Patient-Tailored Cardiac Resynchronization Therapy: Imaging and Exercise Strategies

Philippe Constant Wouters

Patient-Tailored Cardiac Resynchronization Therapy:

Imaging and Exercise Strategies

Philippe Constant Wouters

Patient-Tailored Cardiac Resynchronization Therapy:
Imaging and Exercise Strategies

Cardiale Resynchronisatie Therapie op Maat:
Beeldvorming en Inspanningsstrategiën

(met een samenvatting in het Nederlands)

Proefschrift

ter verkrijging van de graad van doctor aan de
Universiteit Utrecht
op gezag van de
rector magnificus, prof. dr. H.R.B.M. Kummeling,
ingevolge het besluit van het college voor promoties
in het openbaar te verdedigen op
donderdag 24 november 2022 des ochtends te 10.15 uur

door

Philippe Constant Wouters

geboren op 15 april 1994
te Breda

PROMOTOREN:

Prof. dr. P.A.F.M. Doevendans
Prof. dr. F.W. Prinzen

COPROMOTOREN:

Dr. M. Meine
Dr. M.J. Cramer

TABLE OF CONTENTS

PART III   EXPLORING EXERCISE PHSYIOLOGY

APPENDICES

1

**General Introduction
and Thesis Outline**

BACKGROUND

Upon reaching 80 years of age, the heart will have produced approximately 3 billion beats. Not only is the heart a truly fascinating and remarkable organ from a medical perspective, its symbolical value is recognised around the globe and unmistakably intertwined in our culture. Almost equally remarkable are the many technological advancements in the field of cardiology that have contributed to the treatment of this precious organ. A hallmark example of these advancements is cardiac resynchronization therapy (CRT), a device therapy that originated nearly three decades ago [1,2] and is used to treat patients with dyssynchronous heart failure (HF). The present work aims to investigate how outcomes for patients treated with CRT can be improved. To this goal, three focus areas are defined in this thesis: (i) to evaluate the clinical use of electromechanical markers as a means of improving patient selection criteria for CRT; (ii) to investigate the role of cardiac imaging in optimizing placement of the left ventricular (LV) lead; and (iii) to examine exercise physiological aspects in patients with dyssynchronous HF.

PHYSIOLOGY OF THE HEART

For the heart to function, a crucial interplay between electrical conduction and mechanical function exists. Electrical conduction is rhythmically initiated at a frequency of ~70 beats per minute within the aptly named *'pacemaker cells'*, which are concentrated in the sinoatrial node. Conduction is then passed along the atria, but is temporarily halted at the atrioventricular node. This allows the atria to contract and thereby eject blood into the two main chambers of the heart; the ventricles. After this delay, conduction is rapidly propagated through the bundle of His, and is then diverged along the right and left bundle branches and their respective Purkinje fibres. As a result, '*simultaneous'* activation of the right and left ventricle occurs, and blood is ejected in the lungs and the rest of the body, respectively. However, various conditions may disrupt the normal haemodynamic function of the heart and its efficiency, thereby contributing to the development of heart failure (HF).

EPIDEMIOLOGY OF HEART FAILURE

HF is a clinical syndrome, characterised by signs and symptoms that are caused by the hearts inability to regulate adequate blood flow through the body. HF is the final common stage of many diseases of the heart with an estimated prevalence of over 60 million worldwide [3]. Moreover, HF is also the most rapidly '*growing'* cardiovascular condition

globally, and remains a major cause of morbidity and mortality in developed countries. As such, HF represents one of the leading health care problems in the western world [3]. At age 45 years, estimated lifetime risk for HF is at least 20%, with an average five-year survival rate of 57% [3]. Next to non-modifiable risk factors such as age, gender, ethnicity and genetic susceptibility, various (lifestyle) factors that are at least partially modifiable are associated with an increased risk of incident HF. These include dyslipidaemia, hypertension, diabetes mellitus, smoking and physical inactivity [4]. This indicates that a healthy lifestyle is closely related to a reduced risk of HF.

UNDERSTANDING DYSSYNCHRONOUS HEART FAILURE

In the early 1990's, the concept of dyssynchrony-induced redistribution of myocardial fiber strain and blood flow was introduced [5,6]. Indeed, an electrical problem in the native conduction system of the heart can disturb the function of the left ventricle (LV). Both the '*type'* of electrical activation of both ventricles and the *'extent'* of this activation delay are represented by the QRS-complex on the electrocardiogram (ECG). In approximately one third of patients with heart failure, a broadened QRS-complex with left bundle branch block (LBBB) morphology on the ECG is found [7]. LBBB indicates a delayed depolarisation of the left ventricle (LV) free wall, relative to the LV septum, resulting in an asynchronous LV activation. Despite the suggestive name, LBBB on the ECG does not necessarily indicate that the conduction block is located within the left bundle branch [8]. Rather, lesions may also be located within the His-bundle (i.e., intrahisian). In fact, an LBBB pattern on the ECG may even originate in the presence of an intact conduction system at the His-Purkinje level, for example in the case of myocardial lesions [8].

In response to LBBB, cardiac workload is shifted away from the LV septum, and directed towards the LV free wall, thereby impeding cardiac efficiency [10]. This *'septal-to-lateral wall'* shift also becomes apparent when evaluating strain patterns in the LV, since the amount of paradoxical and ineffective systolic stretching in the early-activated septum is markedly increased **(Figure 1)**. These effects are also translated to the molecular and cellular level, as asymmetrical hypertrophy occurs in the later-activated LV free wall [11]. Conversely, in the septum, local hypoperfusion and reduced myocardial work are observed [12]. As a whole, these changes culminate in drastically altered hemodynamic loading conditions, and adverse remodelling of the LV ensues. Here, LV end-systolic volume (LVESV) is increased, and LV ejection fraction is depressed.
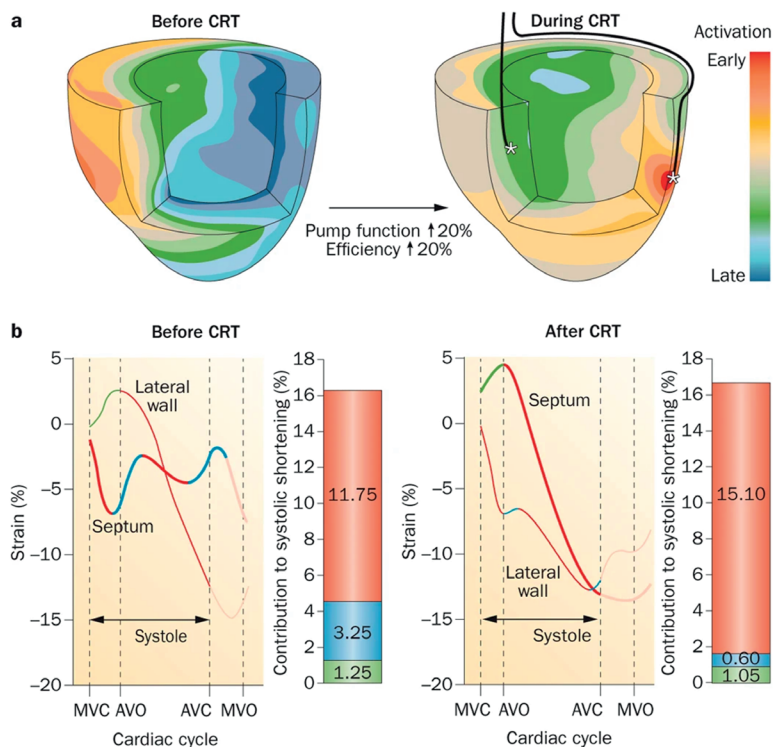
Figure 1. *Sequences of electrical activation (A) and mechanical strain curves (B) in left bundle branch block, before and after cardiac resynchronisation therapy. Reprinted with permission from Vernooy et al. [9].*
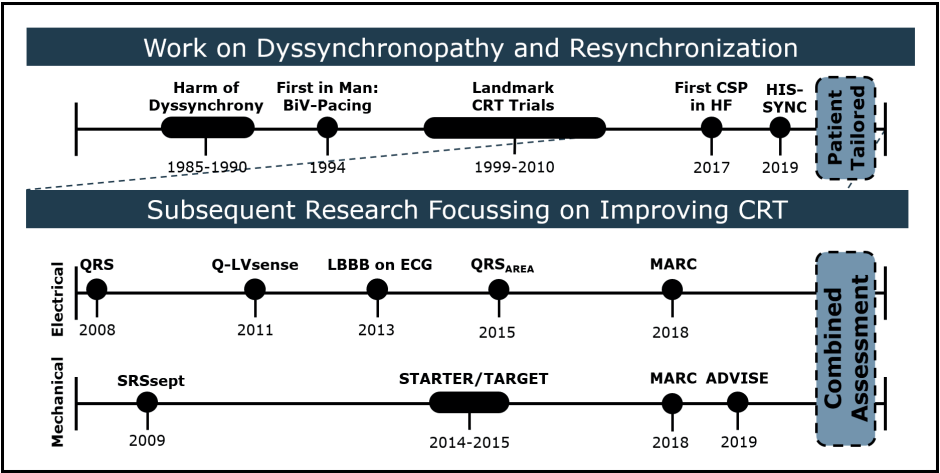
Figure 2. *Previous work on cardiac resynchronization therapy put into perspective using timelines. Legend: ADVISE, Advanced image-supported lead placement; BiV, biventricular; CRT, cardiac resynchronization therapy; CSP, conduction system pacing; ECG, electrocardiogram; LBBB, left bundle branch block; MARC, Markers and Response to CRT; SRSsept, systolic rebound stretch of the septum; STARTER, Speckle Tracking Assisted Resynchronization Therapy for Electrode Region; TARGET, Targeted left ventricular lead placement to guide cardiac resynchronization therapy.*

RESYNCHRONIZING THE HEART

In patients with symptomatic and dyssynchronous HF with a severely depressed LVEF despite optimal medical treatment CRT is considered. CRT is an implantable device therapy that requires the implantation of three pacemaker leads as a means to *"harmonize"* the rhythm of the heart. To this end, leads are placed in the right atrium and right ventricle, respectively. An additional third lead is placed through the coronary sinus, and placed alongside the LV lateral wall. In essence, CRT aims to simultaneously depolarize both ventricles by means of electric stimulation, thereby resynchronising the heart. As a result, CRT largely reverses functional and structural abnormalities that were induced by LBBB, both globally and regionally, and can thereby cure dyssynchronopathy [13]. Physicians determine patient eligibility using guideline criteria [14]. According to the current guidelines, concerning the electrical conduction delay, two ECG features should preferably be present on the ECG:

1. *'The right type'*: a left bundle branch block (LBBB) activation pattern, thought to be characterized by a set of 'typical' ECG characteristics [15].
2. *'The right duration'*: presence of sufficient electrical delay, thought to be characterized by a QRS-duration of at least 150 ms [16].

THE PROBLEM OF CRT NON-RESPONSE

Response following CRT can be measured according to a variety of functional, structural, or clinical endpoints. Although there is no unifying standard definition that truthfully describes response to CRT, the estimate that 30-40% of patients undergoing CRT are non-responders is generally accepted. Potential causes of non-response are multifactorial, and an integrated approach is warranted to optimize results in these patients. Various research attempts have been made to improve CRT **(Figure 2)**.

I – OPTIMIZING PATIENT SELECTION

For successful CRT, that is obviously an electrical therapy, the presence of sufficient baseline electrical dyssynchrony is required. In the absence of such a substrate, CRT may even be detrimental [17]. However, parameters of mechanical dyssynchrony are associated with outcome after CRT as well. Unfortunately, accurate identification of the electrical substrate by evaluating the previously mentioned ECG characteristics is rather complex. For instance, multiple definitions of LBBB-morphology exist [18], inter-observer variability is high [19], and LV electrical activation patterns can either be concealed [8] or mimicked

in the ECG [20]. Moreover, although an electrical substrate can be present, this does not necessarily result in actual *'mechanical'* impairment of the LV. Various parameters of mechanical dyssynchrony have been introduced over the years, including markers that can be assessed visually on the echocardiogram (i.e., Apical Rocking and Septal Flash), or require strain-imaging. It is therefore crucial to investigate how the electrical substrate can best be characterised in an objective manner, and how LV mechanical dysfunction can best be quantified.

The vectorcardiographic QRS_{AREA} has been proposed as a novel marker that objectively identifies the LV electrical substrate [21]. QRS_{AREA} at baseline [22], and its reduction after CRT [23] are independently associated with outcome and response following device implantation, and outperform contemporary QRS characteristics. However, ECG features beyond the QRS-complex are still not evaluated. Use of a deep learning-based approach on the whole ECG may further improve risk stratification.

Previous work also extensively studied methods to quantify LV mechanical discoordination using strain-imaging **(Figure 2)**. Upon its discovery, systolic rebound stretch of the septum (SRSsept) was found to be strongly associated with volumetric response [24] and long-term clinical outcome [25]. SRSsept is also of added value when QRS-duration and LBBB morphology are evaluated [26]. Methods were then explored to optimize acquisition and analysis of SRSsept [27,28], and recently its added value on top of visually assessed dyssynchrony was proven [29]. However, the role of SRSsept has yet to be investigated into a clinical context where QRS_{AREA} is assessed as well. It should therefore be investigated to what extent combined and optimised assessment of both, electrical and mechanical properties, reflect the likeliness of the heart to improve (i.e., reverse remodel) after CRT implantation. And, how this may affect the interpretation of SRSsept in everyday practice.

II − TAILORING LEAD IMPLANTATION

Different LV-lead pacing sites can be reached by navigating the various coronary sinus tributaries. However, landmark trials have consistently demonstrated that, on group level, no LV pacing site is consistently superior or detrimental [30,31]. By contrast, acute haemodynamic studies have shown that, within the patient, the optimal site can be highly variable and is patient-specific [32]. It was found that pacing in-scar was associated with a 6-fold increase in cardiovascular death [33]. Besides using tissue characterisation as a means of predicting response to CRT, imaging can also be used to determine the site of latest mechanical activation **(Figure 3)**. Targeting sites of latest mechanical activation is also associated with response, most notably in patients with intermediate QRS width < 150 ms and those with non-LBBB [34]. This is important, because these patients typically

tend to demonstrate less reverse remodelling and are therefore considered a challenging patient subpopulation. Unfortunately, the percentage of 'successfully' in-target placed LV-leads is highly variable when comparing prospective image-guided studies. Moreover, no dedicated medical device software exists, limiting clinical adoption.

Bogaard et al demonstrated that optimal device settings, when tailored to the patient-specific needs, cannot overcome a suboptimal LV lead position [35]. When comparing differences in Q-LVsense between patients, patients that receive pacing at sites with a longer electrical delay demonstrate more pronounced acute haemodynamic [36] and mid-term echocardiographic response [37]. Unfortunately, *'within'* the patient, Q-LVsense cannot be used to reliably predict the optimal pacing site [38]. Moreover, mapping Q-LVsense in various veins can be time-consuming and cumbersome. CART-Tech recently developed a dedicated medical device that analyses pre-procedural cardiac magnetic resonance (CMR) images to determine the optimal site for LV lead placement [39,40]. Its software visualises these optimal sites using co-registration, superimposed on live 2D-fluoroscopy. It therefore allows for real-time navigation of the LV-lead. However, feasibility of this approach has to be demonstrated in a multicentre setting, and its clinical utility has to be proven when put to the test in a randomised clinical trial.

Pre-procedural		Intra-procedural
Avoid scar	**Target late activation**	**Target late activation**
• MRI: Late gadolinium enhancement	• MRI: 4D-dyssynchrony mapping	• (3D-vector) resynchronization; $\Delta QRS_{(AREA)}$
	• STE: Δ time-to-peak strain	• Intrinsic conduction delay; Q-LV sense
• STE: Low strain amplitude	• Electrocardiographic imaging	• LV-paced dyssynchrony; interlead delays
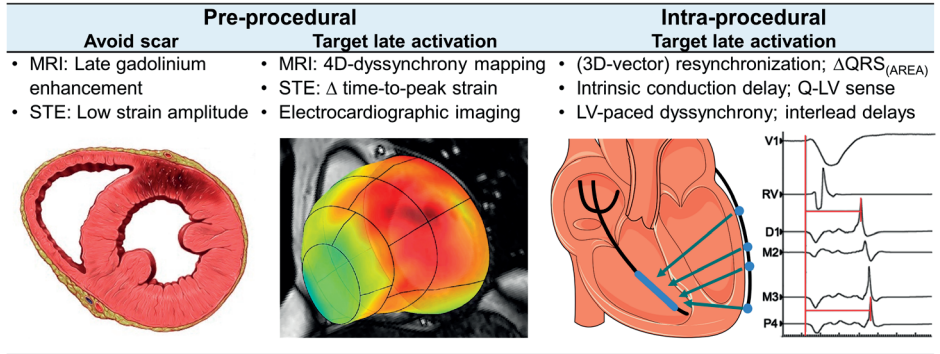
Figure 3. Summary of theoretical framework as to how the optimal left ventricular lead position can be ascertained, based on previous research efforts over the years.

III − EXPLORING EXERCISE PHYSIOLOGY

Although an extensive body of literature exist on methods to improve patient selection and LV lead placement, the role of exercise physiology in recipients of CRT is relatively under-investigated. This is remarkable, because heart failure is a systemic disease which affects various organs in the body [41], and exercise tolerance has a major impact on the quality of life of the patient. Besides 'central' pathology, so called 'peripheral' derangements of skeletal muscle function occur as well [41]. Of course, both types of pathology

contribute to the development of exercise (in)tolerance. Patients with HF may notice these limitations only when performing strenuous activities that require high effort (New York Heart Association [NYHA] class I), but also already during ordinary physical activities (NYHA class II), or even as rapidly as during ordinary daily living activities (NYHA class III).
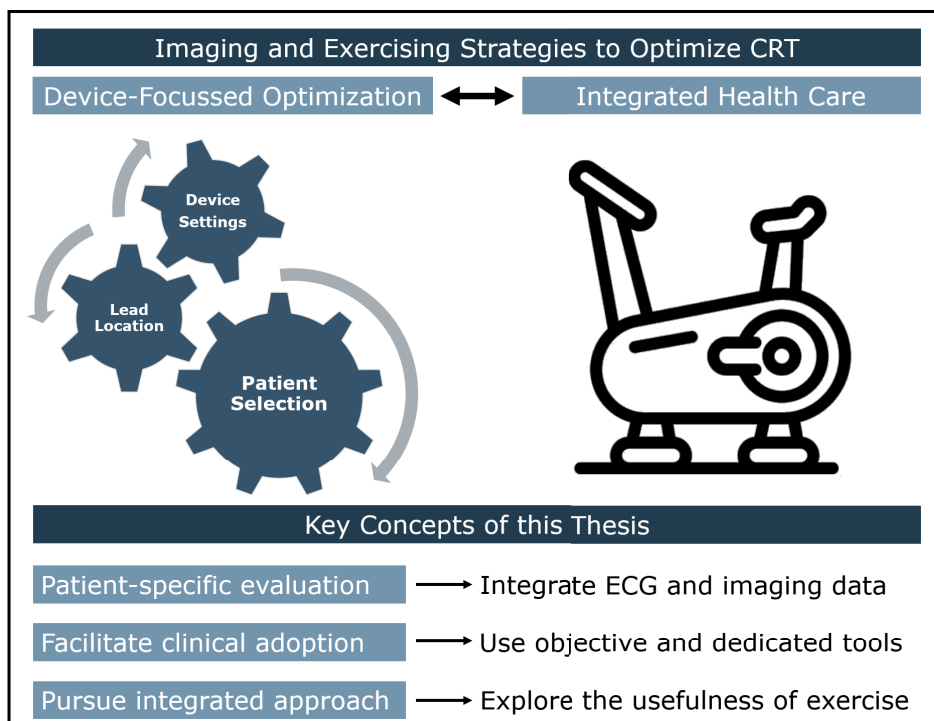
Figure 4. *The main aspects of improving outcomes in patients with heart failure, and focus points of this thesis.*

As discussed above, CRT effectuates electrical resynchronization, which in turn instigates structural reverse remodelling of the dilated LV. It is therefore reasonable to relate a *'structural'* response after CRT to *'functional'* improvements, such as increased exercise capacity and quality of life. However, disagreement between these echocardiographic and functional endpoints is seen surprisingly often, since structural response correlates poorly with actual symptomatic and clinical improvement [42,43]. Hence, where the majority of research on CRT focusses on improving patient selection, LV lead position, or device optimisation, the third part of this thesis will explore how exercise physiology may help improve outcome in patients with dyssynchronous HF.

RESEARCH AIMS OF THIS THESIS

The thesis is divided in three main parts, each focussing on separate research topics **(Figure 4)**. In general, we sought to further explore and (partly) answer the following questions:

1. PART I: How can we optimally incorporate electrical and mechanical properties of the dyssynchronous heart to refine patient selection for CRT?
2. PART II: Which approach allows for optimal placement of the left ventricular lead, tailored to patient-specific characteristics?
3. PART III: Can we improve the diagnostic, prognostic, and therapeutic value of exercise testing and exercise training in the workup of patients eligible for CRT?

OUTLINE OF THIS THESIS

Previous research has improved our understanding of the electromechanical substrate in dyssynchronous heart failure. As a result, new methods to identify the electrical substrate and subsequent mechanical dysfunction (i.e., dyssynchrony or discoordination) have been investigated, which led to insights how these can be used to improve patient selection and guide LV-lead implantation. The present thesis builds on these important insights, aims to further advance these developments, and incorporate these into clinical practice.

Firstly, we sought to refine selection criteria that assess patient eligibility for CRT. In **chapter 2**, an end-to-end explainable deep learning-based approach was developed to objectively identify the electrical substrate using the whole 12-lead ECG. This approach was then compared to QRS_{AREA} and contemporarily used guideline criteria for the prediction both, outcome and echocardiographic response, after CRT. In **chapter 3**, we compared acute changes in either mechanical function (i.e., recoordination) and hemodynamic response (i.e., dP/dt), and investigated their association with response to CRT. **Chapter 4** then focusses on the actual combination of these advanced measures of the electrical substrate and mechanical dysfunction, by simultaneously assessing QRS_{AREA} and SRSsept, respectively.

Secondly, methods to improve LV-lead placement in CRT are investigated. The link between patient-specific electromechanical activation and various resynchronization approaches were explored in **chapter 5.** We try to provide clinicians with insights as to 'who' may benefit from certain strategies of optimized lead placement, and 'how' this can be achieved. Then, in **chapter 6**, the feasibility and outcome of an image-guided approach to navigate the LV-lead in real-time was explored. To this end, 30 patients were prospectively enrolled in three Dutch hospitals. The actual clinical utility of this

1

approach will be further investigated in a larger multicentre randomised controlled trial (ADVISE trial). The protocol of this study is carefully described in **chapter 7**, which also reports on the potential health-economic implications of such an approach.

Thirdly, we explored the role of exercise physiology in patients with (dyssynchronous) heart failure. **Chapter 8** touches upon the feasibility of strain-based discoordination imaging during stress echocardiography in patients with heart failure. In addition, it explores whether exercise may unmask or reduce mechanical dysfunction in these patients. In **chapter 9,** we investigate the relation between various exercise parameters at baseline and echocardiographic response after CRT. Finally, in **chapter 10**, we further explored exercise physiology in a broad context. We sought to explain symptom aetiology in patients with heart failure by investigating central haemodynamics and peripheral skeletal muscle function during exercise testing. In addition, we compared the effects of high-intensity interval training and CRT on these parameters.
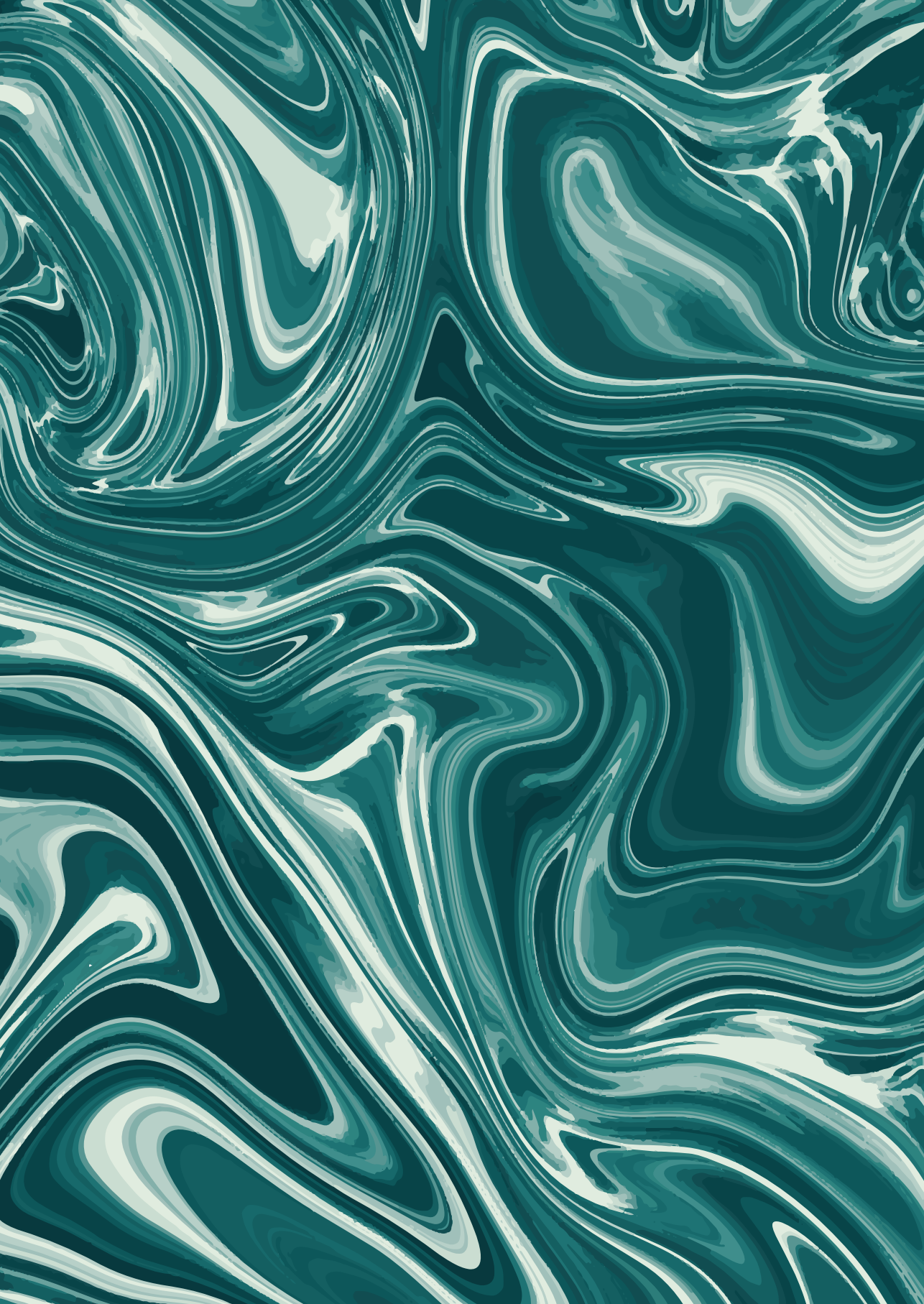
REFERENCES

1. S. Cazeau, P. Ritter, S. Bakdach, *et al.* Four Chamber Pacing in Dilated Cardiomyopathy. *Pacing Clin. Electrophysiol.* **17**, 1974–1979 (1994).

2. P. Bakker, H. Meijburg, H. de Jonge, *et al.* Beneficial effects of biventricular pacing in congestive heart failure. *Pacing Clin Electrophysiol.* **17**, 820 (1994).

3. A. Groenewegen, F. H. Rutten, A. Mosterd, A. W. Hoes. Epidemiology of heart failure. *Eur. J. Heart Fail.* **22**, 1342–1356 (2020).

4. A. L. Bui, T. B. Horwich, G. C. Fonarow. Epidemiology and risk profile of heart failure. *Nat. Rev. Cardiol.* **8**, 30–41 (2011).

5. F. W. Prinzen, C. H. Augustijn, T. Arts, M. A. Allessie, R. S. Reneman. Redistribution of myocardial fiber strain and blood flow by asynchronous activation. *Am. J. Physiol. Circ. Physiol.* **259**, H300–H308 (1990).

6. F. W. Prinzen, W. C. Hunter, B. T. Wyman, E. R. McVeigh. Mapping of regional myocardial strain and work during ventricular pacing: experimental study using magnetic resonance imaging tagging. *J. Am. Coll. Cardiol.* **33**, 1735–1742 (1999).

7. W. Mullens, A. Auricchio, P. Martens, *et al.* Optimized implementation of cardiac resynchronization therapy: a call for action for referral and optimization of care. *Eur. J. Heart Fail.* **22**, 2349–2369 (2020).

8. G. A. Upadhyay, T. Cherian, D. Y. Shatz, *et al.* Intracardiac Delineation of Septal Conduction in Left Bundle-Branch Block Patterns: Mechanistic Evidence of Left Intrahisian Block Circumvented by His Bundle Pacing. *Circulation.* **139**, 1876–1888 (2019).

9. K. Vernooy, C. J. M. Van Deursen, M. Strik, F. W. Prinzen. Strategies to improve cardiac resynchronization therapy. *Nat. Rev. Cardiol.* **11**, 481–493 (2014).

10. O. Sletten, J. Aalen, H. Izci, *et al.* Lateral Wall Dysfunction Signals Onset of Progressive Heart Failure in Left Bundle Branch Block. *JACC Cardiovasc. Imaging.* **14**, 2059–2069 (2021).

11. L. B. van Middendorp, M. Kuiper, C. Munts, *et al.* Local microRNA-133a downregulation is associated with hypertrophy in the dyssynchronous heart. *ESC Hear. Fail.* **4**, 241–251 (2017).

12. K. Vernooy, X. A. A. M. Verbeek, M. Peschar, *et al.* Left bundle branch block induces ventricular remodelling and functional septal hypoperfusion. *Eur. Heart J.* **26**, 91–98 (2005).

13. K. Vernooy, R. N. M. Cornelussen, X. A. A. M. Verbeek, *et al.* Cardiac resynchronization therapy cures dyssynchronopathy in canine left bundle-branch block hearts. *Eur. Heart J.* **28**, 2148–2155 (2007).

14. M. Glikson, J. C. Nielsen, M. B. Kronborg, *et al.* 2021 ESC Guidelines on cardiac pacing and cardiac resynchronization therapy: Developed by the Task Force on cardiac pacing and cardiac resynchronization therapy of the European Society of Cardiology (ESC) With the special contribution of the European Hear. *Eur. Heart J.* (2021), doi:10.1093/eurheartj/ehab364.

15. I. Sipahi, J. C. Chou, M. Hyden, *et al.* Effect of QRS morphology on clinical event reduction with cardiac resynchronization therapy: meta-analysis of randomized controlled trials. *Am. Heart J.* **163**, 260–7.e3 (2012).

16. I. Sipahi, T. P. Carrigan, D. Y. Rowland, B. S. Stambler, J. C. Fang. Impact of QRS Duration on Clinical Event Reduction With Cardiac Resynchronization Therapy: Meta-analysis of Randomized Controlled Trials. *Arch. Intern. Med.* **171**, 1454–1462 (2011).

17. F. Ruschitzka, W. T. Abraham, J. P. Singh, *et al.* Cardiac-Resynchronization Therapy in Heart Failure with a Narrow QRS Complex. *N. Engl. J. Med.* **369**, 1395–1405 (2013).

18. A. M. W. van Stipdonk, R. Hoogland, I. ter Horst, *et al.* Evaluating Electrocardiography-Based Identification of Cardiac Resynchronization Therapy Responders Beyond Current Left Bundle Branch Block Definitions. *JACC Clin. Electrophysiol.* **6**, 193–203 (2020).

19. A. M. W. van Stipdonk, S. Vanbelle, I. A. H. Ter Horst, *et al.* Large variability in clinical judgement and definitions of left bundle branch block to identify candidates for cardiac resynchronisation therapy. *Int. J. Cardiol.* **286**, 61–65 (2019).

20. M. Potse, D. Krause, L. Bacharova, *et al.* Similarities and differences between electrocardiogram signs of left bundle-branch block and left-ventricular uncoupling. *EP Eur.* **14**, v33–v39 (2012).

21. C. J. M. van Deursen, K. Vernooy, E. Dudink, *et al.* Vectorcardiographic QRS area as a novel predictor of response to cardiac resynchronization therapy. *J. Electrocardiol.* **48**, 45–52 (2015).

22. A. M. W. van Stipdonk, I. Ter Horst, M. Kloosterman, *et al.* QRS Area Is a Strong Determinant of Outcome in Cardiac Resynchronization Therapy. *Circ. Arrhythm. Electrophysiol.* **11**, e006497 (2018).

23. M. A. Ghossein, A. M. W. van Stipdonk, F. Plesinger, *et al.* Reduction in the QRS area after cardiac resynchronization therapy is associated with survival and echocardiographic response. *J. Cardiovasc. Electrophysiol.* **32**, 813–822 (2021).

24. B. W. L. De Boeck, A. J. Teske, M. Meine, *et al.* Septal rebound stretch reflects the functional substrate to cardiac resynchronization therapy and predicts volumetric and neurohormonal response. *Eur. J. Heart Fail.* **11**, 863–871 (2009).

25. G. E. Leenders, B. W. L. De Boeck, A. J. Teske, *et al.* Septal rebound stretch is a strong predictor of outcome after cardiac resynchronization therapy. *J. Card. Fail.* **18**, 404–412 (2012).

26. J. Van't Sant, I. A. H. Ter Horst, S. C. Wijers, *et al.* Measurements of electrical and mechanical dyssynchrony are both essential to improve prediction of CRT response. *J. Electrocardiol.* **48**, 601–608 (2015).

27. W. M. Van Everdingen, A. H. Maass, K. Vernooy, *et al.* Comparison of strain parameters in dyssynchronous heart failure between speckle tracking echocardiography vendor systems. *Cardiovasc. Ultrasound*. **15**, 25 (2017).

28. W. M. van Everdingen, J. Walmsley, M. J. Cramer, *et al.* Echocardiographic Prediction of Cardiac Resynchronization Therapy Response Requires Analysis of Both Mechanical Dyssynchrony and Right Ventricular Function: A Combined Analysis of Patient Data and Computer Simulations. *J. Am. Soc. Echocardiogr.* **30**, 1012-1020.e2 (2017).

29. O. A. E. Salden, A. Zweerink, P. Wouters, *et al.* The value of septal rebound stretch analysis for the prediction of volumetric response to cardiac resynchronization therapy. *Eur. Heart J. Cardiovasc. Imaging*. **22**, 37–45 (2021).

30. F. Leyva, A. Zegard, R. J. Taylor, *et al.* Long-term outcomes of cardiac resynchronization therapy using apical versus nonapical left ventricular pacing. *J. Am. Heart Assoc.* **7**, e008508 (2018).

31. J. P. Singh, H. U. Klein, D. T. Huang, *et al.* Left ventricular lead position and clinical outcome in the multicenter automatic defibrillator implantation trial-cardiac resynchronization therapy (MADIT-CRT) trial. *Circulation*. **123**, 1159–1166 (2011).

32. N. Derval, P. Steendijk, L. J. Gula, *et al.* Optimizing hemodynamics in heart failure patients by systematic screening of left ventricular pacing sites: the lateral left ventricular wall and the coronary sinus are rarely the best sites. *J. Am. Coll. Cardiol.* **55**, 566–575 (2010).

33. F. Leyva, P. W. Foley, S. Chalil, *et al.* Cardiac resynchronization therapy guided by late gadolinium-enhancement cardiovascular magnetic resonance. *J. Cardiovasc. Magn. Reson.* **13**, 29 (2011).

34. J. J. Marek, S. Saba, T. Onishi, *et al.* Usefulness of echocardiographically guided left ventricular lead placement for cardiac resynchronization therapy in patients with intermediate QRS width and non-left bundle branch block morphology. *Am. J. Cardiol.* **113**, 107–116 (2014).

35. M. D. Bogaard, P. A. Doevendans, G. E. Leenders, *et al.* Can optimization of pacing settings compensate for a non-optimal left ventricular pacing site? *EP Eur.* **12**, 1262–1269 (2010).

36. M. R. Gold, R. B. Leman, N. Wold, J. L. Sturdivant, Y. Yu. The effect of left ventricular electrical delay on the acute hemodynamic response with cardiac resynchronization therapy. *J. Cardiovasc. Electrophysiol.* **25**, 624–630 (2014).

37. M. R. Gold, U. Birgersdotter-Green, J. P. Singh, *et al.* The relationship between ventricular electrical delay and left ventricular remodelling with cardiac resynchronization therapy. *Eur. Heart J.* **32**, 2516–2524 (2011).

38. W. M. van Everdingen, A. Zweerink, M. J. Cramer, *et al.* Can We Use the Intrinsic Left Ventricular Delay (QLV) to Optimize the Pacing Configuration for Cardiac Resynchronization Therapy With a Quadripolar Left Ventricular Lead? *Circ. Arrhythm. Electrophysiol.* **11**, e005912 (2018).

39. O. A. E. Salden, H. T. van den Broek, W. M. van Everdingen, *et al.* Multimodality imaging for real-time image-guided left ventricular lead placement during cardiac resynchronization therapy implantations. *Int. J. Cardiovasc. Imaging.* **35**, 1327–1337 (2019).

40. W. A. Gathier, O. A. E. Salden, D. J. van Ginkel, *et al.* Feasibility and potential benefit of pre-procedural CMR imaging in patients with ischaemic cardiomyopathy undergoing cardiac resynchronisation therapy. *Netherlands Hear. J.* **28**, 89–95 (2020).

41. T. A. Rehn, M. Munkvik, P. K. Lunde, I. Sjaastad, O. M. Sejersted. Intrinsic skeletal muscle alterations in chronic heart failure patients: a disease-specific myopathy or a result of deconditioning? *Heart Fail. Rev.* **17**, 421–436 (2012).

42. C. Daubert, N. Behar, R. P. Martins, P. Mabo, C. Leclercq. Avoiding non-responders to cardiac resynchronization therapy: a practical guide. *Eur. Heart J.* **38**, 1463–1472 (2017).

43. B. K. Fornwalt, W. W. Sprague, P. BeDell, *et al.* Agreement is poor among current criteria used to define response to cardiac resynchronization therapy. *Circulation.* **121**, 1985–1991 (2010).

PART I

OPTIMIZING PATIENT SELECTION

2

Explainable Electrocardiogram-Based Deep Learning Outperforms Guideline Criteria and QRS$_{AREA}$ for Prediction of Cardiac Resynchronization Therapy Outcome

Philippe C. Wouters*, Rutger R. van de Leur*, Melle B. Vessies, Antonius M.W. van Stipdonk, Mohammed A. Ghossein, Rutger J. Hassink, Pieter A. Doevendans, Pim van der Harst, Alexander H Maass, Frits W. Prinzen, Kevin Vernooy, Mathias Meine, Rene van Es

* Shared first authorship

ABSTRACT

Aims: We sought to identify and visualize ECG features using an explainable deep learning-based algorithm to predict cardiac resynchronization therapy (CRT) outcome. Its performance was compared to current guideline ECG criteria and QRS$_{AREA}$.

Methods and results: A deep learning algorithm, trained on 1.1 million ECGs, was used to compress the median beat ECG, thereby summarizing all ECG features in 21 explainable factors (FactorECG). Pre-implantation ECGs of 1306 CRT patients from three academic centers were converted into their respective FactorECG, and the occurrence of a clinical endpoint (death, left ventricular assist device implantation, or heart transplantation) and echocardiographic non-response (< 15% left ventricular end-systolic volume reduction at 6 months) were analyzed. FactorECG significantly outperformed guideline ECG criteria for clinical outcome (c-statistic = 0.69) and echocardiographic non-response (c-statistic = 0.69). FactorECG performed significantly better for outcome, but similar for echocardiographic response when compared to QRS$_{AREA}$ (c-statistic = 0.61 and c-statistic = 0.70, respectively). FactorECG identified inferolateral T-wave inversion, smaller right precordial S-wave and T-wave amplitude and ventricular rate to be important predictors for both poor outcome and non-response, while increased PR-interval and P-wave duration was only important for poor outcome, and shorter QRS and JTc-duration only for non-response.

Conclusion: Requiring only a standard 12-lead ECG, FactorECG held superior discriminative ability for the prediction of clinical outcome as compared to guideline criteria and QRS$_{AREA}$, without requiring additional clinical variables. End-to-end automated visualisation of ECG features allows for an explainable algorithm, which may facilitate rapid uptake of this personalised decision-making tool in CRT.

INTRODUCTION

In patients with dyssynchronous heart failure (HF), cardiac resynchronization therapy (CRT) can effectively restore left ventricular (LV) electrical activation and mechanical function, thereby improving clinical outcome [1,2]. However, for CRT to be beneficial, sufficient LV electrical conduction delay must be present [3]. Currently, patients are selected based on various requirements set out by different guidelines. However, by itself, a class I indication does not necessarily ensure a sustained response after CRT [4]. Moreover, in patients without typical left bundle branch block (LBBB) morphology or an intermediate QRS-duration of 130 – 150 ms, effectiveness of CRT is variable and still doubted [3]. These patients have no class I indication for CRT, and are thereby at increased risk of not being considered for treatment [5,6]. It is clear, however, that a substantial subpopulation of these patients is likely to benefit, and as such should not be withheld from CRT altogether [5]. Accurate and objective identification of the underlying electrical substrate is therefore crucial to optimize patient selection and ensure optimal treatment.

Currently, electrical characteristics derived from the electrocardiogram (ECG), such as LBBB-morphology and QRS-duration, are used to determine eligibility for CRT [3]. Multiple ECG criteria for LBBB have been defined [7], and inter-observer variability is high [8]. Moreover, a variety of LV electrical activation patterns are concealed in the ECG, further complicating clinical decision making [9]. Recently, QRS_{AREA} has emerged as a new and objective computerized measure [4,10]. QRS_{AREA} is independently associated with survival and echocardiographic response, outperforming LBBB-morphology and QRS-duration [4,10]. As such, QRS_{AREA} partly overcomes the challenges of subjective ECG interpretation, but (subtle) ECG characteristics, also besides the QRS-complex, are still not considered.

Machine learning has gained interest as a means of integrating large amounts of variables, thereby producing advanced clinical decision models. The SEMMELWEIS-CRT score, for example, outperforms many already existing risk scores, but relies on 33 clinical variables [11]. Besides being laborious to use, such models also rely on human interpretation of input variables such as left ventricular ejection fraction (LVEF), New York Heart Association (NYHA), LBBB-morphology and QRS-duration, which are all subjectively assessed. Hence, although such models may predict response to CRT, large amounts of clinical variables will still need to be acquired, extracted and entered in such models [11–13].

A recent development in the field of machine learning, called deep learning, can learn features from the raw ECG signal without the necessity for any human interpretation [14]. Deep learning algorithms may therefore be used to automatically detect, identify and classify ECG abnormalities that are associated with non-response or poor outcome after CRT. Although the need for very large datasets and the lack of interpretability were deemed common drawbacks of deep learning, a novel technique that uses a variational auto-encoder (the FactorECG) was recently introduced [15]. This approach enables physi-

cians to better understand the learned ECG features of deep learning algorithms, and make the technique available to much smaller datasets.

The present study seeks to compare contemporary guideline ECG criteria for CRT implantation and QRS_{AREA} with the FactorECG for the prediction of a combined clinical endpoint and echocardiographic response. In addition, we aim to identify and visualise ECG features associated with these outcome measures.

METHODS

Study design

All data were acquired for routine patient care and handled anonymously, and were collected as part of the multicentre Maastricht-Utrecht-Groningen (MUG) registry [10]. Under these circumstances, informed consent was waived by the Institutional Review Board at the time of the study. All study procedures were performed in compliance with the Declaration of Helsinki.

Only patients who received a de novo CRT-device were considered for the present study. A baseline ECG (within 3 months before implantation) was required for the primary endpoint analysis, whereas paired echocardiographic examination at baseline and follow-up (6 to 12 months) was required for the secondary endpoint. Echocardiographic exams were used to determine LV end-systolic volume (LVESV), and LVEF was calculated using the Simpson's modified biplane method.

The primary endpoint was a combined clinical endpoint consisting of left ventricular assist device (LVAD) implantation, heart transplantation (HTx), and all-cause mortality. Secondary outcome was echocardiographic non-response, defined as relative decrease in LVESV < 15%. In addition, time to first HF-hospitalisation was assessed.

Electrocardiographic data

For all patients, standard 12-lead ECGs were exported and converted into median heart beats using the MUSE ECG system (MUSE version 8, GE Healthcare, Chicago, IL). The median beat data were constructed by aligning all QRS-complexes in the 10 second ECG of the same shape (e.g., excluding premature ventricular complexes), and generating a representative QRS-complex by taking the median voltage [16]. Automated ECG readings were used to derive QRS-duration and other typical ECG parameters. LBBB-morphology was defined according to the 2013 ESC and 2013 AHA criteria at the time, as previously reported [7]. Using these morphological definitions, indications for CRT implantation were determined according to the current ESC 2021 guidelines [3].

To calculate QRS_{AREA}, first all ECGs were semi-automatically recoded into vectorcardiograms, consisting of three orthogonal leads (X, Y, and Z). To this end, the Kors conversion

2

matrix was used in custom Matlab software (MathWorks Inc)[17]. The three orthogonal leads from the vectorcardiogram form a 3D-vector loop, from which QRS_{AREA} was calculated as the sum of the area under the QRS-complex as $\sqrt{X_{AREA}{}^2 + Y_{AREA}{}^2 + Z_{AREA}{}^2}$.

Deep learning approach

A recently developed approach to use deep neural networks in an explainable method, referred to as the FactorECG, was used. Here, the complete median beat ECG is analysed using a variational auto-encoder (VAE), which divided the ECG into morphological features without any assumptions (e.g., an agnostic approach). For this approach, the VAE was pretrained to learn these morphological features (or underlying generative factors) of the ECG, using a dataset of 1.1 million ECGs from the University Medical Centre Utrecht[15]. The VAE is an algorithm that consists of three parts: 1) an encoder DNN, 2) the FactorECG (a compressed version of the ECG in only 32 disentangled continuous factors) and 3) the decoder DNN **(Figure 1A)**. Pretraining of the VAE was performed unsupervised by entering the median beat ECGs into the algorithm and reconstructing the same ECG, while calculating the difference between the original and reconstructed ECG to optimize the network. After training, the encoder was used to determine a distinctive set of 32 continuous variables (the FactorECG) for every ECG. Importantly, it has been shown before that only 21 of the 32 factors encode significant information[15]. Hence, only these 21 factors were used in subsequent models. In the training step, the 21 continuous FactorECG values for every ECG, as calculated by the decoder, are used in Cox and logistic regression models to perform prediction of outcome and response after CRT **(Figure 1B).**

Explainability of the individual ECG factors associated with outcome and response was achieved by visualizing their influence on the median beat ECG morphology. This was done on the model-level by varying the values of the individual ECG factors between -3 and 3, while reconstructing the ECG using the decoder. The other factors were kept constant, which allows for visualization of the distinct median beat ECG morphology that every factor entails. Moreover, patient-level explanations can be obtained by investigating the FactorECG values of that specific ECG, in combination with the coefficients of the model. This way, we can determine which factors were important in a specific patient to make the prediction. Interactive visualizations of the model are available on https://crt.ecgx.ai. The architecture and training procedures for the FactorECG have been described in detail before[15].

Statistical analysis

Baseline characteristics were expressed as mean ± standard deviation (SD), or median with interquartile range (IQR), where applicable. Depending on normality of data, differences in continuous variables were assessed using the Student t test or Mann-Whitney U test. Conversely, categorical variables were tested using the χ2 test or Fisher exact.
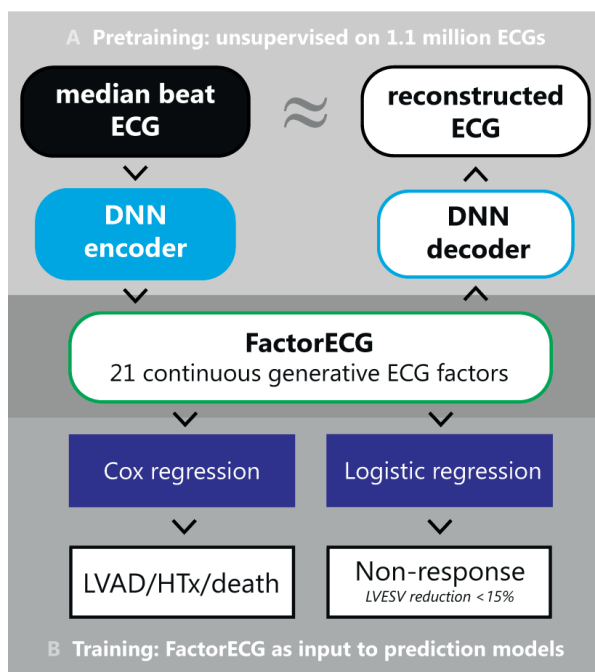
Figure 1. *Schematic representation of the series of algorithms and processes: a variational auto-encoder, the FactorECG and reconstructions. A: in the pretraining phase, the variational auto-encoder is trained on a dataset of 1.1 million median beat ECGs from the University Medical Center Utrecht to learn the underlying factors that generate the ECG. In this process, the VAE learns to reconstruct ECGs as accurate as possible using only the FactorECG continuous factors. B: in the training phase, the 21 significant ECG factors for every median beat ECG in the CRT population are obtained using the encoder. These factors are used as input in Cox and logistic regressions models to predict outcome (composite of LVAD implantation, heart transplantation and death) or non-response (LVESV reduction less than 15% after CRT implantation). Legend: DNN; deep neural network, ECG; electrocardiogram, HTx; heart transplantation, LVAD; left ventricular assist device, LVESV; left ventricular end-systolic volume, VAE; variational auto-encoder.*

Models using different guideline criteria, QRS_{AREA} and the per-patient 21 significant FactorECG values, were compared. For the primary endpoint, Cox proportional hazard models were fitted to take time-to-event into account. The proportional hazards assumption and linearity of the association for continuous variables was verified. Hazards ratios (HRs) were reported to investigate importance of the FactorECG values, which were all standardized. Model fit was assessed using Akaike's Information Criterion (AIC), discrimination using Harell's C-statistic, and calibration using the calibration slope **(Supplemental Table 1 and 2)**. The apparent C-statistic was obtained by applying the model on the original data. Internal validation was performed to obtain the optimism-corrected C-statistic (e.g., a c-statistic corrected for overfitting), and the calibration slope was acquired using 500 bootstrap samples. Confidence intervals (CI) around the C-statistic were obtained using 2000 bootstrap samples. For the secondary endpoint, a similar approach was applied, with logistic regression to predict the binary endpoint of

LVESV non-response < 15%. Odds ratios (OR) and hazard ratios (HR) were reported to investigate the importance of individual standardized FactorECG values.

In a second step, the added value of the models to standard clinical parameters was assessed. Clinical parameters known to be associated with CRT outcome were entered in multivariate models (i.e. Cox regression for outcome and logistic regression for response): sex, age, etiology (i.e. ischemic cardiomyopathy [ICM] or non-ICM), weight, height, baseline NYHA class, rhythm (sinus rhythm or atrial fibrillation), baseline LVEF, baseline end-diastolic volume, baseline interventricular mechanical delay (IVMD), hemoglobin, creatinine levels, and presence of diabetes. As there were missing values of some parameters, multivariate imputation using chained equations was performed using only these clinical parameters as input. Model performance was assessed similarly as for the ECG-only models above. All statistical analyses were performed using Python version 3.8. The Transparent Reporting of a Multivariable Prediction Model for Individual Prognosis or Diagnosis Statement for the reporting of diagnostic models was followed, where applicable [18].

RESULTS

Baseline characteristics

A real-world CRT population was gathered from three Dutch academic hospitals (n = 1946), of which 1492 were eligible after exclusion for RV-pacing and QRS-duration < 120ms. Of the 1492 patients, 1306 had a digital ECG available in the 90 days before implantation and were therefore included in the analysis for the primary endpoint. On average, patients were 68 years [IQR 60-75 years], mostly male (70%) with NYHA II (40%) or III (53%), and 50% non-ICM **(Table 1)**. ESC guideline CRT indication, using the ESC 2013 criteria for LBBB, were as follows: class I 737 (56%), class IIa 401 (31%), class IIb and class III 168 (13%) **(Table 1)**. When applying the AHA criteria for LBBB, indications were as follows: class I 134 (10%), class IIa 786 (60%), class IIb and class III 385 (30%).

Combined clinical endpoint

A total of 385 patients (30%) reached the primary endpoint of LVAD implantation, HTx, or all-cause mortality. The mean follow-up time was 3.5 years [IQR 2.1 – 5.2 years]. Optimism corrected C-statistics were derived for the different predictor sets in predicting the occurrence of the primary endpoint (LVAD, cardiac transplantation, or all-cause mortality; **Table 2**). According to current guideline criteria for CRT implantation, a class I indication was significantly associated with freedom of the primary endpoint, when compared to a non-class I indication. However, this association was only seen when using the ESC (AUC = 0.57 [95% CI 0.54 – 0.60]), but not with the AHA definition (AUC

Table 1. *Baseline characteristics.*

Variable	Missing (n)	Overall (n = 1306)
Age (years)	0	68.3 [60.0-74.7]
Male – n (%)	0	919 (70.4)
ICM – n (%)	0	649 (49.7)
DM – n (%)	2	328 (25.2)
NYHA – n (%)	29	
I		28 (2.2)
II		513 (40.2)
III		672 (52.6)
IV		64 (5.0)
ICD – n (%)	0	1226 (93.9)
NT-proBNP (pmol/L)	605	1379 [587-2845]
LBBB (ESC 2013) – n (%)	0	1028 (78.7)
LBBB (AHA) – n (%)	0	173 (13.3)
QRS$_{AREA}$ (µVs)	0	108.2 [76.0-151.0]
PR (ms)	216	184.0 [164.0-213.5]
QRS duration (ms)	0	158.0 [146.0-172.0]
QTc (ms)	0	486.0 [463.0-510.0]
LVEDV (ml)	355	205.0 [157.1-271.0]
LVESV (ml)	349	151.0 [113.0-209.0]
LVEF (%)	321	24.0 [18.9-30.0]
Primary endpoint (LVAD, HTx or death) – n (%)	0	385 (30)
Duration of follow-up (years)	0	3.48 [2.08-5.24]
LVESV reduction (%)	485	20.9 [0.5-41.4]
LVESV responder – n (%)	485	355 (43)

Legend: DM, diabetes mellitus; ICD, implantable cardioverter defibrillator; ICM, ischemic cardiomyopathy; LVEDV, left ventricular end diastolic volume; LVEF, left ventricular ejection fraction; LVESV, left ventricular end systolic volume; NT-proBNP, N-terminal pro-B-type natriuretic peptide; NYHA, New York Heart Association

= 0.50 [95% CI 0.47 – 0.53]) of LBBB morphology **(Table 2)**. A stronger association with outcome was seen using the FactorECG (AUC = 0.69 [95% CI 0.66 – 0.72]). Moreover, FactorECG had a significantly stronger association with outcome than QRS$_{AREA}$ (AUC = 0.61 [95% CI 0.58 – 0.64]).

When subdividing QRS$_{AREA}$ and FactorECG in four quartiles, better discriminative performance for the occurrence of the primary endpoint was achieved using FactorECG **(Figure 2)**. A significantly higher event free survival at three years was seen in the lowest risk FactorECG group as compared to QRS$_{AREA}$ ≥ 150 µVs (6% versus 11%; *log rank p = 0.01*). Conversely, three-year event free survival for the highest risk FactorECG quartile was significantly worse than in patients with QRS$_{AREA}$ < 75 µVs (37% versus 27%; *log rank p < 0.005*).

Table 2. *Optimism corrected C-statistic for outcome and response.*

	Outcome		Response	
Predictors	**AUC**	**95% CI**	**AUC**	**95% CI**
AHA 2013 criteria	0.50	[0.47-0.53]	0.56	[0.53–0.60]
ESC 2013 criteria	0.57	[0.54-0.60]	0.61	[0.57–0.64]
QRS$_{AREA}$	0.61	[0.58-0.64]	0.70	[0.67–0.74]
FactorECG	0.69	[0.66-0.72]	0.69	[0.65–0.72]
Clinical	0.69	[0.67-0.72]	0.68	[0.64–0.72]
Clinical /FactorECG	0.72	[0.69-0.75]	0.70	[0.67–0.74]

Legend: AUC, area under the curve; AHA, American Heart Association; ESC, European Society of Cardiology; ICM, ischemic cardiomyopathy; LBBB, left bundle branch block.

Heart failure hospitalization

The HF hospitalization endpoint was available in 1081 patients (83%) and occurred in 133 (12%) of patients during a median follow-up of 3.5 years. FactorECG was significantly associated with time to first HF-hospitalization (optimism-corrected AUC = 0.70 [95% CI 0.66 – 0.73]). This was significantly better than the guideline criteria using the ESC criteria (optimism-corrected AUC = 0.57 [95% CI 0.52 – 0.62]), the AHA criteria (optimism-corrected AUC = 0.52 [95% CI 0.48 – 0.57], and QRS$_{AREA}$ (AUC = 0.65 [95% CI 0.61 – 0.69]).

Echocardiographic response

Paired echocardiograms were available in 821 patients. Long-term echocardiographic non-response was observed in 355 patients (43%). All evaluated models were significantly associated with echocardiographic non-response. However, guideline classification performed the worst, using either the ESC (AUC = 0.61 [95% CI 0.57 – 0.64]) or AHA definition (AUC = 0.56 [95% CI 0.53 – 0.60]) of LBBB-morphology. FactorECG (AUC = 0.69[95% CI 0.65 – 0.72]) and QRS$_{AREA}$ (AUC = 0.70 [95% CI 0.67 – 0.74]) had similar associations with non-response but were both significantly stronger associated with response than current guideline recommendations **(Figure 2)**. Differences in the extent of reverse remodelling, stratified according to four groups of FactorECG and QRS$_{AREA}$, was similar **(Figure 2)**.

Subgroup analysis

Performance of FactorECG and QRS$_{AREA}$ were compared, stratified by known subgroups associated with clinical outcome **(Table 3)**. The strongest association of FactorECG was observed in patients with non-ICM (AUC = 0.77 [95%CI 0.73 – 0.81]), which was significantly higher as compared to QRS$_{AREA}$ (AUC = 0.62 [95%CI 0.57 – 0.67]). Using the ESC definition of LBBB-morphology, FactorECG outperformed QRS$_{AREA}$ in patients with LBBB (AUC = 0.71 [95%CI 0.68 – 0.74] versus AUC = 0.61 [95% CI 0.58 – 0.65]), and non-LBBB (AUC= 0.66 [95% CI 0.60 – 0.71] versus AUC = 0.52 [95% CI 0.46 – 0.58]). The same
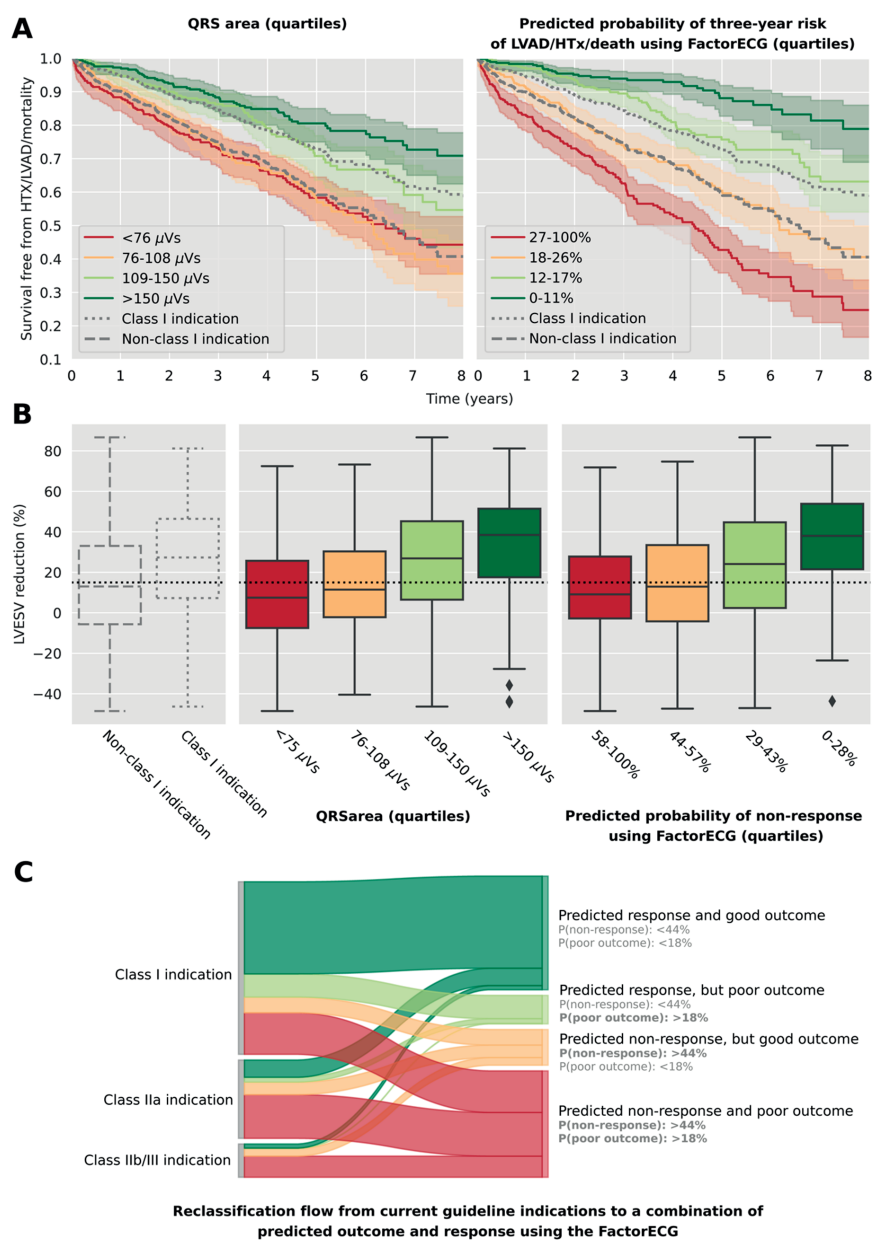
Figure 2. *Clinical utility of FactorECG and QRS_AREA in CRT. QRS_AREA and FactorECG predicted probabilities were divided into four quartiles of equal size. Quartiles of FactorECG better differentiate clinical outcome as compared to QRS_AREA and guidelines using the ESC criteria of LBBB (panel A). Similar associations with echocardiographic response were seen when compared to QRS_AREA, while still outperforming guideline criteria (panel B). Reclassification flow form the guidelines to the FactorECG predictions is shown in panel C. Here, a combination of predicted clinical outcome and response is assessed by setting the probability cut-off at 50% of the data. Probability cut-offs in panel C therefore correspond to the upper two and lower two quartiles in panels A and B combined. Legend: ECG; electrocardiogram, HTx; heart transplantation, LVAD; left ventricular assist device, LVESV; left ventricular end-systolic volume.*

observation was made when evaluating patients with an intermediate QRS-duration, below 150 ms, and patients with ICM. Importantly, FactorECG and QRS_{AREA} demonstrated comparable associations with echocardiographic response, regardless of the subgroup analysed **(Table 3)**.

Table 3. *Optimism corrected C-statistic in various subgroups.*

	Outcome (AUC [95% CI])		Response (AUC [95% CI])	
Subgroup	QRS_{AREA}	FactorECG	QRS_{AREA}	FactorECG
Male	0.60 [0.57-0.63]	0.67 [0.64-0.70]	0.69 [0.65-0.73]	0.70 [0.66-0.74]
Female	0.61 [0.53-0.69]	0.77 [0.71-0.83]	0.70 [0.63-0.77]	0.73 [0.66-0.79]
ICM	0.58 [0.54-0.62]	0.63 [0.60-0.67]	0.65 [0.59-0.70]	0.67 [0.61-0.72]
Non-ICM	0.62 [0.57-0.67]	0.77 [0.73-0.81]	0.72 [0.67-0.77]	0.74 [0.70-0.79]
LBBB*	0.61 [0.58-0.65]	0.71 [0.68-0.74]	0.71 [0.67-0.75]	0.73 [0.69-0.76]
Non-LBBB*	0.52 [0.46-0.58]	0.66 [0.60-0.71]	0.53 [0.43-0.63]	0.55 [0.46-0.65]
QRS ≥150ms	0.62 [0.58-0.66]	0.70 [0.66-0.73]	0.71 [0.67-0.75]	0.73 [0.69-0.77]
QRS <150ms	0.58 [0.53-0.63]	0.72 [0.67-0.76]	0.62 [0.55-0.70]	0.67 [0.60-0.73]

*Legend: AUC, area under the curve; ICM, ischemic cardiomyopathy; LBBB, left bundle branch block. * Morphology evaluated according to ESC 2013 criteria.*

Additional value of clinical model

Readily available patient characteristics, known to be associated with CRT outcome, were entered into a clinical model **(Supplemental Table 3 and 4)** [11]. The clinical model was significantly associated with outcome (AUC = 0.66 [95%CI 0.63 –0.69]), HF hospital-ization (AUC = 0.68 [95% CI 0.64 – 0.72] and response (AUC = 0.60 [95%CI 0.56 – 0.64]). However, for all three endpoints, Factor ECG demonstrated significantly better asso-ciations as compared to the clinical model. Moreover, addition of clinical parameters to FactorECG was of no added value for response (ΔAUC = 0.01), HF hospitalization (ΔAUC = 0.02), and clinical outcome (ΔAUC = 0.02).

Explainable deep learning through factor visualisation

ECG factors that were significantly associated with outcome and response are sum-marised in **Figure 3**. Exact hazard ratios for outcome and odds ratios for non-response are summarised in **Supplemental Table 5 and 6**, respectively. Visualisations of the most important ECG factors, using factor traversals, are shown in **Figure 4**, whereas **Supplemental Figure 1** displays complete 12-lead visualisation of all factors. Factors associated with '*both*' non-response and poor outcome were interpreted as follows: F_1 (absent QRS-notching and ST-deviation, but lateral T-wave inversion), F_9 (transition from LBBB-morphology to more right bundle branch block-morphology with smaller right precordial S-wave amplitudes), F_{10} (increased ventricular rate), and F_{19} (decreased anterior QS-amplitude and lateral notched R). Importantly, F_8 (increased PR-interval and

P-wave duration) was only associated with worse outcome, whereas F_5 (decreased QRS duration and JTc-interval) and F_{26} (decreased QRS-duration and amplitude of the LBBB-morphology) was only associated with non-response.
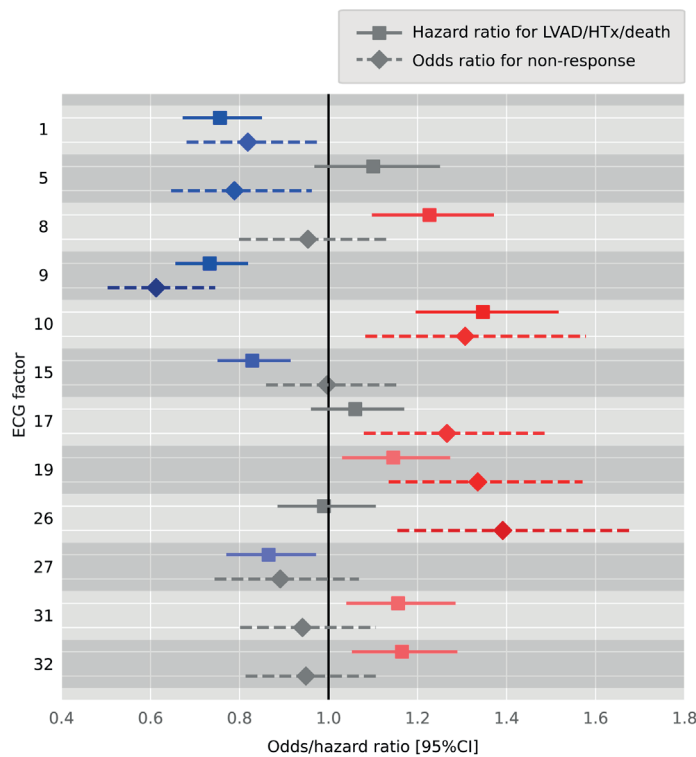
Figure 3. *Hazard and odds ratios for the models predicting either the clinical endpoint or echocardiographic non-response (LVESV reduction < 15%) using the ECG factors as the only input for the model. Colors (red and green) correspond with factor traversal reconstructions in Figure 4. All ECG factors were standardized and hazard and odds ratios can be interpreted as importance scores. Legend: ECG; electrocardiogram, HTx; heart transplantation, LVAD; left ventricular assist device, LVESV: left ventricular end-systolic volume.*

Clinical applicability using risk groups

Using a combination of predictions of the FactorECG algorithm for both echocardiographic non-response and 3-year clinical outcome, four distinct groups could be identified to assist patient selection **(Supplemental Table 7)**. Here, QRS_AREA could not differentiate between good and poor outcome in echocardiographic responders (median QRS_AREA 151 versus 152 μVs, respectively) or non-responders (median QRS_AREA 84 versus 83 μVs, respectively).

In the first group, with both predicted response and good outcome (n = 338), 76% of the patients were responders, and only 14% experienced the primary endpoint during follow-up. In the second group, patients with poor 3-year outcome, despite an

echographic response (n = 72), were more frequently male, had ICM, higher NT-proBNP, high QRS-duration, and the worst ESV and LVEF. Conversely, in the third group, CRT non-responders with good clinical outcome regardless (n = 96) were predominantly characterised by shorter QRS-duration, lowest LVESV, and highest LVEF. In the fourth group of patients, with both poor outcome and non-response, significant more ICM, NYHA III, and non-LBBB was observed as compared to the other subgroups. In this worst performing subgroup (n = 314) the primary endpoint occurred in 46% of the patients during follow-up, and response occurred in only 36% of patients. Other clinical parameters can be found in **Supplemental Table 7**.
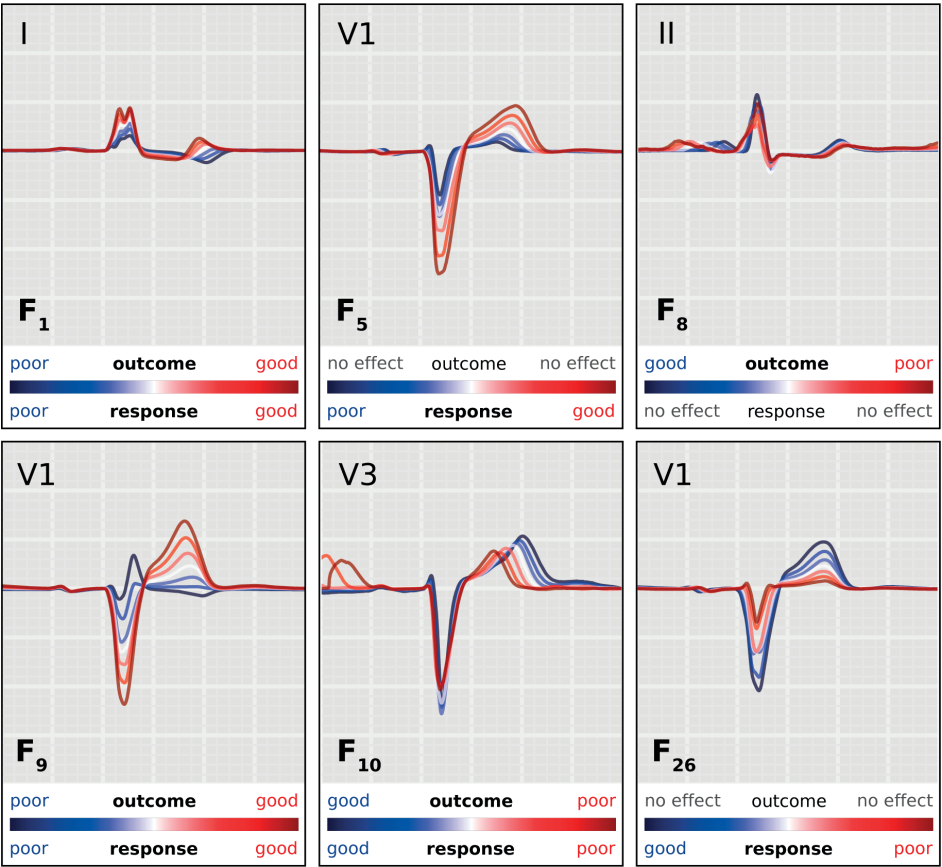
Figure 4. Factor traversals of a subset of the ECG factors associated with both, clinical outcome (composite endpoint of LVAD/HTx/death) and echocardiographic response (LVESV reduction > 15%). In each graph the corresponding factor is varied from -3 (blue) to 3 (red) standard deviations from the mean of 0 (white line), which represents a mean ECG in the CRT population. For each factor, the lead showing the most easily interpretable effect is shown in the upper left corner. Complete 12-lead ECG of all factors can be found in Supplemental Figure 1. Legend: ECG; electrocardiogram, HTx; heart transplantation, LVAD; left ventricular assist device, LVESV; left ventricular end-systolic volume.

In contrast, when using the current ESC guidelines for selection of patients eligible for CRT, in class I patients (n = 499) response occurred in 65% and the primary outcome endpoint in 26% during follow-up. In patients with class IIa (n = 226) or IIb/III (n = 96) indications, response occurred in 50% and 33%, and the primary outcome endpoint in 35% and 37%, respectively. A comparison of the classification in the four FactorECG groups and the guideline-based groups can be found in **Figure 2C**.

2
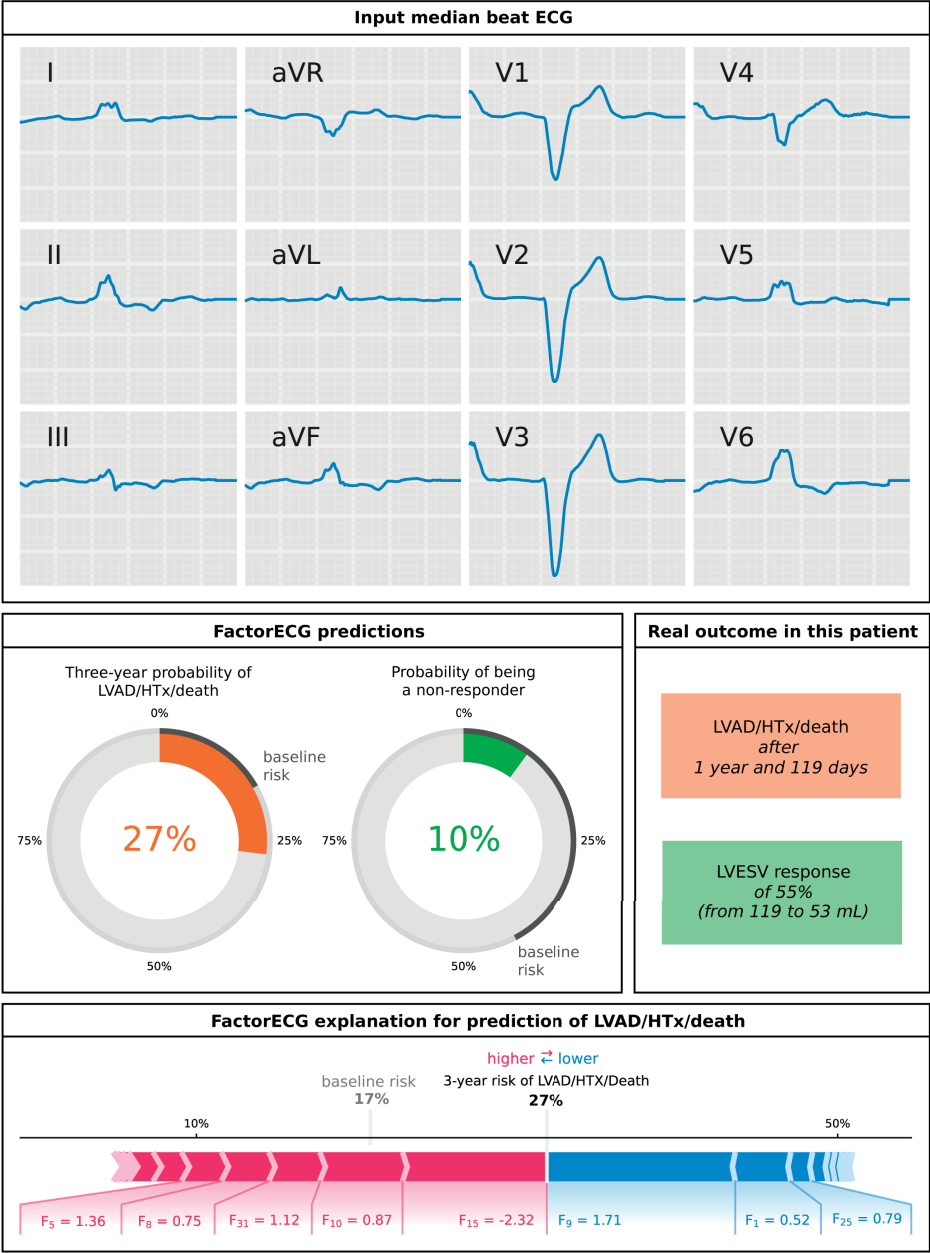
Take Home Figure. *Patient-level example of a prediction with the FactorECG explanation. A standard 12-lead ECG is entered into a deep learning model, which automatically translates this ECG into its FactorECG containing all distinct features. These factors are entered into the Cox and logistic regression models and predicted probabilities for both LVAD/HTx/death and non-response are shown to the user. This patient responded well to CRT, but died within three years regardless. The FactorECG explanations shows that this prediction of high probability of LVAD/HTx/death is driven by factors 15, 10, 31, 8 and 5. These factors represent an increased ventricular frequency in combination with long PR-interval with broad P-wave and lower than average QRS amplitudes. Legend: ECG; electrocardiogram, HTx; heart transplantation, LVAD; left ventricular assist device, LVESV: left ventricular end-systolic volume.*

DISCUSSION

In this large, multicentre, real-world dataset, an explainable deep learning-based algorithm (the FactorECG) was predictive for long-term clinical outcome and echocardiographic response after CRT implantation. FactorECG outperformed contemporary guideline criteria and vectorcardiographic QRS_{AREA} for clinical outcome. Importantly, only a readily available 12-lead ECG is required, since no significant added value was obtained using additional clinical input variables. The user-independent analysis and automated visualization of key ECG features allows for patient-specific interpretation of the algorithm **(Take Home Figure)**, which may facilitate its adoption into clinic practice as a valuable alternative for the selection of CRT candidates. Lastly, an online visualisation tool was created to provide interactive visualizations (https://crt.ecgx.ai).

Deep learning-based prediction of outcome

For the first time, deep learning has been used to predict clinical outcome after CRT using only the raw preprocedural ECG (AUC = 0.69 [96% CI 0.66-0.72]). In contrast, previous studies aimed to predict CRT outcome using machine learning to unify a vast number of clinical variables in a single model. The SEMMELWEIS-CRT score combined 33 clinical variables for the prediction of all-cause mortality, reporting a mean internally calculated AUC of 0.69, derived from 1510 patients in a single centre [11]. Similarly, two other studies combined a plethora of pre-implantation characteristics, including ECG and echocardiography data [12,13]. Kalscheur et al. created a random forest model with 45 variables, and obtained an AUC of 0.74 (95% CI 0.72–0.76) for the 12-month prediction of death or HF hospitalization [13]. Cikes et al. even incorporated 77 variables, including more complex echocardiographic parameters such as strain, septal flash, and right ventricular fractional area change [12]. Their clinical model identified two phenogroups with an HR of 0.35-0.36 for event-free survival, when comparing CRT-D to ICD-only. One study compared an unsupervised principal component analysis model with QRS_{AREA} [19]. Here, similar results for QRS_{AREA} (HR = 0.46 [95% CI 0.39–0.55]) and their model (HR = 0.45 [95% CI 0.38–0.53]) were seen for the composite endpoints of death, LVAD, or HTx.

Differences in primary clinical endpoints in the aforementioned studies complicate a direct comparison with the present study. However, similar or better performance was observed with respect to predicting clinical outcomes [11,13]. Moreover, our approach outperformed QRS_{AREA} with respect to clinical outcome, whereas unsupervised machine learning of baseline QRS-waveforms previously failed to do so [19]. Most importantly, all previously proposed models require collection and calculation of many clinical variables, which are highly operator dependent, cumbersome, and likely to dissuade clinicians to rapidly adopt such an approach [11–13]. In contrast, our proposed approach requires only a standard 12-lead ECG, without the need for additional clinical input variables, or manual

2

selection of the QRS-complex. For research purposes, an online tool has been developed where the ECG can be uploaded, and predictions for CRT outcome can be made (https://crt.ecgx.ai).

Echocardiographic response

In our study, a head-to-head comparison of FactorECG and QRS_{AREA} provided similar results for the prediction of echocardiographic response (AUC = 0.69 and 0.70, respectively). Adding up to 13 clinical variables did not increase performance of either model in our study. However, next to identifying the electrical substrate on the ECG, characterisation of the extent of mechanical impairment is of importance as well, especially in patients with ICM. In fact, adding parameters of mechanical dyssynchrony to QRS_{AREA} improves prediction of 6-month response (AUC = 0.76), and is therefore also likely of added value to FactorECG [4]. Simple multivariate logistic regression models, consisting of only four variables, have also shown to be associated with sustained echocardiographic response (AUC = 0.774), a surrogate marker of stable disease remission [4].

Identifying ECG features beyond the QRS-complex

Our results confirm the known importance of LBBB-morphology and QRS_{AREA} for the prediction of echocardiographic response [4,10]. Using FactorECG, all types of LV conduction delay, as reflected in the QRS-complex, can be represented by combining ECG Factors 5, 9, 19, and 27. Interestingly, although QRS_{AREA} was associated with outcome, ECG factors that incorporate QRS-duration were not associated with outcome **(Figure 4)**. These findings are somewhat in conflict with a meta-analysis in 5813 patients, which showed no benefit of CRT in reducing adverse clinical events in patients with a moderate QRS-duration, below 150 ms [6]. However, in the presence of sufficient electrical substrate, a subset of patients with moderate QRS-prolongation is still likely to respond [3]. This is also underscored by our results, since FactorECG also predicted outcome in patients with QRS-duration < 150 ms (AUC = 0.72). Likewise, when corrected for various other ECG features, no significant association with QRS-duration and outcome remains, as also reported previously [20].

Visualisation of ECG factors identified various other ECG characteristics known to be to be associated with outcome and/or response. One of these factors was the identification of a prolonged PR-interval (F_8), for instance. This factor may be of special relevance, since a first-degree atrioventricular block is frequently observed in patients with HF, but can be corrected by CRT. In fact, it has recently been shown that correction of atrioventricular dromotropathy increases LV filling and LV pump function, which may explain the increased risk of poor outcome in the present study [21]. In addition, the QRS-T angle [22], JTc-interval [23], and T-wave area [24] have been raised as potentially important de-

terminants of response or outcome. However, various other subtle markers of ischemia, dyssynchrony, or risk of arrhythmia may be represented by FactorECG.

Indeed, when evaluated by itself, a large number of other factors can be identified from the ECG [7]. Unfortunately, accurately identifying these factors, and interpreting their interrelated meaning, is highly complex. In the first place because there is lack of consensus [7] and inter-observer disagreement [8] as to what truly defines LBBB-morphology. Matters are further complicated when septal and LV activation patterns are concealed, or wrongly mimicked [9]. Lastly, various unknown ECG-criteria may have remained undetected. Interpretation of the LBBB ECG is therefore complex and misleading. In this regard, FactorECG allows for a unified and agnostic approach, is user-independent, and inherently explainable**.**

Clinical implications

The FactorECG algorithm can be used in every patient that is considered for CRT. When provided with the baseline ECG, the patient-specific ECG-factors that are associated with response and outcome are identified and combined into an individual risk score, and a patient-specific visualisation of these factors is given **(Take Home Figure)**. While similar in size, the CRT non-response *and* poor outcome subgroup, as predicted by the FactorECG, performed worse than patients without a class-I indication for CRT according to the ESC guideline criteria. Importantly, 39% of patients in this worst performing subgroup had a class I indication **(Figure 2C)**. FactorECG therefore enables better classification of eligibility, without compromising the total proportion of patients deemed suitable for CRT implantation.

Future perspectives

Our self-contained ECG-based model was especially effective in the non-ICM population, but additional clinical variables are required to improve performance in patients with ICM. Likely, information about mechanical dyssynchrony is of importance in these patients [4]. In addition, optimal placement of the LV lead is of importance to enhance response in CRT patients. This is particularly important in patients with scar, but also in patients with heterogenous LV electrical activation [9]. In the future, FactorECG may use ECG-derived data to identify the site of latest electrical activation, thereby guiding LV lead implantation [9]. Lastly, prospective studies with FactorECG are warranted to acquire CE certification, allowing its use as a medical device.

Strengths and limitations

Our data was derived from a large multicentre database, and thereby represents a real-world population. Internal validation by means of bootstrapping was performed, which allows for unbiased validation in the complete dataset, and is therefore considered the

2

recommended approach for validation of any prediction model [25]. As a result, performance was not assessed in a single train-test split, because this approach only validates an example model in an arbitrarily chosen and small data subset and produces a poorer model by default [25]. Moreover, by using regular prediction models (i.e. logistic regression and Cox regression) with a limited number of predicting variables as input (only the 21 factors), the risk of overfitting is low.

Many clinicians regard deep learning as a 'black box', which limits trust in such algorithms [15]. However, our approach to make the model inherently explainable may abate this concern, and increase willingness to facilitate clinical adoption of the FactorECG. Furthermore, addition of a few important clinical values might further increase the predictive value of FactorECG. Especially use of strain parameters have shown to be highly predictive, also in addition to QRS_{AREA} [4], or when used in machine-learning models [12]. As a result, no direct comparison with pre-existing scores could be performed [11]. Conversely, our approach only requires a standard 12 lead ECG, and no advanced and highly user dependent measurements are needed.

Conclusions

The FactorECG, an inherently explainable and end-to-end automated deep learning model, can accurately predict both echocardiographic response and long-term clinical outcome in patients eligible for CRT. Moreover, it outperformed contemporary guideline ECG-criteria and QRS_{AREA} with superior discriminative ability, particularly in non-ICM patients. This approach is based solely on a standard 12-lead ECG, requires no additional clinical parameters, and visualises patient-specific key features associated with outcome and response. Besides QRS-morphology, T-wave amplitude and inversion, ventricular rate, and PR-interval and P-wave duration were identified as important ECG factors. The FactorECG thereby facilitates personalised decision making in CRT, while being easy-to-use, allowing rapid uptake for everyday clinical practice.

REFERENCES

1. K. Vernooy, C. J. M. Van Deursen, M. Strik, F. W. Prinzen. Strategies to improve cardiac resynchronization therapy. *Nat. Rev. Cardiol.* **11**, 481–493 (2014).

2. M. R. Gold, J. Rickard, J. C. Daubert, P. Zimmerman, C. Linde. Redefining the Classifications of Response to Cardiac Resynchronization Therapy: Results From the REVERSE Study. *JACC Clin. Electrophysiol.* **7**, 871–880 (2021).

3. M. Glikson, J. C. Nielsen, M. B. Kronborg, *et al.* 2021 ESC Guidelines on cardiac pacing and cardiac resynchronization therapy: Developed by the Task Force on cardiac pacing and cardiac resynchronization therapy of the European Society of Cardiology (ESC) With the special contribution of the European Hear. *Eur. Heart J.* (2021), doi:10.1093/eurheartj/ehab364.

4. P. C. Wouters, W. M. van Everdingen, K. Vernooy, *et al.* Does mechanical dyssynchrony in addition to QRS area ensure sustained response to cardiac resynchronization therapy? *Eur. Hear. journal. Cardiovasc. Imaging* (2021), doi:10.1093/ehjci/jeab264.

5. O. A. E. Salden, K. Vernooy, A. M. W. van Stipdonk, *et al. JACC Clin. Electrophysiol.*, in press, doi:10.1016/j.jacep.2019.11.018.

6. I. Sipahi, T. P. Carrigan, D. Y. Rowland, B. S. Stambler, J. C. Fang. Impact of QRS Duration on Clinical Event Reduction With Cardiac Resynchronization Therapy: Meta-analysis of Randomized Controlled Trials. *Arch. Intern. Med.* **171**, 1454–1462 (2011).

7. A. M. W. van Stipdonk, R. Hoogland, I. ter Horst, *et al.* Evaluating Electrocardiography-Based Identification of Cardiac Resynchronization Therapy Responders Beyond Current Left Bundle Branch Block Definitions. *JACC Clin. Electrophysiol.* **6**, 193–203 (2020).

8. A. M. W. van Stipdonk, S. Vanbelle, I. A. H. Ter Horst, *et al.* Large variability in clinical judgement and definitions of left bundle branch block to identify candidates for cardiac resynchronisation therapy. *Int. J. Cardiol.* **286**, 61–65 (2019).

9. P. C. Wouters, K. Vernooy, M. J. Cramer, F. W. Prinzen, M. Meine. Optimizing lead placement for pacing in dyssynchronous heart failure: The patient in the lead. *Hear. Rhythm.* **18**, 1024–1032 (2021).

10. M. A. Ghossein, A. M. W. van Stipdonk, F. Plesinger, *et al.* Reduction in the QRS area after cardiac resynchronization therapy is associated with survival and echocardiographic response. *J. Cardiovasc. Electrophysiol.* **32**, 813–822 (2021).

11. M. Tokodi, W. R. Schwertner, A. Kovács, *et al.* Machine learning-based mortality prediction of patients undergoing cardiac resynchronization therapy: the SEMMELWEIS-CRT score. *Eur. Heart J.* **41**, 1747–1756 (2020).

12. M. Cikes, S. Sanchez-Martinez, B. Claggett, *et al.* Machine learning-based phenogrouping in heart failure to identify responders to cardiac resynchronization therapy. *Eur. J. Heart Fail.* **21**, 74–85 (2019).

13. M. M. Kalscheur, R. T. Kipp, M. C. Tattersall, *et al.* Machine Learning Algorithm Predicts Cardiac Resynchronization Therapy Outcomes. *Circ. Arrhythmia Electrophysiol.* **11**, e005499 (2018).

14. R. R. van de Leur, M. J. Boonstra, A. Bagheri, *et al.* Big Data and Artificial Intelligence: Opportunities and Threats in Electrophysiology. *Arrhythmia Electrophysiol. Rev.* **9**, 146–154 (2020).

15. R. R. van de Leur, M. N. Bos, K. Taha, *et al. medRxiv*, in press, doi:10.1101/2022.01.04.22268759.

16. GE Healthcare. Marquette 12SL ECG Analysis Program Physician's Guide. 2012. Chicago, United States: Accessed April 30, 2020. https://www.gehealthcare.com/products/diagnostic-cardiology/marquette-12sl. (available at https://www.gehealthcare.com/products/diagnostic-cardiology/marquette-12sl).

2

17. J. A. Kors, G. van Herpen, A. C. Sittig, J. H. van Bemmel. Reconstruction of the Frank vectorcardio-gram from standard electrocardiographic leads: diagnostic comparison of different methods. *Eur. Heart J.* **11**, 1083–1092 (1990).

18. G. S. Collins, J. B. Reitsma, D. G. Altman, K. G. M. Moons. Transparent Reporting of a multivariable prediction model for Individual Prognosis Or Diagnosis (TRIPOD): the TRIPOD Statement. *Br. J. Surg.* **102**, 148–158 (2015).

19. A. K. Feeny, J. Rickard, K. M. Trulock, *et al.* Machine Learning of 12-Lead QRS Waveforms to Identify Cardiac Resynchronization Therapy Patients With Differential Outcomes. *Circ. Arrhythm. Electro-physiol.* **13**, e008210 (2020).

20. M. J. H. Khidir, V. Delgado, N. Ajmone Marsan, M. J. Schalij, J. J. Bax. QRS duration versus morphol-ogy and survival after cardiac resynchronization therapy. *ESC Hear. Fail.* **4**, 23–30 (2017).

21. F. C. W. M. Salden, P. R. Huntjens, R. Schreurs, *et al.* Pacing therapy for atrioventricular dromotropa-thy: a combined computational-experimental-clinical study. *Eur. Eur. pacing, arrhythmias, Card. Electrophysiol. J. Work. groups Card. pacing, arrhythmias, Card. Cell. Electrophysiol. Eur. Soc. Cardiol.* (2021), doi:10.1093/europace/euab248.

22. R. Sweda, Z. Sabti, I. Strebel, *et al.* Diagnostic and prognostic values of the QRS-T angle in patients with suspected acute decompensated heart failure. *ESC Hear. Fail.* **7**, 1817–1829 (2020).

23. A. H. Maass, K. Vernooy, S. C. Wijers, *et al.* Refining success of cardiac resynchronization therapy using a simple score predicting the amount of reverse ventricular remodelling: results from the Markers and Response to CRT (MARC) study. *Europace.* **20** (2018). pp. e1–e10.

24. E. B. Engels, E. M. Végh, C. J. M. van Deursen, *et al.* T-Wave Area Predicts Response to Cardiac Resynchronization Therapy in Patients with Left Bundle Branch Block. *J. Cardiovasc. Electrophysiol.* **26**, 176–183 (2015).

25. E. W. Steyerberg, F. E. J. Harrell. Prediction models need appropriate internal, internal-external, and external validation. *J. Clin. Epidemiol.* **69**, 245–247 (2016).

SUPPLEMENTARY MATERIAL

Supplemental Table 1. *Akaike's Information Criterion and calibration slope for outcome.*

Predictors	C-statistic	C-statistic, corrected	AIC	Calibration slope
AHA 2013 criteria	0.51 [0.49-0.54]	0.50 [0.47-0.53]	5067	0.47
ESC 2013 criteria	0.57 [0.54-0.60]	0.57 [0.54-0.60]	5041	1.07
QRS$_{AREA}$	0.61 [0.58-0.64]	0.61 [0.58-0.64]	5023	1.07
FactorECG	0.71 [0.68-0.73]	0.69 [0.66-0.72]	4927	0.89
Clinical	0.70 [0.67-0.73]	0.69 [0.67-0.72]	4987	0.92
Clinical / FactorECG	0.75 [0.72-0.77]	0.72 [0.69-0.75]	4835	0.86

The apparent c-statistic was obtained by applying the model on the original data, while internal validation was performed to obtain the optimism corrected c-statistic and calibration slope. Legend: AHA, American Heart Association; AIC, Akaike's Information Criterion; ESC, European Society of Cardiology.

Supplemental Table 2. *Akaike's Information Criterion and calibration slope for response.*

Predictors	C-statistic	C-statistic, corrected	AIC	Calibration slope
AHA 2013 criteria	0.57 [0.54 – 0.60]	0.56 [0.53 – 0.60]	1112	0.93
ESC 2013 criteria	0.61 [0.57 – 0.64]	0.61 [0.57 – 0.64]	1090	0.95
QRS$_{AREA}$	0.70 [0.67 – 0.74]	0.70 [0.67 – 0.74]	1018	0.99
FactorECG	0.72 [0.68 – 0.76]	0.69 [0.65 – 0.72]	1043	0.81
Clinical	0.70 [0.67 – 0.74]	0.68 [0.64 – 0.72]	1062	0.82
Clinical / FactorECG	0.75 [0.72 – 0.78]	0.70 [0.67 – 0.74]	1036	0.74

The apparent c-statistic was obtained by applying the model on the original data, while internal validation was performed to obtain the optimism corrected c-statistic. Legend: AHA, American Heart Association; AIC, Akaike's Information Criterion; ESC, European Society of Cardiology.

Supplemental Table 3. *Clinical model for outcome.*

	Covariate	Coefficient	Hazard Ratio	95% CI	p-value
1	Age	0.01	1.01	[1.00-1.02]	0.112
2	ICM	-0.04	0.96	[0.77-1.21]	0.753
3	DM	0.16	1.17	[0.92-1.48]	0.194
4	LVEDV	0.0	1.00	[1.00-1.00]	0.013
5	LVEF	-0.0	1.00	[0.98-1.02]	0.769
6	Female	-0.39	0.68	[0.50-0.91]	0.010
7	Haemoglobin	0.07	1.08	[0.98-1.18]	0.114
8	IVMD	-0.01	0.99	[0.99-1.00]	0.001
9	Creatinine	0.01	1.01	[1.00-1.01]	<0.001
10	Length	0.0	1.00	[1.00-1.00]	0.057
11	NYHA II	0.87	2.39	[0.75-7.58]	0.139
	NYHA III	1.51	4.52	[1.44-14.18]	0.010
	NYHA IV	1.88	6.53	[1.98-21.52]	0.002
12	Sinus rhythm	-0.45	0.64	[0.49-0.83]	0.001
13	Weight	-0.01	0.99	[0.98-1.00]	0.002

Legend: DM, diabetes mellitus; ICM, ischemic cardiomyopathy; IVMD, interventricular mechanical delay; LVEDV, left ventricular end diastolic volume; LVEF, left ventricular ejection fraction; NYHA, New York Heart Association

Supplemental Table 4. *Clinical model for response.*

	index	Coefficient	Odds Ratio	95% CI	p-value
0	Intercept	-2.62	0.07	[0.00-1.25]	0.071
1	Age	-0.0	1.00	[0.98-1.01]	0.842
2	Weight	0.01	1.01	[1.00-1.02]	0.229
3	Length	0.0	1.00	[1.00-1.00]	0.054
4	LVEF	0.02	1.02	[1.00-1.04]	0.085
5	Haemoglobin	0.16	1.17	[1.02-1.36]	0.028
6	LVEDV	0.0	1.00	[1.00-1.00]	0.887
7	IVMD	-0.02	0.99	[0.98-0.99]	<0.001
8	Sinus rhythm	-0.69	0.50	[0.33-0.76]	0.001
9	Creatinine	0.0	1.00	[1.00-1.01]	0.014
10	Female	-0.03	0.97	[0.66-1.44]	0.883
11	ICM	0.32	1.37	[0.99-1.91]	0.060
12	NYHA II	0.46	1.59	[0.66-3.84]	0.302
	NYHA III	0.75	2.12	[0.87-5.13]	0.097
	NYHA IV	1.01	2.74	[0.88-8.54]	0.082
13	DM	-0.1	0.90	[0.63-1.29]	0.577

Legend: DM, diabetes mellitus; ICM, ischemic cardiomyopathy; IVMD, interventricular mechanical delay; LVEDV, left ventricular end diastolic volume; LVEF, left ventricular ejection fraction; NYHA, New York Heart Association

Supplemental Table 5. *Hazard ratios for individual ECG Factors and outcome.*

FactorECG Covariate	Coefficient	Hazard Ratio	95% CI	p-value
1	-0.28	0.76	[0.67-0.85]	<0.001
5	0.10	1.10	[0.97-1.25]	0.143
6	-0.00	1.00	[0.90-1.10]	0.937
8	0.20	1.23	[1.10-1.37]	<0.001
9	-0.31	0.73	[0.66-0.82]	<0.001
10	0.30	1.35	[1.20-1.52]	<0.001
11	0.01	1.01	[0.91-1.12]	0.822
12	-0.04	0.96	[0.87-1.07]	0.486
13	-0.09	0.91	[0.82-1.01]	0.079
15	-0.19	0.83	[0.75-0.91]	<0.001
16	0.05	1.05	[0.94-1.18]	0.343
17	0.06	1.06	[0.96-1.17]	0.246
19	0.14	1.15	[1.03-1.27]	0.012
22	-0.03	0.97	[0.87-1.07]	0.519
23	0.10	1.10	[0.99-1.22]	0.063
25	-0.07	0.93	[0.83-1.05]	0.244
26	-0.01	0.99	[0.89-1.11]	0.854
27	-0.14	0.87	[0.77-0.97]	0.015
30	-0.10	0.90	[0.81-1.00]	0.052
31	0.15	1.16	[1.04-1.29]	0.007
32	0.15	1.17	[1.05-1.29]	0.003

Legend: CI, confidence interval.

Supplemental Table 6. *Odds ratios for individual ECG Factors and non-response.*

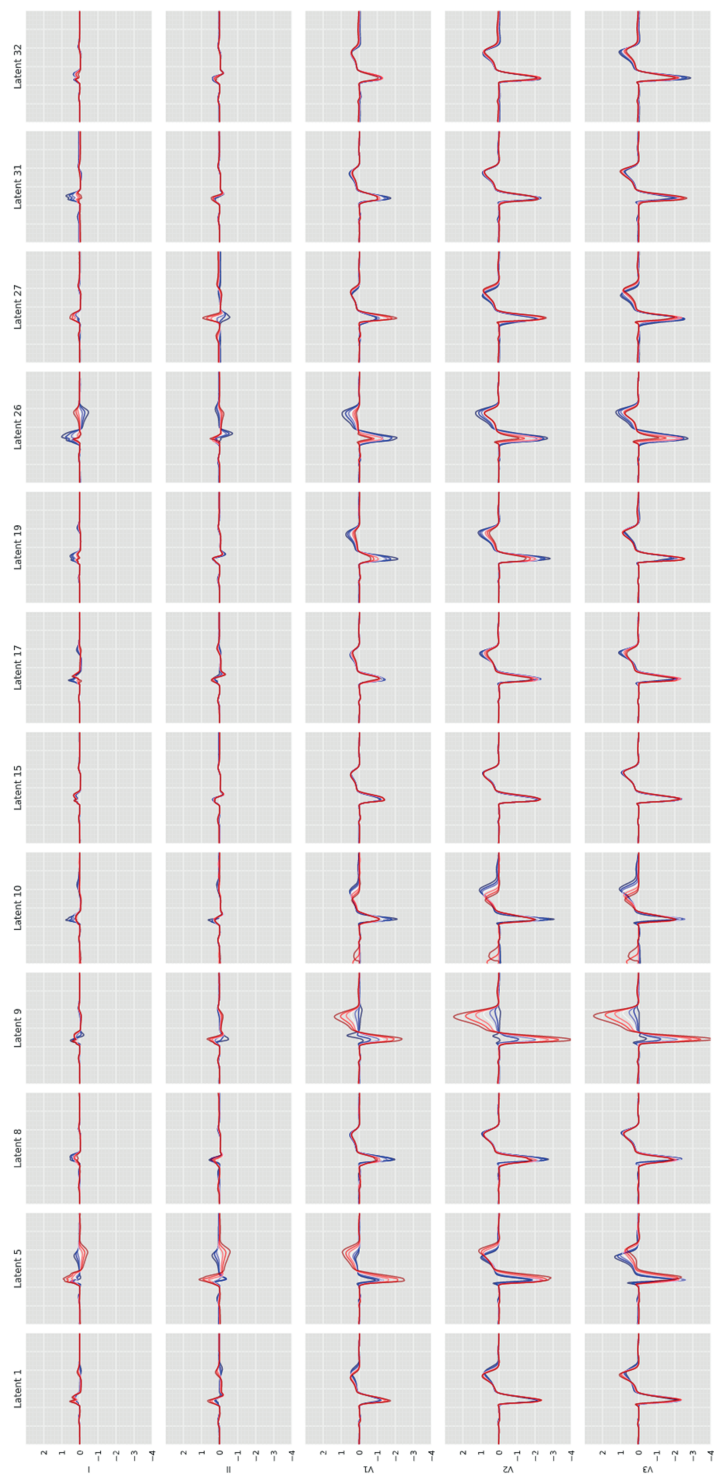| Response				
index	**Coefficient**	**Odds Ratio**	**95% CI**	**p-value**
Intercept	-0.22	0.80	[0.69-0.93]	0.004
1	-0.20	0.82	[0.68-0.98]	0.033
5	-0.24	0.79	[0.65-0.96]	0.019
6	0.01	1.01	[0.87-1.19]	0.865
8	-0.05	0.95	[0.80-1.14]	0.601
9	-0.49	0.61	[0.50-0.75]	<0.001
10	0.27	1.31	[1.08-1.58]	0.005
11	0.10	1.10	[0.94-1.30]	0.240
12	-0.16	0.85	[0.72-1.02]	0.078
13	-0.03	0.97	[0.81-1.15]	0.692
15	-0.00	1.00	[0.86-1.16]	0.964
16	0.08	1.08	[0.92-1.28]	0.334
17	0.24	1.27	[1.08-1.49]	0.004
19	0.29	1.34	[1.14-1.57]	<0.001
22	-0.04	0.96	[0.82-1.12]	0.585
23	0.08	1.09	[0.93-1.28]	0.304
25	0.14	1.15	[0.95-1.40]	0.159
26	0.33	1.39	[1.15-1.68]	<0.001
27	-0.11	0.89	[0.74-1.07]	0.213
30	0.06	1.06	[0.90-1.26]	0.489
31	-0.06	0.94	[0.80-1.11]	0.462
32	-0.05	0.95	[0.81-1.11]	0.507

Legend: CI, confidence interval.

Supplemental Table 7. *Patient characteristics, stratified according to four quartiles as predicted by FactorECG.*

Variable	Overall (n=821)	NR+PO+ (n=314)	NR+PO- (n=96)	NR-PO+ (n=72)	NR-PO- (n=338)
Age (years)	67.0 [59.3-74.0]	69.0 [62.0-75.0]	65.8 [56.8-74.0]	68.3 [61.0-77.0]	64.3 [58.0-72.8] †
Male – n (%)	567 (69.1)	248 (79.0)	63 (65.6)	49 (68.1)	206 (60.9) *
ICM – n (%)	388 (47.3)	188 (59.9)	49 (51.0)	31 (43.1)	119 (35.2) *
DM – n (%)	186 (22.7)	72 (22.9)	22 (22.9)	19 (26.4)	73 (21.7)
NYHA – n (%)					†
I	17 (2.1)	4 (1.3)	1 (1.1)	0 (0)	12 (3.6)
II	316 (39.1)	94 (30.3)	47 (49.5)	25 (35.7)	150 (45.2)
III	443 (54.8)	196 (63.2)	44 (46.3)	39 (55.7)	164 (49.4)
IV	32 (4.0)	16 (5.2)	3 (3.2)	6 (8.6)	6 (1.8)
ICD – n (%)	773 (94.2)	297 (94.6)	89 (92.7)	71 (98.6)	315 (93.2)
NT-proBNP (pmol/L)	1353 [560-2856]	2103 [1032-3875]	797 [323-1800]	2531 [938-5456]	881 [409-1879] *
LBBB (ESC 2013) – n (%)	670 (81.6)	208 (66.2)	78 (81.2)	67 (93.1)	317 (93.8) *
LBBB (AHA) – n (%)	112 (13.7)	39 (12.4)	10 (10.4)	15 (21.1)	48 (14.2)
QRS$_{AREA}$ (µVs)	115.0 [80.1-156.4]	82.4 [62.7-105.4]	84.4 [68.2-110.1]	151.6 [115.6-184.9]	151.2 [119.9-183.2] *
PR (ms)	182.0 [162.0-206.5]	204.0 [174.0-236.0]	174.0 [160.0-192.0]	186.0 [166.0-209.0]	174.0 [158.0-192.0] *
QRSd (ms)	160.0 [146.0-174.0]	154.0 [142.0-170.0]	148.0 [133.5-154.0]	170.0 [158.0-188.0]	165.0 [154.0-178.0] *
QTc (ms)	484.0 [462.0-508.0]	478.0 [453.2-506.0]	464.5 [432.8-486.0]	518.5 [491.0-541.0]	488.5 [470.0-508.0] *
LVEDV (ml)	206.0 [158.0-271.0]	214.0 [169.0-275.0]	185.0 [138.5-260.5]	249.5 [187.2-309.5]	193.0 [155.3-262.2] †
LVESV (ml)	152.0 [114.0-209.0]	164.2 [122.4-206.0]	130.7 [97.8-196.2]	199.3 [136.0-241.2]	143.5 [108.9-204.4] *
LVEF (ml)	24.0 [19.0-30.0]	23.0 [18.0-28.8]	27.8 [21.0-34.7]	20.0 [15.2-25.0]	25.0 [19.7-31.6] *
ESC indication – n (%)					*
Class I	499 (60.8)	121 (38.5)	40 (41.7)	60 (83.3)	278 (82.2)
Class IIa	226 (27.5)	130 (41.4)	34 (35.4)	10 (13.9)	52 (15.4)
Class IIb/III	96 (11.7)	63 (20.1)	22 (22.9)	2 (2.8)	8 (2.4)
Primary endpoint – n (%)	243 (29.6)	143 (45.5)	18 (18.8)	35 (48.6)	47 (13.9)*
LVESV reduction (%)	19.4±31.0	6.1±32.2	15.7±27.3	24.0±26.3	31.8±26.4*
LVESV non-response – n (%)	355 (43.2)	199 (63.4)	46 (47.9)	24 (33.3)	86 (25.4)*

*Legend: DM, diabetes mellitus; ICD, implantable cardioverter defibrillator; ICM, ischemic cardiomyopathy; LVEDV, left ventricular end diastolic volume; LVEF, left ventricular ejection fraction; LVESV, left ventricular end systolic volume; NT-proBNP, N-terminal pro-B-type natriuretic peptide; NR: non-responder, NYHA, New York Heart Association, PO: poor outcome. * p < 0.001; † p < 0.005.*

2

Supplemental Figure 1. *Complete 12-lead visualization of all ECG factors. In each graph the corresponding factor is varied from -3 (blue) to 3 (red) standard deviations from the mean of 0 (white line), which represents a mean ECG in the CRT population.*
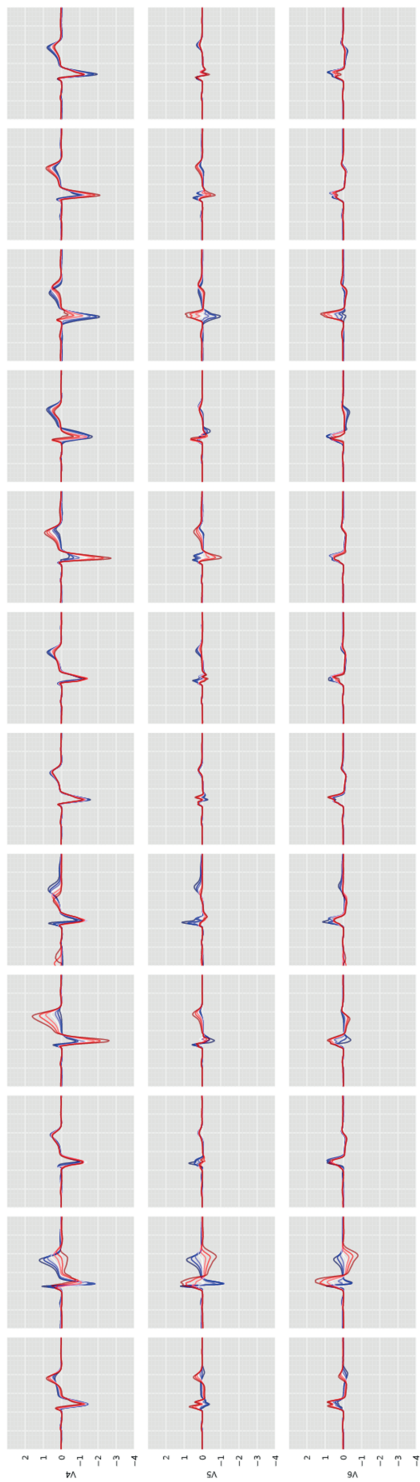
Supplemental Figure 1. Complete 12-lead visualization of all ECG factors (continued). In each individual graph, the corresponding factor is varied from −3 (blue) to 3 (red) standard deviations from the mean of 0 (white line), which represents a mean ECG in the CRT population.

3

Acute Recoordination Rather Than Functional Hemodynamic Improvement Determines Reverse Remodelling by Cardiac Resynchronisation Therapy

Philippe C. Wouters[*], Geert E. Leenders[*], Maarten J. Cramer, Mathias Meine, Frits W. Prinzen, Pieter A. Doevendans, Bart W.L. De Boeck

* First two authors contributed equally

ABSTRACT

Purpose: Cardiac resynchronisation therapy (CRT) improves left ventricular (LV) function acutely, with further improvements and reverse remodelling during chronic CRT. The current study investigated the relation between acute improvement of LV systolic function, acute mechanical recoordination, and long-term reverse remodelling after CRT.

Methods: In 35 patients, LV speckle tracking longitudinal strain, LV volumes & ejection fraction (LVEF) were assessed by echocardiography before, acutely within three days, and six months after CRT. A subgroup of 25 patients underwent invasive assessment of the maximal rate of LV pressure rise (dP/dt_{max},) during CRT-implantation. The acute change in dP/dt_{max}, LVEF, systolic discoordination (internal stretch fraction [ISF] and LV systolic rebound stretch [SRSlv]) and systolic dyssynchrony (standard deviation of peak strain times [2DS-SD18]) was studied, and their association with long-term reverse remodelling were determined.

Results: CRT induced acute and ongoing recoordination (ISF from 45±18 to 27±11 and 23±12%, p<0.001; SRS from 2.27±1.33 to 0.74±0.50 and 0.71±0.43%, p<0.001) and improved LV function (dP/dt_{max} 668±185 vs. 817±198 mmHg/s, p<0.001; stroke volume 46±15 vs. 54±20 and 52±16ml; LVEF 19±7 vs. 23±8 and 27±10%, p<0.001). Acute recoordination related to reverse remodelling (r=0.601 and r=0.765 for ISF & SRSlv, respectively, p<0.001). Acute functional improvements of LV systolic function however, neither related to reverse remodelling nor to the extent of acute recoordination.

Conclusion: Long-term reverse remodelling after CRT is likely determined by (acute) recoordination rather than by acute hemodynamic improvements. Discoordination may therefore be a more important CRT-substrate that can be assessed and acutely restored.

INTRODUCTION

Previous studies have demonstrated that the clinical benefits of cardiac resynchronization therapy (CRT) are accompanied by improvements of left ventricular (LV) function and reverse remodelling [1]. Based on the assumption that acute improvements in hemodynamic parameters both reflect effective resynchronisation and convey longer-term beneficial effects of CRT, acute increases in stroke volume and maximum rate of LV pressure rise (dP/dt_{max}) have been applied to assess CRT-response since the very beginning of CRT development [2–6]. Invasive dP/dt_{max} has been used to quantify acute de- and resynchronisation effects in animal studies [7], to guide LV placement [8,9], and to optimize atrioventricular and interventricular delay in the setting of clinical research [5,10,11]. On the contrary, measures of baseline mechanical dyssynchrony (i.e. temporal dispersion in myocardial shortening) and discoordination (i.e. reciprocal shortening and stretching) have been shown to identify the mechanical substrate of CRT and relate to longer-term benefits, but acute effects and response mechanisms have little been studied [12,13]. Moreover, a direct comparison of these two approaches has not been performed yet.

A considerable part of the remodelling processes involved in CRT appears to be linked to local mechanics [14–16]. This comparative study therefore set out on the hypothesis that long-term improvement of LV function (i.e. ejection fraction) and reverse remodelling after CRT is determined by acute recoordination of LV contraction, rather than by a functional response characterised by acute hemodynamic improvements.

METHODS

Study population and study protocol

A total of 35 patients with good echocardiographic image quality who underwent CRT implantation were prospectively included in the present study. All patients had severe symptomatic heart failure (New York Heart Association class [NYHA]) II-IV, LV ejection fraction (LVEF) <35%) despite optimal medical therapy and had a QRS-width ≥120ms with an LBBB-morphology. Transthoracic echocardiography was performed in each patient before, within 3 days after, and six months after CRT implantation. In a subgroup of 25 patients, device settings were optimized by maximizing the invasively determined maximal rate of LV pressure rise (dP/dt_{max}) during the implantation procedure [17]. In the remaining 10 patients, algorithms based on the intracardiac electrogram implemented in the devices were used for device optimization [18]. Echocardiographic response to CRT was assessed by the reduction in LV end-systolic volume, with responders defined as patients with >15% reduction at six months ("long-term") follow-up [19].

Echocardiographic and strain imaging protocol

Echocardiography was performed on a Vivid 7 ultrasound machine (General Electric, Milwaukee, USA) using a M3S transducer. A minimum of 3 loops were acquired at breath hold and analyzed offline (Echopac version 6.0.1, General Electric). Pulsed Doppler flow profiles at LV inflow (mitral valve opening & closure) and outflow (aortic valve opening & closure) as well as at the right ventricular outflow tract (pulmonary valve opening) were employed for cardiac event timing. Systole was defined as the interval between mitral and aortic valve closure. For deformation imaging, dedicated narrow sector single wall images of the septum, anteroseptum, anterior, lateral, posterior, and inferior wall were prospectively acquired at 51-109 frames per second. For each wall, longitudinal strain curves at the basal, midventricular and apical segments (i.e. 18-segment model) were derived by speckle tracking with the onset of the QRS as zero reference. The obtained traces were further post-processed along with cardiac event timing markers in a custom-made toolbox (STOUT: Speckle tracking Toolbox Utrecht), yielding spatially encoded and time-normalized deformation data over the entire LV [20]. Stroke volume (SV), LVEF, LV end-systolic (LVESV) and end-diastolic (LVEDV) volumes by biplane Simpson's method were analysed by one (GL), and all deformation and dyssynchrony measurements independently by another (BDB) observer. Both were blinded to each other and to the invasive dP/dt_{max} measurements.

Dyssynchrony and discoordination parameters

Inter-ventricular mechanical delay (IVMD) was defined as the delay between pulmonary and aortic valve opening. Intra-ventricular LV-dyssynchrony was defined as the standard deviation of time to peak strain in all segments (2DS-SD18). As a surrogate marker of mechanical work-inefficiency, discoordination was assessed as the internal stretch fraction (ISF) and systolic rebound stretch (SRSlv)[21–23]. To calculate ISF, each strain rate curve was automatically split into their respective shortening (negative strain) and stretching (positive strain) components. The average strain rate of all LV segments was then determined for the these shortening and stretching components separately. The *fraction* of total systolic stretch (i.e. wasted work) relative to total systolic shortening (i.e. constructive work) determined ISF **(Supplemental Figure 1)**[21]. Conversely, as a more specific index of systolic wasted work by itself, SRSlv was calculated. Here, all systolic stretch that occurs immediately after prematurely terminated shortening was summed and averaged over the total amount of LV segments **(Figure 1)** [20,23].

LV dP/dt_{max} measurements during device implantation

Device implantation was performed under local anaesthesia. Right ventricular apical (RV) and atrial leads were placed transvenously at conventional positions. The LV lead was aimed at a tributary of the coronary sinus overlying the LV free wall. Leads were connected to a CRT-defibrillator in all patients.
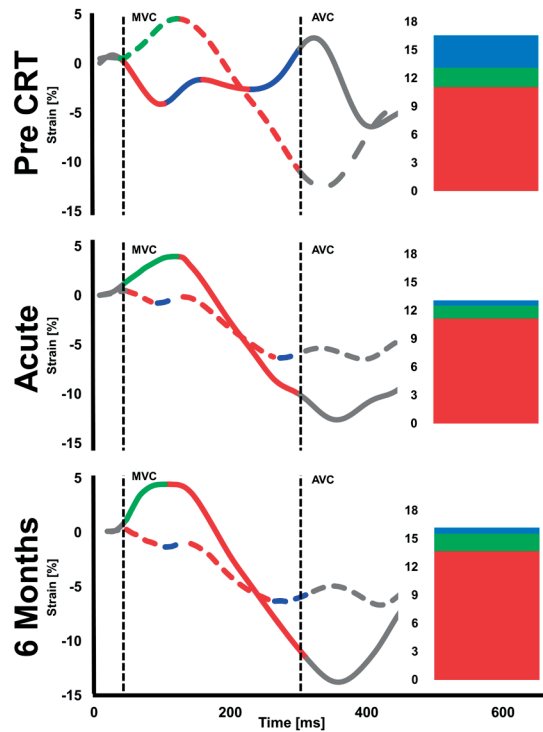
Fig 1 *Systolic rebound stretch as part of a biphasic response in recoordination. Left ventricular systolic rebound stretch (SRSlv) is calculated as the total amount of systolic stretching that occurs after prematurely terminated shortening during systole (i.e. strain-amplitudes of positive longitudinal strain), averaged over the total number of segments. Compared to baseline, an acute reduction in the amount of systolic rebound stretch (blue; i.e. wasted work) of the left ventricle is seen upon biventricular pacing, without concomitant improvement in systolic shortening (red; i.e. constructive work). Conversely, improvement in systolic shortening becomes apparent after six months of prolonged biventricular stimulation. Note that for illustrative purposes only two segmental strain curves, both of the septum (solid lines) and lateral wall (dashed lines), are displayed for a representative CRT responder.*

LV dP/dt$_{max}$ was obtained by placing a pressure wire (PressureWire^{TM} Certus, St. Jude Medical Inc., St. Paul, MN, USA) in the LV via femoral arterial access. After baseline measurement of LV dP/dt$_{max}$, the acute effect of CRT on LV dP/dt$_{max}$ was derived automatically from continuous, digitized invasive pressure measurements digitized at 100 Hz (Radi Analyzer Physio Monitor v1.0 beta4, St. Jude Medical, Inc., St. Paul, MN, USA). Measurements were averaged over 10 seconds for each setting. Premature ventricular beats and the first post-extrasystolic beat were manually excluded from analysis. AV- and VV-delays were optimized to maximize the increase in LV dP/dt$_{max}$ compared to baseline. [17] Paced AV-delays were shortened by 20ms steps from 240ms to 80ms. VV-delay optimization was performed at the previously determined optimal AV-delay starting with LV pre-activation by 80 ms followed by lengthening of the VV delay by steps of 20 ms until RV pre-activation by 80 ms.

Statistical analysis

Statistical analysis was performed using SPSS version 25.0 (SPSS Inc., Chicago, Illinois). Values are presented as mean and standard deviation (SD) for continuous variables, and as numbers and percentages for categorical variables. Assumptions on homogeneity of variances and normally distributed residuals were checked by Levene's test and Q-Q plots respectively. Comparison of continuous data between responders and non-responders was performed by independent samples t-test. Comparison of continuous data over time was performed by repeated measurements analysis of variance (ANOVA). Categorical data were compared by chi-square or Fischer's exact test as appropriate. Bonferroni post-hoc correction for multiple comparisons was applied when applicable. For the direct comparison of the relationship between acute improvements and long-term response, Pearson correlation were restricted to the subset of 25 patients with complete dP/dt$_{max}$, dyssynchrony, and discoordination measurements. A p-value <0.05 was considered statistically significant.

RESULTS

Patient population

Mean age of the study population was 65±11 years, 60% were male, 83% were in NYHA functional class III, heart failure aetiology was ischemic in 46%. LV lead placement was posterior or posterolateral in 15 (43%), lateral in 18 (51%) and anterolateral in 2 (6%) patients. Echocardiographic data including all volumetric, dyssynchrony and discoordination parameters at baseline, immediately after implant & at six months follow up was available for all patients (n=35). The subgroup with LV dP/dt$_{max}$-guided optimization comprised 25 patients enabling the direct comparison of acute LV dP/dt$_{max}$ augmentation and acute recoordination with long-term response. Baseline LV dP/dt$_{max}$ was determined during sinus rhythm (n=20), atrial pacing (due to sick sinus, n=2) and RV pacing (pacing-dependent AV-Block, n=3) and was on average 668±185 mmHg/s.

Baseline characteristics of this subgroup with dP/dt$_{max}$ data as well as of the entire study population stratified according to response are provided in **Supplemental Table 1**. In total, 20 patients (57%) were classified as echocardiographic responder. Non-responders were similar to responders concerning all baseline clinical characteristics.

Recoordination, hemodynamic improvement, and reverse remodelling after CRT

In the entire group, initiation of CRT acutely improved coordination (ISF & SRSlv) and synchrony (IVMD, 2DS-SD18) along with augmented LVEF, SV and LV dP/dtmax **(Supplemental Table 2)**. Acute recoordination and resynchronisation were maintained over

time. Interestingly, the acute improvement of LV coordination was exclusively caused by a reduction of paradoxical systolic stretch (both systolic stretch and SRSlv), at unchanged systolic shortening. Inversely, longer-term CRT further improved recoordination in terms of a further decline in ISF exclusively by an increase in the systolic shortening fraction without effect on paradoxical stretch. Stroke volume increased acutely upon starting CRT, but remained constant during six months follow-up, while LVEF continued to increase due to a balanced reduction in LVEDV and LVESV **(Supplemental Figure 2)**.

The effects of CRT on LV coordination and hemodynamic function, stratified according to response, are displayed graphically in **Figure 2**. At baseline, responders had higher baseline values of discoordination (ISF 53±17 vs. 35±13 %, p=0.003; SRSlv 3.01±1.26 vs. 1.28±0.56 %, p<0.001) and dyssynchrony (IVMD 62±20 vs. 39±28 ms, p=0.012; 2DS-SD18 158±42 vs. 125±43 ms, p=0.026) compared to non-responders. As seen in the entire group, both responders and non-responders showed an immediate reduction in systolic stretch and IVMD upon CRT initiation, finally reaching similar values during acute CRT. However, in view of the lower baseline values, the absolute reduction in systolic stretch was smaller in non-responders and became insignificant when expressed in relative terms by ISF. Similarly, the reduction of 2D-SD18 by CRT did not reach significance in non-responders **(Supplemental Figure 2)**. Significant long-term improvement of myocardial shortening, with the associated further decrease in ISF, was only present in responders. Responders and non-responders showed a similar acute hemodynamic response, both expressed in terms of dP/dt$_{max}$ and ejection fraction **(Figure 2)**. However, only in the responder group EF continued to rise during longer lasting CRT.
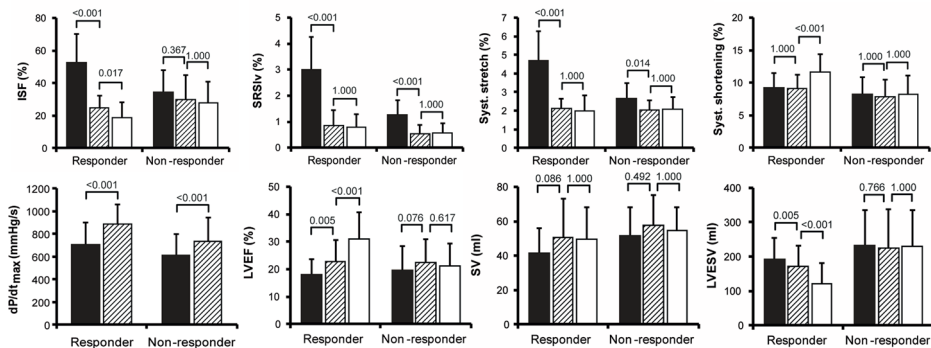
Fig 2 *Evolution of discoordination and left ventricular hemodynamic function stratified according to response. Mean and standard deviation values of discoordination (upper panels) and parameters of left ventricular hemodynamic function and dimensions (lower panels). Results are shown before, directly after and six months after CRT (black, shaded, and white bars, respectively) in responders and non-responders. Note that acutely after CRT, coordination improves by reduction of systolic stretch, whereas during long-term follow-up systolic stretch remains stable but systolic shortening improves in responders. ISF, internal stretch fraction; SRSlv, systolic rebound stretch of the septum; dP/dt$_{max}$, maximum rate of LV pressure rise; SV, stroke volume; LVEF, left ventricular ejection fraction; LVESV, LV end-systolic-volume.*

Relation of acute improvements with long-term response

Acute recoordination parameters were closely related to reverse remodelling and ΔLVEF after six months **(Table 1)**. The best predictor of reverse remodelling was the acute reduction of systolic rebound stretch within the LV (ΔSRSlv; R=0.767, p<0.001). Similar relations with reverse remodelling were found for *baseline* measurements of discoordination (R=0.796 and R=0.581 for SRSlv and ISF, respectively: both p<0.001) and dyssynchrony (R=0.475, p=0.005 and R=0.518, p=0.001 for IVMD and 2D-SD18 respectively). In contrast, acute increases in LV dP/dt$_{max}$, LVEF and SV neither predicted long-term response (i.e. reverse remodelling and ΔLVEF) after six months **(Table 1)** nor did they correlate with the extent of acute recoordination and resynchronisation **(Supplemental Table 3)**. Additionally, acute improvements in mitral regurgitation effective regurgitant orifice (ΔMRero; R=0.064, p=0.778) and RV tricuspid annular plane systolic excursion (ΔTAPSE; R=0.101, p=0.630) were unrelated to long-term reverse remodelling as well.

Table 1. Relation of acute improvements with reverse remodelling and changes in LVEF (n=25)

Parameter	6-months ΔLVESV (%)		6-months ΔLVEF (%-point)	
	R	p-value	R	p-value
Acute recoordination				
ΔISF (%-point)	**0.601**	**<0.001**	**0.578**	**0.002**
ΔSystolic stretch (%-point)	**0.676**	**<0.001**	**0.628**	**<0.001**
ΔSRSlv (%-point)	**0.765**	**<0.001**	**0.694**	**<0.001**
Acute resynchronisation				
ΔIVMD (ms)	0.133	0.554	0.140	0.535
Δ2D-SD18 (ms)	**0.500**	**0.011**	**0.451**	**0.023**
ΔQRS (ms)	0.188	0.368	0.131	0.533
Acute improvement of systolic function				
ΔdP/dt$_{max}$ (%)	0.251	0.277	0.173	0.409
ΔSV (%)	0.047	0.830	0.250	0.249
ΔLVEF (%-point)	0.237	0.265	0.392	0.077

For a uniform representation, all changes Δ express a physiologic improvement, i.e. decrements for discoordination & dyssynchrony parameters, and increments for function parameters such that relations are positive if both parameters improve. Abbreviations: ISF, internal stretch fraction; SRSlv, left ventricular systolic rebound stretch; 2DS-SD18, standard deviation of time to peak strain; IVMD, interventricular mechanical delay; LVEDV, left ventricular (LV) end-diastolic volume; LVESV, LV end-systolic volume; SV, stroke volume; LVEF, LV ejection fraction; dP/dt$_{max}$, maximum rate of LV pressure rise.

DISCUSSION

This study demonstrates that the extent of acute mechanical recoordination achieved upon CRT-initiation, specifically SRSlv, is highly predictive of volumetric response to CRT at six months follow-up. In contrast, our results substantiate that an acute functional response (i.e. hemodynamic improvement of LV systolic function) poorly relates to the

extent of acute LV recoordination, and therefore poorly predicts longer-term remodelling **(Figure 3)**. Moreover, this study strongly suggests a bimodal response to CRT: an immediate alleviation of dyssynchrony and of paradoxical systolic stretch in particular, followed by a true improvement of myocardial shortening on the longer-term **(Figure 1)**. Taken together, these findings emphasize the importance of correction of local derangements in cardiac mechanics to trigger reverse remodelling after CRT.

3
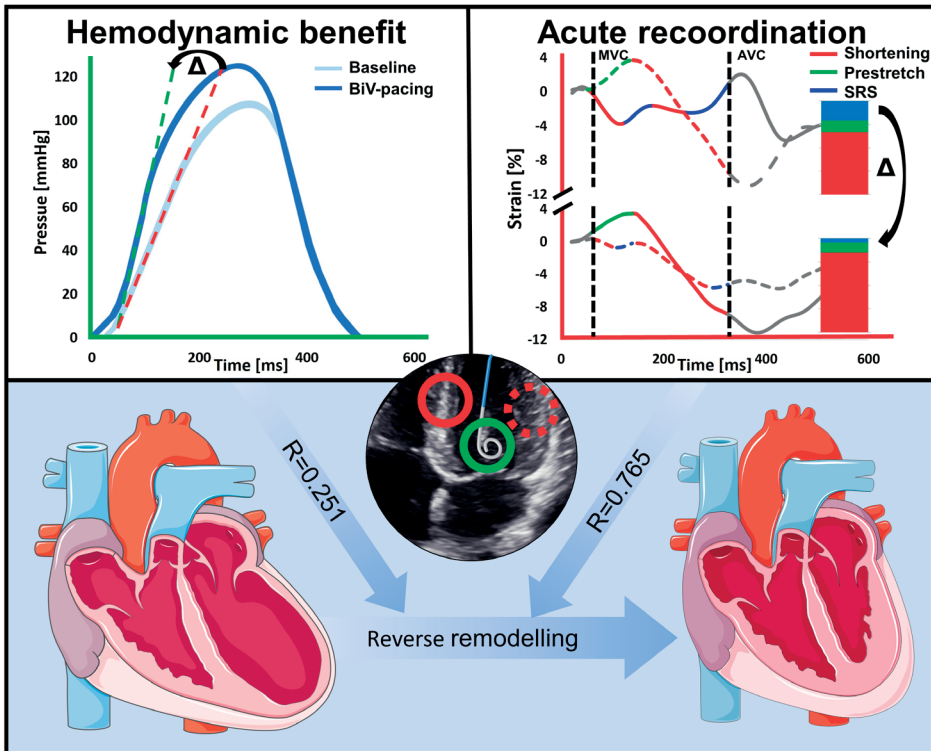
Fig 3 *Visual abstract summarizing the main study methods and results. Biventricular (BiV) pacing elicited an acute LV functional response, reflected by an acute increase (Δ) in invasively determined LV dP/dt$_{max}$ (top left panel). BiV pacing also induced acute recoordination of LV deformation (top right panel), predominantly characterised by acute reduction (Δ) in paradoxical systolic rebound stretch of the LV (SRSlv). As such, a smaller fraction of the work that was performed during systole was internally wasted by segments paradoxically stretching. This ensues in a lower internal strain fraction (ISF, not displayed), thereby signifying higher efficiency. When comparing acute improvements in LV systolic function and acute recoordination, the parameter most strongly related to reverse remodelling was the extent of acute recoordination, and not acute hemodynamic response.*

Acute functional hemodynamic improvements fail to predict long-term response

In the present study, acute hemodynamic changes, whether invasively assessed by LV dP/dt$_{max}$, or echocardiographically by LVEF and stroke volume did not relate to resynchronisation and failed to predict long-term reverse remodelling. These data challenge the historical assumptions that the best achievable acute functional response, as reflected

by e.g. dP/dt_{max}, reflects optimal resynchronization, predicts a favorable longer-term outcome, and -in extenso- may represent targets for CRT-optimization. These assumptions predominantly followed numerous observations that CRT induces immediate and sustained improvements in both mechanical activation synchrony as well as in hemodynamic parameters, most notably dP/dt_{max} [2–6,8,9,14,24–27]. Nevertheless, preclinical evidence to support acute functional response as a predictor of longer-term remodelling is sparse and clinical patient data conflicting. Importantly, only one study suggested **Δ**dP/dt_{max} as a predictor of long-term reverse remodelling [28]. In contrast, Stellbrink et al. and Bogaard et al. independently demonstrated that volumetric and clinical responders to CRT, were found among those with both very high and with minimal acute ΔdP/dt_{max} [17,29]. In analogy, echocardiographic subanalyses of the REVERSE-trial and the PROSPECT-trial demonstrated no relation between the acute increase in LVEF and long-term effects of CRT on reverse remodelling and clinical outcome [24,30]. Therefore, acute and chronic improvements seem part of a heterogeneous spectrum of CRT response, subject to many additional variables. This notion is further supported by the absence of a clear relation between **Δ**dP/dt_{max} and acute recoordination in the present study.

Acute reversal of paradoxical stretch and mechanical inefficiency mediate CRT response

The current study clearly suggests longer-term reverse remodelling to be significantly mediated by the extent to which CRT can acutely improve mechanical coordination through acute reversal of paradoxical systolic stretch. We have previously demonstrated that CRT response at six months involves a redistribution and homogeneization of systolic strain amplitudes by improving local and global myocardial shortening proportionally to the reduction in paradoxical systolic stretch [21]. The most specific stretch component associated with improved shortening and response in that study was the systolic rebound stretch that abunds at the septum [21]. To this end, the added prognostic value of high baseline SRS of the septum (and correction thereof), in addition to simple visual assessment of dyssynchrony, has recently been proven in 200 CRT recipients, both in patients with LBBB and non-LBBB [12].

Similar results have been obtained when evaluating changes in recoordination after six months in terms of strain-based myocardial work. Here, homogenization of systolic work was demonstrated primarily through mitigation of wasted (i.e. paradoxical) work [31]. Recently, Duchenne et al demonstrated that acute redistribution of regional LV work, specifically from the lateral wall towards the septum, determined long-term reverse remodelling [32]. With regional systolic strain representing the main determinant of regional myocardial work in that study, redistribution of work through reversal of wasted work was based on reversal of septal paradoxical stretch also in that study. As opposed to the present study, indices of discoordination and/or myocardial work have not been di-

rectly compared to invasive hemodynamic measures such as dP/dt_{max} before. However, because both ISF and SRS of the septum at baseline show close correlation with the septum-to-lateral wall ratio of myocardial work, similar results are to be expected when using afterload-integrated indices of wasted work in the septum [33].

CRT-induced recoordination follows a biphasic response

Besides its direct comparison with acute hemodynamic parameters of LV systolic function, the current study extends the findings of previous studies by also demonstrating that the conversion of stretching into shortening follows a biphasic response. Immediately after onset of biventricular pacing, LV coordination improved almost exclusively by a reduction of paradoxical myocardial systolic stretch, whereas longer-term improvements nearly exclusively involved an increase in myocardial systolic shortening **(Figure 2)**. This biphasic response suggests that, whereas the acute reduction of stretch can be attributed to retiming of ventricular activation and contraction, actual long-term improvements involve secondary mechanisms activated in response to chronic application of CRT.

It is becoming increasingly clear that the chronic response to CRT involves complex molecular, cellular and electrical modifications that are specific to dyssynchronous heart failure and its cure by CRT [15,16,27,34]. Although many of the mechano-feedback pathways remain to be elucidated, abnormal stretch is considered an important mediator for local genetic, cellular and electrical remodelling [27,35,36]. Hence, we postulate that restoration of normal contraction patterns may reverse these processes and instigate longer-term improvements. Exemplary in this regard are the findings of Aiba et al. in a canine model of dyssynchronous heart failure. Although immediate restoration of regional strain homogeneity by CRT elicited only minor improvements in LV pump function, considerable reverse molecular remodeling and restoration of regional molecular and electrophysiologic homogeneity ensued [15]. We therefore postulate that homogenisation and restoration of normal shortening mechanics play a key role in the mediation of long-term reverse remodelling, that is, in the transition from short to long-term benefit following CRT [27].

Additionally, one of the unique and primary mechanisms by which CRT is believed to convey its longer-term benefits, is through improved myocardial efficiency of ventricular contraction [2,22,37]. By definition, segments that shorten against the pressures in systole perform positive work, whereas segments that lengthen (stretch) are subjected to negative (paradoxical) work. Hence, by expressing the fraction of total shortening that is internally dissipated into paradoxical stretch, the internal strain fraction (ISF) conceptually reflects myocardial work inefficiency, or "wasted work" [37,38]. As such, the observed attenuation of paradoxical systolic stretch at unchanged shortening underlying the immediate ISF-decrease in our study, complies well with the concept that CRT

augments cardiac function at unchanged or even diminished energy cost [2]. Conversely, we observed a reduction in end-diastolic volumes paralleled by augmented total shortening at six months, a pattern reminiscent of the gradual, true reverse remodelling observed in successful heart failure drug trials.

Potential clinical implications

Our results show that acute recoordination and functional improvement of LV systolic function are unrelated, and as such question the use of acute hemodynamic improvements as a herald of long-term structural benefit of CRT. Rather, our results point to a prominent role of correction of discoordinated myocardial deformation and in particular the reversal of paradoxical systolic (rebound) stretch as key mechanisms in achieving long-term reverse remodelling and improved LVEF.

Since a stronger reduction of systolic stretching within the septum is associated with a two-fold larger reduction in LVESV, optimizing the extent of recoordination achieved upon initiation of biventricular pacing can be of interest as well [12]. Because CRT can restore discoordination acutely, our results also point to the potential role of discoordination-imaging of as a means of optimization device settings (e.g. electrode selection) directly after CRT implantation, but further research is warranted.

To fulfil its future clinical potential and to allow for integration in prediction models, methods of assessing discoordination will need to be further automatized, quantified and visualized in physiologically meaningful and clinically feasible ways [39,40]. Promising in this regard are the latest technical advances permitting near-instantaneous, on-scanner implementations of indices such as total and wasted work with encouraging first clinical results.

Study limitations

Because of non-consecutive enrollment of the patients, the potential influence of selection bias cannot be excluded. Our findings should therefore be confirmed in a larger cohort of unselected patients who underwent CRT implantation. Less preload-dependent hemodynamic measures may be more predicative of a volumetric response than LV dP/dt$_{max}$, SV or LVEF. For example, invasive determination of stroke work was not performed [41]. Also, because no blood pressure data was systematically collected at the time of echocardiography, myocardial wasted work, which incorporates afterload, could not be calculated. The primary goal of the current study was however to explore the mechanisms responsible for CRT response rather than to find the best echocardiographic method to assess those factors. Echocardiography and invasive hemodynamic assessments were not performed simultaneously. All patients were however in a stable clinical condition and echocardiographic examinations were performed within a few days from the implantation procedure. In the majority of cases, baseline and paced LV

dP/dt$_{max}$ were measured only once and in non-randomized order. Repeated and randomized measurements, as incorporated in some optimization systems [5], improve the reliability of the measurements and might augment their predictive performance.

CONCLUSION

3

Long-term echocardiographic response after cardiac resynchronisation therapy is likely related to acute recoordination, specifically by attenuation of paradoxical systolic rebound stretch, rather than acute hemodynamic improvement of LV systolic function **(Figure 3)**. The present findings underscore the relevance of LV recoordination as an *acute* mechanistic pathway for long term reverse remodelling processes after biventricular pacing, and thereby provide physiological insights that further support the ability of discoordination-imaging to predict and asses CRT response [12]. Although consistent, our results are confined to the limitations of a small selected cohort of patients and should be interpreted accordingly.

REFERENCES

1. A. C. Pouleur, D. Knappe, A. M. Shah, *et al.* Relationship between improvement in left ventricular dyssynchrony and contractile function and clinical outcome with cardiac resynchronization therapy: The MADIT-CRT trial. *Eur. Heart J.* **32**, 1720–1729 (2011).

2. G. Nelson, R. Berger, B. Fetics, *et al.* Left Ventricular or Biventricular Pacing Improves Cardiac Function at Diminished Energy Cost in Patients With Dilated Cardiomyopathy and Left Bundle-Branch Block. *Circulation.* **102**, 3053–3059 (2000).

3. G. Nelson, C. Curry, B. Wyman, *et al.* Predictors of Systolic Augmentation From Left Ventricular Preexcitation in Patients With Dilated Cardiomyopathy and Intraventricular Conduction Delay. *Circulation.* **101**, 2703–2709 (2000).

4. D. A. Kass, C. H. Chen, C. Curry, *et al.* Improved left ventricular mechanics from acute VDD pacing in patients with dilated cardiomyopathy and ventricular conduction delay. *Circulation.* **99**, 1567–1573 (1999).

5. A. Auricchio, C. Stellbrink, M. Block, *et al.* Effect of pacing chamber and atrioventricular delay on acute systolic function of paced patients with congestive heart failure. The Pacing Therapies for Congestive Heart Failure Study Group. The Guidant Congestive Heart Failure Research Group. *Circulation.* **99**, 2993–3001 (1999).

6. O. A. Breithardt, C. Stellbrink, A. P. Kramer, *et al. J. Am. Coll. Cardiol.*, in press, doi:10.1016/S0735-1097(02)01987-3.

7. X. A. A. M. Verbeek, K. Vernooy, M. Peschar, R. N. M. Cornelussen, F. W. Prinzen. Intra-ventricular resynchronization for optimal left ventricular function during pacing in experimental left bundle branch block. *J. Am. Coll. Cardiol.* **42**, 558–567 (2003).

8. M. D. Bogaard, P. A. Doevendans, G. E. Leenders, *et al.* Can optimization of pacing settings compensate for a non-optimal left ventricular pacing site? *EP Eur.* **12**, 1262–1269 (2010).

9. C. Butter, A. Auricchio, C. Stellbrink, *et al.* Effect of resynchronization therapy stimulation site on the systolic function of heart failure patients. *Circulation.* **104**, 3026–3029 (2001).

10. A. Auricchio, J. Ding, J. C. Spinelli, *et al.* Cardiac resynchronization therapy restores optimal atrioventricular mechanical timing in heart failure patients with ventricular conduction delay. *J. Am. Coll. Cardiol.* **39**, 1163–1169 (2002).

11. A. Auricchio, C. Stellbrink, S. Sack, *et al. J. Am. Coll. Cardiol.*, in press, doi:10.1016/S0735-1097(02)01895-8.

12. O. A. E. Salden, A. Zweerink, P. Wouters, *et al.* The value of septal rebound stretch analysis for the prediction of volumetric response to cardiac resynchronization therapy. *Eur. Heart J. Cardiovasc. Imaging.* **22**, 37–45 (2021).

13. A. H. Maass, K. Vernooy, S. C. Wijers, *et al.* Refining success of cardiac resynchronization therapy using a simple score predicting the amount of reverse ventricular remodelling: results from the Markers and Response to CRT (MARC) study. *Europace.* **20** (2018). pp. e1–e10.

14. K. Vernooy, R. N. M. Cornelussen, X. A. A. M. Verbeek, *et al.* Cardiac resynchronization therapy cures dyssynchronopathy in canine left bundle-branch block hearts. *Eur. Heart J.* **28**, 2148–2155 (2007).

15. T. Aiba, G. G. Hesketh, A. S. Barth, *et al.* Electrophysiological consequences of dyssynchronous heart failure and its restoration by resynchronization therapy. *Circulation.* **119**, 1220–1230 (2009).

16. B. Andreas, A. Takeshi, H. Victoria, *et al.* Cardiac Resynchronization Therapy Corrects Dyssynchrony-Induced Regional Gene Expression Changes on a Genomic Level. *Circ. Cardiovasc. Genet.* **2**, 371–378 (2009).

3

17. M. D. Bogaard, P. Houthuizen, F. A. Bracke, *et al.* Baseline left ventricular dP/dtmax rather than the acute improvement in dP/dtmax predicts clinical outcome in patients with cardiac resynchronization therapy. *Eur. J. Heart Fail.* **13**, 1126–1132 (2011).

18. J. Yan, S. Zhang, D. Huang, *et al.* Evaluation of the therapeutic effects of QuickOpt optimization in Chinese patients with chronic heart failure treated by cardiac resynchronization. *Sci. Rep.* **8**, 4259 (2018).

19. S. S. D., F. Elyse, B. Mikhail, *et al.* Effect of Cardiac Resynchronization Therapy on Reverse Remodeling and Relation to Outcome. *Circulation.* **122**, 985–992 (2010).

20. B. W. L. De Boeck, B. Kirn, A. J. Teske, *et al.* Three-dimensional mapping of mechanical activation patterns, contractile dyssynchrony and dyscoordination by two-dimensional strain echocardiography: Rationale and design of a novel software toolbox. *Cardiovasc. Ultrasound.* **6**, 22 (2008).

21. B. W. L. De Boeck, A. J. Teske, M. Meine, *et al.* Septal rebound stretch reflects the functional substrate to cardiac resynchronization therapy and predicts volumetric and neurohormonal response. *Eur. J. Heart Fail.* **11**, 863–871 (2009).

22. F. W. Prinzen, K. Vernooy, B. W. L. DeBoeck, T. Delhaas. Mechano-energetics of the asynchronous and resynchronized heart. *Heart Fail. Rev.* **16**, 215–224 (2011).

23. B. Kirn, A. Jansen, F. Bracke, *et al.* Mechanical discoordination rather than dyssynchrony predicts reverse remodeling upon cardiac resynchronization. *Am. J. Physiol. Circ. Physiol.* **295**, H640–H646 (2008).

24. M. St John Sutton, S. Ghio, T. Plappert, *et al.* Cardiac resynchronization induces major structural and functional reverse remodeling in patients with New York Heart Association class I/II heart failure. *Circulation.* **120**, 1858–1865 (2009).

25. P. Steendijk, S. A. Tulner, J. J. Bax, *et al.* Hemodynamic effects of long-term cardiac resynchronization therapy: analysis by pressure-volume loops. *Circulation.* **113**, 1295–1304 (2006).

26. W. Mullens, T. Verga, R. A. Grimm, *et al. J. Am. Coll. Cardiol.*, in press, doi:10.1016/j.jacc.2008.08.079.

27. F. W. Prinzen, A. Auricchio. The "Missing" Link Between Acute Hemodynamic Effect and Clinical Response. *J. Cardiovasc. Transl. Res.* **5**, 188–195 (2012).

28. S. G. Duckett, M. Ginks, A. K. Shetty, *et al. J. Am. Coll. Cardiol.*, in press, doi:10.1016/j.jacc.2011.04.042.

29. C. Stellbrink, O. A. Breithardt, A. Franke, *et al.* Impact of cardiac resynchronization therapy using hemodynamically optimized pacing on left ventricular remodeling in patients with congestive heart failure and ventricular conduction disturbances. *J. Am. Coll. Cardiol.* **38**, 1957–1965 (2001).

30. L. A. Pires, S. Ghio, E. S. Chung, *et al.* Relationship Between Acute Improvement in Left Ventricular Function to 6-Month Outcomes After Cardiac Resynchronization Therapy in Patients With Chronic Heart Failure. *Congest. Hear. Fail.* **17**, 64–69 (2011).

31. J. Vecera, M. Penicka, M. Eriksen, *et al.* Wasted septal work in left ventricular dyssynchrony: a novel principle to predict response to cardiac resynchronization therapy. *Eur. Heart J. Cardiovasc. Imaging.* **17**, 624–632 (2016).

32. J. Duchenne, J. M. Aalen, M. Cvijic, *et al.* Acute redistribution of regional left ventricular work by cardiac resynchronization therapy determines long-term remodelling. *Eur. Heart J. Cardiovasc. Imaging* (2020), doi:10.1093/ehjci/jeaa003.

33. A. Zweerink, G. J. de Roest, L. Wu, *et al.* Prediction of Acute Response to Cardiac Resynchronization Therapy by Means of the Misbalance in Regional Left Ventricular Myocardial Work. *J. Card. Fail.* **22**, 133–142 (2016).

34. K. Chakir, S. K. Daya, T. Aiba, *et al.* Mechanisms of enhanced beta-adrenergic reserve from cardiac resynchronization therapy. *Circulation.* **119**, 1231–1240 (2009).

35. J. ichi Sadoshima, Y. Xu, H. S. Slayter, S. Izumo. Autocrine release of angiotensin II mediates stretch-induced hypertrophy of cardiac myocytes in vitro. *Cell*. **75**, 977–984 (1993).

36. W. Mullens, J. Bartunek, W. H. Wilson Tang, *et al.* Early and late effects of cardiac resynchronization therapy on force-frequency relation and contractility regulating gene expression in heart failure patients. *Hear. Rhythm*. **5**, 52–59 (2008).

37. K. Russell, M. Eriksen, L. Aaberge, *et al.* A novel clinical method for quantification of regional left ventricular pressure–strain loop area: a non-invasive index of myocardial work. *Eur. Heart J.* **33**, 724–733 (2012).

38. C. K. Larsen, J. M. Aalen, C. Stokke, *et al.* Regional myocardial work by cardiac magnetic resonance and non-invasive left ventricular pressure: a feasibility study in left bundle branch block. *Eur. Heart J. Cardiovasc. Imaging* (2019), doi:10.1093/ehjci/jez231.

39. E. Donal, V. Delgado, E. Galli. Mechanical dyssynchrony is better understood and it might be a good news for heart failure patients. *Eur. Hear. J. - Cardiovasc. Imaging* (2020), doi:10.1093/ehjci/jeaa216.

40. J. Gorcsan, C. P. Anderson, B. Tayal, *et al.* Systolic Stretch Characterizes the Electromechanical Substrate Responsive to Cardiac Resynchronization Therapy. *JACC Cardiovasc. Imaging*. **12**, 1741–1752 (2019).

41. A. Zweerink, O. A. E. Salden, W. M. van Everdingen, *et al.* Hemodynamic Optimization in Cardiac Resynchronization Therapy: Should We Aim for dP/dtmax or Stroke Work? *JACC Clin. Electrophysiol.* **5**, 1013–1025 (2019).

SUPPLEMENTARY MATERIAL

Supplemental Table 1. Baseline characteristics of the entire study population and the dP/dt$_{max}$-subgroup

Parameter	Responders (n=20)	Non-responders (n=15)	P-value	All Patients (n=35)	dP/dt $_{max}$ (n=25)	P-value
Age (yrs)	67±10	62±12	0.163	65±11	66±10	0.781
Male (%)	13 (65)	8 (53)	0.511	21 (60)	15 (60)	1.000
Ischemic aetiology (%)	9 (45)	7 (47)	1.000	16 (46)	11 (44)	1.000
QRS (ms)	175±22	173±33	0.789	174±27	175±28	0.906
120 – 150 (%)	3 (15)	3 (20)		6 (17)		
> 150 (%)	17 (85)	12 (80)		29 (83)		
Sinus rhythm (%)	19 (95)	14 (93)	1.000	33 (94)	23 (92)	1.000
NYHA class	2.9±0.3	3.0±0.5	0.335	2.9±0.4	3.1±0.3	0.115
II	2	2		4	0	
III	18	11		29	23	
IV	0	2		2	2	
B-blocker (%)	12 (60)	11 (73)	0.489	23 (66)	16 (64)	1.000
ACEi/ARB (%)	17 (85)	15 (100)	0.244	32 (91)	23 (92)	1.000
Spironolactone (%)	9 (45)	10 (67)	0.306	19 (54)	14 (56)	1.000
Diuretics (%)	20 (100)	15 (100)	1.000	35 (100)	25 (100)	1.000
LVEDV (ml)	235±68	284±101	0.096	256±86	254±88	0.914
LVESV (ml)	196±58	236±99	0.143	213±79	212±82	0.971
LVEF (%)	18±6	19±7	0.726	19±6	18±7	0.924
SV (ml)	42±14	51±16	0.088	46±15	44±14	0.670
MRero (mm^2)	6.7±6.9	10.7±7.6	0.127	8.4±7.4	9.6±7.7	0.252
Heart rate (bpm)	68±10	69±14	0.741	69±12	71±11	0.424
LV lead position (%)			0.129			0.240
Post/postlat	9 (45)	6 (40)		15 (43)	11 (44)	
Lateral	10 (50)	8 (53)		18 (52)	12 (48)	
Anterolateral	1 (5)	1 (7)		2 (6)	2 (8)	
dP/dt$_{max}$ (mmHg/s)	713±188	618±176	0.208	668±185	668±185	NA

Legend: NYHA class, New York Heart Association class; ACEi/ARB, angiotensin converting enzyme inhibitor or angiotensin receptor blocker use; LVEDV, left ventricle (LV) end-diastolic volume; LVESV, LV end-systolic volume; SV, stroke volume; LVEF, LV ejection fraction; MRero, mitral regurgitation effective regurgitant orifice; dP/dt$_{max}$, maximum rate of LV pressure rise.

3

Supplemental Table 2. Overall evolution of discoordination, dyssynchrony, and ventricular function parameters in the entire study population (n=35)

Parameter	Baseline	Acute	6 Months	P-values Overall	Baseline vs. Acute	Acute vs. 6 Months
ISF (%)	45±18	27±11	23±12	<0.001	<0.001	0.022
Systolic stretch (%)	3.86±1.62	2.13±0.48	2.06±0.73	<0.001	<0.001	1.000
Systolic shortening (%)	8.89±2.35	8.63±2.34	10.24±3.18	<0.001	1.000	0.002
SRSlv (%)	2.27±1.33	0.74±0.50	0.71±0.43	<0.001	<0.001	1.000
2DS-SD18	144±45	121±33	111±44	0.004	0.066	0.468
IVMD	52±27	13±29	10±28	<0.001	<0.001	1.000
LVEDV (ml)	256±86	249±97	219±104	<0.001	0.585	<0.001
LVESV (ml)	211±80	195±87	167±96	<0.001	0.005	0.001
LVEF (%)	19±7	23±8	27±10	<0.001	<0.001	0.007
SV (ml)	46±15	54±20	52±16	0.003	0.025	1.000
MRero (mm^2)	8.4±7.4	5.9±5.5	5.9±6.4	0.010	0.006	0.334
TAPSE (mm)	15.4±5.6	16.3±4.0	17.1±4.9	0.043	0.144	0.366
Heart rate (bpm)	69±12	69±11	68±9	0.675	1.000	0.782
dP/dtmax (mmHg/s)	668±185	817±198	-	-	<0.001	-

Legend: ISF, internal stretch fraction; SRSlv, left ventricular systolic rebound stretch; 2DS-SD18, standard deviation of time to peak strain; IVMD, interventricular mechanical delay; LVEDV, left ventricular (LV) end-diastolic volume; LVESV, LV end-systolic volume; LVEF, LV ejection fraction; SV, stroke volume; MRero, mitral regurgitation effective regurgitant orifice; TAPSE, tricuspid annular plane systolic excursion; dP/dt$_{max}$, maximum rate of LV pressure rise.

Supplemental Table 3. Relation of acute recoordination & resynchronisation parameters with those representing acute hemodynamic improvement (n=25)

Parameter	Acute ΔdP/dt$_{max}$ (%)		Acute ΔSV (%)		Acute ΔLVEF (%-point)	
	R	p-value	R	p-value	R	p-value
Acute recoordination						
ΔISF (%-point)	0.201	0.334	0.005	0.980	0.077	0.720
ΔSRSlv (%-point)	-0.050	0.814	-0.079	0.720	-0.186	0.385
Acute resynchronisation						
ΔIVMD (ms)	0.381	0.080	0.309	0.186	0.346	0.125
Δ2D-SD18 (ms)	0.302	0.143	0.089	0.685	0.317	0.131

For a uniform representation, all changes Δ express a physiologic improvement, i.e. decrements for discoordination & dyssynchrony parameters, and increments for function parameters such that relations are positive if both parameters improve. Other abbreviations: see Table 1 in the main document.
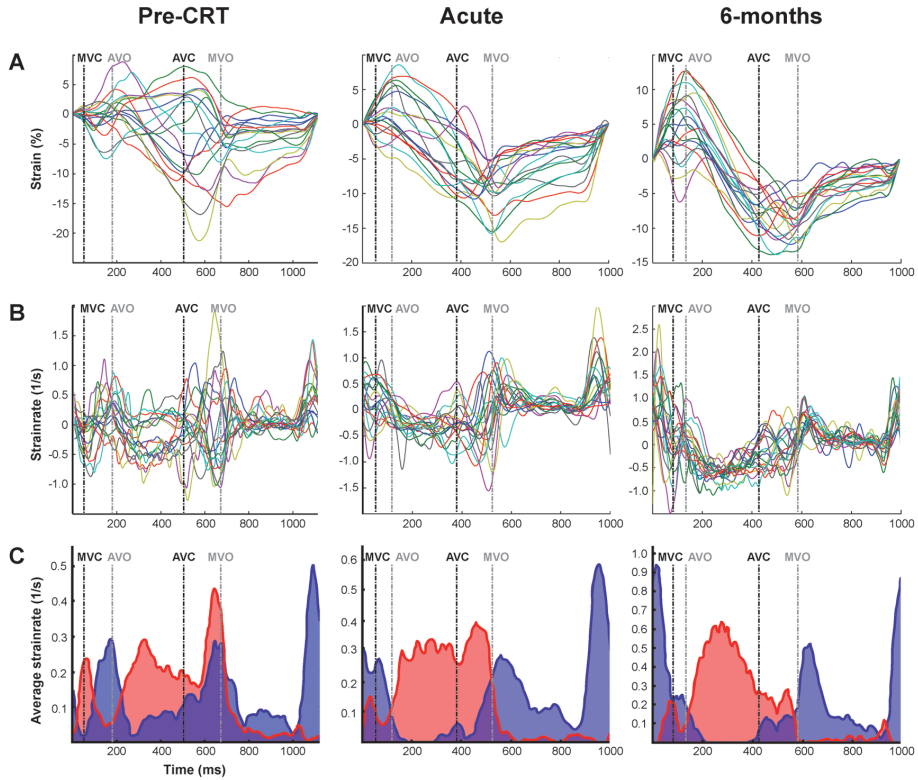
Supplemental Fig 1. *Calculation of internal stretch fraction. Calculation of internal stretch fraction (ISF) exemplified before, acutely after and six months after CRT. Segmental strain curves of all 18 LV segments (panel A) are first differentiated over time into segmental strain rate curves (panel B). Segmental strain rate curves are then split into a shortening (i.e. negative strain rate) and stretching (i.e. positive strain rate) component. Subsequently, the average strain rate of all LV segments is determined for the shortening and stretching components separately (panel C; dark red and blue lines, respectively). As such, displayed over time, red areas signify the average amount of LV shortening, whereas blue areas signify stretching of the LV. During systole (i.e. between MVC and AVC), overlapping areas (purple) indicate simultaneous systolic shortening and stretching (i.e. ISF). As such, dividing systolic shortening by systolic stretching results in systolic ISF. MVC, mitral valve closure; AVC, aortic valve closure.*
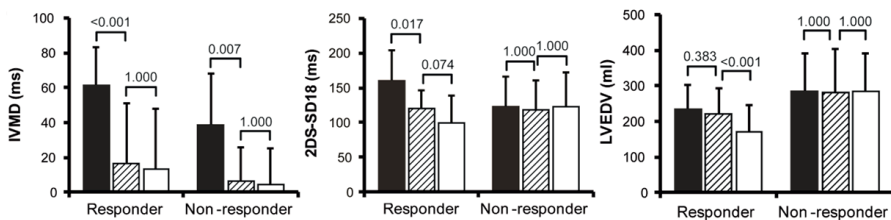
Supplemental Fig 2 *Evolution of dyssynchrony and end-diastolic volume stratified according to response. Mean and standard deviation values of dyssynchrony and left ventricular end-diastolic volume measurements before, directly after and six months after CRT (black, shaded, and white bars, respectively) in responders and non-responders. IVMD, interventricular mechanical delay; 2DS-SD18, standard deviation of time-to-peak strain in 18 segments; LVEDV: left ventricle end-diastolic volume.*

4

Does Mechanical Dyssynchrony in Addition to QRS$_{AREA}$ Ensure Sustained Response to Cardiac Resynchronization Therapy?

Philippe C. Wouters, Wouter M. van Everdingen, Kevin Vernooy, Bastiaan Geelhoed, Cornelis P. Allaart, Michiel Rienstra, Alexander H. Maass, Marc A. Vos, Frits W. Prinzen, Mathias Meine, Maarten J. Cramer.

ABSTRACT

Aims: Judicious patient selection for cardiac resynchronization therapy (CRT) may further enhance treatment response. Progress has been made by using improved markers of electrical dyssynchrony and mechanical discoordination, using QRS_{AREA}, and systolic rebound stretch of the septum (SRSsept) or systolic stretch index (SSI), respectively. To date, the relation between these measurements has not yet been investigated.

Methods and results: A total of 240 CRT patients were prospectively enrolled from six centers. Patients underwent standard 12-lead electrocardiography, and echocardiography, at baseline, 6-month, and 12-month follow-up. QRS_{AREA} was derived using vectorcardiography, and SRSsept and SSI were measured using strain-analysis. Reverse remodelling was measured as the relative decrease in left ventricular end-systolic volume, indexed to body surface area (ΔLVESVi). Sustained response was defined as ≥ 15% decrease in LVESVi, at both 6 and 12-month follow-up. QRS_{AREA} and SRSsept were both strong, multivariable adjusted, variables associated with reverse remodelling. SRSsept was associated with response, but only in patients with QRS_{AREA} ≥ 120 μVs (AUC = 0.727 versus 0.443). Combined presence of SRSsept ≥ 2.5% and QRS_{AREA} ≥ 120 μVs significantly increased reverse remodelling compared to high QRS_{AREA} alone (ΔLVESVi 38±21 versus 22±21%). As a result, 92% of LBBB-patients with combined electrical and mechanical dysfunction were *sustained* volumetric responders, as opposed to 51% with high QRS_{AREA} alone.

Conclusion: Parameters of mechanical dyssynchrony are better associated with response in the presence of a clear underlying electrical substrate. Combined presence of high SRSsept and QRS_{AREA}, but not high QRS_{AREA} alone, ensures a sustained response after CRT in LBBB patients.

INTRODUCTION

Cardiac resynchronization therapy (CRT) alleviates symptoms and greatly reduces morbidity and mortality in patients with dyssynchronous heart failure. Although CRT in general is highly effective, response is variable, and some patients experience no clinical benefit or sometimes even deleterious effects of CRT outcome [1]. It is therefore that judicious selection of patients is of great importance.

Patient selection criteria dictate that heart failure patients are deemed eligible for CRT based on the presence of sufficient electrical substrate, characterized by left bundle branch block (LBBB) QRS-morphology and a prolonged QRS-duration [2]. Unfortunately, various definitions of LBBB morphology exist, and defining QRS-morphology is hampered by significant inter-observer disagreement [3]. Improvements have been made using QRS$_{AREA}$, which has a stronger association with survival and volumetric response after CRT, independently of QRS morphology [4,5]. Since QRS$_{AREA}$ can be easily retrieved from a standard ECG, it is readily implementable in everyday practice.

Because, by itself, an electrical substrate does not *necessarily* contribute to significant deterioration of left ventricular (LV) function, measuring mechanical discoordination can be beneficial as well [6]. The extent of mechanical impairment can be reflected by the amount of stretching that occurs during systole (i.e., systolic rebound stretch of the septum [SRSsept]), also referred to as 'wasted work' [7-9] **(Figure 1)**. Strain-imaging can therefore be used as a tool to quantify the severity of LV systolic impairment that can be attributed to the underlying electrical conduction delay, and by extent determine ones probability to respond to CRT.

Although the importance of QRS$_{AREA}$ and SRSsept have been demonstrated separately, both have yet to be integrated into a single model [5,10]. It is presently unknown whether measuring mechanical discoordination is still of added value in patients with a clear electrical substrate when defined by QRS$_{AREA}$ [4]. In addition, research often solely focusses on response after 6 months, without evaluating whether CRT-induced reverse remodelling, and by extent clinical benefit, is sustained. To this purpose, the present study set out to investigate whether the presence of high QRS$_{AREA}$ with accompanying LV discoordination results in more pronounced 6-month and 12-month LV reverse remodelling, when compared to high QRS$_{AREA}$ alone. We hypothesize that the presence of *combined* electrical and mechanical dysfunction are of added benefit, especially in predicting a lasting CRT-response.
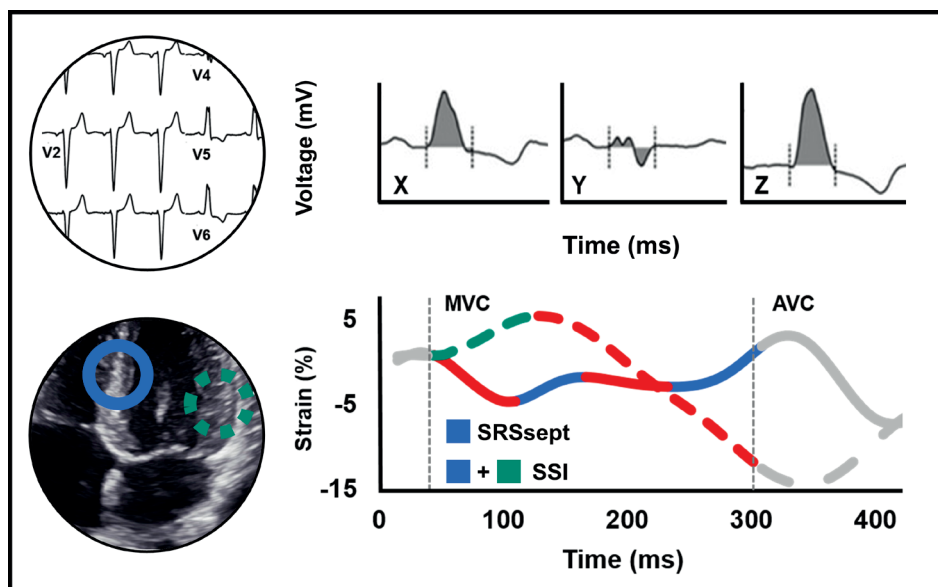
Figure 1. *QRS$_{AREA}$ was derived using vectorcardiograms, recoded from the conventional 12-lead ECG (upper panel). Indices of discoordination were determined using speckle tracking echocardiography (lower panel). Legend: AVC, aortic valve closure, MVC, mitral valve closure; SRSsept systolic rebound stretch of the septum; SSI, systolic stretch index.*

METHODS

Study design

The present study reports a predefined subanalysis of the prospective multicenter Markers and Predictors of Response (MARC) study, which reported 6-month outcome only [5]. The MARC study was primarily designed to investigate various markers for response in patients with *de novo* implantation of a CRT device (clinicaltrials.gov: NCT01519908). The study was initiated and executed by six centers within the framework of the Center for Translational Molecular Medicine (CTMM), project COHFAR (grant 01C-203). All ECGs and echocardiograms were analyzed by a core laboratory, blinded to both clinical patient history and volumetric response (University Medical Center of Utrecht, the Netherlands). Data underlying the present article is under management of the statistical core laboratory (University Medical Center of Groningen, the Netherlands). The present study complied with the Declaration of Helsinki and was approved by the review boards of all participating centers. All patients provided written informed consent.

Study participants

Patients were deemed eligible upon adhering to European and American guideline criteria for CRT at the time of inclusion (February 2012 to November 2013). Patients in sinus rhythm, LV ejection fraction (LVEF) < 35%, and LBBB ≥ 130 ms *or* non-LBBB ≥ 150

ms were included. In addition, patients had New York Heart Association (NYHA) class II or III heart failure symptoms, despite receiving optimal medical therapy. Exclusion criteria included renal insufficiency (<30 mL/min/1.73 m^2), previous resynchronization or anti-bradycardia pacing therapy, right bundle branch block, recent myocardial infarction, permanent atrial fibrillation or flutter, and permanent second or third degree atrioventricular block.

Study protocol

Each patient received a CRT device, programmed at implant to DDD-mode with sensed atrioventricular delay 90 ms, paced atrioventricular delay 130 ms; and interventricular delay 0 ms. Optimization of AV and/or VV delay was performed according to local protocols. A 12-lead digital ECG and echocardiograms were obtained, at baseline, 6-month and 12-month follow-up. LVEF and cardiac dimensions were calculated using Simpson's modified biplane method [11]. The primary study endpoint was LV end-systolic volume reduction, indexed to body surface area using the Du Bois formula (ΔLVESVi) [12]. Since body size is associated with reverse remodelling, indexation was performed to allow for superior, standardized, inter-individual comparison [11]. Echocardiographic response was defined as follows: non-response, LVESVi < 15%; response, LVESVi 15-30%; super-response LVESVi ≥ 30%. Sustained remodelling was defined as LVESVi ≥ 15% at *both* 6 and 12-month follow-up, relative to baseline.

Electrocardiographic data

Standard 12-lead ECG's were analyzed by the ECG core laboratory in order to calculate QRS$_{AREA}$, QRS duration, and define LBBB morphology. ECGs were semi-automatically recoded into vectorcardiograms, each consisting of three orthogonal leads (X, Y, and Z), using the Kors conversion matrix in custom made Matlab software (MathWorks Inc.) **(Figure 1)**. The three orthogonal leads from the vectorcardiogram together form a 3D-vector loop, from which QRS$_{AREA}$ was calculated as $(X_{area}^2 + Y_{area}^2 + Z_{area}^2)^{1/2}$. Presence of LBBB was determined retrospectively according to morphological features from to the European Society of Cardiology (ESC) and the American Heart Association/American College of Cardiology/Heart Rhythm Society (AHA/ACC/HRS) .

Mechanical dyssynchrony and discoordination

Speckle-tracking echocardiography was performed on GE and Philips equipment. A focused view of the septum and conventional apical 4-chamber view were acquired. Onset of QRS-complex and closure time of the aortic valve, using Pulsed-wave Doppler images of the LV outflow tract, were used to define systole. Images were traced alongside the endocardial border of the septum and LV lateral wall (LVlw), excluding the apex. Analysis was performed on vendor-independent software (TomTec Cardiac Performance

Analysis, TomTec Imaging Systems GmbH, Unterschleissheim, Germany). SRSsept and systolic stretch index (SSI) were calculated as indices of mechanical discoordination. For SRSsept, tracings in the *focused* septal view were used whenever possible (61% of patients).

SRSsept was defined as the sum of stretch that occurred in the septum following prematurely terminated shortening, during systole **(Figure 1)** [7]. SSI was subsequently calculated by adding the amount of prestretch that occurred in the LVlw to SRSsept [13]. Contemporary, timing-based, markers of inter- and intraventricular were assessed as well. Interventricular mechanical delay (IVMD) was measured as the difference between left and right ventricular pre-ejection intervals, using pulsed wave Doppler. Apical rocking and septal flash were assessed visually, defined as a short rocking motion of the apex and rapid short inward motion of the septum respectively [14].

Statistical analysis

Statistical tests were performed in SPSS version 25 (IBM, Armonk, NY, USA). Continuous data were expressed using mean ± standard deviation (normally distributed variables) or as median, interquartile range (non-normally distributed variables). Categorical data were described by an absolute number of occurrences and associated frequency (%). Data of two subgroups were compared using a t-test or Mann–Whitney U test, dependent on normality of the data. In the case of multiple subgroups, a one-way ANOVA was used with Bonferroni post hoc test where applicable. Fisher's χ2 test was used for categorical data.

To test the association between discoordination and QRS_{AREA} at baseline and LVESVi-reduction at follow-up, univariate and multivariate adjusted linear regression analyses were performed with correction for potential confounders. Confounders were selected based on parameters that showed an association with ΔLVESVi in univariate analysis with $P < 0.1$. Variables that were added to the final model using backward selection were: sex, age, ischaemic cardiomyopathy, LBBB morphology, QRS duration, QRS_{AREA}, apical rocking, septal flash, IVMD, SRSsept and SSI. Assumptions of multivariable linear regression were checked for the existence of non-linearity, heteroskedasticity, and multicollinearity by graphical analyses and correlations tests. Normality of residuals was tested by a Q-Q plot.

Based on the presence of sufficient baseline electrical substrate (i.e. high QRS_{AREA}) and/or concomitant discoordination (i.e. high SRSsept), the study population was divided into four subgroups. To this end, optimal cut-off values were determined on the basis off highest sensitivity and specificity for discrimination of responders (≥ 15% LVESVi-reduction) from non-responders, using the Youden index.

RESULTS

A total of 240 patients were prospectively included, of whom paired LVESVi measurements at both 6 and 12 months were available in 200. Participants were predominantly male (62%) with a mean age of 66 and an average QRS duration of about 180 ms **(Table S1)**. The majority of patients were NYHA II (63%), with ischemic cardiomyopathy (ICM) in 42% of cases. Overall, LVESV$_i$ decreased by 22 ± 24% (75 ± 31 mL/m^2 versus 58 ± 31 mL/m^2), with 61% of patients being a volumetric responder.

Sustained versus non-sustained remodelling

A total of 114 patients (57%) demonstrated sustained remodelling. Following initial non-response at 6 months, 19 patients demonstrated delayed reverse remodelling after 12 months (ΔLVESVi 23±13%; p < 0.001) **(Figure 2)**. Conversely, 12 delayed non-responders demonstrated initial reverse remodelling, which was not sustained at 12-month follow-up (ΔLVESVi -30±22%; p < 0.001). Reliability of LVESV measurements was excellent, with intra- and interclass correlation coefficients of 0.994 and 0.988 respectively (P < 0.001).
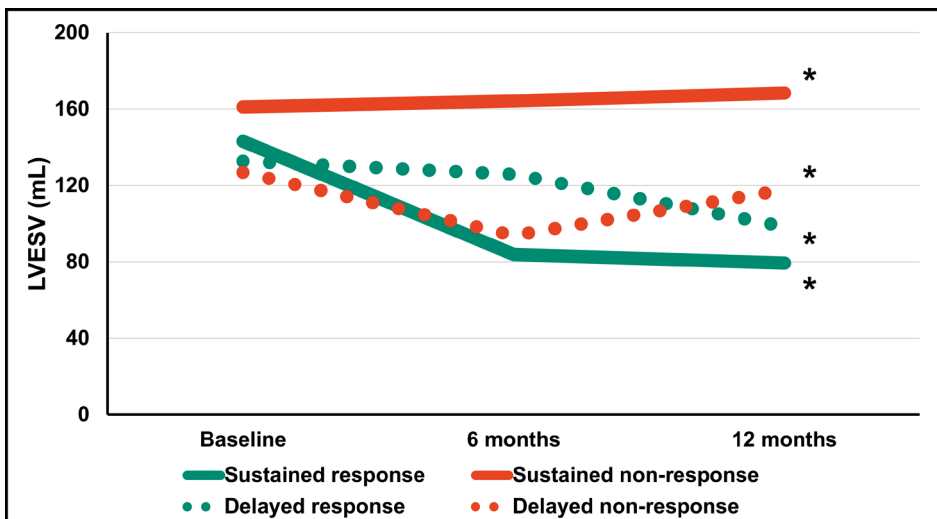
Figure 2. *Changes in left ventricular end-systolic volume over the course of 6 and 12 month follow-up periods. * p < 0.05 between 6 and 12 months.*

Mechanical discoordination and reverse remodelling

Differences in various baseline characteristics on the basis of low QRS$_{AREA}$ and high QRS$_{AREA,}$ with and without concomitant mechanical discoordination, are summarized in **Table S2**. A total of 11 variables were selected for univariate linear regression analysis **(Table 1)**. Significant multivariable adjusted associations with ΔLVESVi, after *both* 6

months and 12 months, were revealed for QRS$_{AREA}$ (β = 0.283 and β = 0.473) and SRSsept (β = 0.177 and β = 0.211), respectively. Other echocardiographic predictors were only significant at either 6 months (IVMD; β = 0.180) or 12 months (apical rocking; β = 0.189). When comparing SSI and SRSsept, only the latter proved to be associated with reverse remodelling after multivariate adjustment. Intra-observer reliability for SRSsept was high with an intraclass correlation coefficient of 0.89 (P < 0.001) [10].

Table 1. *Univariate and multivariate analysis for 6 and 12-month reduction in LVESVi*

	Univariate – 6M		Multivariate – 6M		Multivariate – 12M	
	β	P-value	β	P-value	β	P-value
Male sex – n (%)	-0.168	0.014	-	-	-	-
Age (years)	-0.169	0.013	-0.150	0.022	-0.225	0.001
ICM – n (%)	-0.320	<0.001	-	-	-	-
LBBB – n (%) [ESC]	0.250	<0.001	0.137	0.069	-	-
QRS duration (ms)	0.128	0.072	-0.177	0.031	-0.225	0.008
QRS$_{AREA}$ (µVs)	0.437	<0.001	0.283	0.002	0.473	<0.001
Apical rocking – n (%)	0.313	<0.001	0.125	0.081	0.189	0.007
Septal Flash – n (%)	0.233	0.001	-	-	-	-
IVMD (ms)	0.369	<0.001	0.180	0.020	-	-
SRSsept (%)	0.372	<0.001	0.177	0.014	0.211	0.003
SSI (%)	0.394	<0.001	-	-	-	-

Legend: β, standardized regression coefficient (represents the number of standard deviations that the outcome will change as a result of one standard deviation change in the predictor); 6M, 6-month follow-up; 12M, 12-month follow-up; ICM, ischemic cardiomyopathy; LBBB, left bundle branch block; IVMD, interventricular mechanical delay; SRSsept, systolic rebound stretch of the septum; SSI, systolic stretch index.

Disagreement between electrical substrate and mechanical dyssynchrony

The optimal cut-off value for QRS$_{AREA}$ (AUC = 0.674; p < 0.001) and SRSsept (AUC = 0.652; p = 0.001) were 120 µVs and 2.5% respectively **(Figure S1, A)**. However, baseline QRS$_{AREA}$ and SRSsept were poorly related to each other (R = 0.358; P-value < 0.001) **(Figure S1, B)**. Of all patients, 9% had isolated high SRSsept, whereas high QRS$_{AREA}$ without concomitant SRSsept was found in 26% of cases (Cohen's Kappa = 0.318). When combining these two cut-off values with age and apical rocking [10], multivariate logistic regression analysis demonstrated good associations with 6-month response (AUC = 0.757; p < 0.001) and sustained response (AUC = 0.774; p < 0.001) **(Table S3)**.
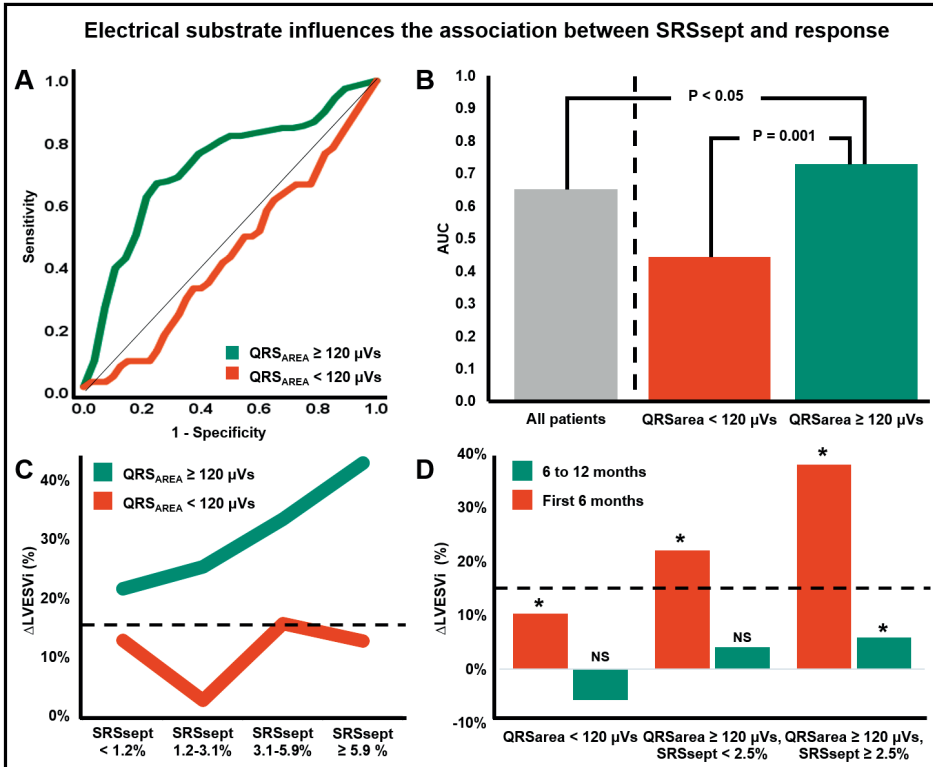
Graphical abstract. *Combined assessment of SRSsept and high QRS$_{AREA}$ significantly improves the association with 6-month response, when compared to SRSsept alone (A, B). The amount of SRSsept is positively associated with response after 6 months, but only in patients with high QRS$_{AREA}$ (C). Simultaneous presence of both high QRS$_{AREA}$ and SRSsept, indicative of coupled electrical and mechanical delay, greatly enhances the extent of reverse remodelling after CRT (D). * p < 0.05.*

The importance of combined electromechanical dysfunction

Baseline SRSsept was increasingly associated with ΔLVESVi, but only in patients with QRS$_{AREA}$ ≥ 120 µVs (AUC = 0.727 versus 0.443; p-between = 0.001) **(Graphical abstract A-C; Table S4)**. Assesment of QRS$_{AREA}$ in addition to SRSsept significantly improved the association with 6-month response, as compared to SRSsept alone (AUC = 0.727 versus AUC = 0. 652; p < 0.05) **(Graphical abstract B)**. This assocation was near-identical for patient with and without ICM (ΔAUC = 0.008; NS). In patients with high QRS$_{AREA}$, simultaneous presence of high SRSsept resulted in significantly more 6-month reverse remodelling than in patients with QRS$_{AREA}$ ≥ 120 µVs alone (ΔLVESVi 38±21 versus 22±21%; p = 0.001) **(Graphical abstract, D)**.

Only in patients with both high QRS$_{AREA}$ and SRSsept, reverse remodelling was continued significantly between 6 and 12-month follow-up (ΔLVESVi 6±23%; p = 0.028) **(Graphical abstract, D)**. Presence of SRSsept consistently enhanced response in patients with QRS$_{AREA}$ ≥ 120 µVs, even in patients with very high baseline QRS$_{AREA}$ (≥ 155

μVs) **(Figure 3)**. Moreover, 90% of patients with both high QRS$_{AREA}$ and SRSsept (n = 59) were volumetric responders, as opposed to only 54% of patients with only QRS$_{AREA}$ ≥ 120 μVs (n = 48). Lastly, 68% of patients with both elevated QRS$_{AREA}$ and SRSsept were classified as super-responder, as opposed to 40% of patients with high QRS$_{AREA}$ alone.
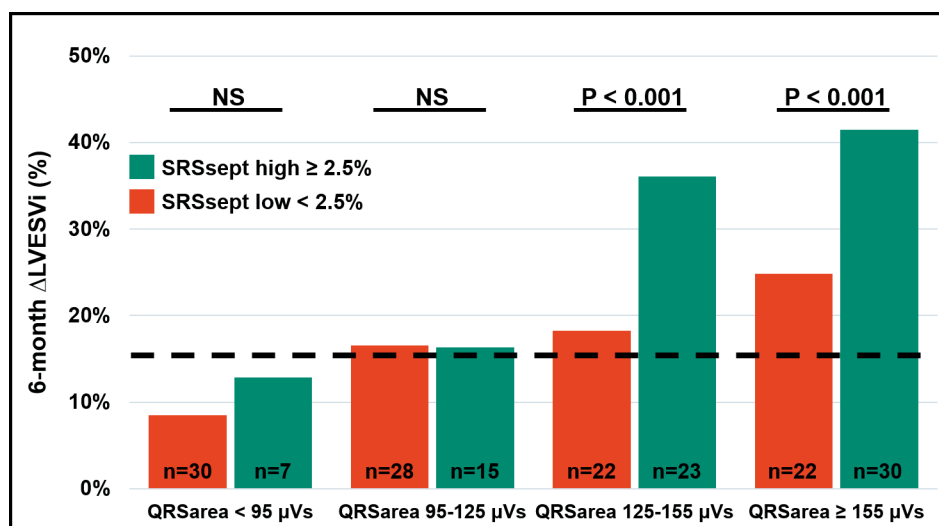
Figure 3. Influence of either the presence (green) or absence (gray) of high SRSsept for various quartiles of baseline electrical dyssynchrony.

Sustained remodelling and varying pattern of dyssynchrony

Using the ESC or AHA criteria for LBBB, 31% and 69% of patients were classified as non-LBBB, respectively. The additive benefit of SRSsept in non-LBBB was significant only when using strict AHA criteria **(Figure 4).** In LBBB patients however, simultaneous presence of high SRSsept ensured sustained remodelling when compared to high QRS$_{AREA}$ alone, both according to ESC (n=49 versus n=39) and AHA (n=23 versus n=19) criteria.

DISCUSSION

The most pertinent finding of the present prospective multicenter study is that both SRSsept and QRS$_{AREA}$ are associated with sustained reverse remodelling, after multivariable adjustment. More specifically, the identification of SRSsept ≥ 2.5%, rather than QRS$_{AREA}$ alone, appears to be especially of added value in achieving *sustained* remodelling in LBBB patients with high QRS$_{AREA}$.
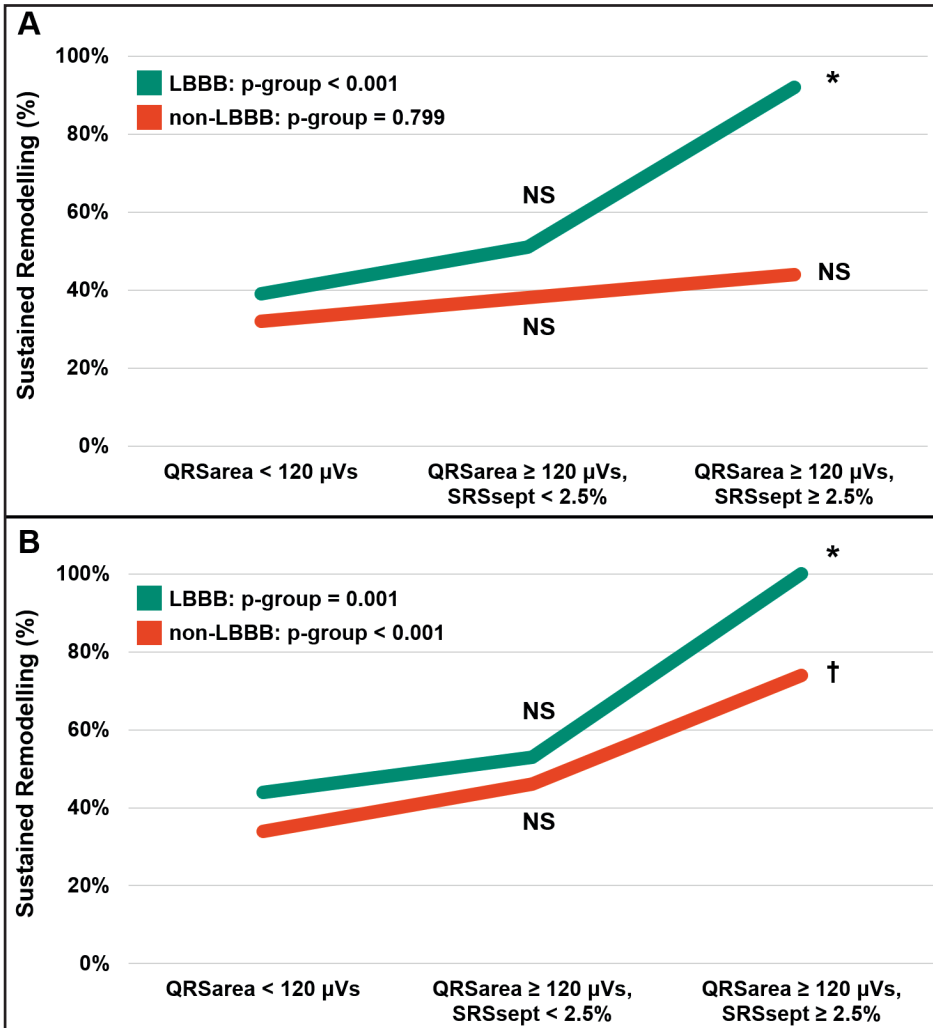
Figure 4. *Presence of mechanical discoordination in patients with high QRS$_{AREA}$ ensures sustained reverse remodelling in patients with LBBB (green) according to ESC (upper panel) or AHA (lower panel) criteria. * p < 0.001 compared to both categories; † p = 0.001 compared to QRS$_{AREA}$ < 120 µVs.*

Enhanced identification of electrical substrate using QRS$_{AREA}$

Despite an average QRS-duration of 180 ms, 39% of patients were non-responders. As such, current guideline criteria for an electrical substrate are incapable of ensuring a volumetric response. QRS$_{AREA}$ is derived objectively from the ECG, reflects LV activation delay, and is inversely associated with scar [15,16]. QRS$_{AREA}$ may as such be preferred above the more subjective QRS morphology [3]. The subjectivity of LBBB morphology is further underscored by our results, since the added benefit of SRSsept in non-LBBB patients was dependent on the definition used. Also, reduction of QRS$_{AREA}$ more strongly predicts

response to CRT than QRS duration or LBBB morphology [4]. In particular, QRS_{AREA} was independently associated with both all-cause mortality and echocardiographic response [4]. QRS_{AREA} therefore better reflects the electrical substrate amenable to resynchronization than its traditional counterparts, especially in patients with non-LBBB morphology, who would otherwise be deemed less suitable candidates for CRT [4,17]. It is currently unknown to which degree high levels of QRS_{AREA} can be found in patients with QRS duration below 130 ms, and whether these patients are likely to respond to CRT.

Indices of mechanical discoordination in CRT

Although apical rocking is an easy visual assessment, it is no quantifiable measure, subjectively assessed, and has limited inter-observer reproducibility [18]. In contrast to both IVMD and apical rocking, SRSsept was consistently of added value to elevated QRS_{AREA}, both at 6 and 12-month follow-up. Since a *reduction* of SRSsept, but not IVMD, is associated with reverse remodelling, SRSsept is also more likely to reflect the amenable mechanical substrate to CRT [19].

Discoordination-imaging in CRT patients aims to capture the contradictory contraction pattern that occurs during systole, and thereby quantify the extent by which LBBB causes LV dysfunction [19]. Because regional septal dysfunction is a major contributor to deteriorated LV function in CRT patients, SRSsept indirectly reflects LV discoordination as a whole [20]. Using a concept similar to our approach [7,10,19], myocardial work elegantly combines strain-imaging with a single non-invasive estimate of LV pressure [20,21]. Wasted myocardial work thereby essentially represents a measure of paradoxical systolic stretching, *indexed* to blood pressure.

Aalen et al. demonstrated higher predictive power of septal-to-LVlw work difference when compared to SSI in predicting reverse remodelling (AUC = 0.77 versus 0.73). In contrast to our work, simultaneous assessment of MRI-derived septal viability was used instead of QRS_{AREA}. [18]. Importantly however, MRI-derived septal viability was incorporated *only* into the analysis of myocardial work, whereas this was neglected with respect to SSI. In another recent study from Gorcsan et al. [13], similar or superior outcomes were reported using SSI in nearly 500 patients, when compared to myocardial work [18]. To date, no direct comparison between either method has been conducted investigating clinical endpoints. Regardless, SRSsept has previously been thoroughly investigated and should be considered a robust parameter with good intra-observer reliability [7,8,10]. Future studies, integrating electrical substrate assessment with both, septal dysfunction *and* septal viability, may demonstrate further improvement in response prediction.

Combined electrical and mechanical dysfunction ensures CRT response

Previous work already emphasized that no parameter, aimed at characterizing LV mechanical inefficacy, should be interpreted on its own, without also evaluating the

underlying electrical substrate. In particular, lack of sufficient electrical dyssynchrony (i.e., QRS-duration < 130 ms) generally precludes benefit from CRT, regardless of the presence of mechanical dyssynchrony [22]. Conversely, also in patients with QRS-duration ≥ 130 ms, non-electrical substrates such as (septal) scarring and myocardial stiffness may affect mechanical dysynchrony, which is unlikely to be corrected by CRT [9,18].

Our findings are therefore in agreement with this work, since we were unable to demonstrate additional benefit of SRSsept in patients with relatively low levels of baseline electrical dyssynchrony. However, over two-thirds of all patients with both elevated QRS$_{AREA}$ and SRSsept were classified as super-responders, with only one in ten patients becoming volumetric non-responders. In addition, over 90% of LBBB patients were sustained remodellers.

Clinical implications for strain-analysis

The identification of potential super-responders and sustained remodellers, as a surrogate marker of stable disease remission and subsequent sustained prognostic benefits [12], may be useful in the process of deciding which patients are eligible to receive CRT without an implantable cardioverter–defibrillator [23]. More appropriate discrimination between CRT with and without implantable cardioverter–defibrillator is especially valuable in low-to-middle income countries who maintain lower cost-effectiveness thresholds, thereby increasing referral and implant rates.

Unfortunately, because of previously conflicting results, echocardiographic analysis of mechanical dyssynchrony still holds no place in contemporary practice revolving patient selection for CRT [24]. Strain-based parameters of discoordination are however much more promising than timing-based indices, and should be further investigated in randomized trials [7,8,10,19]. New studies, prospectively investigating discoordination-indices, are therefore highly awaited. Especially given that the negative results from PROSPECT, which was a non-randomized study, were published well over a decade ago [24].

Study limitations

Our findings should be interpreted in the context of limitations inherent to its nonrandomized design. However, our results were derived prospectively from a relatively large sample size in a multicenter setting of unselected patients, were reproducible at multiple time points, and therefore robust. Moreover, core laboratory analysis minimized measurement variability for echo and QRS$_{AREA}$. For SRSsept, optimal image quality of the septum was ensured by acquiring focused septal views with high framerate in only 61% of cases. Also, although various vendors were used for image-acquisition, our use of vendor-independent software limited its influence on our results [25]. Conversely, with varying image-quality and different vendors, our study also reflects a real-world situation, and at the same time underscores how the quality of SRSsept may be improved

even further. Because no focused LVlw views were acquired for calculation of SSI, no definite conclusions can be drawn with respect to potential non-inferiority of SRSsept, relative to SSI.

Conclusion

Our work demonstrates, for the first time, the importance and practicability of the combined assessment of QRS_{AREA} and SRSsept in a real-world setting. Mechanical disco-ordination, in the presence of an underlying electrical substrate, ensures responsiveness to CRT with high certainty in the majority of patients. Discoordination-imaging may therefore be particularly useful in identifying super-responders and patients who will show sustained disease remission.

REFERENCES

1. K. Vernooy, C. J. M. Van Deursen, M. Strik, F. W. Prinzen. Strategies to improve cardiac resynchronization therapy. *Nat. Rev. Cardiol.* **11**, 481–493 (2014).

2. M. Brignole, A. Auricchio, G. Baron-Esquivias, *et al.* 2013 ESC Guidelines on cardiac pacing and cardiac resynchronization therapy: The Task Force on cardiac pacing and resynchronization therapy of the European Society of Cardiology (ESC). *Europace.* **15**, 1070–1118 (2013).

3. A. M. W. van Stipdonk, R. Hoogland, I. ter Horst, *et al.* Evaluating Electrocardiography-Based Identification of Cardiac Resynchronization Therapy Responders Beyond Current Left Bundle Branch Block Definitions. *JACC Clin. Electrophysiol.* **6**, 193–203 (2020).

4. M. A. Ghossein, A. M. W. van Stipdonk, F. Plesinger, *et al.* Reduction in the QRS area after cardiac resynchronization therapy is associated with survival and echocardiographic response. *J. Cardiovasc. Electrophysiol.* **32**, 813–822 (2021).

5. A. H. Maass, K. Vernooy, S. C. Wijers, *et al.* Refining success of cardiac resynchronization therapy using a simple score predicting the amount of reverse ventricular remodelling: results from the Markers and Response to CRT (MARC) study. *Europace.* **20** (2018). pp. e1–e10.

6. O. A. Smiseth, J. M. Aalen. Mechanism of harm from left bundle branch block. *Trends Cardiovasc. Med.* **29**, 335–342 (2019).

7. B. W. L. De Boeck, A. J. Teske, M. Meine, *et al.* Septal rebound stretch reflects the functional substrate to cardiac resynchronization therapy and predicts volumetric and neurohormonal response. *Eur. J. Heart Fail.* **11**, 863–871 (2009).

8. G. E. Leenders, B. W. L. De Boeck, A. J. Teske, *et al.* Septal rebound stretch is a strong predictor of outcome after cardiac resynchronization therapy. *J. Card. Fail.* **18**, 404–412 (2012).

9. J. Lumens, B. Tayal, J. Walmsley, *et al.* Differentiating Electromechanical from Non-Electrical Substrates of Mechanical Discoordination to Identify Responders to Cardiac Resynchronization Therapy. *Circ. Cardiovasc. Imaging.* **8**, e003744 (2015).

10. O. A. E. Salden, A. Zweerink, P. Wouters, *et al.* The value of septal rebound stretch analysis for the prediction of volumetric response to cardiac resynchronization therapy. *Eur. Heart J. Cardiovasc. Imaging.* **22**, 37–45 (2021).

11. R. M. Lang, L. P. Badano, V. Mor-Avi, *et al.* Recommendations for cardiac chamber quantification by echocardiography in adults: an update from the American Society of Echocardiography and the European Association of Cardiovascular Imaging. *Eur Hear. J Cardiovasc Imaging.* **28**, 1-39.e14 (2015).

12. P. W. X. Foley, S. Chalil, K. Khadjooi, *et al.* Left ventricular reverse remodelling, long-term clinical outcome, and mode of death after cardiac resynchronization therapy. *Eur. J. Heart Fail.* **13**, 43–51 (2011).

13. J. Gorcsan, C. P. Anderson, B. Tayal, *et al.* Systolic Stretch Characterizes the Electromechanical Substrate Responsive to Cardiac Resynchronization Therapy. *JACC Cardiovasc. Imaging.* **12**, 1741–1752 (2019).

14. I. Stankovic, C. Prinz, A. Ciarka, *et al.* Relationship of visually assessed apical rocking and septal flash to response and long-term survival following cardiac resynchronization therapy (PREDICT-CRT). *Eur. Heart J. Cardiovasc. Imaging.* **17**, 262–269 (2016).

15. F. Plesinger, A. M. W. van Stipdonk, R. Smisek, *et al.* Fully automated QRS area measurement for predicting response to cardiac resynchronization therapy. *J. Electrocardiol.* **63**, 159–163 (2020).

4

16.   E. B. Engels, M. Mafi-Rad, A. M. W. van Stipdonk, K. Vernooy, F. W. Prinzen. Why QRS Duration Should Be Replaced by Better Measures of Electrical Activation to Improve Patient Selection for Cardiac Resynchronization Therapy. *J. Cardiovasc. Transl. Res.* **9**, 257–265 (2016).

17.   A. M. W. van Stipdonk, I. Ter Horst, M. Kloosterman, *et al.* QRS Area Is a Strong Determinant of Outcome in Cardiac Resynchronization Therapy. *Circ. Arrhythm. Electrophysiol.* **11**, e006497 (2018).

18.   J. M. Aalen, E. Donal, C. K. Larsen, *et al.* Imaging predictors of response to cardiac resynchronization therapy: left ventricular work asymmetry by echocardiography and septal viability by cardiac magnetic resonance. *Eur. Heart J.* **41**, 3813–3823 (2020).

19.   P. C. Wouters, G. E. Leenders, M. J. Cramer, *et al.* Acute recoordination rather than functional hemodynamic improvement determines reverse remodelling by cardiac resynchronisation therapy. *Int. J. Cardiovasc. Imaging*. **37**, 1903–1911 (2021).

20.   K. Russell, M. Eriksen, L. Aaberge, *et al.* A novel clinical method for quantification of regional left ventricular pressure–strain loop area: a non-invasive index of myocardial work. *Eur. Heart J.* **33**, 724–733 (2012).

21.   F. W. Prinzen, J. Lumens. Investigating myocardial work as a CRT response predictor is not a waste of work. *Eur. Heart J.* **41**, 3824–3826 (2020).

22.   J. Beshai, R. Grimm, S. Nagueh, *et al.* Cardiac-resynchronization therapy in heart failure with narrow QRS complexes. *Hear. Metab.* **369**, 38 (2008).

23.   L. Køber, J. J. Thune, J. C. Nielsen, *et al.* Defibrillator Implantation in Patients with Nonischemic Systolic Heart Failure. *N. Engl. J. Med.* **375**, 1221–1230 (2016).

24.   E. S. Chung, A. R. Leon, L. Tavazzi, *et al.* Results of the Predictors of Response to CRT (PROSPECT) trial. *Circulation*. **117**, 2608–2616 (2008).

25.   W. M. Van Everdingen, A. H. Maass, K. Vernooy, *et al.* Comparison of strain parameters in dyssynchronous heart failure between speckle tracking echocardiography vendor systems. *Cardiovasc. Ultrasound*. **15**, 25 (2017).

SUPPLEMENTARY MATERIAL

Table S1. *Baseline characteristics of patients with paired volumetric data at 6 months.*

	Paired LVESVi (n=213)	Non-responders (n=83)	Responders (n=130)	P-value
Demographics				
Male sex – n (%)	132 (62)	59 (71)	73 (56)	0.031
Age (years)	66 ± 9.8	67±9	65±10	0.094
BSA (m^2)	1.9 (1.8-2.1)	2.0 (1.8-2.1)	1.9 (1.8-2.1)	0.304
ICM – n (%)	90 (42)	48 (58)	42 (32)	<0.001
NYHA class – n (%)				0.486
Class II	133 (63)	49 (59)	84 (65)	
Class III	79 (37)	34 (41)	45 (35)	
History of AF – n (%)	27 (13)	11 (13)	16 (12)	0.836
Diabetes – n (%)	56 (26)	24 (29)	32 (25)	0.525
Renal dysfunction – n (%)	10 (5)	4 (5)	6 (5)	1.000
Electrocardiography				
LBBB – n (%)*	138 (67)	43 (53)	95 (75)	0.001
QRS duration (ms)	178 (165-191)	174 (160-185)	180 (167-194)	0.028
QRS_AREA (μVs)	136 ± 47	117±41	147±47	<0.001
PR interval (ms)	185 (168-210)	187 (175-216)	184 (163-201)	0.224
Echocardiography				
LV EDV (mL)	180 (145-239)	179 (135-249)	180 (147-225)	0.392
LV ESV (mL)	135 (99-184)	133 (100-178)	135 (100-177)	0.316
LV ejection fraction (%)	26 ± 8	25±9	26±7	0.730
Apical rocking – n (%)	135 (63)	38 (46)	97 (75)	<0.001
Septal flash – n (%)	102 (50)	28 (35)	74 (59)	<0.001
IVMD (ms)	47 ± 29	37 ± 28	54 ± 27	<0.001
SRSsept (%)	2.9 ± 2.8	2.0 ± 2.1	3.5 ± 3.0	<0.001
SSI (%)	4.2 ± 3.3	3.0 ± 2.4	5.1 ± 3.6	<0.001

*Legend: AF, atrial fibrillation; EDV, end-diastolic volume; ESV, end-systolic volume; ICM, ischemic cardiomyopathy; LBBB, left bundle branch block; LV, left ventricular; IVMD, interventricular mechanical delay; SRSsept, systolic rebound stretch of the septum; SSI, systolic stretch index. * According to the ESC definition.*

Table S2. Differences in baseline characteristics based on electromechanical subgroups.

	Low QRS$_{AREA}$ (n=89)	Only high QRS$_{AREA}$ (n = 50)	High QRS$_{AREA}$ and SRSsept (n = 59)	P-value*
Demographics				
Male sex – n (%)	66 (74)	33 (66)	24 (41)	<0.001
Age (years)	66±9.3	66±9.3	65±11	0.579
BSA (m^2)	2.0 (1.8-2.1)	1.9 (1.8-2.1)	1.8 (1.7-2.0)	<0.001
ICM – n (%)	40 (56)	16 (33)	18 (31)	0.006
NYHA class – n (%)				<0.001
Class II	34 (47)	41 (85)	39 (66)	
Class III	37 (51)	7 (15)	20 (34)	
History of AF – n (%)	14 (19)	5 (10)	5 (9)	0.145
Diabetes – n (%)	25 (35)	14 (29)	11 (19)	0.122
Renal dysfunction – n (%)	6 (8)	0 (0)	4 (7)	0.133
Electrocardiography				
LBBB – n (%)*	31 (43)	40 (83)	50 (85)	<0.001
QRS duration (ms)	164 (155-178)	183 (172-195)	187 (177-200)	<0.001
QRS$_{AREA}$ (µVs)	90±18	159±34	167±40	<0.001
PR interval (ms)	192 (176-223)	180 (162-202)	178 (165-199)	0.002
Echocardiography				
LV EDV (mL)	174 (149-249)	184 (140-229)	177 (147-242)	0.787
LV ESV (mL)	131 (97-183)	138 (100-180)	133 (104-191)	0.771
LV ejection fraction (%)	26±7.9	26±8.6	25±8.2	0.492
Apical rocking – n (%)	36 (50)	28 (58)	51 (86)	<0.001
Septal flash – n (%)	29 (34)	29 (58)	35 (63)	<0.001
IVMD (ms)	34±28	53±28	61±25	<0.001
SRSsept (%)	1.7±2.0	1.1±0.7	5.8±2.3	<0.001
SSI (%)	2.6±2.4	2.9±1.6	7.3±2.9	<0.001

*Legend: AF, atrial fibrillation; EDV, end-diastolic volume; ESV, end-systolic volume; ICM, ischemic cardiomyopathy; LBBB, left bundle branch block; LV, left ventricular; IVMD, interventricular mechanical delay; SRSsept, systolic rebound stretch of the septum; SSI, systolic stretch index. * According to the ESC definition.*

Table S3. *Simple multivariate logistic regression model for sustained volumetric response.*

	Response at 6 months		Sustained response	
	OR [95%CI]	P-value	OR [95%CI]	P-value
Constant	3.361	0.332	10.607	0.080
Age (per year)	0.969 [0.935-1.004]	0.078	0.946 [0.910-0.983]	0.006
High QRS$_{AREA}$ (yes)	2.703 [1.350-5.413]	0.005	2.468 [1.149-5.301]	0.021
High SRSsept (yes)	1.989 [0.949-4.170]	0.069	2.192 [1.015-4.737]	0.046
Apical rocking (yes)	2.285 [1.124-4.645]	0.022	2.642 [1.217-5.734]	0.014

Legend: β, logistic regression coefficient OR, odds ratio; CI, confidence interval; SRSsept, systolic rebound stretch of the septum.

4

Table S4. *Parameters of left ventricular dyssynchronous dysfunction determining a volumetric response, six months after cardiac resynchronization therapy.*

Predictor	AUC	P-value	Cut-Off	Positive	Negative	Sens (%)	Spec (%)
QRSarea < 120 µVs (n = 72)							
SRSsept	0.443	0.416	≥ 2,5%	16	54	17%	72%
IVMD	0.576	0.286	≥ 40 ms	27	43	43%	64%
ApRock	0.471	0.671	Present	36	36	47%	48%
QRSarea ≥ 120 µVs (n = 113)							
SRSsept*	0.727	0,000	≥ 2,5%	59	48	67%	79%
IVMD	0.694	0,001	≥ 40 ms	81	26	79%	57%
ApRock*	0.721	0,000	Present	32	31	84%	61%

* p-value < 0.01, when compared to QRS$_{AREA}$ < 120 µVs.
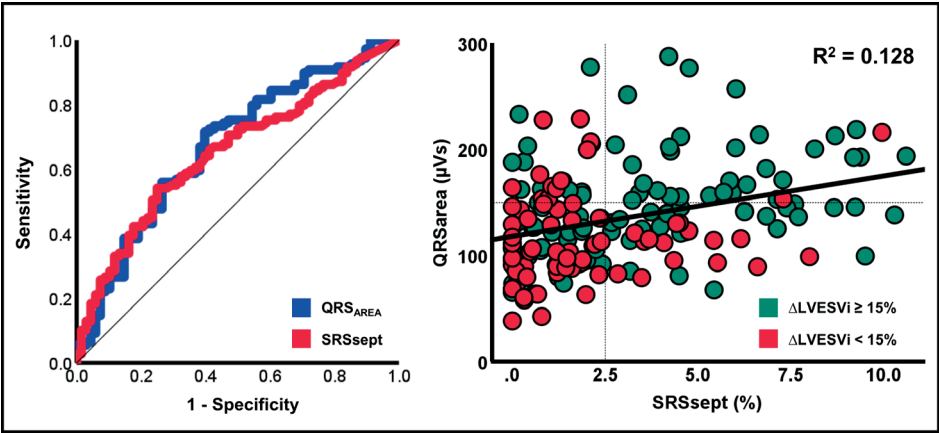
Figure S1. *Optimal cut-off values were produced for QRS$_{AREA}$ and SRSsept (A), which are two largely distinct mechanisms of LBBB-induced dyssynchronopathy (B).*

PART II

TAILORING LEAD PLACEMENT

5

Optimizing Lead Placement for Pacing in Dyssynchronous Heart Failure: the Patient in the Lead

Philippe C. Wouters, Kevin Vernooy, Maarten J. Cramer, Frits W. Prinzen, Mathias Meine.

ABSTRACT

Cardiac resynchronisation therapy (CRT) greatly reduces morbidity and mortality in patients with dyssynchronous heart failure. However, despite tremendous effort, response has been variable and can be further improved. Although optimizing left ventricular lead placement (LVLP) is arguably the cornerstone of CRT, the procedure of LVLP using the transvenous approach has remained largely unchanged for over two decades. Improvements have been developed using scar location and electrical and/ or mechanical mapping. Moreover, recent interest in conduction system pacing (CSP) as an alternative to biventricular pacing emerged. CSP is promising, but may not be suitable for all patients with dyssynchronous heart failure. This review underscores the importance of a patient-tailored approach and discusses the potential applications of both CSP and targeted biventricular CRT.

INTRODUCTION

Biventricular pacing (BVP) has been an established device therapy in the treatment of patients with dyssynchronous heart failure (HF) for over 20 years now, but various challenges remain [1]. The cornerstones of obtaining maximal response in cardiac resynchronization therapy (CRT) is optimizing left ventricular (LV) lead placement (LVLP) [2]. It is therefore striking that the actual procedure of lead implantation has remained largely unaltered, with the majority of leads being placed empirically, without evaluation of the underlying electromechanical substrate. As an alternative to conventional BVP, two distinct approaches to improve contemporary LVLP are being investigated.

One method of optimizing LVLP is by stimulating the native conduction system (i.e. conduction system pacing [CSP]), which drastically alters the way we place the LV lead altogether. Alternatively, LVLP may also be improved by using a guided and target-based approach for transvenous lead deployment [1]. Although CSP and targeted BVP both seem promising, determining the optimal LVLP can be difficult. Not only is it unclear which patients would benefit from CSP compared to BVP, but, equally important, uncertainty exists concerning how to determine the optimal pacing target in BVP. In this review, we discuss the potential applications and shortcomings of both approaches and forward the importance of a target-based approach that is tailored to the patient. The etiology of LV conduction delay and mechanisms that complicate CSP and targeted BVP also are discussed.

Heterogeneity of abnormal left intraventricular conduction

Various conditions that result in scar or fibrosis may cause functional and/or structural damage to the His-Purkinje system or LV myocardium **(Figure 1)** [3]. In turn, significantly impaired inter- and intraventricular conduction may occur. An important conduction delay is characterized by QRS-prolongation (QRS ≥ 130 ms) on the surface ECG, but considerable heterogeneity among left bundle branch block (LBBB) patterns exists [4]. These differences are dependent on the location (proximal versus distal and myocardial) and the extent (focal versus diffuse) of the lesion causing the conduction disorder. Consequentially, not all cardiac segments will necessarily exhibit the same extent of activation delay. Pacing a segment that exhibits significantly more electrical dyssynchrony will therefore result in more pronounced reduction in LV activation times than can be achieved by pacing relatively early activated segment [5]. It can therefore be argued that, for BVP, differences in ventricular activation warrant different positions of the LV lead in order to obtain optimal resynchronization. To this end, accurate distinction between true LBBB and non-LBBB seems important. Although specific ECG-criteria for LBBB have been defined, various definitions exist and lack of inter-observer agreement complicates clinical decision making [6]. Moreover, impaired myocardial conduction can mimic LBBB

QRS-morphology, even in the absence of concomitant His-Purkinje lesions [7]. Interpretation of the LBBB-ECG can therefore be difficult and misleading, since a variety of distinct septal and LV activation patterns are concealed [8]. Regardless of ECG-classification, both subgroups (i.e. LBBB and non-LBBB) are treated using the same empirical approach of transvenous LVLP. This in part explains the lower response rates associated with non-LBBB, despite the potential presence of an electrical substrate that is amendable to CRT [9].

Proximal and distal left bundle-branch block

To determine the best pacing strategy in LBBB, it is crucial to know where the conduction disorder is located. The term LBBB is often used interchangeably as both a clinical condition and an anatomical entity. Anatomically speaking however, an LBBB pattern is not necessarily located within the left bundle branch itself. This became particularly clear after a study from Narula as early as 1977, where full normalization of the QRS complex was reported after pacing the His-bundle in patients with LBBB [10]. It was however not until recently that Upadhyay et al. clearly showed that nearly half of patients with LBBB have a proximal conduction block [8]. In the case of 'proximal' LBBB, lesions are actually localized *within* the bundle of His (i.e. left intrahisian block). As a result, electrical impulses are blocked at this point, and left intraventricular activation ensues solely after (undisrupted) activation of the right ventricle (RV) has reached the LV endocardium through transseptal conduction [3]. Electrical impulses thereby bypass the native conduction system but rather are transmitted through the myocardium. The result is significantly delayed LV activation, which often occurs in a distinct homogenous fashion.

A 'distal' LBBB is present in about 18% of patients with LBBB QRS-morphology [8]. Here, the block is located below the His-bundle (i.e. infrahisian block), within the left bundle branch itself. LV conduction is blocked along the trajectory of the left bundle fascicles, and intraventricular activation continues following a similar pattern of transseptal activation originating from the RV. Importantly, the variability in the location of a conduction block in patients with LBBB was elegantly demonstrated by Upadyay et al. as well. Despite complying with strict definitions of LBBB, mapping studies revealed that one-third of LBBB-patients have intact His-Purkinje activation and normal transseptal activation times **(Figure 1)** [8,11]. This suggests that the cause of the electrical delay likely lies elsewhere in the LV myocardium, despite exhibiting an LBBB morphology.

Nonspecific intraventricular conduction delay

Lastly, nonspecific intraventricular conduction delay can also be present. Here, more complex and heterogeneous patterns of ventricular activation are present [4]. These patterns can be reflected on the ECG as a broad QRS complex in the absence of typical features of right bundle branch block (RBBB) and LBBB. In the context of an underlying
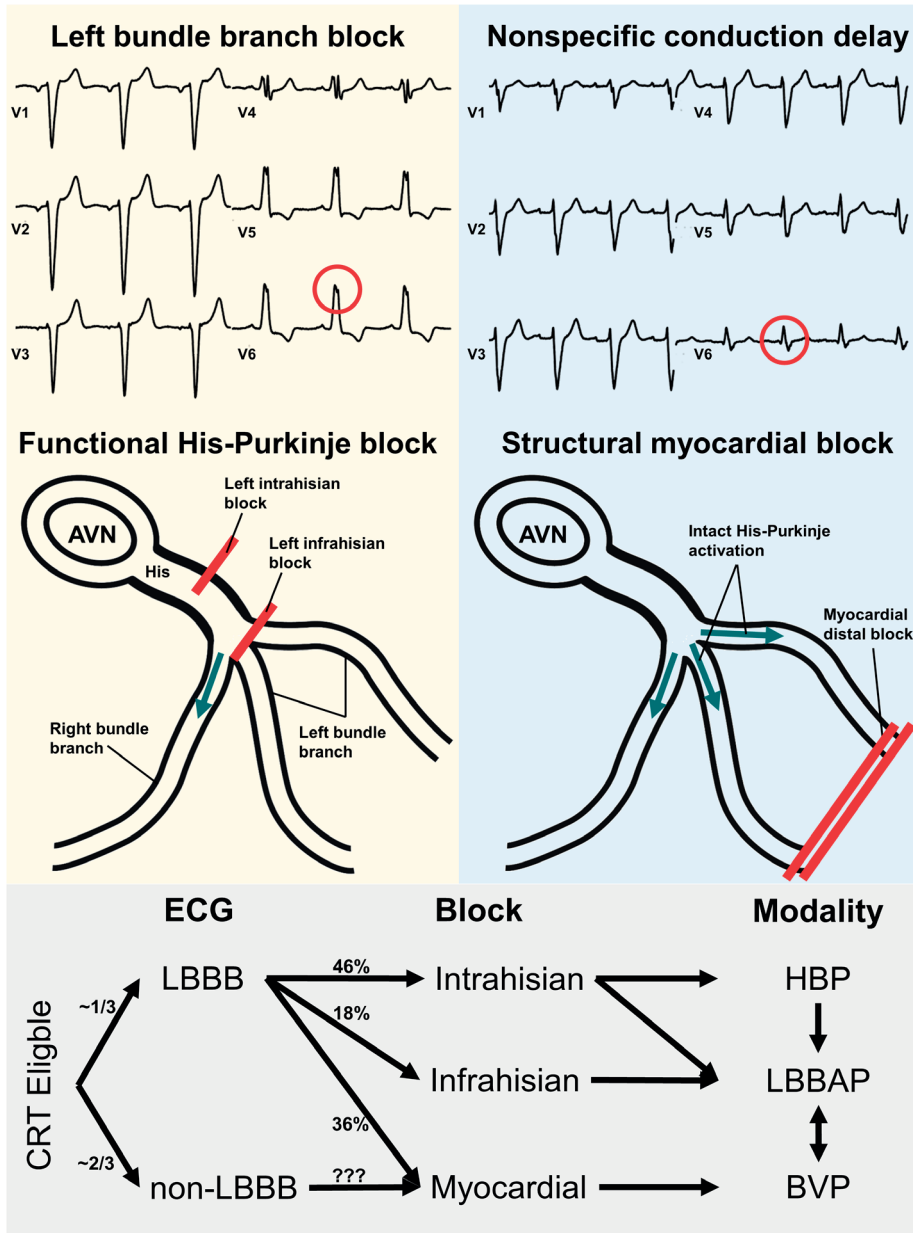
Figure 1. *Differences in the origin of conduction block that result in left bundle branch block morphology. A typical LBBB morphology on the surface ECG may originate from a conduction block in the bundle of His, left bundle branch or elsewhere in the myocardium (i.e. intact His-Purkinje activation). The latter is most frequently seen in non-typical LBBB morphology. Legend: BVP, biventricular pacing; CRT, cardiac resynchronization therapy; HBP, His-bundle pacing; LBBAP, left bundle branch area pacing; LBBB, left bundle branch block.*

electrical substrate that can be corrected by CRT, these patients are commonly referred to as non-LBBB [9]. Derval et al. performed invasive 3D electroanatomic mapping to illustrate the fundamental differences in LV activation patterns in non-LBBB (average QRS ~150ms) when compared to LBBB (AHA/HRS/ACC criteria) [4]. Purkinje potentials at the site of LV endocardial breakthrough were identified in all non-LBBB patients, whereas this was never the case for LBBB [4]. In addition, non-LBBB was characterized by activation that originated from multiple (instead of a single) endocardial LV breakthroughs at the septum, with distinct areas of localized pockets of slow conduction along the LV free wall. Consequentially, failing to meet both Strauss and AHA/HRS/ACC criteria (i.e. non-LBBB) reliably excludes damage to the His-Purkinje system with a specificity of 91% [8]. Although CRT in patients with non-LBBB is debatable, 30% to 50% of these patients exhibit dominant LV electrical delay that is amendable to CRT [9,12]. As such, they should not be withheld from treatment.
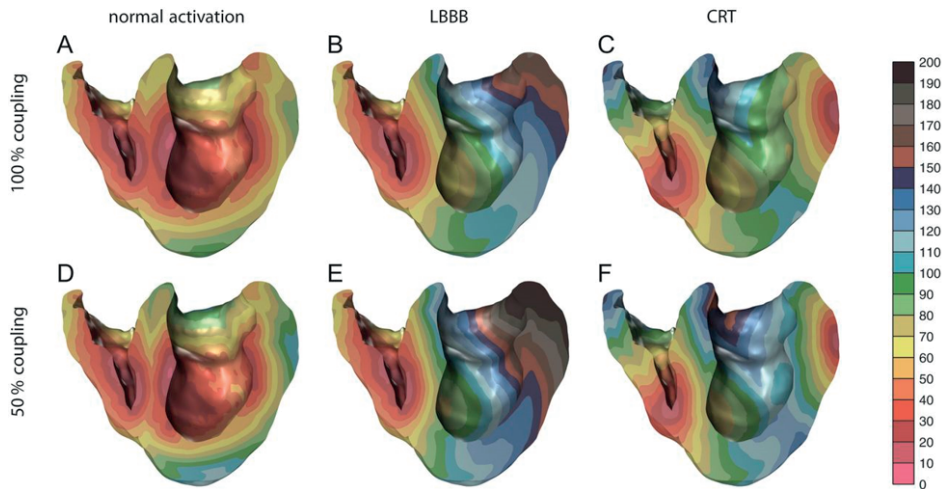
Figure 2. *Simulated ventricular electrical activation patterns in patients with (lower panel) and without (upper panel) electromechanical uncoupling. In contrast to normal activation (A), electrical activation delay with LBBB-morphology may be cause by functional lesions within the native conduction system (B) or structural myocardial damage (D). Co-existing structural and functional lesions further aggravate this delay (E), which can be less effectively resynchronized (F) when compared to LBBB alone (C). Reproduced from Potse et al. by permission of Oxford University Press* [7].

The challenge of electromechanical dissociation

Mechanical discoordination, when caused by electrical dyssynchrony, is thought to contribute to impaired LV function and is therefore an important substrate for CRT as well [13]. Importantly, the extent of electromechanical uncoupling is variable and dependent on electrical and nonelectrical substrates, including regional hypocontractiliy and myocardial scar **(Figure 2)** [7,14]. Here, lack of coupling implies electrical depolarization of a cardiac segment without synchronous myocardial fiber shortening. Due to uncoupling

however, sites of latest mechanical activation occur more frequently in a non-laterally located segment than electrical activation, which complicates selection of optimal transvenous LVLP [14]. Based on our understanding of conduction disorders that cause dyssynchrony, two distinct approach to enhance LVLP in dyssynchronous HF can be proposed **(Figure 1)**.

Current and future approaches to resynchronization

In contrast to resynchronizing the heart by pacing both ventricles near-simultaneously in BVP, direct stimulation of the His-Purkinje system through CSP is possible as well. To this end, there has been a resurgence in interest for His-bundle pacing (HBP) in CRT. Other alternative strategies for CSP include left bundle branch pacing (LBBP) and LV septal pacing (LVSP). Because of their practical overlap, both are collectively referred to as left bundle branch area pacing (LBBAP) [15]. Unlike HBP and LBBP however, LVSP activates fast conducting superficial subendocardial fibers and therefore does not require capture of the native conduction system [16]. CSP allows for physiological ventricular activation with fast (endocardial-initiated) impulse conduction, evidenced by near complete normalization of the QRS **(Figure 3)** [17].

Comparing conduction system pacing to biventricular pacing

The primary benefit of CSP is its potential to establish physiological ventricular activation. Additional advantages of CSP include the independence from limited venous access or phrenic nerve stimulation. Although Abdelrahman et al. demonsrated the feasibility and effectiveness of HBP in patients with a standard RV-pacing indication, few studies are performed where HBP was applied in a cohort of patients with dysysnchronous HF [18]. Huang et al. demonstrated in 56 patients that, after a three year follow-up, patients who received permanent HBP drastically improved their LV ejection fraction (LVEF) by over 50% of baseline value [17]. Nonetheless, in ~25 to 50% of patients, permanent HBP is not feasible due to fixation failure or inadequate thresholds necessary for the correction of LBBB, despite complying with criteria for LBBB morphology [17,19]. These findings are in line with the mapping study of Upadhyay et al., who demonstrated that less than half of patients with a strict LBBB pattern had a true intrahisian conduction block [8].

Because the relatively low percentage of patients with intrahisian block, LBBAP may be a more interesting approach of CSP in the majority of patients. LBBAP requires less precision than HBP and lower and more stable pacing capture thresholds can be achieved [15]. LBBP therefore circumvents many of the technical limitations of HBP, resulting in a significantly better feasibility of 90-98% in LBBB patients [20]. Moreover, LVEF-improvement after HBP and LBBP is near-identical, but significantly better than during BVP (24% versus 17%) [19]. A recent study showed the first results for LVSP in 27 patients [16].

LVSP resulted in more pronounced QRS reduction than BVP, although acute hemodynamic benefit (AHB) appeared to be similar when compared to conventional CRT [16].

Taken together, both HBP and LBBAP are exciting alternatives to conventional BVP with promising early evidence of safety and efficacy. Lead positioning in LBBAP is however less critical than during HBP, rendering it less technically challenging and more widely applicable for the majority of patients and implanters. Unfortunately long term results concerning safety (e.g. dislodgement, potential septal perforation, challenging lead extraction) and hard clinical endpoints in large randomized trials are still lacking. Moreover, because a key aspect of LVSP is to bypass slow conduction across the septum (30 to 70 ms in LBBB), it remains to be investigated whether LBBAP can resynchronize LV activation in patients with normal septal activation. It is in this regard important to realize some LBBB and most non-LBBB patients have intact Purkinje activation and exhibit LV activation onset within the septum that is comparable to that of patients with narrow QRS **(Figure 2; B versus D)** [4,7]. CSP may therefore be best suited for LBBB patients with a functional His-Purkinje lesion (i.e. potential super-responders), although these patients may invariably improve with BVP as well **(Figure 1)**. In non-LBBB however, optimally targeting the LV free wall (i.e. BVP) seems more appropriate [9].
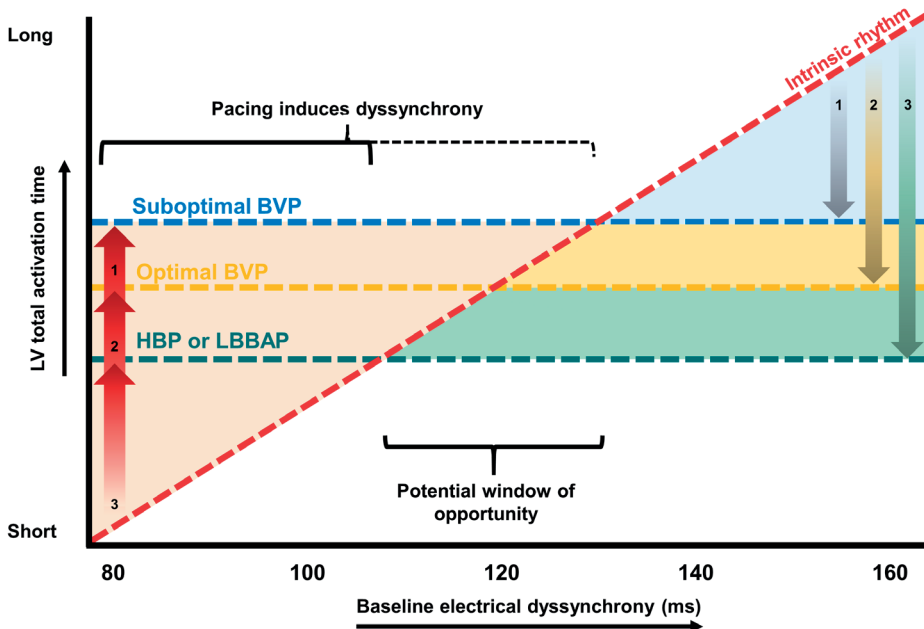
Figure 3. The effect of various pacing modalities on LV activation time. The effect of BVP (dotted blue or yellow line) and CSP (dotted green line) on LV total activation time are illustrated. Depending on the amount of baseline electrical dyssynchrony without pacing (dotted red line), pacing can be beneficial (downward arrows) or potentially detrimental (upward arrows). When compared to BVP with a suboptimal LV lead position (arrow 1), total LV activation time can be decreased further when an optimal position is ensured (arrow 2), or when CSP is applied (arrow 3). Note that, in theory, patients with low baseline dyssynchrony may also benefit from CSP. Based on data from Ploux et al. [12]. For abbreviations, please see Figure 1.

The fallacy of empirical lead placement in CRT

### RV lead position and LV-only pacing

Studies that investigated whether a non-apical RV-load position, closer to the His-Purkinje system, could improve outcome in CRT found no differences in echocardiographic or clinical endpoints as opposed to a conventional RV-lead position [21]. However, paced effects (e.g. interlead delays) were not used to determine optimal RV-lead position. Alternatively, preserving intrinsic conduction via the right bundle branch altogether in LV-only pacing appears to be a safe but non-superior alternative to BVP [22]. Most studies were however limited by suboptimal comparison between BVP and LV-only pacing, since the important aspect of fusion with intrinsic right bundle conduction during LV-only pacing was not always taken into consideration [23]. The ongoing AdaptResponse trial investigates RV-synchronized LV-only fusion pacing compared to BVP, and will be the first trial that is sufficiently powered to assess hospitalization and mortality outcomes [24]. It remains to be investigated whether the potential utility of RV-paced wavefronts in reducing transseptal conduction times is a prerequisite for optimal resynchronization in selected patients [25]. This may hold especially true in LV-only patients where fusion with the right bundle conduction is inadequate. It is in this regard important to note that fusion is highly sensitive to the intrinsic atrioventricular conduction time [26].

The optimal LV pacing site is patient specific

Accumulated evidence in over 4200 patients from various landmark trials taught us that, on group level, no single site is *consistently* superior (or inferior) to another with respect to long term outcome [21,27,28]. Conversely, the inter- and intra-individual heterogeneity of the optimal LV pacing site becomes apparent in many interventional studies where AHB was systematically explored during BVP at various sites. Pacing a suboptimal site improves the maximum rate of LV pressure rise (dP/dt_{max}) on average by ±13%. Combining the results of all studies suggests that this can be further improved by an additional 9 percentage points (range 3-16%) when the optimal site is targeted **(Figure 4; Supplemental Table 1)** [2,29]. Although the question remains to what extent AHB contributes to clinical improvement, each patient will benefit from the largest improvement of LV function [30]. We should acknowledge that hemodynamic variation may in part originate from bias caused by multiple measurements, physiological variability and analytical error of dP/dt_{max} assessment. Nonetheless, most studies limited the amount of samples and prevented bias by rigorous methodology.

The robustness of these findings as a whole is also underscored by a more recent study. Van Everdingen et al. demonstrated that considerable intra-individual hemodynamic variation occurs even among different electrode configurations of a quadripolar lead, spaced at minimum just 20 mm apart [31]. This may be explained by the substantial but unpredictable differences in LV propagation seen upon electrocardiographic imag-

ing, despite pacing adjacent LV electrodes [32]. We may therefore conclude that the influence of a variety of factors on optimal LVLP is reflected by the large individual variation in paced effects and hemodynamics, and LVLP is highly patient specific. Since measures of both LV dP/dt$_{max}$ and stroke work were consistent across all studies, these findings emphasize the need for individualized targeting of the optimal pacing site [30]. In line with this, one study proved that successfully pacing a pre-defined and patient-specific segment resulted in more pronounced AHB when compared to empirical placement [33]. It is therefore not surprising that simply adding LV-pacing vectors through multipoint pacing is not necessarily beneficial when compared to optimized BVP, supporting the notion that optimizing lead placement is at least equally important [31,34]. Conversely, because BVP (i.e. epicardial LV-stimulation) is hampered by relatively slow wavefront propagation, adequate depolarization may be particularly difficult to achieve in patients with very pronounced LV dilatation [35]. Whether programming multipoint pacing with the widest electrode spacing and minimal delay can result in better outcomes, which may be especially useful in non-LBBB patients and/or clear LV enlargement, remains to be demonstrated [31,34,35]. One important question remains however: besides avoiding in-scar pacing, on what basis should we determine the optimal location for LVLP [36]?
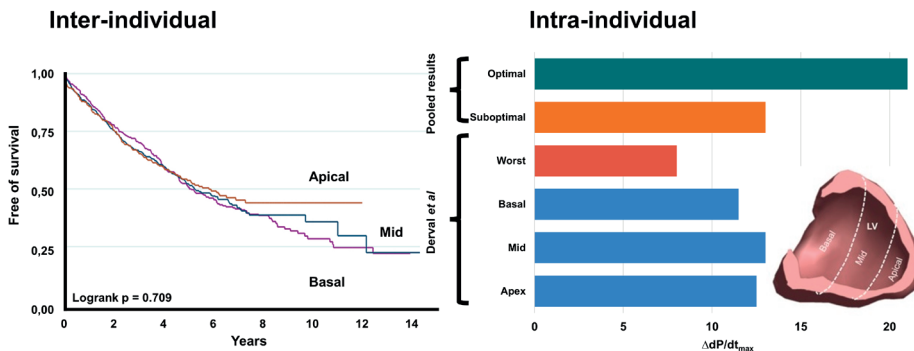
Figure 4. *The fallacy of empirical transvenous lead placement. On group level, similar clinical outcomes are reported concerning total mortality regardless of left ventricular lead location (left panel, from Leyva et al. [21]). Alternatively, the pooled results of Derval et al. and various other acute hemodynamic studies demonstrate the potential improvement when targeting the patient-individual optimal segment instead of a conventional location [29]. Importantly, no one site is consistently superior to others, underscoring the unpredictability and heterogeneity of the optimal target amongst different patients (right panel). For further reading, please see Supplementary Table 1.*

Targeted lead placement in biventricular CRT

Electrically guided

Gold et al. found that BVP with the lead positioned at the longest electrical delay (e.g. higher QLVs) correlates to increased AHB and predicts reverse remodeling [37]. Importantly, while QLVs may be used to select the optimal vein, QLVs cannot be used for selection of the optimal electrode of a quadripolar lead when placed in an already optimal

area [32,38]. A possible explanation is that a correlation with LV end-systolic volume (LVESV) reduction seems driven by shorter QLV values (cut-off value of ~95 ms) and appears to be most applicable when large disparities between the measured QLV are present [5,38]. Moreover, when compared to an anatomical approach, QLV-guided implantation may only be beneficial in patients with typical LBBB morphology [39].

Because of small differences in intrinsic activation delay when LVLP is already optimal, electrical indices such as LV-paced to RV-sensed wavefront propagation (i.e. LVp-RVs) correlate poorly to QLV as well [32]. LV-paced activation effects are therefore highly unpredictable when based on stimulation site alone, despite widely variable acute electrical responses [32,38]. Where QLV is a measure of *intrinsic* electrical dyssynchrony, the difference between left and right paced-to-sensed interlead delays (LVp-RVs > RVp-LVs) can be used as a measure of *paced* LV-dyssynchrony. Paced LV-dyssynchrony is associated with scar and local electrical disturbances and is independently associated with non-response, even in addition to QLV [40,41]. Regardless, paced-to-sensed interlead delays are not associated with LVLP or acute stroke work increase, underscoring the heterogeneity of optimal LVLP [38]. Additionally, LV latency as indicated by stimulus-to-QRS onset ≥ ~40 ms can also be measured, which may be used to predict mortality and HF-hospitalization [42]. Although LV latency is associated with ischemic etiology, its presence can be related to any cause of impaired impulse propagation, prolonged refractoriness or conduction disorders. Alternatively, pre-implantation electrocardiographic imaging (e.g. body surface mapping or ECG-imaging), or paced reduction of QRS_{AREA} may allow for more accurate distinction between optimal and suboptimal cardiac segments [9,43].

5

Table 1. *Prospective image-guided studies with a control group investigating targeted lead placement.*

Study	Bai et al.[48]	Khan et al. [44]	Saba et al.[45]	Sommer et al.[49]	Bertini et al.[46]	Stephansen et al.[50]
Patients (No.)	104	220	187	182	100	122
Design	Cohort	RCT	RCT	RCT	Cohort[†]	RCT
Blinded	Yes	Yes	Yes	Yes	NR	Yes
Method	Echo[‡]	Echo	Echo	CT and Echo	Echo and MRI[§]	Echo, Rb-PET, CT
Male (%)	67	79	73	79	75	75
LBBB (%)	100	99	53	100	53	100
QRS (ms)	154	158	159	166	155	169
ICM (%)	59	56	62	49	47	50
ΔLVESV (%)						
Guided	33[¶]	46±33	30±29	34±23	39[¶]	25±36
Control	13	26±23	20±25	33±23	22	22±23
p-value	0.428	0.001	P<0.05	NS	NR	0.71

[†] With retrospective control group; [‡] intracardiac echocardiography coupled with vector velocity imaging; [§] > 75% LGE In ICM or subendocardial fibrosis for NICM; [¶] No relative reduction reported, calculated from group results. Legend: NR, not reported; NS = not significant.

Image-guided

Three out of six studies comparing image-guided LVLP with an empirical approach report significantly more reverse remodeling and/or percentage of responders in the treatment group [44–46] **(Table 1)**. However, in the TARGET and STARTER studies, assessment of strain at the apex could not be performed, even though an apical position may be optimal in a substantial amount of patients **(Supplemental Table 2)** [21]. Although, the utility of strain for detecting scarred segments is poor with a sensitivity of only 33%, these positive effects can therefore not solely be attributed to targeting the latest mechanically activated segment [47].
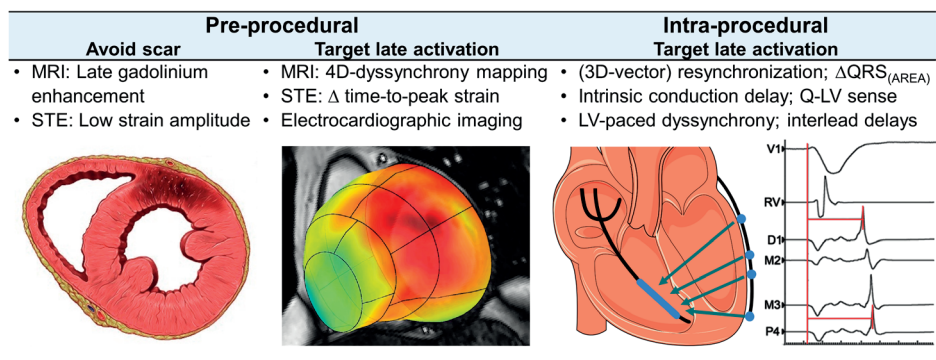
In contrast to TARGET and STARTER, two studies allowed targeting electrically delayed segments using QLV-guidance in the control group and were unable to demonstrate significant differences in reverse remodeling between both groups [49,50]. Stephansen et al., who performed QLV-mapping in any accessible coronary sinus branch, concluded that this approach is equally effective when compared to an echo-guided approach based on a mechanical delay [50]. Importantly however, procedure time was significantly longer, radiation doses were higher, more in-scar pacing occurred, and optimization of inter-ventricular pacing delay was only performed in the electrically-guided group. Lastly, it should be considered that LVLP in patients with LBBB and QRS duration ≥ 150 ms is less critical, since these patients already have a clear electrical substrate, regardless of the segment targeted [12]. In line with this, superior outcomes associated with image-guided LVLP in the STARTER trial were almost completely driven by patients with non-LBBB and patients with QRS duration below 150 ms [51].

Which modality should we use for guidance?

Various methods to determine optimal lead location can be considered before and during implantation of a biventricular pacemaker **(Figure 5)**. It is in this regard of particular importance that in-scar pacing is avoided, due to its 6-fold increased risk of cardiovascular death or HF-hospitalisation [36]. In LBBB patients, an electrically guided approach may be non-inferior compared to an image-guided approach [50]. In patients with non-LBBB morphology however, image-guided LVLP resulted in superior outcome compared to contemporary placement, whereas a QLV-guided approach failed to do so [39,51]. While the previously mentioned limitations of an electrically-guided approach should be considered, image-guided approaches may have insufficiently utilized potential as well.

Because better outcomes are associated when targeting late LV electrode activation and optimizing paced-to-sensed interlead delays, (further) improving LVLP during the procedure can also be considered [5,40–42]. Intra-individually however, LV-paced electrical effects are highly variable, unpredictable, and correlate poorly to intrinsic electrical delay [32,38]. Finally, knowing where to optimally place the lead is meaningless when a target cannot be reached, and suboptimal positions can only be partly improved by optimiz-

ing device programming [2]. The difficulty and variability of targeted LVLP is illustrated by the frequency of within-target LVLP, ranging from 30 to 63% between all studies **(Supplemental Table 2)**. Whether *intra-operative* visualization of optimal targets, for example using fusion with fluoroscopy, can increase these numbers warrants further investigation.

Pre-procedural		Intra-procedural
Avoid scar	**Target late activation**	**Target late activation**
• MRI: Late gadolinium enhancement • STE: Low strain amplitude	• MRI: 4D-dyssynchrony mapping • STE: Δ time-to-peak strain • Electrocardiographic imaging	• (3D-vector) resynchronization; $\Delta QRS_{(AREA)}$ • Intrinsic conduction delay; Q-LV sense • LV-paced dyssynchrony; interlead delays

5

Figure 5. Examples of pre- and intra-procedural methods for selecting the optimal left ventricular lead location. The optimal target for left ventricular lead placement is determined by assessing scar tissue (left) and electromechanical activation patterns (middle). In addition, various paced effects can be considered to further assist implanting physicians during the procedure. The list is not all-encompassing. Legend: LV, left ventricular; MRI, magnetic resonance imaging; STE, speckle-tracking echocardiography.

CONCLUSION

Amongst patients eligible for CRT there is great diversity of both the extent and location of conduction disorders causing an electromechanical delay. Unfortunately, this distinction cannot be made based on the surface ECG and does not influence LVLP in our current practice. Contemporary lead placement in BVP is therefore hampered by an empirical approach, despite clear evidence for considerable intra-individual variation in the segment that results in optimal AHB. As an alternative to BVP, future strategies presumably include HBP for patients with conduction disorders within the bundle of His, and LBBAP in patients exhibiting infrahisian block. However, patients with non-LBBB have normal septal activation and are therefore less likely to benefit from CSP. BVP with the LV lead targeted away from scar and towards late activated segments may provide the best results for these patients.

REFERENCES

1. K. Vernooy, C. J. M. Van Deursen, M. Strik, F. W. Prinzen. Strategies to improve cardiac resynchronization therapy. *Nat. Rev. Cardiol.* **11**, 481–493 (2014).

2. M. D. Bogaard, P. A. Doevendans, G. E. Leenders, *et al.* Can optimization of pacing settings compensate for a non-optimal left ventricular pacing site? *EP Eur.* **12**, 1262–1269 (2010).

3. N. Y. Tan, C. M. Witt, J. K. Oh, Y.-M. Cha. Left Bundle Branch Block. *Circ. Arrhythmia Electrophysiol.* **13**, e008239 (2020).

4. N. Derval, J. Duchateau, S. Mahida, *et al.* Distinctive Left Ventricular Activations Associated with ECG Pattern in Heart Failure Patients. *Circ. Arrhythmia Electrophysiol.* **10**, e005073 (2017).

5. M. R. Gold, U. Birgersdotter-Green, J. P. Singh, *et al.* The relationship between ventricular electrical delay and left ventricular remodelling with cardiac resynchronization therapy. *Eur. Heart J.* **32**, 2516–2524 (2011).

6. A. M. W. van Stipdonk, R. Hoogland, I. ter Horst, *et al.* Evaluating Electrocardiography-Based Identification of Cardiac Resynchronization Therapy Responders Beyond Current Left Bundle Branch Block Definitions. *JACC Clin. Electrophysiol.* **6**, 193–203 (2020).

7. M. Potse, D. Krause, L. Bacharova, *et al.* Similarities and differences between electrocardiogram signs of left bundle-branch block and left-ventricular uncoupling. *EP Eur.* **14**, v33–v39 (2012).

8. G. A. Upadhyay, T. Cherian, D. Y. Shatz, *et al.* Intracardiac Delineation of Septal Conduction in Left Bundle-Branch Block Patterns: Mechanistic Evidence of Left Intrahisian Block Circumvented by His Bundle Pacing. *Circulation.* **139**, 1876–1888 (2019).

9. O. A. E. Salden, K. Vernooy, A. M. W. van Stipdonk, *et al. JACC Clin. Electrophysiol.*, in press, doi:10.1016/j.jacep.2019.11.018.

10. O. S. Narula. Longitudinal dissociation in the His bundle. Bundle branch block due to asynchronous conduction within the His bundle in man. *Circulation.* **56**, 996–1006 (1977).

11. A. Auricchio, C. Fantoni, F. Regoli, *et al.* Characterization of left ventricular activation in patients with heart failure and left bundle-branch block. *Circulation.* **109**, 1133–1139 (2004).

12. S. Ploux, R. Eschalier, Z. I. Whinnett, *et al.* Electrical dyssynchrony induced by biventricular pacing: Implications for patient selection and therapy improvement. *Hear. Rhythm.* **12**, 782–791 (2015).

13. O. A. E. Salden, A. Zweerink, P. Wouters, *et al.* The value of septal rebound stretch analysis for the prediction of volumetric response to cardiac resynchronization therapy. *Eur. Heart J. Cardiovasc. Imaging.* **22**, 37–45 (2021).

14. F. Maffessanti, T. Jadczyk, R. Kurzelowski, *et al.* The influence of scar on the spatio-temporal relationship between electrical and mechanical activation in heart failure patients. *EP Eur.* **22**, 777–786 (2020).

15. L. Heckman, P. Vijayaraman, J. Luermans, *et al.* Novel bradycardia pacing strategies. *Heart* (2020), doi:10.1136/heartjnl-2020-316849.

16. F. C. W. M. Salden, J. G. L. M. Luermans, S. W. Westra, *et al.* Short-Term Hemodynamic and Electrophysiological Effects of Cardiac Resynchronization by Left Ventricular Septal Pacing. *J. Am. Coll. Cardiol.* **75**, 347–359 (2020).

17. W. Huang, L. Su, S. Wu, *et al.* Long-term outcomes of His bundle pacing in patients with heart failure with left bundle branch block. *Heart.* **105**, 137–143 (2019).

18. M. Abdelrahman, F. A. Subzposh, D. Beer, *et al.* Clinical Outcomes of His Bundle Pacing Compared to Right Ventricular Pacing. *J. Am. Coll. Cardiol.* **71**, 2319–2330 (2018).

19. S. Wu, L. Su, P. Vijayaraman, *et al*. Left bundle branch pacing for Cardiac Resynchronization Therapy: Non-randomized on treatment comparison with His Bundle Pacing and Biventricular Pacing. *Can. J. Cardiol*. (2020), doi:10.1016/j.cjca.2020.04.037.

20. L. Su, S. Wang, S. Wu, *et al*. Long-Term Safety and Feasibility of Left Bundle Branch Pacing in a Large Single-Center Study. *Circ. Arrhythmia Electrophysiol*. **0** (2021), doi:10.1161/CIRCEP.120.009261.

21. F. Leyva, A. Zegard, R. J. Taylor, *et al*. Long-term outcomes of cardiac resynchronization therapy using apical versus nonapical left ventricular pacing. *J. Am. Heart Assoc*. **7**, e008508 (2018).

22. S. Skaf, B. Thibault, P. Khairy, *et al*. Impact of Left Ventricular vs Biventricular Pacing on Reverse Re-modelling: Insights From the Evaluation of Resynchronization Therapy for Heart Failure (EARTH) Trial. *Can. J. Cardiol*. **33**, 1274–1282 (2017).

23. E. Trucco, J. M. Tolosana, E. Arbelo, *et al*. Improvement of Reverse Remodeling Using Electrocardiogram Fusion-Optimized Intervals in Cardiac Resynchronization Therapy: A Randomized Study. *JACC Clin. Electrophysiol*. **4**, 181–189 (2018).

24. G. Filippatos, D. Birnie, M. R. Gold, *et al*. Rationale and design of the AdaptResponse trial: a prospective randomized study of cardiac resynchronization therapy with preferential adaptive left ventricular-only pacing. *Eur. J. Heart Fail*. **19**, 950–957 (2017).

25. N. Varma. Left ventricular electrical activation during right ventricular pacing in heart failure patients with LBBB: Visualization by electrocardiographic imaging and implications for cardiac resynchronization therapy. *J. Electrocardiol*. **48**, 53–61 (2015).

26. N. Varma, D. O'Donnell, M. Bassiouny, *et al*. Programming Cardiac Resynchronization Therapy for Electrical Synchrony: Reaching Beyond Left Bundle Branch Block and Left Ventricular Activation Delay. *J. Am. Heart Assoc*. **7**, e007489 (2018).

27. L. A. Saxon, B. Olshansky, K. Volosin, *et al*. Influence of left ventricular lead location on outcomes in the COMPANION study. *J. Cardiovasc. Electrophysiol*. **20**, 764–768 (2009).

28. J. P. Singh, H. U. Klein, D. T. Huang, *et al*. Left ventricular lead position and clinical outcome in the multicenter automatic defibrillator implantation trial-cardiac resynchronization therapy (MADIT-CRT) trial. *Circulation*. **123**, 1159–1166 (2011).

29. N. Derval, P. Steendijk, L. J. Gula, *et al*. Optimizing hemodynamics in heart failure patients by systematic screening of left ventricular pacing sites: the lateral left ventricular wall and the coronary sinus are rarely the best sites. *J. Am. Coll. Cardiol*. **55**, 566–575 (2010).

30. A. Zweerink, O. A. E. Salden, W. M. van Everdingen, *et al*. Hemodynamic Optimization in Cardiac Resynchronization Therapy: Should We Aim for dP/dtmax or Stroke Work? *JACC Clin. Electrophysiol*. **5**, 1013–1025 (2019).

31. W. M. van Everdingen, A. Zweerink, O. A. E. Salden, *et al*. Pressure-Volume Loop Analysis of Multipoint Pacing With a Quadripolar Left Ventricular Lead in Cardiac Resynchronization Therapy. *JACC. Clin. Electrophysiol*. **4**, 881–889 (2018).

32. B. J. Wisnoskey, N. Varma. Left ventricular paced activation in cardiac resynchronization therapy patients with left bundle branch block and relationship to its electrical substrate. *Hear. Rhythm O2*. **1**, 85–95 (2020).

33. A. K. Shetty, S. G. Duckett, M. R. Ginks, *et al*. Cardiac magnetic resonance-derived anatomy, scar, and dyssynchrony fused with fluoroscopy to guide LV lead placement in cardiac resynchronization therapy: a comparison with acute haemodynamic measures and echocardiographic reverse remodelling. *Eur. Heart J. Cardiovasc. Imaging*. **14**, 692–699 (2013).

34. C. Leclercq, H. Burri, A. Curnis, *et al*. Cardiac resynchronization therapy non-responder to responder conversion rate in the more response to cardiac resynchronization therapy with MultiPoint Pacing (MORE-CRT MPP) study: Results from Phase i. *Eur. Heart J*. **40**, 2979–2987 (2019).

5

35. N. Varma, J. 2nd Baker, G. Tomassoni, *et al.* Left Ventricular Enlargement, Cardiac Resynchronization Therapy Efficacy, and Impact of MultiPoint Pacing. *Circ. Arrhythm. Electrophysiol.* **13**, e008680 (2020).

36. F. Leyva, P. W. Foley, S. Chalil, *et al.* Cardiac resynchronization therapy guided by late gadolinium-enhancement cardiovascular magnetic resonance. *J. Cardiovasc. Magn. Reson.* **13**, 29 (2011).

37. M. R. Gold, R. B. Leman, N. Wold, J. L. Sturdivant, Y. Yu. The effect of left ventricular electrical delay on the acute hemodynamic response with cardiac resynchronization therapy. *J. Cardiovasc. Electrophysiol.* **25**, 624–630 (2014).

38. W. M. van Everdingen, A. Zweerink, M. J. Cramer, *et al.* Can We Use the Intrinsic Left Ventricular Delay (QLV) to Optimize the Pacing Configuration for Cardiac Resynchronization Therapy With a Quadripolar Left Ventricular Lead? *Circ. Arrhythm. Electrophysiol.* **11**, e005912 (2018).

39. J. P. Singh, R. D. Berger, R. N. Doshi, *et al.* Targeted Left Ventricular Lead Implantation Strategy for Non-Left Bundle Branch Block Patients: The ENHANCE CRT Study. *JACC. Clin. Electrophysiol.* **6**, 1171–1181 (2020).

40. N. Ueda, T. Noda, I. Nakajima, *et al.* Clinical impact of left ventricular paced conduction disturbance in cardiac resynchronization therapy. *Hear. Rhythm.* **17**, 1870–1877 (2020).

41. A. Gauthey, E. Willemen, J. Lumens, *et al.* Impact of paced left ventricular dyssynchrony on left ventricular reverse remodeling after cardiac resynchronization therapy. *J. Cardiovasc. Electrophysiol.* **31**, 494–502 (2020).

42. D. Yagishita, Y. Yagishita, S. Kataoka, *et al.* Left Ventricular Stimulation With Electrical Latency Predicts Mortality in Patients Undergoing Cardiac Resynchronization Therapy. *JACC Clin. Electrophysiol.* **7**, 796–805 (2021).

43. M. A. Ghossein, A. M. W. van Stipdonk, F. Plesinger, *et al.* Reduction in the QRS area after cardiac resynchronization therapy is associated with survival and echocardiographic response. *J. Cardiovasc. Electrophysiol.* **32**, 813–822 (2021).

44. F. Z. Khan, M. S. Virdee, C. R. Palmer, *et al.* Targeted left ventricular lead placement to guide cardiac resynchronization therapy: The TARGET study: A randomized, controlled trial. *J. Am. Coll. Cardiol.* **59**, 1509–1518 (2012).

45. S. Saba, J. Marek, D. Schwartzman, *et al.* Echocardiography-Guided Left Ventricular Lead Placement for Cardiac Resynchronization Therapy. *Circ. Hear. Fail.* **6**, 427–434 (2013).

46. M. Bertini, D. Mele, M. Malagù, *et al.* Cardiac resynchronization therapy guided by multimodality cardiac imaging. *Eur. J. Heart Fail.* **18**, 1375–1382 (2016).

47. Z. Bakos, E. Ostenfeld, H. Markstad, *et al.* A comparison between radial strain evaluation by speckle-tracking echocardiography and cardiac magnetic resonance imaging, for assessment of suitable segments for left ventricular lead placement in cardiac resynchronization therapy. *EP Eur.* **16**, 1779–1786 (2014).

48. R. Bai, L. Di Biase, P. Mohanty, *et al.* Positioning of Left Ventricular Pacing Lead Guided by Intracardiac Echocardiography with Vector Velocity Imaging During Cardiac Resynchronization Therapy Procedure. *J. Cardiovasc. Electrophysiol.* **22**, 1034–1041 (2011).

49. A. Sommer, M. B. Kronborg, B. L. Nørgaard, *et al.* Multimodality imaging-guided left ventricular lead placement in cardiac resynchronization therapy: a randomized controlled trial. *Eur. J. Heart Fail.* **18**, 1365–1374 (2016).

50. C. Stephansen, A. Sommer, M. B. Kronborg, *et al.* Electrically vs. imaging-guided left ventricular lead placement in cardiac resynchronization therapy: a randomized controlled trial. *EP Eur.* (2019), doi:10.1093/europace/euz184.

51. J. J. Marek, S. Saba, T. Onishi, *et al.* Usefulness of echocardiographically guided left ventricular lead placement for cardiac resynchronization therapy in patients with intermediate QRS width and non-left bundle branch block morphology. *Am. J. Cardiol.* **113**, 107–116 (2014).

5

SUPPLEMENTARY MATERIAL

Supplemental Table 1. Studies demonstrating that optimal acute hemodynamic benefit is site specific.

Study	Butter et al. [1]	Dekker et al. [2]	Gold et al. [3]	Bogaard et al. [4]	Derval et al. [5]	Strik et al. [6]	Zweerink et al. [7]
Patients (No.)	30	11	14	16	35	26	43
Sites (No.) [†]	2	4-6	2	≥ 2	11	2–6	4
ΔdP/dt$_{max}$ (%)							
Optimal [‡]	12	20	39	30	31	14	17
Non-optimal	5	9	24	19	15	11	12
ΔSW%							
Optimal	NR	66	NR	NR	NR	NR	80
Non-optimal	NR	21	NR	NR	NR	NR	53
p-value	<0.001	NR	NR	<0.001	<0.001	<0.01	< 0.001

[†] Dekker et al paced the epicard and Derval et al the endocard, the other studies investigated transvenous lead positions.
[‡] Butter and Gold reported anterior segments as 'non-optimal' pacing sites, Strik et al investigated best versus basolateral positions, and Zweerink et al compared the optimal versus distal electrode of quadripolar leads. Legend: NR, not reported; SW, stroke work.

Supplemental Table 2. Variability of optimal left ventricular lead location and the ability to reach it.

Hemodynamic studies							
Study	Butter et al. [1]	Dekker et al. [2]	Gold et al. [3]	Bogaard et al. [4]	Derval et al. [5]	Strik et al. [6]	Zweerink et al. [7]
Patients (No.)	30	11	14	16	35	26	43
Sites (No.)	2	4-6	2	≥ 2	11	2–6	4
Best segment							
Basal	NR	27%	57%	19%	NR	NR	NR
Mid	NR	36%	50%	63%	NR	NR	NR
Apex	NR	26%	43%	19%	NR	NR	NR

Image-guided studies						
Study	Bai et al.	Khan et al.	Saba et al.	Sommer et al.	Bertini et al.	Stephansen et al.
Lead position						
Concordant	NR	63 vs. 45	30 vs. 12	49 vs. 43	58 vs. NR	60 vs. 30
Adjacent	NR	25 vs. 28	55 vs. 55	44 vs. 54	36 vs. NR	32 vs. 57
Remote	NR	10 vs. 24	15 vs. 33	1 vs. 2	6 vs. NR	8 vs. 13

Note: For references to image-guided studies used above, please see table 1 of the original manuscript.

SUPPLEMENTARY REFERENCE LIST

1. C. Butter, A. Auricchio, C. Stellbrink, *et al.* Effect of resynchronization therapy stimulation site on the systolic function of heart failure patients. *Circulation*. **104**, 3026–3029 (2001).

2. A. L. A. J. Dekker, B. Phelps, B. Dijkman, *et al.* Epicardial left ventricular lead placement for cardiac resynchronization therapy: Optimal pace site selection with pressure-volume loops. *J. Thorac. Cardiovasc. Surg.* **127**, 1641–1647 (2004).

3. M. R. Gold, A. Auricchio, J. D. Hummel, *et al.* Comparison of stimulation sites within left ventricular veins on the acute hemodynamic effects of cardiac resynchronization therapy. *Hear. Rhythm*. **2**, 376–381 (2005).

4. M. D. Bogaard, P. A. Doevendans, G. E. Leenders, *et al.* Can optimization of pacing settings compensate for a non-optimal left ventricular pacing site? *EP Eur.* **12**, 1262–1269 (2010).

5. N. Derval, P. Steendijk, L. J. Gula, *et al.* Optimizing hemodynamics in heart failure patients by systematic screening of left ventricular pacing sites: the lateral left ventricular wall and the coronary sinus are rarely the best sites. *J. Am. Coll. Cardiol.* **55**, 566–575 (2010).

6. M. Strik, S. Ploux, P. R. Huntjens, *et al.* Response to cardiac resynchronization therapy is determined by intrinsic electrical substrate rather than by its modification. *Int. J. Cardiol.* **270**, 143–148 (2018).

7. A. Zweerink, O. A. E. Salden, W. M. van Everdingen, *et al.* Hemodynamic Optimization in Cardiac Resynchronization Therapy: Should We Aim for dP/dtmax or Stroke Work? *JACC Clin. Electrophysiol.* **5**, 1013–1025 (2019).

5

6

Real-Time Image-Guided Lead Placement in Cardiac Resynchronization Therapy: Feasibility and Outcome in a Multicenter Setting

Philippe C. Wouters, Frebus J. van Slochteren, Anton E. Tuinenburg, Pieter A. Doevendans, Maarten J. Cramer, Peter-Paul H.M. Delnoy, Vincent F. van Dijk, Mathias Meine.

ABSTRACT

Background: Image-guidance to assist left ventricular (LV) lead placement may improve outcome after cardiac resynchronization therapy (CRT), but previous approaches and results varied greatly, and multicentre feasibility is lacking altogether. **Objective:** We sought to investigate the multicentre feasibility of *'real-time'* image-guidance to assist LV lead placement for CRT.

Methods: In 30 patients from three hospitals, cardiac magnetic resonance imaging (CMR) was performed to identify myocardial scar and late mechanical activation (LMA). LMA was determined using radial strain, plotted over time. Segments without scar but clear LMA were classified as optimal for LV lead placement, according to an accurate 36-segment model of the whole heart. LV leads were navigated, in real-time, using image-overlay with fluoroscopy. After 6 months, echocardiographic response and super-response were defined as ≥ 15% or ≥ 30% reduction in LV end-systolic volume (LVESV), respectively.

Results: Real-time image-guidance was successfully performed in all CRT patients (age 66±10 years; 59% male, 62% non-ischemic cardiomyopathy; 69% left bundle branch block). LV leads were placed as follows: within (14%), adjacent (62%), or remote (24%) from the pre-defined target. According to the conventional 18-segment model, a remote position occurred only once (3%). On average, 86% of patients demonstrated a volumetric response (mean LVESV-reduction 36±29%), and 66% of all patients were super-responders.

Conclusion: Real-time image-guidance for LV lead placement in CRT was feasible in a multicentre setting. Efficacy will be further investigated in the randomised controlled 'Advanced Image Supported Lead Placement in Cardiac Resynchronization Therapy' trial (ADVISE; NCT05053568).

INTRODUCTION

Over the years, various approaches have been studied to prevent non-response after cardiac resynchronization therapy (CRT), or further improve treatment efficacy in patients already demonstrating a response [1]. To this end, optimising left ventricular (LV) lead placement (LVLP) remains crucial, since optimal device programming cannot overcome a suboptimal position [2]. Regardless, the process of LVLP itself has remained largely unaltered, as LV leads are still routinely placed empirically [3].

It has been shown previously that placing the lead remote from scar and within late electromechanically activated segments improves response [4,5]. The optimal LV lead location is therefore highly variable and patient-specific [2,6]. Although initial prospective studies were encouraging [4,5], feasibility of in-target LVLP, efficacy, and methodology varied largely [6,7]. In addition, most studies were performed in a single-centre setting [6,7]. Despite its potential benefits, further development of a guided patient-tailored approach in everyday practice is still lacking.

Because of inconsistent results, the optimal strategy for LVLP is still debated [3]. In contrast to echocardiography, cardiac magnetic resonance imaging (CMR) does not suffer from high user-dependence or poor acoustic windows. In addition, CMR allows for whole-heart analysis, not confined to a limited amount of segments of the LV lateral wall [8]. Moreover, CMR is characterised by excellent spatial resolution, without the need for ionizing radiation, and is the gold standard technique for the identification of scar and myocardial viability [9].

The present study therefore set out to study the feasibility, and preliminary efficacy, of a dedicated device for image-guided LVLP, in a multicentre setting.

METHODS

Study design

We prospectively included 30 consecutive patients from three participating centres. Patients with a class I and class IIa guideline indication for a de novo CRT implantation were eligible [3]. Exclusion criteria were impediments for CMR (i.e., claustrophobia, contrast allergy), and permanent atrial fibrillation. LV ejection fraction (LVEF) and cardiac dimensions were calculated using Simpson's modified biplane method. The primary endpoint was reduction of LV end-systolic volume (ΔLVESV), 6-month after CRT implantation. Ischemic cardiomyopathy (ICM) was defined using clinical history or presence of ≥ 5% of the LV myocardial volume on LGE-CMR being scar. Volumetric response was defined as LVESV-reduction ≥ 15%, whereas super-response was defined as decrease of LVESV ≥ 30%. In addition, at 2 months (interquartile range [IQR] 2-3 months), absolute

reduction in log-transformed N-terminal pro-brain natriuretic peptide (NT-proBNP) was calculated. The trial was registered at the Netherlands Trial Register (Trial NL8506) and approved by the Medical Research Ethics Committee Utrecht. All patients gave written informed consent.

Image acquisition and processing

Within 3 months before CRT implantation, standard clinical CINE-CMR with late gadolinium enhancement (LGE) sequences (1 month [IQR 0-2]) were acquired, as previously described [10]. Short axis CMR images where used to determine LV lead targets. Automated identification of LV lead targets was done using CARTBox software [CARTTech B.V., Utrecht, The Netherlands]. Myocardial scar was assessed by applying a full-width at half maximum algorithm on LGE scans **(Fig 1)**. This technique uses half the maximal signal within scar as the threshold for myocardial scar pixels. Manual correction was applied when necessary. For late mechanical activation (LMA), feature tracking postprocessing of the CINE sequences was used to determine myocardial deformation in the radial direction. As a means of enhancing interpretability and improving signal-to-noise ratio, the magnitude of radial deformation was calculated and projected, over time, on geometrical 2D and 3D cardiac models. This resulted in 4-Dimensional Mechanical
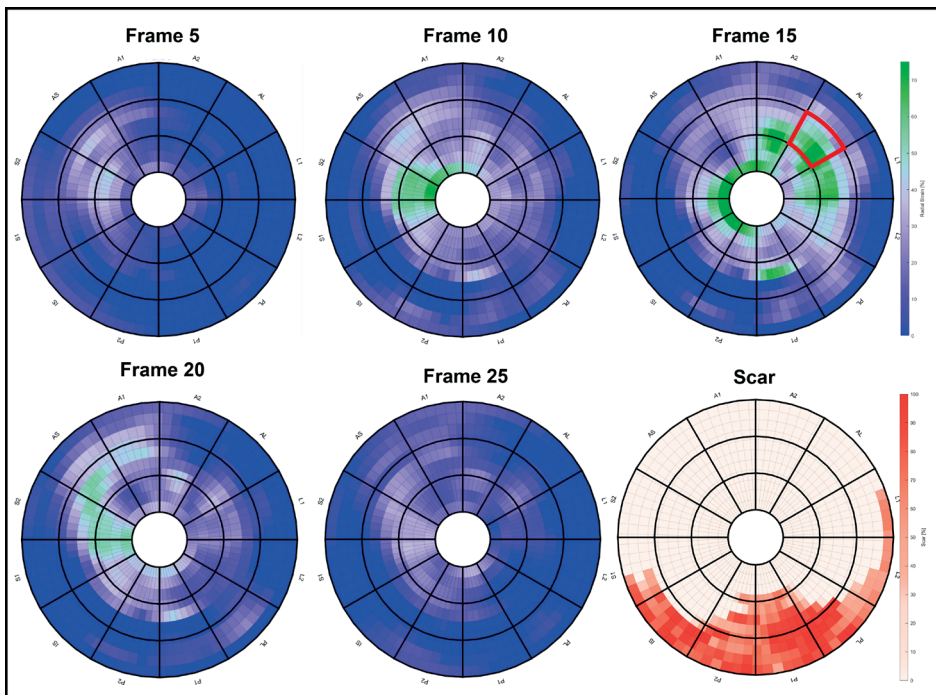
Fig 1. Mechanical activation starts early at the septum (frame 5), and progresses heterogeneously towards the mid-anterolateral region of the left ventricle lateral wall (frame 15). Conversely, the posterior and posterolateral wall show scar.

Activation Plots (4D-MAP), where the radial strain amplitude is displayed over time. Sites of LMA were identified as having the latest high radial strain amplitude, as displayed in a patient specific fashion **(Fig 1)**.

LV lead target specification

Earlier image-guided LVLP studies used the 16 segment American Heart Association (AHA) models [11–13]. By contrast, we incorporated a more specific 36-segment model, which allowed us to differentiate between more segments deemed relevant for LVLP. A predefined decision model was used to assist clinical decision making, and improve reproducibility and user-independence of target selection for LVLP. Segments with myocardial scar were avoided at all time, whereas LMA, as evidenced on the 4D-MAP, was targeted. Apical segments were analysed, but the apical 'cap' was excluded as potential LV lead target. The electrode closest to the pre-defined target was selected, with due consideration of favourable stimulation thresholds and absence of phrenic nerve stimulation.

6

## CRT Implantation and electrical measurements

Implantations were performed according to local protocols, always using quadripolar leads. Electrical activation delay was measured, defined as the intrinsic interval between Q on the ECG and local LV sensing delay on the intracardiac electrogram at a given LV pacing site (Q-LVsense). At the end of the procedure, implanting physicians were asked to self-evaluate whether image-guidance affected their approach.

Image overlay using model-to-image registration

For the registration of the 3D CMR-derived LV surface models with live fluoroscopy (i.e., model-to-image fusion), both a 3D and 2D technique can be used. Because 3D methods impose excessive radiation burden and are not available in all operating theatres, an easy to use 2D image-registration technique to register the 3D LV surface model was developed. The 3D and 2D fusion techniques were evaluated for non-inferiority in the first 5 patients of this study **(Supplemental Appendix)**. Upon validation, only the 2D registration technique was applied in all subsequent patients.

In brief, EP Navigator [Philips Healthcare, Best, The Netherlands], and CART-Box Suite Light [CART-Tech B.V., Utrecht, The Netherlands] were used. Live 3D-CMR to 2D-flurosco-py registration was performed using two separate 2D-fluoroscopic registrations. Here, two acquisitions of the LV and coronary venous anatomy were acquired during balloon occlusion and contrast infusion, using an offset of at least 60 degrees (typically, LAO40 and RAO30). Image fusion was performed using anatomical landmarks **(Fig 2)**. The image overlay, containing scar and the LMA target area, was superimposed on fluoroscopic images during the implantation procedure, aimed at increasing spatial lead-to-target proximity **(Fig 2)**.

RAO 30 **LAO 45**

RADIAL STRAIN

LV LEAD TARGET

SCAR TISSUE
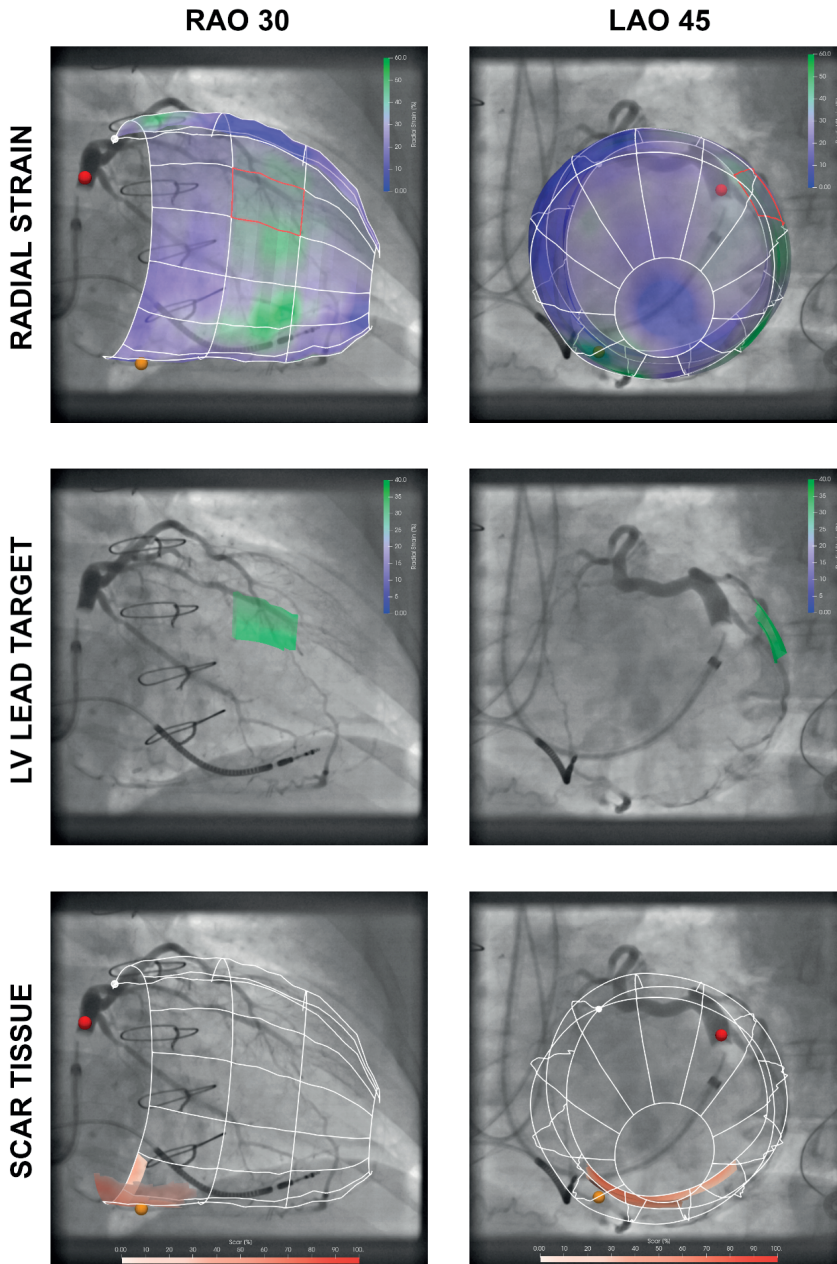
Fig 2. *Model-to-image registration to guide left ventricular lead implantation in real-time. The 36-segment mesh is derived from cardiac magnetic resonance imaging, and is superimposed on dual-view fluoroscopic venograms, using the right anterior oblique (RAO, left column) and left anterior oblique (LAO, right column) acquisitions. Sites of latest mechanical activation (green, upper panels) are targeted, scar tissue (red, lower panels) is avoided. In this case, the most suitable target for lead implantation is determined as mid-lateral 1, and displayed to the implanting physician (middle panel). The red dot indicates the coronary sinus, and orange dot the middle cardiac vein.*

Allocation of final lead position

Final LV lead positions, relative to the pre-defined target, were determined at the end of the study by two observers, blinded to targets, patient characteristics, and outcome. Because defining final LV lead position is unreliable using fluoroscopy only [14], the same model-to-image registration approach on 2D-fluoroscopic images was performed. Only slight agreement was found when comparing LVLP based on fluoroscopy only [15] with model-to-image registration (Cohen's kappa = 0.078; p = 0.536), confirming the necessity of the latter registration technique.

Statistical analysis

Statistics were performed in SPSS version 26 (IBM, Armonk, NY, USA). Depending on normal distribution, continuous data were expressed using mean ± standard deviation, or as median and interquartile range (IQR). Categorical data were expressed as the absolute number of occurrences and associated frequency (%). Independent subgroups were compared using a t-test or Mann–Whitney U test, where appropriate. Fisher's exact test was used to compare nominal variables. One-way ANOVA was used to compare three categories of lead locations. Inter-observer reliability was determined using intraclass correlation coefficient (ICC), or Cohen's kappa for categorical variables. All statistical tests performed were two-tailed, and a p-value < 0.05 was considered statistically significant.

RESULTS

Thirty consecutive patients were included and underwent CRT implantation between December 2019 and May 2021. One patient had no suitable venous anatomy and required epicardial lead placement, resulting in exclusion from further analysis. All 29 remaining patients successfully underwent image-guidance in real-time **(Table 1)**. Scar burden, relative to the whole LV, was ≥ 5% in ten patients (median 7.75% [5.2-13.7]).

Multicentre feasibility of live image fusion

Complete CMR analysis was completed within two days after data transfer. Image fusion at the catheter laboratory was performed in 22±7 minutes for 3D fusion, and within 5 minutes for 2D fusion. According to operating physicians, image-fusion was displayed on time in 96% of cases. Average duration of LV lead placement was 50±35 minutes, with a total procedure time of 120±45 minutes. On average, 55±28 ml contrast fluid was used. Radiation dose area was lower using the 2D-fusion method as compared to using the 3D-rotational fluoroscopy (2805±4051 versus 4840±2625 µGy/m2; p = 0.299).

Table 1. Baseline clinical characteristics of study population.

	Total (n=29)	Responders (n=25)	Non-responders (n=4)	P-value
Clinical characteristics				
Male sex – n (%)	17 (59)	13 (52)	4 (100)	0.121
Age (years)	66±10	66±11	64±9	0.766
Non-ICM – n (%)	18 (62)	17 (68)	1 (25)	0.107
NYHA II – n (%)	16 (55)	13 (52)	3 (75)	0.606
NT-proBNP (pg/mL)	1529±1580	1494±1596	1897±1917	0.739
Electrocardiographic parameters				
LBBB – n (%)†	20 (69)	19 (76)	1 (25)	0.076
QRS duration (ms)	169±20	170±19	159±23	0.285
Medication				
β-blocker – n (%)	23 (79)	21 (84)	2 (50)	0.180
ACEi/ARB – n (%)	27 (93)	23 (92)	4 (100)	1.000
Spironolactone – n (%)	12 (41)	9 (36)	3 (75)	0.279
Echocardiographic parameters				
LVEDV (ml)	209±79	212±85	190±12	0.604
LVESV (ml)	163±68	166±72	141±15	0.503
LVEF (%)	23±7	22±7	26±4	0.310
TAPSE (mm)	18±5	18±5	21±5	0.192

Legend: ACEi, angiotensin-converting-enzyme inhibitor; ARB, angiotensin-II receptor blocker; DBP, diastolic blood pressure; EDV, end-diastolic volume; EF, ejection fraction; ESV, end-systolic volume; ICM, ischemic cardiomyopathy; IVMD, interventricular mechanical delay; LBBB, left bundle branch block; LV, left ventricular; NT-proBNP, N-terminal pro-brain natriuretic peptide; NYHA, New York Heart Association; TAPSE, tricuspid annular plane systolic excursion. † According to the ESC definition.

LV lead positioning and target allocation

Based on the 36-segment model, inter-observer comparison reproduced the exact same primary target selection in 63% of cases, and an adjacent one in 32%. There was substantial agreement when evaluating final LV lead location categories, based on the primary target of the two different observers (Cohen's kappa = 0.680; p < 0.001).

Fig 3 displays '*final*' lead distribution, with the majority of leads positioned within (n = 4; 14%) or adjacent (n = 18; 62%) to the pre-defined target. According to either the 36-segment or conventional 18-segment AHA model, a remote position was acquired in 24% or 3% of patients, respectively. Documented explanations for deviation of the advised primary target were lack of venous access (n = 5), high pacing thresholds (n = 2), phrenic nerve stimulation (n = 1), or unstable lead position (n = 1).
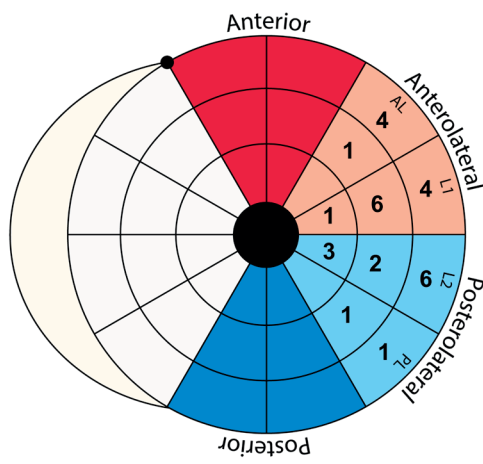
Fig 3. *Bullseye plot according to the 36-segment model (individual parts) and traditional 18-segment model (colorized parts). Leads were distributed across ten different locations,* whereas 8 different segments were identified as optimal

Electrical properties

Q-LVsense of the stimulation electrode (average 157±35 ms) was similar when stratified to lead position (≥ 150 ms, regardless of vicinity to the target), and unaffected by presence of scar **(Fig 4)**. Intrinsic LV electrical delay, normalized to QRS-duration (Q-LVsense/QRSd), was not associated with a volumetric response (AUC = 0.542; p = 0.793). When separated at the median, high versus low Q-LVsense/QRSd was not associated with ΔLVESV (37±28% versus 32±28%; p = 0.572). Pacing thresholds at the final electrode were 0.9±0.5 V. At 2-month and 6-month follow-up, 2-month biventricular pacing percentage was on average 95±13% (< 95% in four patients). No LV pacing vectors were altered, and no shocks were delivered.
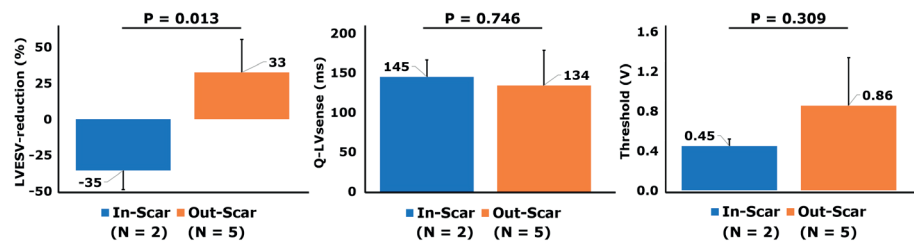
Fig 4. *In patients with ischemic cardiomyopathy and left ventricular (LV) lateral wall scar, scar at the LV pacing electrode was associated with less reverse remodelling, but electrical properties could not differentiate between in versus out-scar pacing.*
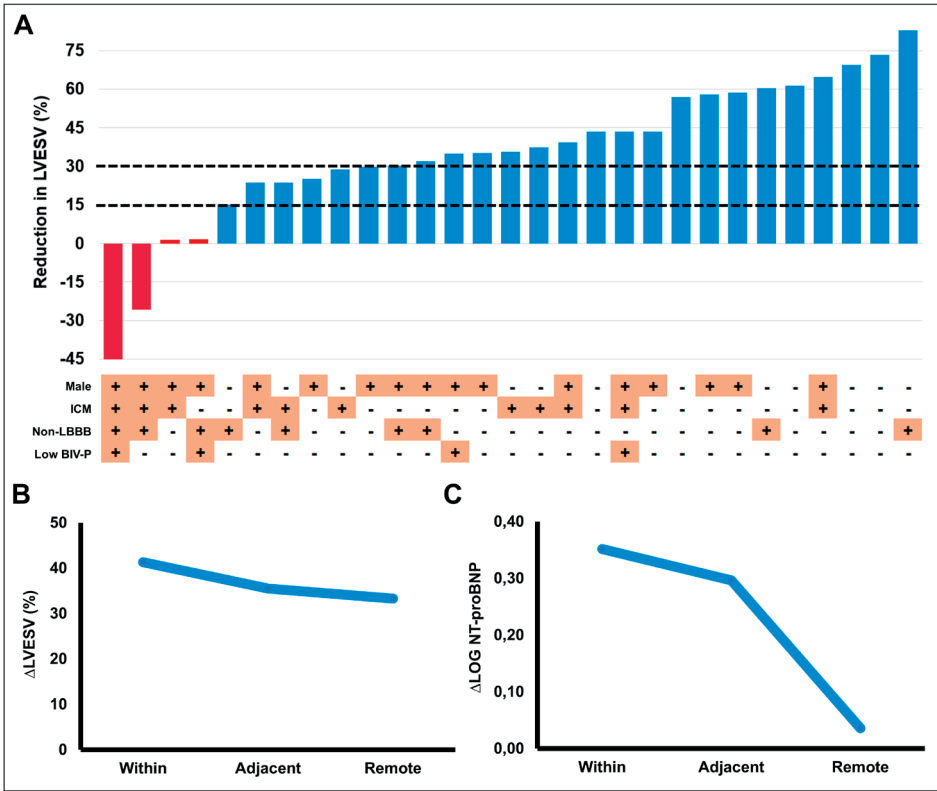
Fig 5. *Echocardiographic and neurohumoral response. In total, 86% of patients were volumetric responders (A). Although ΔLVESV was not significantly related to lead position (B), an association with log-reduction in NT-proBNP was observed (C). Legend: BIV-P, biventricular pacing < 95%; ICM, ischemic cardiomyopathy; LBBB, left bundle branch block; LVESV, left ventricular end-systolic volume; NT-proBNP, N-terminal pro-brain natriuretic peptide.*

Volumetric and neurohumoral response

In total, average reduction in LVESV was 36±29%, with 86% of all patients being volumetric responders, and 66% super-responders **(Fig 5A)**. Volumetric response rates were 95% in non-ICM, 94% in left bundle branch block (LBBB), 73% in ICM, and 67% in non-LBBB. No baseline variables were significantly different in non-responders. In-scar pacing was unavoidable in two cases, which were both non-responders with a mean '*increase'* in LVESV of 35±14% **(Fig 4)**. Excluding in-scar pacing, LVESV-reduction in patients with and without ICM (33±17% versus 45±21; p = 0.158) or non-LBBB and LBBB (35±28 versus 43±18; p = 0.380) was non-significantly different.

Volumetric response was comparable between different anatomical LV lead locations **(Fig 5B)**. Absolute LVEF increased on average by 13±12%, with 45% of patients having their LVEF increased to ≥ 35% **(Table 2)**. Inter-observer reliability for echocardiographic measurements of LVESV was excellent (ICC = 0.990 [95% confidence interval

0.956-0.998]; p < 0.001). Log-transformed NT-proBNP decreased significantly at 2-month follow-up (3.03 versus 2.82; p = 0.013), with a non-significant trend between NT-proBNP and lead position (η^2 = 0.220; p = 0.199) **(Fig 5C)**.

Table 2. Changes in echocardiographic function.

Variable	Baseline	6-months	P-value
LVEDV (ml)	209±79	153±68	<0.001
LVESV (ml)	163±68	101±55	<0.001
LVEF (%)	22±7	35±12	<0.001
IVMD (ms)	87±85	34±31	0.002
TAPSE (mm)	18±5	18±7	0.759
RV S' (cm/s)	10±3	12±4	0.036

Legend: EDV, end-diastolic volume; EF, ejection fraction; ESV, end-systolic volume; IVMD, interventricular mechanical delay; LV, left ventricular; RV S', right ventricular systolic velocity (S'); TAPSE, tricuspid annular plane systolic excursion

6

Influence of image-guidance on decision making

Before image-guidance, the pre-implantation user questionnaire revealed a mid-(antero) lateral position as most frequently preferred target by the physician. The 4D-MAP analysis identified a target adjacent or remote from the physicians' target in 39% and 33% of cases, respectively. Implanting physicians noted that image-guidance significantly altered the implantation by navigating towards another target in 38% of cases. In 19% of all cases, another vein was chosen.

DISCUSSION

Our study is the first to demonstrate the use of real-time guided LVLP in a multicentre setting, using an accurate 36-segment model. Within- or adjacent-from-target LVLP occurred in 76% of cases, with 86% of patients classified as responders. Live model-to-image fusion, combing CMR and dual-view fluoroscopic venograms, is therefore feasible in a multicentre setting **(Graphical Abstract)**.

Determinants of response to CRT

Although patient characteristics also determine response to CRT, a poor LV-lead position within scar likely explained non-response in two out of four non-responders **(Fig 4)**. Importantly, if in-scar pacing could be avoided, despite a clear scar burden, response rates were high in patients with ICM and non-LBBB. Here, image-guidance is likely most valuable, since these patients typically demonstrate heterogeneous LV electrical activation, have smaller target sites, and demonstrate poorer outcome after CRT when compared to DCM or LBBB patients [6]. Conversely, optimal pacing areas are relatively larger in patients

with LBBB and DCM [6], which may explain why no clear association was found between lead-to-target proximity and response. Especially considering only one patient had the LV lead implanted in a *'truly'* remote position (ie, according to the 18-segment model). Regardless, response rates of 95% in LBBB and non-ICM are rare [7,16], and the contributing role of image-guidance in this patient group should therefore not be excluded.
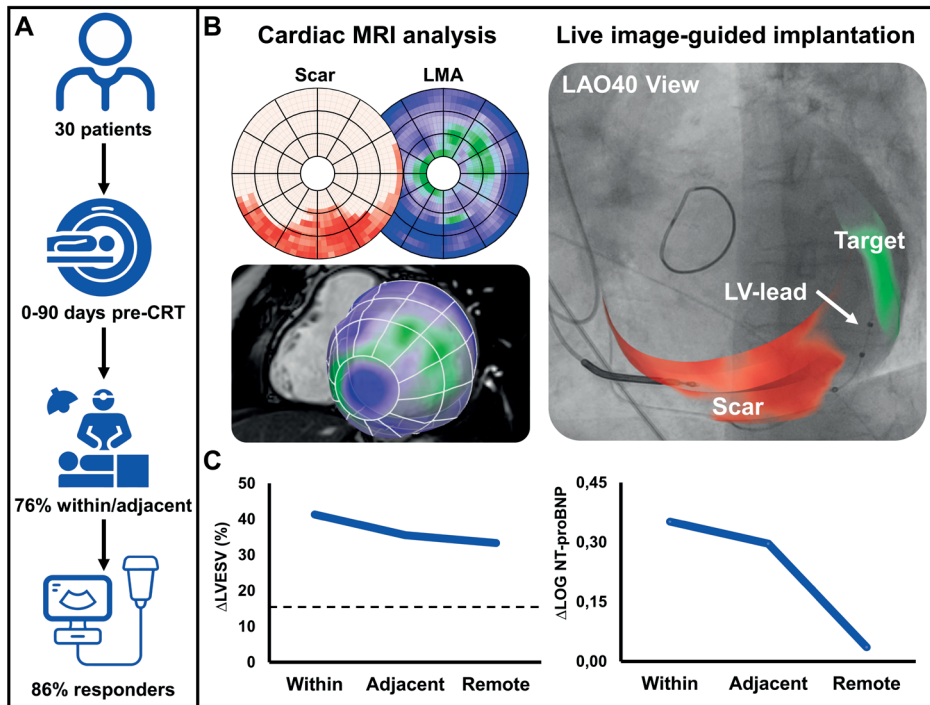
Graphical Abstract. *Study overview (A), methodology (B), and outcomes (C) of real-time image-guided left ventricular lead placement in a multicentre setting.*

Feasibility in multicentre setting

Image-guidance was successfully performed in all CRT patients. Notwithstanding limited venous access or high pacing thresholds, which precluded optimal LVLP in some patients, a near-optimal position was acquired in the majority of cases. In addition, implantation times compared favorably with all previously conducted live image-guide studies [11-13].

When comparing differences in spatial lead-to-target proximity, "adjacent" LVLP, according to 36-segments, can be considered similar to "within" target in the 18-segment model **(Fig 2)**. As was the case in our study (76% within or adjacent in the 36 segment model), previous research that investigated *'live'* image-guided LVLP in conventional models also reported high in-target success rates of 71-83% [11-13]. This is substantially

higher than the 30-63% reported by studies lacking real-time fluoroscopic overlay [6]. Unfortunately, feasibility of their approaches was tested in single centre settings only, and with smaller sample sizes [11–13]. Moreover, the percentage of 6-month volumetric responders was lower at 60% [12,13], or not investigated [11]. Lastly, these studies enrolled more patients with LBBB [11–13], and included comparable amounts of patients with ICM [12,13].

Live image-guided lead implantation

Several important methodological differences can be appreciated when comparing our approach with the aforementioned studies [11–13]. One study required CMR acquisition and CRT implantation in a single session, which complicates its use in clinical practice [11]. Previous studies targeted segments with the most delayed time-to-minimum volume, using regional volume-over-time curves [11,12]. By contrast, our approach used custom built feature-tracking software and used time-dependant visualisation of mechanical activation. This likely reduced the influence of noise and improved interpretability when compared to conventional approaches, as underscored by the substantial inter-observer agreement for target selection in the present study. To our knowledge, previous studies did not report reproducibility of target selection. Lastly, traditional larger segment models, as used in previous studies, less accurately portray spatial lead-to-target proximity, and limit how precise regions with scar and LMA can be visualized and targeted.

Electrical guiding as alternative

Maximising the Q-LVsense interval is a well-recognised strategy to enhance response to CRT. Although Q-LVsense is associated with CRT response on group level [7], it cannot differentiate optimal from suboptimal segments in individual patients [17]. Differentiation is especially difficult when Q-LVsense is high, or when differences in Q-LVsense at various locations of a quadripolar lead are small, which is the case when leads are already placed in or near an optimal location [6,17]. Hence, lack of association between Q-LVsense and remodelling is also reflected by our results, since average Q-LVsense at the stimulation electrode was ≥ 150 ms, and similar across patients with different LV lead locations. Mapping Q-LVsense in all suitable epicardial veins may prove more effective, but this approach is time consuming and cumbersome [16]. Moreover, Q-LVsense guidance provides no additional benefit in patients with non-LBBB [18], which is the most important group of patients for optimising lead placement in the first place [6]. By contrast, image-guidance has shown to be beneficial in this subgroup, and can pre-procedurally characterize the mechanical delays of the whole LV lateral wall [4].

Clinical relevance and outlook

Besides preventing non-response, image-guidance may also further increase the amount of reverse remodelling. Indeed, super-response is associated with better

clinical improvement, less HF-hospitalisation, and lower mortality when compared to LVESV-reduction of 15-30% [1]. As a result, despite CMR being costly, an image-guided technique may prove cost-effective [19]. Lastly, conduction system pacing (CSP) has been proposed as an alternative for transvenous lead placement in CRT patients [6]. However, long-term follow-up data is still awaited, and similar response rates of about 70% have been demonstrated in 345 CSP patients [20]. Hence, CSP does not ensure response to CRT either, and an image-guided approach may compare equally favourable, especially in non-LBBB or ICM [6].

Limitations

Although promising, our results should be interpreted with caution, in the context of a non-randomised design. The randomized multicentre 'Advanced Image Supported Lead Placement in Cardiac Resynchronization Therapy' trial (ADVISE; NCT05053568) will address this important limitation [19]. Although the high proportion of LBBB may have influenced our results, patient characteristics were comparable to previous live image-guided studies [11–13]. Although descriptive subgroup analyses were provided for hypothesis-generating purposes, analyses were underpowered due to limited sample size. As a result, the effect of LV lead location and response warrants further research. Although CMR has high spatial resolution, better temporal resolution is achieved using speckle-tracking echocardiography. Alternatively, cardiac computed tomography may be more suitable in patients with a pre-existing ICD implanted, and can also asses venous anatomy [13]. Lastly, as Sommer et al. clearly illustrated, accurate identification of LVLP using fluoroscopy is not without its pitfalls due to variable cardiac anatomy and high observer-dependent interpretation [14]. However, our model-to-image registration-approach likely reduced risk of misclassification, without the need for post-CRT computer tomography.

CONCLUSIONS

Use of CMR as a radiation-free and non-invasive imaging technique to guide LV lead implantation is feasible in a multicentre setting, since 76% of leads were implanted in close proximity to the target, and 86% of patients demonstrated a volumetric response with a mean reduction in LVESV of 36%. Accurate segmental analysis, time-dependant visualisation of radial strain, and real-time image-fusion may have contributed to these promising results. The randomised controlled ADVISE trial will further study the clinical efficacy following the present approach [19].

REFERENCES

1. C. Ypenburg, R. J. van Bommel, C. J. W. Borleffs, *et al.* Long-term prognosis after cardiac resynchronization therapy is related to the extent of left ventricular reverse remodeling at midterm follow-up. *J. Am. Coll. Cardiol.* **53**, 483–490 (2009).

2. M. D. Bogaard, P. A. Doevendans, G. E. Leenders, *et al.* Can optimization of pacing settings compensate for a non-optimal left ventricular pacing site? *EP Eur.* **12**, 1262–1269 (2010).

3. M. Glikson, J. C. Nielsen, M. B. Kronborg, *et al.* 2021 ESC Guidelines on cardiac pacing and cardiac resynchronization therapy: Developed by the Task Force on cardiac pacing and cardiac resynchronization therapy of the European Society of Cardiology (ESC) With the special contribution of the European Hear. *Eur. Heart J.* (2021), doi:10.1093/eurheartj/ehab364.

4. J. J. Marek, S. Saba, T. Onishi, *et al.* Usefulness of echocardiographically guided left ventricular lead placement for cardiac resynchronization therapy in patients with intermediate QRS width and non-left bundle branch block morphology. *Am. J. Cardiol.* **113**, 107–116 (2014).

5. F. Z. Khan, M. S. Virdee, C. R. Palmer, *et al.* Targeted left ventricular lead placement to guide cardiac resynchronization therapy: The TARGET study: A randomized, controlled trial. *J. Am. Coll. Cardiol.* **59**, 1509–1518 (2012).

6. P. C. Wouters, K. Vernooy, M. J. Cramer, F. W. Prinzen, M. Meine. Optimizing lead placement for pacing in dyssynchronous heart failure: The patient in the lead. *Hear. Rhythm.* **18**, 1024–1032 (2021).

7. D. B. Fyenbo, A. Sommer, B. L. Nørgaard, *et al.* Long-term outcomes in a randomized controlled trial of multimodality imaging-guided left ventricular lead placement in cardiac resynchronization therapy. *EP Eur.*, euab314 (2022).

8. R. M. Lang, L. P. Badano, V. Mor-Avi, *et al.* Recommendations for cardiac chamber quantification by echocardiography in adults: an update from the American Society of Echocardiography and the European Association of Cardiovascular Imaging. *Eur Hear. J Cardiovasc Imaging.* **28**, 1-39.e14 (2015).

9. Z. Bakos, E. Ostenfeld, H. Markstad, *et al.* A comparison between radial strain evaluation by speckle-tracking echocardiography and cardiac magnetic resonance imaging, for assessment of suitable segments for left ventricular lead placement in cardiac resynchronization therapy. *EP Eur.* **16**, 1779–1786 (2014).

10. O. A. E. Salden, H. T. van den Broek, W. M. van Everdingen, *et al.* Multimodality imaging for real-time image-guided left ventricular lead placement during cardiac resynchronization therapy implantations. *Int. J. Cardiovasc. Imaging.* **35**, 1327–1337 (2019).

11. J. M. Behar, P. Mountney, D. Toth, *et al.* Real-Time X-MRI-Guided Left Ventricular Lead Implantation for Targeted Delivery of Cardiac Resynchronization Therapy. *JACC. Clin. Electrophysiol.* **3**, 803–814 (2017).

12. A. K. Shetty, S. G. Duckett, M. R. Ginks, *et al.* Cardiac magnetic resonance-derived anatomy, scar, and dyssynchrony fused with fluoroscopy to guide LV lead placement in cardiac resynchronization therapy: a comparison with acute haemodynamic measures and echocardiographic reverse remodelling. *Eur. Heart J. Cardiovasc. Imaging.* **14**, 692–699 (2013).

13. J. Gould, B. S. Sidhu, B. J. Sieniewicz, *et al.* Feasibility of intraprocedural integration of cardiac CT to guide left ventricular lead implantation for CRT upgrades. *J. Cardiovasc. Electrophysiol.* **32**, 802–812 (2021).

14. A. Sommer, M. B. Kronborg, B. L. Nørgaard, *et al.* Left and right ventricular lead positions are imprecisely determined by fluoroscopy in cardiac resynchronization therapy: a comparison with

6

cardiac computed tomography. *Eur. Eur. pacing, arrhythmias, Card. Electrophysiol. J. Work. groups Card. pacing, arrhythmias, Card. Cell. Electrophysiol. Eur. Soc. Cardiol.* **16**, 1334–1341 (2014).

15. J. P. Singh, H. U. Klein, D. T. Huang, *et al.* Left ventricular lead position and clinical outcome in the multicenter automatic defibrillator implantation trial-cardiac resynchronization therapy (MADIT-CRT) trial. *Circulation.* **123**, 1159–1166 (2011).

16. C. Stephansen, A. Sommer, M. B. Kronborg, *et al.* Electrically vs. imaging-guided left ventricular lead placement in cardiac resynchronization therapy: a randomized controlled trial. *EP Eur.* (2019), doi:10.1093/europace/euz184.

17. W. M. van Everdingen, A. Zweerink, M. J. Cramer, *et al.* Can We Use the Intrinsic Left Ventricular Delay (QLV) to Optimize the Pacing Configuration for Cardiac Resynchronization Therapy With a Quadripolar Left Ventricular Lead? *Circ. Arrhythm. Electrophysiol.* **11**, e005912 (2018).

18. J. P. Singh, R. D. Berger, R. N. Doshi, *et al.* Targeted Left Ventricular Lead Implantation Strategy for Non-Left Bundle Branch Block Patients: The ENHANCE CRT Study. *JACC. Clin. Electrophysiol.* **6**, 1171–1181 (2020).

19. P. C. Wouters, C. van Lieshout, V. F. van Dijk, *et al.* Advanced image-supported lead placement in cardiac resynchronisation therapy: protocol for the multicentre, randomised controlled ADVISE trial and early economic evaluation. *BMJ Open.* **11**, e054115 (2021).

20. P. Vijayaraman, S. Ponnusamy, Ó. Cano, *et al.* Left Bundle Branch Area Pacing for Cardiac Resynchronization Therapy: Results From the International LBBAP Collaborative Study Group. *JACC Clin. Electrophysiol.* **7**, 135–147 (2021).

SUPPLEMENTARY MATERIAL

CRT Implantation and electrical measurements

In brief, right atrial and right ventricular leads were placed, preferably in the right atrium appendage and right ventricular septum, respectively. In all patients, a quad-ripolar LV lead was implanted through the coronary sinus. Using live image-overlay, the vein deemed most suitable to facilitate lead placement at the pre-defined target was attempted first. In all patients, procedure times and radiation dose were collected. In addition, pacing threshold and phrenic nerve stimulation threshold were assessed at all stimulation electrodes.

Image overlay using model-to-image registration

For the registration of the 3D LV surface models with live fluoroscopy (i.e., model-to-image fusion), both a 3D and 2D technique have been used. For the 3D technique, a rotational scan was acquired using interventional cone beam cardiac tomography equipment. Subsequently, a 3D DICOM file with myocardial scar and the implantation target were registered with the reconstructed 3D rotational scan, as described previously in Salden et al [1]. A drawback of the 3D technique is the necessity to acquire a 3D rotational scan, solely for the purpose of registration of the 3D LV surface models, whereas the rest of the intervention is done based on 2D fluoroscopy. This technique is not available in all operating theatres, and imposes excessive radiation burden [1]. To overcome this issue, an easy to use 2D image registration technique to register the 3D LV surface model was developed. This new technique was validated in the first 5 patients in this study, and upon validation the 2D registration technique was applied in the subsequent patients **(Supplemental Figure 1)**.

For the 2D registration technique, EP Navigator [Philips Healthcare, Best, The Netherlands], and CART-Box Suite Light [CART-Tech B.V., Utrecht, The Netherlands] was used. Live 3D-CMR to 2D-fluroscopy registration was performed using two separate 2D-fluoroscopic registrations. Here, two acquisitions of the LV and coronary venous anatomy were acquired during balloon occlusion and contrast infusion, using an offset of at least 60 degrees (typically, LAO40 and RAO30). Image fusion was performed using anatomical landmarks (coronary sinus, middle cardiac vein, cardiac silhouette), in line with Babic et al. **(Figure 2)** [2]. In RAO30, the 3D LV surface model was oriented in the corresponding angles and the coronary sinus was aligned nearby the base of the 3D LV surface model. Subsequently the 3D middle cardiac vein marker was aligned with the corresponding 2D location. In LAO40, the 3D LV surface model was oriented in the corresponding angles and aligned with the 2D fluoroscopy based on the cardiac silhouette. The location was fine-tuned based on the 3D markers of the coronary sinus, and middle cardiac vein. After the registration step, the overlay image, containing scar and

6

the target area information, was shown to the cardiologist by a color scale on the large display in the operating theater **(Figure 2)**.

Echocardiographic analysis

Echocardiograms were obtained before (0 months [IQR -2-0]) and 6 months after CRT implantation (6 months [IQR 5-6]). LVEF and cardiac dimensions were calculated using Simpson's modified biplane method [3]. Interventricular mechanical delay (IVMD) was measured as the difference between left and right ventricular pre-ejection intervals, using pulsed wave Doppler. RV-function was assessed using tricuspid annular plane systolic excursion (TAPSE) using M-mode, and tissue doppler imaging-derived tricuspid lateral annular systolic velocity wave (RV S').

Validation of 3D-3D versus 3D-2D registration

The validation of the 2D registration was performed in five patients. The results are shown in **Supplemental Table 1**. The results are a pointwise subtraction of the vertices of the ground truth LV surface model and the LV surface model that is registered based on two 2D images.

Supplemental Table 1. Summary of registration differences when comparing 3D scan versus two separate 2D fluoroscopic images.

Patient	Threshold (4% of max circumference)	max circumferential error	max longitudinal error	max radial error
1	10.5mm (4%)	9.7mm (3.6%)	9.9mm (3.7%)	7.7mm (2.9%)
2	11.3mm (4%)	10.9mm (3.8%)	9.7mm (3.4%)	10.2mm (3.6%)
3	9.6mm (4%)	2.2mm (0.9%)	1.8mm (0.7%)	2.0mm (0.8%)
4	9.3mm (4%)	8.0mm (3.4%)	7.7mm (3.3%)	7.4mm (3.2%)
5	9.2mm (4%)	3.8mm (1.7%)	1.2mm (0.53%)	3.8mm (1.7%)

Thresholds of the maximum difference in registration were 4% of the circumference and length of the heart. The results are a pointwise subtraction of the ground truth mesh and the mesh that is registered based on two 2D images.

6
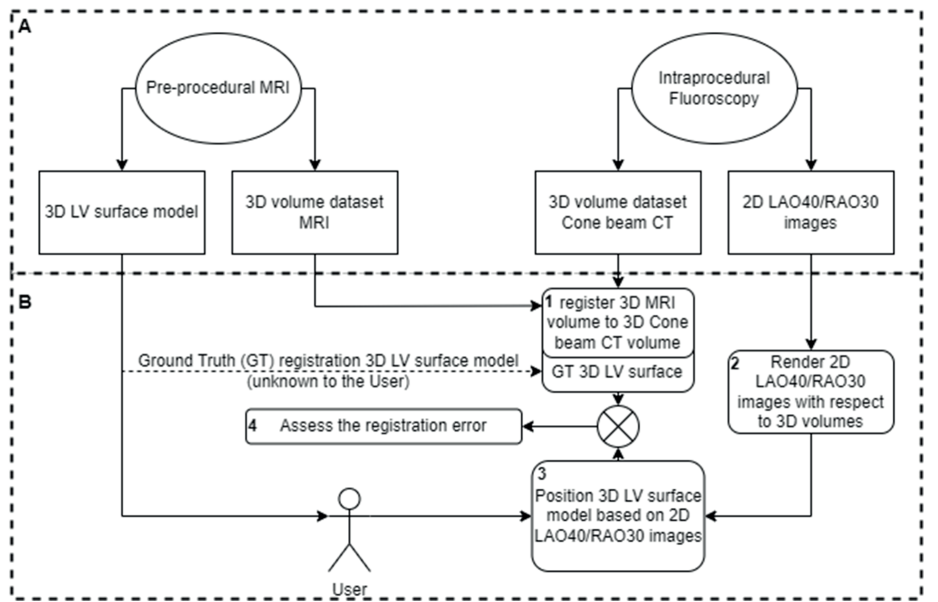
Supplemental Figure 1: Schematic overview of the registration validation process. Panel A: data acquisition. Panel B: registration steps. Step 1: Register the 3D MRI volume to the 3D Cone beam CT volumes. Step 2: render the 2D LAO40 and RAO40 images with respect to the 3D Cone beam CT volume. Step 3: Position the 3D LV surface mesh based on the anatomical landmarks (coronary sinus, middle cardiac vein, cardiac silhouette). Step 4: distract the ground truth (GT) and the registered 3D LV surface models to assess the registration accuracy.

SUPPLEMENTAL REFERENCES

1. O. A. E. Salden, H. T. van den Broek, W. M. van Everdingen, *et al.* Multimodality imaging for real-time image-guided left ventricular lead placement during cardiac resynchronization therapy implantations. *Int. J. Cardiovasc. Imaging*. **35**, 1327–1337 (2019).
2. A. Babić, H. H. Odland, E. Lyseggen, *et al.* An image fusion tool for echo-guided left ventricular lead placement in cardiac resynchronization therapy: Performance and workflow integration analysis. *Echocardiography*. **36**, 1834–1845 (2019).

7

Advanced Image-Supported Lead Placement in Cardiac Resynchronization Therapy: Protocol for the Multicenter, Randomized Controlled ADVISE Trial and Early Economic Evaluation

Philippe C. Wouters, Chris van Lieshout, Vincent F. van Dijk,
Peter-Paul H.M. Delnoy, Pieter A.F.M. Doevendans, Maarten J. Cramer,
Geert W.J. Frederix, Frebus J. van Slochteren*, Mathias Meine*.

Last two authors contributed equally

ABSTRACT

Introduction: Achieving optimal placement of the left ventricular (LV) lead in cardiac resynchronization therapy (CRT) is a prerequisite in order to achieve maximum clinical benefit, and is likely to help avoid non-response. Pacing outside scar tissue and targeting late activated segments may improve outcome. The present study will be the first randomized controlled trial to compare the efficacy of *real-time* image-guided LV lead delivery to conventional CRT implantation. In addition, to estimate the cost-effectiveness of targeted lead implantation, an early decision analytic model was developed, and described here.

Methods and analysis: A multicenter, interventional, randomised, controlled trial will be conducted in a total of 130 patients with a class I or IIa indication for CRT implantation. Patients will be stratified to ischemic heart failure aetiology and 1:1 randomized to either empirical lead placement or live image-guided lead placement. Ultimate lead location and echocardiographic assessment will be performed by core laboratories, blinded to treatment allocation and patient information. Late gadolinium enhancement cardiac MRI (LGE-CMR) and CINE-CMR with feature-tracking post processing software will be used to semi-automatically determine myocardial scar and late mechanical activation. The subsequent treatment file with optimal LV-lead positions will be fused with the fluoroscopy, resulting in live target-visualisation during the procedure. The primary endpoint is the difference in percentage of successfully targeted LV-lead location. Secondary endpoints are relative percentage reduction in indexed LV end-systolic volume, a hierarchical clinical endpoint, and quality of life. The early analytic model was developed using a Markov-model, consisting of seven mutually exclusive health states.

Ethics and dissemination: The protocol was approved by the Medical Research Ethics Committee Utrecht (NL73416.041.20). All participants are required to provide written informed consent. Results will be submitted to peer-reviewed journals. The trial is registered at a ClinicalTrials.gov (NCT05053568) and Netherlands Trial Register (Trial NL8666).

INTRODUCTION

Chronic heart failure is a major global health concern with a 5-year mortality rate of about 50%. In about one-third of these patients, heart failure is accompanied by left ventricular (LV) conduction delay (i.e. QRS-duration ≥ 130 ms), which is a predictor for worse prognosis [1,2]. Cardiac resynchronization therapy (CRT) greatly reduces morbidity and mortality in these patients, but the extent of response is inconsistent and highly dependent on adequate LV lead placement (LVLP). In-scar LVLP greatly increases risk of cardiovascular death and HF-hospitalisation [3], whereas pacing in an area of late activation is likely to improve outcome [4–6]. Moreover, a suboptimal lead position cannot be compensated by optimizing device programming [7], rendering adequate LVLP arguably the cornerstone of this device therapy.

Because the optimal location is highly variable and patient-specific, an individualised and targeted approach is often warranted [8]. Previous research has demonstrated the benefits of image-guided lead delivery as a mean of improving clinical outcome [8,9]. However, most studies did not allow for electrical guidance in the control group and allowed for only eight potential targets for lead deployment, thereby limiting the accuracy of lead deployment and increasing the odds of fortuitous "in-target" lead placement [10,11]. Moreover, no large studies allowed for real-time visualisation of optimal targets, and most of the image-guided studies were not conducted in a true multicenter setting. As such, the current evidence for image-guided LVLP has remained relatively limited, and contemporary LVLP is still largely based on an empirical strategy [1].

The present study protocol describes the first multicenter randomized controlled trial investigating advanced image supported lead placement in CRT (ADVISE). The primary aim of the study is to demonstrate the feasibility of reaching pre-defined segments through accurate image-guidance, using an 18-segment LV lateral wall model with live visual guidance during the implantation. The secondary objective is to investigate the clinical efficacy by evaluating differences in the extent of LV reverse remodeling, a hierarchical clinical endpoint and quality of life between both groups. Lastly, a Health Technology Assessment will be conducted to determine the expected cost-effectiveness of a patient-tailored approach for targeted lead placement.

METHODS AND ANALYSIS

The ADVISE-CRT trial is a multicenter, randomised, controlled trial that is blinded to the patient and assessors of outcome **(Figure 1)**. Assessment of LV dimension, LV function, and lead location will be performed by core laboratories. Patients will be stratified according to aetiology of heart failure in order to assure equal distribution of patients

with ischemic cardiomyopathy (ICM) and non-ICM patients in both groups. All 130 patients will be 1:1 allocated to either image-guided or empirical LVLP using variable block-randomization:

- Intervention group: live visualised, fluoroscopy-fused, image-guided, lead placement on the basis of avoiding scar and targeting late mechanically activated segments.
- Control group: empirical standard-of-care lead placement in line with current CRT implantation guidelines with electrical guiding on the basis of Q-LV sense[4].

Baseline assessments
- Clinical evaluation (NYHA, ECG).
- Echocardiography and cardiac MRI.
- Two quality of life questionnaires.

MRI analysis and target allocation
- Semi-automated analysis of scar and mechanical activation.
- Target allocation based on pre-specified decision-model.

1:1 variable block-randomization

Image-guided
- Image-guided placement.
- Q-LV sense optimization.
- AV/VV-delay per operator.

Usual-care
- Empirical lead placement.
- Q-LV sense optimization.
- AV/VV-delay per operator.

6 months
- Clinical evaluation (NYHA, ECG).
- Echocardiography.
- Two quality of life questionnaires.

12 & 24 months
- Two quality of life questionnaires
- Clinical events (hospitalisation, LVAD, transplant, death)

Figure 1. *Flow-chart presenting the course of the study.*

Study population

Patients are prospectively enrolled in at least three, and at most six, Dutch academic and peripheral centres. Consecutive patients eligible for CRT with a class I or IIa indication, with or without defibrillator function, according to the 2016 European Society of Cardiology Guidelines for the diagnosis and treatment of acute and chronic heart failure are considered. In addition, some additional criteria for study participation apply **(Table 1)**.

Table 1. *ADVISE inclusion and exclusion criteria*

Inclusion criteria
- Heart failure with LVEF ≤ 35%;
- NYHA class II, III, or IV (ambulatory);
- Optimal medical treatment that is tolerable;
- LBBB with QRS ≥ 130 ms, *or* non-LBBB with QRS ≥ 150 ms.

Exclusion criteria
- Age < 18 years or incapacitated adult;
- Contraindication for CMR (gadolinium; contrast agents; metal);
- Atrial fibrillation; either permanent or during CMR;
- Severe renal insufficiency (GFR < 30 ml/min/1.73 m^2);
- Participation in other potentially confounding trials.

Overview of assessments

Prior to device implantation, all patients will undergo echocardiographic examination and cardiac magnetic resonance imaging (CMR). CMR feature-tracking (CMR-FT) analyses will be performed in both study groups, after which optimal LV-lead location will be determined. Randomization will occur after targets for lead deployment have been defined, after which targets cannot be altered. All patients will receive two quality of life questionnaires (EQ-5D-5L and Kansas City Cardiomyopathy Questionnaire) at four time-points: before implantation and at six months, 12 months, and 24 months after implantation. A 12-lead ECG will be performed before, directly after, and six months after implantation. During the procedure, various LV-paced effects will be measured. Ultimate lead location will be assessed through registration of the 18-segment LV lateral wall model onto the LAO40 and RAO30 fluoroscopy images, similar to the method described by Singh and colleagues, [12]. A global schedule of all assessments is summarised **(Figure 2)**.

CMR analysis and target allocation

Clinical standard short axis CINE acquisitions with a minimum of 25 frames per R-R interval, at max 8mm slice thickness and no slice gap, and LGE acquisitions at max 8mm slice thickness will be performed in the participating hospitals. Cardiac MRI scans may be acquired at most six months before implantation, in case of no (suspicion of) recent ischaemic events. Post processing will be performed in a centralized fashion using a dedicated software toolbox (CARTBox, CART-Tech B.V., Utrecht, The Netherlands). The CARTBox analysis results in a treatment file, which will be used as an overlay with live fluoroscopy during the implantation procedure in the intervention group. Semi-automated and deep-learning assisted contouring CMR-FT analysis will be performed to quantify myocardial deformation and identify the tissue with the latest mechanical contraction. Scar transmurality will be identified based on the LGE acquisitions. Three dimensional maps of mechanical activation and scar transmurality are combined and

used to define the optimal tissue (targets) for the LV lead. Targets will then be allocated on the basis of a pre-specified decision-model by two investigators, blinded to each other.

Segments that contain myocardial scar will be disregarded, whereas segments with latest mechanical activation will be considered most appropriate. Because multiple regions may be deemed suitable, a maximum of three of the most suitable segments will be ranked and considered for implantation in that order of priority. In the case of initial disagreement, consensus will follow after discussion. Of note, the original unprocessed CMR will be available at the discretion of the implanting cardiologist, also in the control group.

Time point	Enrolment -3 months	Allocation Day 0	Post-allocation Day 3	Post-allocation 6 months	Close-out 24 months
ENROLMENT					
Screening	X				
Informed consent	X				
Cardiac MRI	X				
Echocardiography	X			X	
Electrocardiogram	X		X	X	
NYHA class	X			X	
Questionnaires	X			X	X
Target allocation	X				
Treatment allocation		X			
INTERVENTIONS					
Image-guided		⟶			
Empirical		⟶			
ASSESMENTS					
LV-lead location		X			
Procedural aspects [a]		X			
Technical aspects		X			
LVESVi- reduction	X			X	
Resynchronisation [b]	X			X	
QRS$_{AREA}$	X		X	X	
Mortality		X	X	X	X
HF Hospitalisation		X	X	X	X
Adverse events		X	X	X	X

Figure 2. SPIRIT time schedule of enrolment, interventions, and assessments for the ADVISE-CRT trial. [a] *Includes implantation time, radiation exposure, and electrode configurations;* [b] *e.g., indices of mechanical recoordination such as SRSsept.*

Echocardiography

Transthoracic echocardiographic examinations will be performed at baseline and six months after CRT implantation at each participating centre. A standard local protocol used for strain-imaging in CRT candidates will be used, with special attention to high quality images of the LV. To this end, each acquired image will include at least three separate beats, and LV strain images will be frame-rate optimized by using the narrow-

est sector width possible. LV volumes and function will be assessed using Simpson's bi-plane method [13]. Mechanical dyssynchrony (e.g. apical rocking) will be assessed as well. All examinations will be analysed by an echocardiography core laboratory using vendor-independent software.

Randomization and blinding procedures

After baseline assessments and subsequent identification of optimal targets for LVLP, computer-generated variable block 1:1 randomization to either image-guided (intervention) or empirical (control) implantation will be performed (Castor EDC, Amsterdam the Netherlands). Randomization will be stratified according to ischemic or non-ischemic heart failure etiology. Study data will be collected, recorded, logged and managed in compliance with Good Clinical Practice guidelines. All study data are recorded in an electronic case report form (eCRF), where any changes in data entry are logged. All data entered, including perioperative data related to device implantation and optimization, are collected and entered into the eCRF by either the coordinating investigator and/or research nurse. External data validation will be managed by a study monitor, designated by a contract research organization. Both the patient and core laboratories assessing endpoint data (fluoroscopically determined LVLP and echocardiography) will be blinded to the intervention. After six month follow-up has been completed by all patients, unblinding is allowed. After six months, no observer-dependent endpoint data remains to be collected, and electrode reselection is allowed where indicated.

Device implantation

Implantation of CRT, unrestricted by manufacturer or the presence or absence of defibrillator, will occur under local anaesthesia and light intravenous sedation according to standard procedure. In the control group, LVLP will occur at discretion of the physician but in line with current guidelines using quadripolar LV leads (i.e. based on an empirical strategy, guided by Q-LV sense). Q-LV sense is measured unipolar and defined as the time interval between QRS onset on the surface ECG and the maximum voltage *change* over time (i.e. dV/dt), recorded on the electrocardiogram. The LV electrode with the longest Q-LV sense in combination with acceptable pacing threshold and without diaphragmatic stimulation will be selected. In the image-guided intervention group, 2-dimensional fluoroscopic images are co-registered to the previously derived CARTBox treatment file from CMR postprocessing, and visualised in real-time in conjunction with the live fluoroscopy used during the implantation procedure **(Figure 3)**. The LV-lead will be deployed on the basis of the pre-defined target. Only when multiple electrodes are within the target region, electrode selection based on electrical properties (e.g. Q-LV sense) is applied.
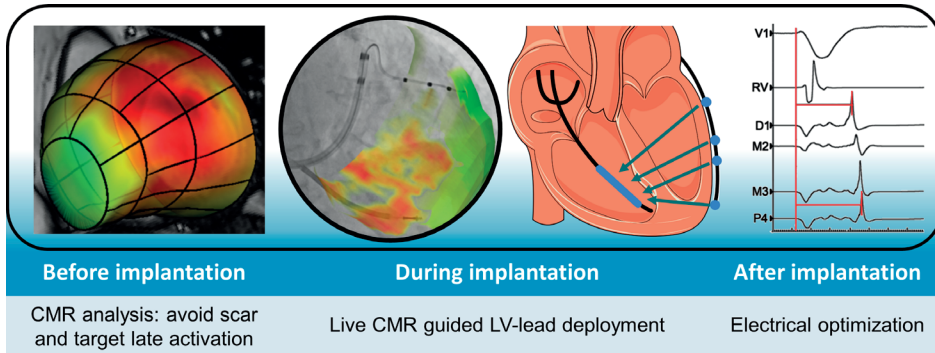
Figure 3. *Workflow for advanced image-guided LV-lead placement. Adapted from Wouters et al [8]. CMR, cardiac magnetic resonance imaging. LV, left ventricular.*

During the procedure, pacing capture thresholds, phrenic nerves stimulation, intrinsic electrical delay (i.e. Q-LV sense) and various LV-paced effects (i.e. LV-pace to RV-sense and RV-pace to LV-sense) will be determined for each electrode of the quadripolar lead positions. When the ultimate lead position has been established, LAO40 and RAO 30 fluoroscopic imaging will be performed to determine the exact final lead location. Final LV lead location will be determined by two investigators, blinded to treatment group and outcome of each other. LVLP will be determined through registration of the CMR-derived LV lateral wall model onto the LAO40 and RAO30 fluoroscopy images, similar to the method described by Singh and colleagues [12]. Adverse events which are possibly related to CARTBox or the procedure, reported spontaneously by the subject or observed by the investigator or his staff, will be recorded in an electronic database.

Endpoints

The ability to achieve successful image-guidance will be based on differences in the percentage of within, adjacent, or remote from the target(s) selected for lead placement. Here, adjacent segments include diagonal segments. Secondary outcomes are relative reduction in LV end-systolic volume indexed to body surface area (LVESVi), proportional difference in volumetric response (≥ 15% LVESVi-reduction), differences in quality of life, and differences in the CRT response score. The latter is a hierarchical clinical endpoint based on HF-hospitalisation and/or death within 12 months, relative LVESVi-change, and change in NYHA class [14]. Other outcome measures include the following: implantation procedure time, fluoroscopy time, contrast dose, device or procedure-related complications, change in QRS duration and QRS_{AREA}, indices of mechanical recoordination, and LV-lead parameters (Q-LV sense, pacing threshold, phrenic stimulation). Lastly, a Health Technology Assessment concerning the additional value of image-guided LVLP in terms of healthcare expenditure revolving heart failure care will be performed. This

assessment will be based on a previously conducted early economic analysis, which is described in this article.

Sample size

When comparing image-guided and contemporary implantation of CRT, the proportional difference in within-target LVLP ranges between 6 and 30%, and thus varies considerably [8]. In contrast, ADVISE targets segments approximately half the size of areas used in previous studies, rendering the chance of fortuitously successful in-target implantation in either study group much smaller.

We therefore hypothesized that image-guidance will result in a proportional difference in within-target LVLP of at least 27% when compared to empirical lead placement. In order to demonstrate this proportional difference using a two-sided Fisher exact test with 80% power and alpha = 0.05, a total of 114 successfully implanted patients are needed.

Concerning the secondary endpoint of LV reverse remodelling, given an expected standard deviation below 25%, a significant difference in LVESVi reduction between both groups of at least 13% can be detected in 116 patients. Accounting for failed implantations, loss to follow-up and incomplete (echocardiographic) data in about 10% of cases, total sample size necessary was set at 130 patients.

Statistical analysis

An intention-to-treat analysis will be performed to assess LV-lead location and echocardiographic response. In echocardiographic non-responders where electrode reselection is feasible, transition of control patients towards the treatment group may occur after six months. To account for this potential cross-over, an additional per-protocol analysis may be performed with respect to long-term clinical endpoints and the HTA.

The primary endpoint concerning LV-lead location will be defined categorically as being within, adjacent, or remote from the pre-defined target. A two-tailed Fisher exact test will be performed to assess differences in lead location between both groups. Because in principle, the effect of a targeted approach is considered to result in a unidirectional change in lead location, a one-tailed Fisher exact test may be performed as well.

Secondary endpoints will be analysed according to treatment allocation and lead location using Student's *t*-test and one-way ANOVA, or the Wilcoxon's rank sum test and Kruskal-Wallis wherever applicable. Lastly, intra- and inter-observer agreement of the echocardiography core laboratory analysis of LV reverse remodelling will be demonstrated by computing intraclass correlation coefficients in approximately 25 echocardiograms. A p-value < 0.05 will be considered significant.

Patient and public involvement

Patients are part of our multidisciplinary consortium, both before and during the study, and are as such involved in the design and conduct of the study. The priority of the research question, patient communication, study logistics, and methods of recruitment have been informed by discussions with patients representing our study population.

Ethics and dissemination

The ADVISE trial will be conducted according to the principles of the Helsinki Declaration II and Good Clinical Practice guidelines. The protocol has been written in accordance with the Standard Protocol Items: Recommendation For Interventional Trials (SPIRIT) checklist [15]. The study protocol has been approved by the Medical Research Ethics Committee Utrecht (NL73416.041.20), and has been registered at ClinicalTrials. gov (NCT05053568) and Netherlands Trial Register (Trial NL8666). All participants are required to provide written informed consent, prior to study procedures. Patients are currently being enrolled, with the first patient included in February 2021. Results will be disseminated at various presentations and will be submitted to peer-reviewed journals.

Early economic evaluation

To estimate the expected impact on cost and effects of image-guided LVLP in CRT, an early decision analytic model was developed using a Markov-model consisting of seven mutually exclusive health states (**Figure 4**). These health states were identified in collaboration with clinical experts and based on available literature **(Supplemental Table 1-2)**. In brief, a group of 1.000 individuals with heart failure were simulated, receiving either contemporary or image-guided LVLP. The analysis was performed from a societal perspective, including both direct healthcare costs and, where applicable, productivity losses due to absence from work. Model cycle length was one month, and model time horizon was 120 months. This model was developed in Microsoft Excel, version 2010/2016 (Microsoft, Redmond, WA, USA).

Treatment of patients/structure of the model

Patients with heart failure enter the model after the index CRT procedure (4:1 CRT-D versus CRT-P) where all patients are deemed to be in stable condition. After implantation, sequentially patients may 'transition' towards various 'health states', namely: cardiac decompensation (at most three times), Left Ventricle Assist Device (LVAD) implantation, or heart transplant. Detailed overviews of healthcare provided for each of the health states are found in **Supplemental Table 1-2**. Each health state is assigned a different probability of all-cause mortality.
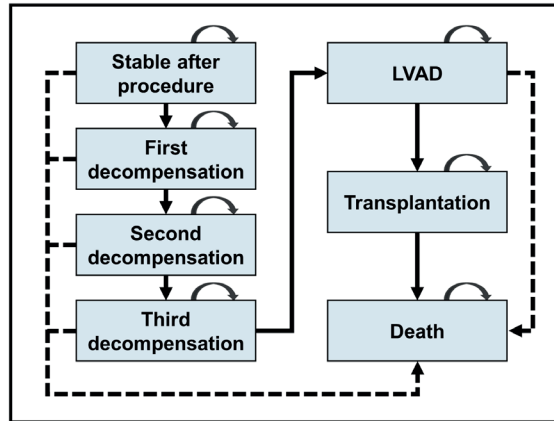
Figure 4. *Seven 'health states' (squares) were defined. Patients either remain in their state during follow-up (inward arrows), or relocate towards the next sequential health state (uninterrupted arrows). Each transition is assigned its own probability of occurrence. When death occurs, other health states may be skipped (dashed arrows). Note that the assumption was made that post-CRT patients with ≤ 2 decompensations will not receive LVAD or transplantation. LVAD, Left Ventricle Assist Device.*

7

Input parameters

Different sources were used to identify input parameters and parameter values. The majority of parameter values were retrieved from existing scientific literature. Where data was not publicly available, expert opinion and data from UMC Utrecht were used. Given the nature of this early analysis, no definitive data is currently available that combines clinical effects and costs for image-guided LVLP. Input values for effects and costs were therefore estimated by experts.

Clinical Outcomes & image-guided lead placement effectiveness

For standard care, an assumed percentage of responders (LVESV-reduction ≥ 15%) was set at 60% (17). For the additional effects of image-guided LVLP the percentage of responders was increased with steps of 2.5% to a maximum of 97.5%. We also analysed the situation for when 70% of patients receiving standard care are responders. First decompensation probability, the arrow from stable to first decompensation in **Figure 4**, was based on a weighted average for hospitalization probabilities for responders and non-responders (18). Transfer probabilities between other health states were assumed to be equal between standard care and care with image-guided LVLP and were based on clinical outcomes which were retrieved from literature (19-21). Most important index procedure complications were pneumothorax, lead dislocation, bleeding and pocket infection. Probabilities of these complications occurring were based on previous research conducted at the UMCU and were assumed not to differ between image-guided LVLP and standard care (22).
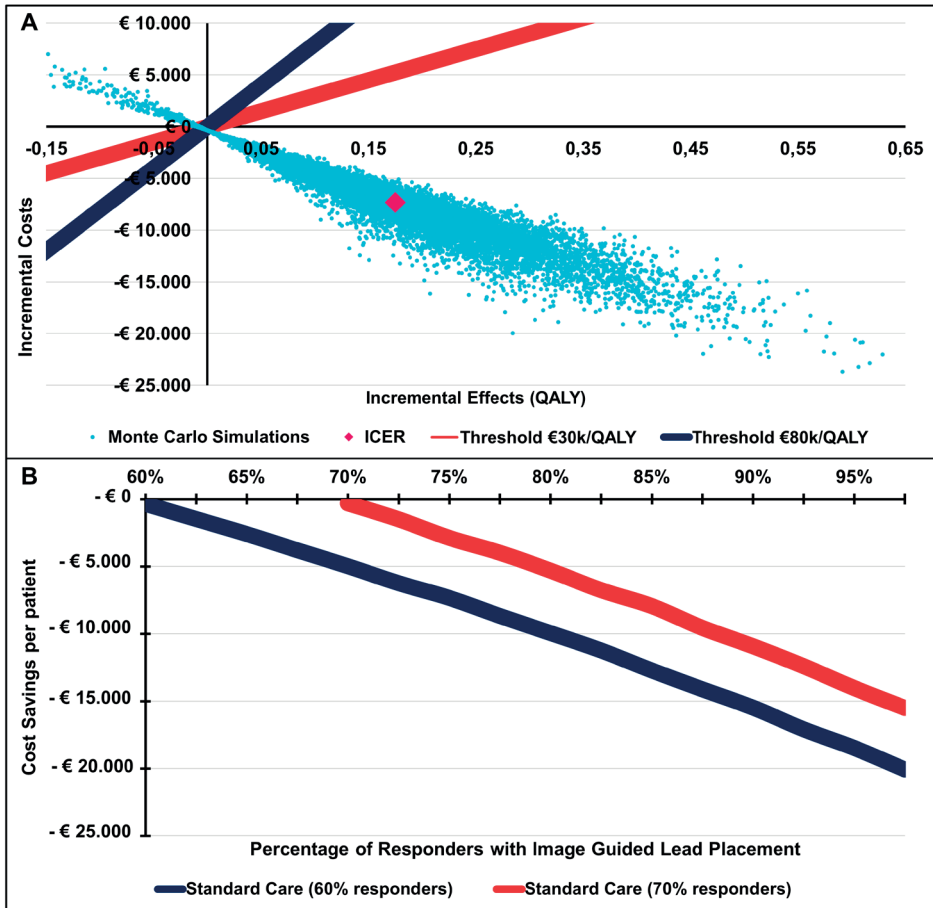
Figure 5. *A: Cost-Effectiveness Plane for image-guided lead placement. The graph shows the iterations (blue dots) in comparison to the cost effectiveness thresholds for €30.000/QALY and € 80.000/QALY (red and blue lines). B: Potential cost savings with image-guided lead placement, based on the proportional difference in responders. Legend: ICER, Incremental Cost Effectiveness Ratio (∆€/∆QALY); QALY, Quality Adjusted Life Year.*

Cost-effectiveness estimation for image-guidance

Based on 10,000 Monte Carlo iterations in the probabilistic sensitivity analyses, **Figure 5A** shows the cost-effectiveness plane. Here, the Monte Carlo iterations are represented by the blue dots. Mean cost difference was found to be -€7.329 (95%-CI: -€15.760 to € 323) and mean Quality Adjusted Life Year (QALY) gain was 0.17 (95%-CI: -0.02 to 0.40). The majority of iterations (96%) resulted in cost saving and an incremental health gain for image-guided LVLP, as compared to standard care.

When the effectiveness of standard care is considered to be 70%, and the effectiveness of CMR guided LVLP is varied between 70% and 95%, the results shown in **Figure**

5B were found. Even at relatively small improvements in the proportion of responders, image-guided LVLP leads to cost savings ranging from € 317 to € 20.069.

One-way sensitivity analysis

In the one-way sensitivity analysis, we varied input parameter value with -20% and +20%, this means the values of all parameters were altered one-by-one. By doing this for all model input parameters, the influence of each parameter on model outcome is demonstrated. The one-way sensitivity analysis showed that the parameters with the greatest influence on the outcomes of the economic evaluation were; i) the percentage of responders for standard care, and ii) the percentage of responders for care with image guided LVLP. This entails that changes in the value of these parameters will most likely change the outcomes of the economic evaluation the most.

DISCUSSION

7

Electrical versus image-guided strategy

Although the STARTER and TARGET study demonstrated the benefit of an image-guided approach for LVLP, they were performed in a time where electrical guiding (using QLV-sense) was not yet routinely performed [10,16]. However, QLV-guidance is nowadays readily available in many centres, and therefore, the results STARTER and TARGET cannot be directly extrapolated to current practice [4,17].

It is therefore noteworthy that only one study carefully investigated both an electrically guided approach (using QLV-sense) and an image-guided approach in a direct comparison [18]. Although Stephansen et al., reported non-inferiority of an electrical approach, we need to consider that these patients had typical LBBB with an average QRS-duration of 169 ms. This is in contrast to patients with non-LBBB morphology, where a QLV-guided approach fails to result in superior outcome when compared to contemporary lead placement [19]. In these patients, an image-guided strategy appears to be more beneficial [16]. Ultimately, electrically-guided and mechanically guided approaches each have their own strengths and limitations, and both may have yet to reach their full potential [8].

Methods used for left ventricular lead placement

Because in-scar pacing is associated with a six fold increased risk for cardiovascular death or hospitalization for HF, avoiding in-scar pacing is of utmost importance [3]. We therefore used CMR with late gadolinium enhancement, which is considered the gold-standard for detection of myocardial scar and has a higher spatial resolution than [82]Rubidium

positron emission tomography [20]. In contrast, the utility of strain imaging using echocardiography for detecting scar is poor with a sensitivity of only 33% [21].

In addition to avoiding scar, feature tracking is performed on CMR CINE sequences in order to determine viable segments with late mechanical activation. Although CMR has lower temporal resolution than speckle-tracking echocardiography, its benefits include the ability to sequence the whole heart and the lack of need for adequate acoustic windows. In addition, strain analysis from CMR is subject to less bias and variability and can be done semi-automatically.

Live fusion and target visualisation

Regardless of the methods used, it is inevitable that there will always be patients in which a target cannot be reached. In particular, the variability and difficulty of reaching a pre-defined target is evidenced by the wide range of remote-from-target lead location, as reported in previous studies [8]. Although venous access is undoubtedly a limiting factor, visualizing target for lead deployment *during* the procedure most likely enhances the proportion of optimally placed leads, since the implanter strives to implant the LV lead as close as possible to the target tissue in a patient specific fashion. Although the feasibility of live fusion has been demonstrated in two previous studies [22,23], they were limited by a small sample size and non-randomized design.

Early economic analysis

The analysis resulted in a robust model outcome for image-guided LVLP in CRT, demonstrating a mean cost savings of approximately €7.000 with simultaneous incremental health gain, relative to standard empirical LVLP. Although results are highly dependent on proportional differences in response, cost-savings are likely feasible even at relatively small clinical improvements. Because any decision analytic model is a simplified version of the actual healthcare pathway, definitive clinical effectiveness must be awaited from data gathered by the ADVISE trial. However, should the estimated mean cost savings hold, a meaningful improvement in cost-effectiveness can be realised. This may be especially valuable in low-to-middle income countries, where referral and implant rates are still relatively lacking [24].

Strengths and limitations

Our study is primarily limited by its relatively small sample size, and as a consequence, lack of primary *clinical* endpoint with sufficient power to detect differences in LVESVi-changes below 13% between both groups. Regardless, the present study is the first *multicenter* randomized controlled trial set out to investigate live CMR-guided LVLP in CRT, thereby providing data in a real-world setting. CMR is however less suitable for patients with prior device implantation due to magnetic field inhomogeneities, reduc-

ing image quality. Although CMR-FT has a lower temporal resolution when compared to speckle-tracking echocardiography, it may suffer from less noise and inter-observer dependence. Moreover, our technique allows for gold-standard scar detection, accurate segmentation, and live visualization of suitable targets for lead deployment. Lastly, although fluoroscopy-based determination of LVLP has limited reproducibility, simultaneous co-registration with our MRI-derived LV lateral wall model may improve its accuracy [25].

Future perspectives

Previous studies were conducted without performing QLV-guidance in the control group, and were limited by using at most two recruiting centres [10,16,18]. Moreover, to date, no studies utilized *live* image-guidance in a randomized controlled design. Should our study be able to detect more LV reverse remodelling and/or better clinical outcome, an important step has been set towards more widespread adoption of image-guided strategies for optimized LVLP in CRT.

7

REFERENCES

1. M. Brignole, A. Auricchio, G. Baron-Esquivias, *et al.* 2013 ESC Guidelines on cardiac pacing and cardiac resynchronization therapy: The Task Force on cardiac pacing and resynchronization therapy of the European Society of Cardiology (ESC). *Europace*. **15**, 1070–1118 (2013).

2. N. M. Hawkins, M. C. Petrie, M. R. MacDonald, K. J. Hogg, J. J. V. McMurray. Selecting patients for cardiac resynchronization therapy: Electrical or mechanical dyssynchrony? *Eur. Heart J*. **27**, 1270–1281 (2006).

3. F. Leyva, P. W. Foley, S. Chalil, *et al.* Cardiac resynchronization therapy guided by late gadolinium-enhancement cardiovascular magnetic resonance. *J. Cardiovasc. Magn. Reson*. **13**, 29 (2011).

4. M. R. Gold, U. Birgersdotter-Green, J. P. Singh, *et al.* The relationship between ventricular electrical delay and left ventricular remodelling with cardiac resynchronization therapy. *Eur. Heart J*. **32**, 2516–2524 (2011).

5. F. Z. Khan, M. S. Virdee, P. A. Read, *et al.* Effect of low-amplitude two-dimensional radial strain at left ventricular pacing sites on response to cardiac resynchronization therapy. *J. Am. Soc. Echocardiogr*. **23**, 1168–1176 (2010).

6. A. C. Kydd, F. Z. Khan, W. D. Watson, *et al.* Prognostic benefit of optimum left ventricular lead position in cardiac resynchronization therapy: follow-up of the TARGET Study Cohort (Targeted Left Ventricular Lead Placement to guide Cardiac Resynchronization Therapy). *JACC. Heart Fail*. **2**, 205–212 (2014).

7. M. D. Bogaard, P. A. Doevendans, G. E. Leenders, *et al.* Can optimization of pacing settings compensate for a non-optimal left ventricular pacing site? *EP Eur*. **12**, 1262–1269 (2010).

8. P. C. Wouters, K. Vernooy, M. J. Cramer, F. W. Prinzen, M. Meine. Optimizing lead placement for pacing in dyssynchronous heart failure: The patient in the lead. *Hear. Rhythm*. **18**, 1024–1032 (2021).

9. Y. Jin, Q. Zhang, J. Mao, B. He. Image-guided left ventricular lead placement in cardiac resynchronization therapy for patients with heart failure: a meta-analysis. *BMC Cardiovasc. Disord*. **15**, 36 (2015).

10. F. Z. Khan, M. S. Virdee, C. R. Palmer, *et al.* Targeted left ventricular lead placement to guide cardiac resynchronization therapy: The TARGET study: A randomized, controlled trial. *J. Am. Coll. Cardiol*. **59**, 1509–1518 (2012).

11. S. Saba, J. Marek, D. Schwartzman, *et al.* Echocardiography-Guided Left Ventricular Lead Placement for Cardiac Resynchronization Therapy. *Circ. Hear. Fail*. **6**, 427–434 (2013).

12. J. P. Singh, H. U. Klein, D. T. Huang, *et al.* Left ventricular lead position and clinical outcome in the multicenter automatic defibrillator implantation trial-cardiac resynchronization therapy (MADIT-CRT) trial. *Circulation*. **123**, 1159–1166 (2011).

13. N. B. Schiller, P. M. Shah, M. Crawford, *et al.* Recommendations for quantitation of the left ventricle by two-dimensional echocardiography. American Society of Echocardiography Committee on Standards, Subcommittee on Quantitation of Two-Dimensional Echocardiograms. *J. Am. Soc. Echocardiogr. Off. Publ. Am. Soc. Echocardiogr*. **2**, 358–367 (1989).

14. M. Packer. Development and Evolution of a Hierarchical Clinical Composite End Point for the Evaluation of Drugs and Devices for Acute and Chronic Heart Failure: A 20-Year Perspective. *Circulation*. **134**, 1664–1678 (2016).

15. A.-W. Chan, J. M. Tetzlaff, P. C. Gøtzsche, *et al.* SPIRIT 2013 explanation and elaboration: guidance for protocols of clinical trials. *BMJ Br. Med. J*. **346**, e7586 (2013).

16. J. J. Marek, S. Saba, T. Onishi, *et al.* Usefulness of echocardiographically guided left ventricular lead placement for cardiac resynchronization therapy in patients with intermediate QRS width and non-left bundle branch block morphology. *Am. J. Cardiol.* **113**, 107–116 (2014).

17. M. R. Gold, R. B. Leman, N. Wold, J. L. Sturdivant, Y. Yu. The effect of left ventricular electrical delay on the acute hemodynamic response with cardiac resynchronization therapy. *J. Cardiovasc. Electrophysiol.* **25**, 624–630 (2014).

18. C. Stephansen, A. Sommer, M. B. Kronborg, *et al.* Electrically vs. imaging-guided left ventricular lead placement in cardiac resynchronization therapy: a randomized controlled trial. *EP Eur.* (2019), doi:10.1093/europace/euz184.

19. J. P. Singh, R. D. Berger, R. N. Doshi, *et al.* Targeted Left Ventricular Lead Implantation Strategy for Non-Left Bundle Branch Block Patients: The ENHANCE CRT Study. *JACC. Clin. Electrophysiol.* **6**, 1171–1181 (2020).

20. P. Hunold, H. Jakob, R. Erbel, J. Barkhausen, C. Heilmaier. Accuracy of myocardial viability imaging by cardiac MRI and PET depending on left ventricular function. *World J. Cardiol.* **10**, 110–118 (2018).

21. Z. Bakos, E. Ostenfeld, H. Markstad, *et al.* A comparison between radial strain evaluation by speckle-tracking echocardiography and cardiac magnetic resonance imaging, for assessment of suitable segments for left ventricular lead placement in cardiac resynchronization therapy. *EP Eur.* **16**, 1779–1786 (2014).

22. J. M. Behar, P. Mountney, D. Toth, *et al.* Real-Time X-MRI-Guided Left Ventricular Lead Implantation for Targeted Delivery of Cardiac Resynchronization Therapy. *JACC. Clin. Electrophysiol.* **3**, 803–814 (2017).

23. A. K. Shetty, S. G. Duckett, M. R. Ginks, *et al.* Cardiac magnetic resonance-derived anatomy, scar, and dyssynchrony fused with fluoroscopy to guide LV lead placement in cardiac resynchronization therapy: a comparison with acute haemodynamic measures and echocardiographic reverse remodelling. *Eur. Heart J. Cardiovasc. Imaging.* **14**, 692–699 (2013).

24. K. Dickstein, C. Normand, A. Auricchio, *et al.* CRT Survey II: a European Society of Cardiology survey of cardiac resynchronisation therapy in 11 088 patients—who is doing what to whom and how? *Eur. J. Heart Fail.* **20**, 1039–1051 (2018).

25. A. Sommer, M. B. Kronborg, B. L. Nørgaard, *et al.* Left and right ventricular lead positions are imprecisely determined by fluoroscopy in cardiac resynchronization therapy: a comparison with cardiac computed tomography. *Eur. Eur. pacing, arrhythmias, Card. Electrophysiol. J. Work. groups Card. pacing, arrhythmias, Card. Cell. Electrophysiol. Eur. Soc. Cardiol.* **16**, 1334–1341 (2014).

7

SUPPLEMENTARY MATERIAL

Supplemental Table 1. Cost calculations for input parameters.

	Quantity	Unit Cost (€)	Total Cost (€)	Source
Index Procedure				
Diagnostics				
Cardiac MRI	1	376.91	376.91	(1)
Cardiac Ultrasound	1	139.49	139.49	(1)
Thorax X-Ray	1	61.27	61.27	(1)
Lab work	2	44.46	88.92	(1)
CRT				
Procedural Costs	1	1,432.74	1,432.74	(2)
Biventricular ICD	0.8	12,387.68	9,910.14	(2)
Biventricular Pacemaker	0.2	6,644.83	1,328.97	(2)
Admission				
General Ward Admission	2	668.24	1,336.48	(3)
			14,814.14	
Procedural Complications				
Pocket Infection				
PET/CT Thorax	1	850.99	850.99	(1)
Transesophageal Ultrasound	1	263.81	263.81	(1)
ICD Removal	1	1,039.19	1,039.19	(2)
Pocket Revision	1	956.46	956.46	(2)
ICD Implantation	1	1,045.41	1,045.41	(2)
ICD Device	1	11,594.87	11,594.87	(2)
General Ward Admission	7	668.27	4,677.89	(3)
			20,428.62	
Pneumothorax				
Thorax X-Ray	1	61.27	61.27	(1)
Thorax Drain	1	788.27	788.27	(1)
General Ward Admission	3	668.24	2,004.72	(3)
			2,854.26	
Wire Dislocation				
Thorax X-Ray	2	61.27	122.54	(1)
Replacement CRT Leads	1	600.75	600.75	(2)
General Ward Admission	2	668.24	1,336.48	(3)
			2,059.77	
Follow-up				
Outpatient Visit	1	169.86	169.86	(1)
Lab work	1	44.46	44.46	(1)
			214.32	

Supplemental Table 2. Cost calculations for various health states.

	Quantity	Unit Cost (€)	Total Cost (€)	Source
Additional Healthcare Costs Model Health States				
Decompensation I				
Cardiac Ultrasound	1	139.49	139.49	(1)
General Ward Admission	7	668.24	4,677.68	(3)
			4,817.17	
Decompensation II				
Cardiac Ultrasound	1	139.49	139.49	(1)
Central Venous Line	1	365.38	365.38	(1)
Cardiac Care Unit Admission	14	1,986.48	27,810.72	(3)
			28,316.59	
Decompensation III				
Cardiac Ultrasound	1	139.49	139.49	(1)
Central Venous Line	1	365.38	365.38	(1)
Implantation Ventricle Assist Device (LVAD)	1	5,388.58	5,388.58	(2)
Materials LVAD	1	87,292.15	87,292.15	(2)
Cardiac Care Unit Admission	28	1,986.48	55,621.44	(3)
			148,807.04	
LVAD				
Considered equal to Decompensation III	1	148,807.04	**148,807.04**	(1-3)
Transplantation				
Heart Transplantation including Admission	1	37,579.47	**37,579.47**	(4)

7

SUPPLEMENTAL REFERENCES

1. Performance and Tariffs Specialist Medical Care (Prestaties en tarieven medisch-specialistische zorg) [Internet]. Nederlandse Zorgauthoriteit (Netherlands Healthcare Authorirty) 2018 [cited 24-11-2020]. Available from: https://puc.overheid.nl/nza/doc/PUC_13408_22/.
2. Internal Calculation Department of Cardiology, UMC Utrecht
3. L. Hakkaart-van Roijen NvdL, C. Bouwmans, T. Kanters, S. Swan Tan. Methodologie van kostenon-derzoek en referentieprijzen voor economische evaluaties in de gezondheidszorg (Manual for cost analyses, methods and referenceprices for economic evaluations in healthcare). Diemen, the Netherlands: Zorginstituut Nederland (Netherlands National Healthcare Institute); 2016.
4. Open data van de Nederlandse Zorgauthoriteit [Internet]. Nederlandse Zorgauthoriteit (Netherlands Healthcare Authority). 2020. Available from: www.opendisdata.nl
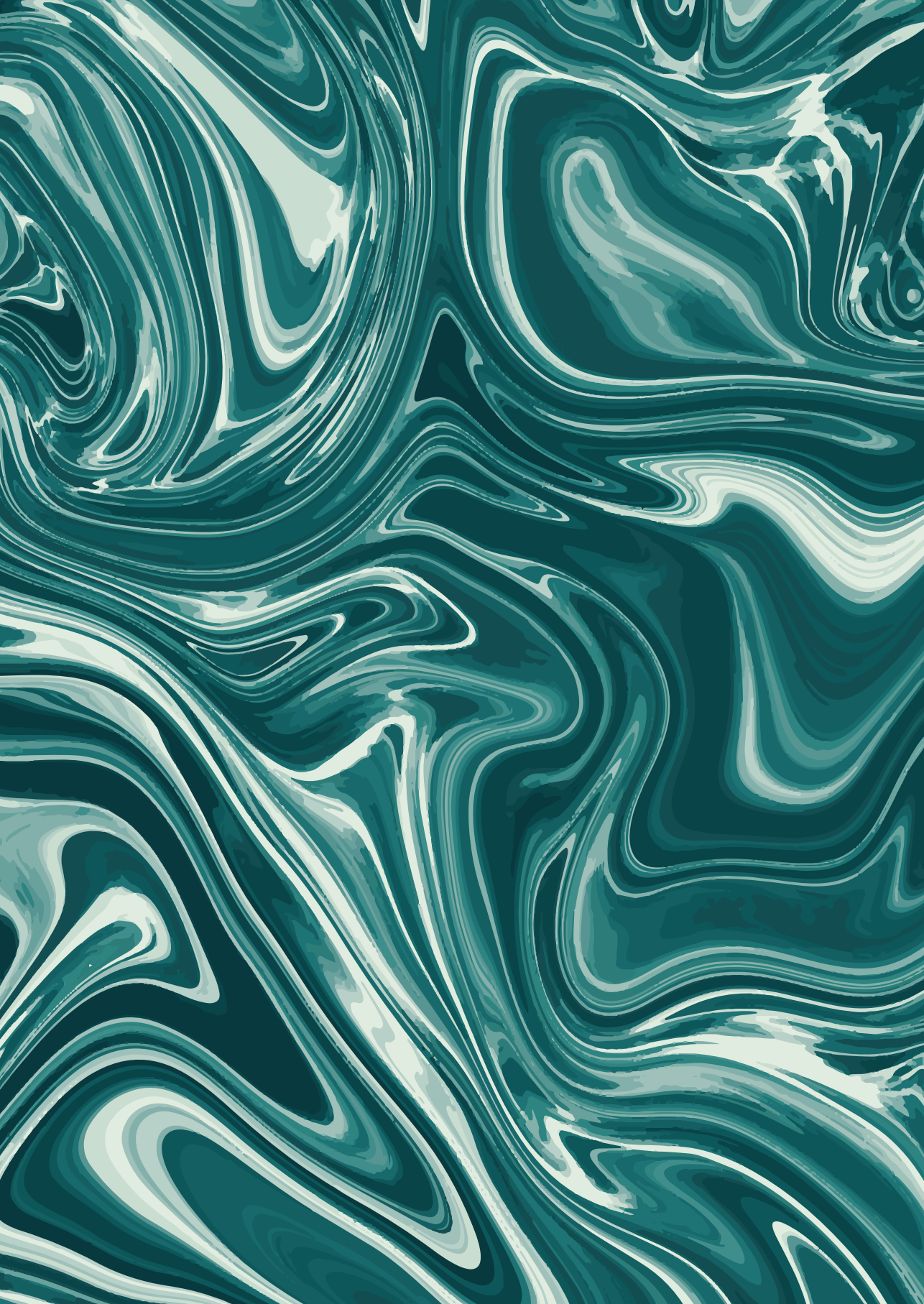
PART III

EXPLORING EXERCISE PHSYIOLOGY

8

Strain-Based Discoordination Imaging During Exercise in Heart Failure with Reduced Ejection Fraction: Feasibility and Reproducibility

Louis S. Fixsen, Philippe C. Wouters, Richard G.P. Lopata, Hareld M.C. Kemps

ABSTRACT

Purpose: Various parameters of mechanical dyssynchrony have been proposed to improve patient selection criteria for cardiac resynchronization therapy (CRT), but sensitivity and specificity are lacking. However, echocardiographic parameters are consistently investigated at rest, whereas heart failure (HF) symptoms predominately manifest during submaximal exertion. Although strain-based predictors of response are promising, feasibility and reproducibility during exercise has yet to be demonstrated.

Methods: Speckle-tracking echocardiography was performed in patients with HF at two separate visits. Echocardiography was performed at rest, during various exercise intensity levels, and during recovery from exercise. Systolic rebound stretch of the septum (SRSsept), systolic shortening (SS), and septal discoordination index (SDI) were calculated.

Results: Echocardiography was feasible in about 70-80% of all examinations performed during exercise. Of these acquired views, 84% of the cine-loops were suitable for analysis of strain-based mechanical dyssynchrony. Test-retest variability and intra- and interoperator reproducibility at 30% and 60% of the ventilatory threshold (VT) were about 2.5%. SDI improved in the majority of patients at 30% and 60% of the VT, with moderate to good agreement between both intensity levels.

Conclusion: Although various challenges remain, exercise echocardiography with strain analysis appears to be feasible in the majority of patients with dyssynchronous heart failure. Inter- and intra-observer agreement of SRSsept and SDI up to 60% of the VT were comparable to resting values. During exercise, the extent of SDI was variable, suggesting a heterogeneous response to exercise. Further research is warranted to establish its clinical significance.

INTRODUCTION

For over 20 years, cardiac resynchronization therapy (CRT) has been an established device therapy for patients with heart failure (HF) with depressed left ventricular (LV) ejection fraction and LV conduction delay [1]. In addition to an electrical substrate amendable to CRT, patients that benefit from resynchronization are typically characterised by signs of mechanical dyssynchrony as well [2].

Echocardiographic assessment of such parameters has been increasingly investigated as a method to better screen patients eligible for CRT [3–5]. Nonetheless, randomised clinical trials that implemented parameters of mechanical dyssynchrony have thus far shown insufficient predictive ability to actually affect clinical decision making [6]. Consequently, clinical and echocardiographic response to CRT remains suboptimal in 30-40% of patients [7,8].

There are various potential explanations for the lacking sensitivity and specificity of echocardiographic measures of mechanical dyssynchrony. First, parameters that were investigated prospectively often assessed relative timing differences within the LV [6,9]. Instead, analysis of deformation characteristics (i.e. discoordination in LV strain) may better reflect myocardial work inefficiency [10,11]. Second, echocardiographic evaluation of dyssynchrony is almost without exception performed at rest [6]. This is somewhat surprising, since patients with HF predominantly experience symptoms during exercise as a consequence of failing compensatory mechanisms. Mechanical dyssynchrony may therefore be exercise-dependent as well. Previous research has shown that echocardiographic parameters at rest do not necessarily represent (dys)synchrony during exercise [6,12,13]. Dyssynchrony during exercise may therefore be a superior predictor of response to CRT than parameters measured at rest alone [14–16]. However, to date, strain-based discoordination parameters have not yet been investigated.

Systolic rebound stretch of the septum (SRSsept), and acute restoration thereof, has been demonstrated as a strong predictor of response to CRT before [3,17,18]. SRSsept is a promising deformation-based parameter because it reflects myocardial work inefficiency within the septum [19]. SRSsept has been validated both in computer models and patients, and may better reflect the mechanical substrate that is amenable to CRT than other indices of mechanical dyssynchrony [20].

For example, dyssynchrony can be overlooked at rest (i.e. "exercise-induced unmasking") or disappear during exertion. To date, estimation of exercise-dependent discoordination using a strain-based parameter and its potential value has not been investigated. This is in part because assessment of SRSsept during exercise is challenging and faces a number of confounding factors (e.g. body motion and increased respiration, blood pressure and heart rate) that will affect the accuracy and interpretation of these measurements. The present exploratory study sought to investigate the feasibility and reproducibility [21] of SRSsept during exercise.

We determined the feasibility, test-retest variability, and the inter- and intra-observer reproducibility of SRSsept in heart failure patients during exercise tests. In addition, we evaluated potential exercise-induced unmasking or disappearance of SRSsept. Patients performed the exercise tests during two separate visits such that the reproducibility of the measurements could be determined. Additionally, variations in SRSsept during exercise were explored.

METHODS

Patients (n=18) with stable CHF that attended the outpatient clinic of the Máxima Medical Centre (Veldhoven, The Netherlands) were prospectively included. All patients provided written informed consent. The study protocol conformed to the principles outlined in the Declaration of Helsinki on research in human subjects and to the procedures of the regional Medical Ethics Committee.

Patients included in the study must have HF with an LVEF ≤ 35%. Patients were excluded if they had: a myocardial infarction or unstable angina less than 3 months prior to inclusion; any diseases (orthopaedic, vascular, pulmonary or neuromuscular) that limited exercise capacity such that exercise tests were not feasible; clinical signs of decompensated heart failure; documented ventricular tachycardia or ischemia during exercise; intra-cardiac shunts or congenital heart disease limiting exercise capacity.

Each patient made three visits to the hospital. The first visit consisted of a routine clinical examination and incremental (symptom limited) exercise test with respiratory gas analysis in order to determine the ventilatory threshold (VT). The VT was used to determine exercise intensity of the submaximal exercise performed in visits 2 and 3. Exercise echocardiography was performed by the same sonographer during visit 2 and 3). Ultrasound data were also acquired before (i.e. rest) and after (i.e. recovery) the exercise bouts.

Symptom limited incremental exercise testing

After the initial clinical examination, a symptom limited, incremental exercise test with respiratory gas analysis was performed on a cycle ergometer (Lode Corival, Groningen, The Netherlands), using an individualised ramp protocol aiming at a total test duration of 8-12 minutes. Patients were instructed to maintain a pedalling frequency of 70 rotations per minute. A twelve-lead electrocardiogram (ECG) was recorded continuously. Peak oxygen uptake (peak VO$_2$) was defined as the average value of oxygen uptake during the last 15 seconds of exercise. VT was assessed by the V-slope method [22]. If symptom limited exercise test had already been performed within the previous 3 months, these data were used to establish the exercise protocol for exercise echocardiography.

Exercise echocardiography measurements

The exercise protocol was performed on an Echo Cardiac Stress table (Lode, Groningen, The Netherlands). Patients were placed in a supine position and rotated an additional 45 degrees around the longitudinal axis. The exercise protocol was constructed from the results of the symptom limited incremental exercise test with respiratory gas analysis and consisted of three 2-minute exercise bouts, respectively at 30%, 60%, 90% of the VT **(Figure 1a)**.

Two-dimensional ultrasound DICOM cine-loops were acquired with a Philips Epiq 7C scanner (Philips Healthcare, Best, The Netherlands) equipped with an X5-1 transducer. The cine-loops had a resolution of 800 by 600 pixels and a frame rate of 50 to 90 frames per second. For the septal strain analysis, zoomed-in (i.e., narrow aperture), high frame rate (90 Hz) cine-loops of the inter-ventricular septum were acquired (**Figure 1b**). LV end-diastolic and end-systolic volumes and ejection fraction were assessed by the bi-plane Simpson's disk method. Mitral valve closure (MVC) and aortic valve closure (AVC) were determined at rest from Doppler flow measurements. Where Doppler measurements were unavailable these were determined visually from parasternal long-axis cine-loops. Data were excluded for image quality reasons if there was an incomplete view of the septum through the entire cardiac cycle; either due to significant image artefacts, out-of-plane motion of the heart, or structures preventing transmission of ultrasound.

8
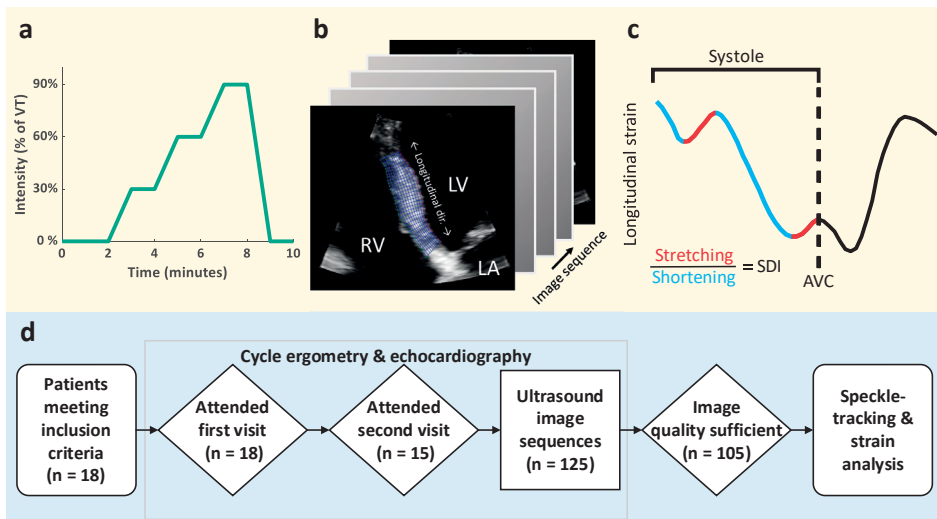
Fig. 1 *Study overview. **a** Heart failure patients were subjected to echocardiography during exercise at various intensity levels of the ventilatory threshold (VT). **1b & 1c** This was followed by segmentation and and automated analyses of septal systolic rebound stretch (SRSsept). **1d** Flowchart of ultrasound data processing; from cycle ergometry to speckle tracking-based strain analysis. Legend: AVC, aortic valve closure; LA, left atrium; LV, left ventricle; RV, right ventricle; SDI, septal discoordination index; SRSsept, septal rebound stretch of the septum; VT, ventilatory threshold.*

Systolic and diastolic times vary non-linearly with changes in heart rate from rest [23]. Timing of AVC and cardiac cycle length were therefore scaled to account for changes in the ratio between systolic and diastolic times relative to rest, using data from Bombardini et al. [23]. Systolic and diastolic times during stress and relaxation at the provided heart rates were fitted to a curve with smoothing splines. Each patient's measured heart rate during exercise and recovery was then evaluated along the fitted lines, yielding an estimate of expected change in systolic and diastolic time.

Speckle tracking

Speckle tracking was performed on DICOM image sequences using a custom strain imaging toolbox implemented in MATLAB (revision 2019b, 64-bit, The Mathworks Inc. Natick, MA, USA), previously described in detail by Lopata et al. [24]. The septum was segmented from the closest visible portion in the direction of the apex until the level of the mitral and tricuspid valves, or the closest visible point distal of the valves (**Figure 1b**). Segmentation of the septum was performed by two independent observers (LF and PW) who were blinded to outcome (i.e. resting/exercise phase). A mesh of 11 radial by 31 longitudinal points was generated over the segmented area, obeying a local coordinate system. A 2-D block matching algorithm was then used to estimate inter-frame displacements of different regions of pixels and mapped to the intersecting points of the mesh. Cumulative strain in the longitudinal direction was calculated with a least-squares strain estimator, taking the spatial derivative of the deformation of the mesh from the initially segmented configuration. The resulting strain field over the visible septal region was then averaged, yielding septal longitudinal strain over time.

Mechanical discoordination indices

The determination of SRSsept has previously been described in detail by De Boeck et al [3]. In short, average deformation throughout the visible septum (blue segmented area in **Figure 1b**) at each time point was used to create curves of longitudinal strain over time. Longitudinal strain within the systolic period was grouped into shortening and stretching components (**Figure 1c**, blue and red portions respectively). SRSsept as an index of *wasted* septal work was thereafter calculated as the sum of systolic stretch within the septum that occurs directly after premature termination of longitudinal shortening. Conversely, systolic shortening (SS) was defined as the absolute sum of shortening during systole, a measure of *effective* work performed. Increased blood pressure during exercise exertion typically leads to a reduction in the overall magnitude of systolic strains, therefore complicating the comparison of systolic strain magnitudes during exercise. We therefore calculated the *ratio* between SRSsept and SS, here referred to as the septal discoordination index (SDI) [25], as shown in **Figure 1c**. This yields a measure of relative wasted and constructive work in the septum [26].

Table 1: Characteristics of the cohort included in this study.

	Total (n = 18)	Paired Data (n = 15)
General characteristics		
Male gender	17 (94%)	14 (93%)
Age (yr)	67 (59 - 74)	71 (64 - 75)
BMI (kg/m^2)	26.2 (23.2 - 30.7)	24.7 (22.6 - 30.6)
NYHA I	4 (22%)	4 (27%)
NYHA II	8 (44%)	7 (46%)
NYHA III	6 (33%)	4 (27%)
Comorbidities		
Ischemic cardiomyopathy	9 (50%)	6 (40%)
Medication		
Beta blockers	17 (94%)	14 (93%)
ACE-inhibitors/Angiotensin II receptor blockers	18 (100%)	15 (100%)
Diuretics	14 (78%)	12 (80%)
Aldosterone antagonists	7 (39%)	5 (33%)
ECG characteristics		
Sinus rhythm	18 (100%)	15 (100%)
QRS duration (ms)	131 ± 30.1	129 ± 29
QRS duration ≥ 130 (ms)	10 (56%)	8 (53%)
LBBB	8 (44%)	6 (40%)
Lab results		
NT-proBNP (pmol/l)	125 (67 - 205)	125 (67 - 205)
Echocardiography		
End-diastolic volume (ml)	174 (148 – 231)	171 (144 - 225)
End-systolic volume (ml)	124 (96.4 – 177)	121 (96 - 173)
Ejection fraction (%)	28.6 (26.5 - 33.1)	29.0 (24.3 - 33.3)

Legend: BMI = body mass index, NYHA = New York Heart Association, ACE = Angiotensin-converting enzyme, ARB = Angiotensin II receptor blockers, ECG = electrocardiogram, LBBB = Left bundle branch block, NT-proBNP = N-terminal prohormone of brain natriuretic peptide.

8

Statistical analysis

The similarity of the septal longitudinal strain curves (i.e. cumulative strain in the longitudinal direction) from each visit was assessed by Pearson's correlation at each exercise intensity level. Prior to correlation, the strain curves were normalised both in amplitude and number of samples (i.e., if there was a discrepancy in heartrate between the two visits); longer cardiac cycles were down-sampled to match the length of the shorter cycle. Intra- and inter-observer agreement was assessed through Bland-Altman analysis. Limits of agreement are given in absolute strain values. Continuous variables are presented as means with standard deviation and dichotomous data as percentages. The paired Student's t-test was used to assess differences between consecutive measurements. A

significance level of 0.05 was used. The test-retest, intra-observer, and inter-observer reliability of SRSsept was assessed by calculating the intraclass correlation coefficient (ICC), using a two-way mixed effects model to determine the absolute agreement of single measurements. Agreement between exercise-induced changes in SDI at different exercise intensity levels was assessed using Cohen's kappa coefficient. All data were analysed in MATLAB.

RESULTS

Feasibility

Of the 18 patients that were included and attended the first echocardiographic visit, 15 patients also attended the second visit (median 7 days apart; 165 total possible cine-loops). All but one patient were male, and half of the patients had an ischemic cardiomy-opathy **(Table 1)**. Ultimately, 137 cine-loops were acquired (83% of potential loops). As such, in 88% of the 33 distinct patient visits at least 2 out of 3 sequences during exercise were successfully acquired. Of the acquired cine-loops, 20 loops were excluded due to insufficient image quality and 12 sequences due to the patient only attending one visit. Therefore, 105 image sequences (77% of acquired loops) remained for strain analysis, in 12 of the 18 patients **(Figure 1d)**.

Table 2 shows an overview of the data included in the strain analysis. The remaining loops were graded at each measurement point (baseline, 30%, 60% and 90% of VT, and recovery) in terms of image quality (good, moderate and poor). Grading was based on the image contrast, definition of tissue structures, image plane stability, and presence of artefacts (or lack thereof). The number of cine-loops of a poor quality increased from 12 to 42% between rest (baseline) and high intensity exercise (90% VT). The mean length of ejection (during which SRSsept was calculated) was 0.34 ± 0.05 seconds, resulting in an average of 30.7 ± 4.6 frames during ejection.

Agreement and variability

Longitudinal strain was calculated in the septal region of the acquired ultrasound cine-loops **(Figure 2)**. In the first visit, prior to 90% VT, the patient with LBBB-type strain ceased the exercise protocol. There was generally good strain curve similarity between visits, with some differences in overall magnitude and period between tests. Median correlation (baseline, 0.91; 30%, 0.81; 60%, 0.86; 90%, 0.89; recovery, 0.86) ranged between 0.81 in the worst case (30% of VT) and 0.91 in the best case (baseline). However, interquartile ranges of correlation increased greatly between the baseline measurement and all further intensities. There was no significant correlation between image quality grade and strain curve similarity.

Table 2: *Summary of patient heart rate (median and interquartile range) and ultrasound data acquired at each intensity that were included in the final strain analysis.*

	Baseline	**30% VT**	**60% VT**	**90% VT**	**Recovery**
Heart rate					
Visit 1	60 (55 - 63)	79 (68 - 83)	90 (78 - 94)	97 (81 - 106)	78 (70 - 96)
Visit 2	63 (55 - 69)	76 (70 - 83)	85 (79 - 89)	94 (87 - 102)	88 (74 - 92)
Number					
Acquired	24	30	27	27	29
Attended twice	22 (91.7%)	25 (83.3%)	26 (96.3%)	24 (88.9%)	28 (96.6%)
Sufficient quality	20 (83.3%)	20 (66.7%)	22 (81.5%)	19 (70.4%)	24 (82.8%)
Image quality					
Good	9 (45%)	10 (50%)	8 (36.4%)	3 (15.8%)	8 (33.3%)
Moderate	9 (45%)	9 (45%)	10 (45.5%)	9 (47.4%)	8 (33.3%)
Poor	2 (10%)	1 (5%)	4 (18.2%)	7 (36.8%)	8 (33.3%)

Legend: VT = ventilatory threshold.
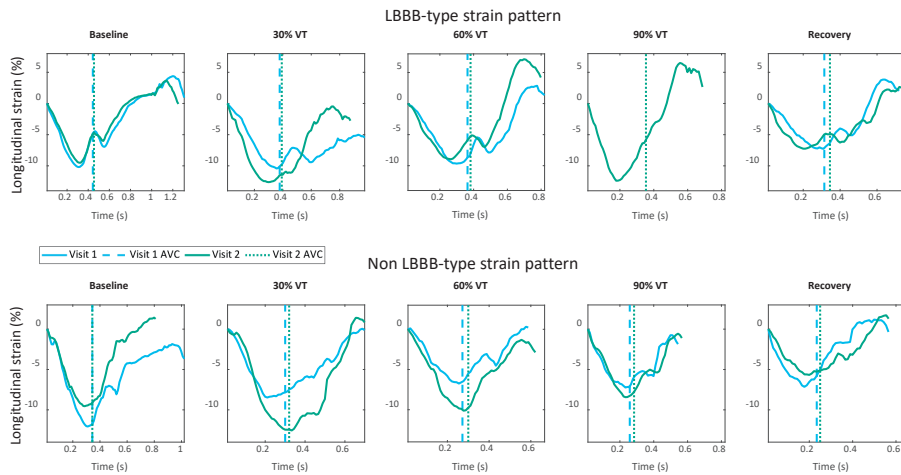
Fig. 2 *Septal strain curves in a patient with an LBBB-type strain pattern (upper), as seen in [20], and a patient with non LBBB-type strain pattern (lower), during each exercise intensity. Curves begin at mitral valve closure, with aortic valve closure (AVC) marked by dotted and dashed lines. Blue lines show strain during visit 1, green visit 2*

Bland-Altman plots showing the test-retest agreement of SRSsept are shown in **Figure 3** (upper row). Agreement for SRSsept at 30% and 60% of VT was comparable to agreement at baseline, with differences in SRSsept below 5% (mean ± standard deviation: baseline, 0.66 ± 1.67%; 30% VT, -0.81 ± 1.98%; 60% VT, 0.03 ± 1.67%). During higher exercise intensity (specifically 90%) and recovery, the confidence interval was wider and measurements with a large bias between visits were present.
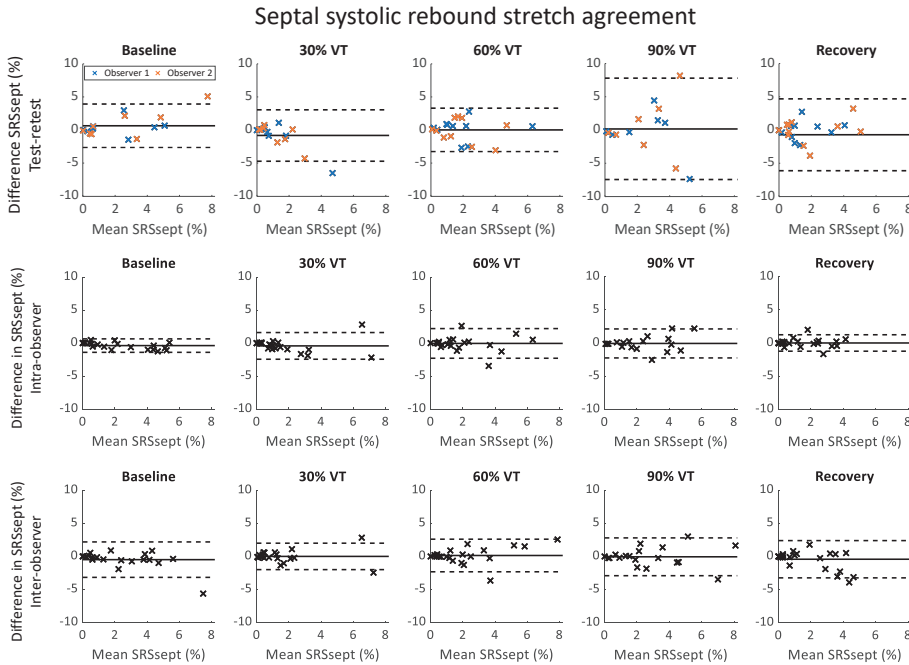
Fig. 3 Bland-Altman plots showing test-retest (upper), intra-observer (middle) and inter-observer (lower) differences in septal systolic rebound stretch (SRSsept). Different colour denotes observer (upper only).

Intra-observer limits of agreement for SRSsept were lowest at baseline (mean -0.37 ± 0.52%), and consistently increased when exercise continued to intensify. Limits of agreement remained within 2.3% at all exercise intensities and during recovery (**Figure 3**, middle row). Conversely, inter-observer limits of agreement for SRSsept were within 2.8% at baseline (mean -0.48 ± 1.37%) and remained similar for all intensities (**Figure 3**, lower row).

Test-retest agreement for SDI (**Figure 4**, upper row) was comparable at rest, 30% and 60% of VT and in recovery (baseline, 0.07 ± 0.31; 30% VT, -0.10 ± 0.24; 60% VT, -0.02 ± 0.30; recovery, 0.03 ± 0.30). However, at 90% VT agreement was poor (0.01 ± 0.75). Intra-observer agreement of SDI (**Figure 4**, middle row) during exercise far exceeded the variability at baseline (baseline, -0.02 ± 0.08) but remained similar during exercise and recovery, and was comparable to baseline test-rest agreement. Likewise, inter-observer agreement of SDI was comparable to baseline test-retest agreement, other than at 30% of VT where the variability was lower (0.03 ± 0.12).
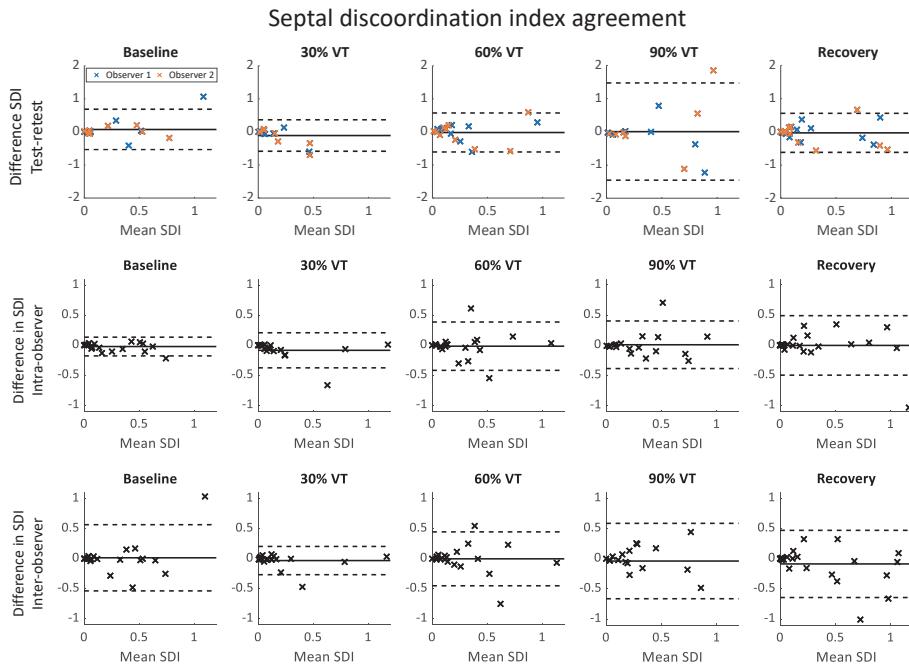
Fig. 4 *Bland-Altman plots showing test-retest (upper), intra-observer (middle) and inter-observer (lower) differences in septal discoordination index (SDI). Different colour denotes observer (upper only).*

Reliability

Intraclass correlation coefficients (ICCs) for test-retest, intra-observer, and inter-observer reliability of SRSsept are shown in **Table 3**. Test-retest reliability was highest for baseline measurements and at 60% of VT (ICCs = 0.82 and 0.66, respectively). There was poor test-retest reliability of SRSsept at 30%, 90%, and in recovery (ICCs = 0.23, 0.04 and 0.27 respectively). Intra- and inter-observer reliability was good at all exercise intensities (ICC ≥ 0.86 and ICC ≥ 0.80, respectively).

SDI shows poor test-retest reliability at 30% and 90% of VT (ICC = 0.32 and 0.16, respectively). Reliability is moderate to good elsewhere (ICCs = 0.50 to 0.77). Intra-observer reliability of SDI is good (ICC > 0.74) for all intensities. Inter-observer reliability of SDI is lowest at baseline (ICC = 0.66).

Table 3: Intraclass correlation coefficients and coefficient of variation of strain parameters, septal systolic rebound stretch (SRS-sept), and the septal discoordination index (SDI) at each exercise intensity.

	Baseline	30% VT	60% VT	90% VT	Recovery
SRSsept					
Intraclass correlation coefficient					
Test-retest	0.82	0.23	0.66	0.04	0.27
Intra-observer	0.95	0.86	0.88	0.89	0.97
Inter-observer	0.80	0.88	0.83	0.82	0.86
SDI					
Intraclass correlation coefficient					
Test-retest	0.50	0.32	0.64	0.16	0.77
Intra-observer	0.98	0.86	0.74	0.87	0.80
Inter-observer	0.66	0.92	0.72	0.76	0.75

Exercise induced changes in septal systolic rebound stretch

There were 15 distinct sets of cine-loops that contained examinations performed at rest and at 30% and 60% of the VT (i.e., the reproducible exercise intensities). Exercise-induced changes in SDI relative to rest were variable, since consistent improvement (n = 8), consistent worsening (n = 4) or a reciprocal response (n = 3) were observed. Agreement (i.e. relative improvement versus relative worsening) between exercise-induced ΔSDI at 30% and 60% of the VT were moderate to good (Cohen K = 0.57 and 0.73 for observer 1 and 2 respectively). Relative to baseline, the majority of patients demonstrated an improvement in mechanical coordination at 30% and 60% of the VT, with on average a 58% or 38% reduction in SDI, respectively. Conversely, a 32% and 64% increase in SDI was seen in the cases with consistent exercise-induced deterioration of strain-efficiency at 30% and 60% of the VT respectively **(Figure 5)**.

Septal discoordination index
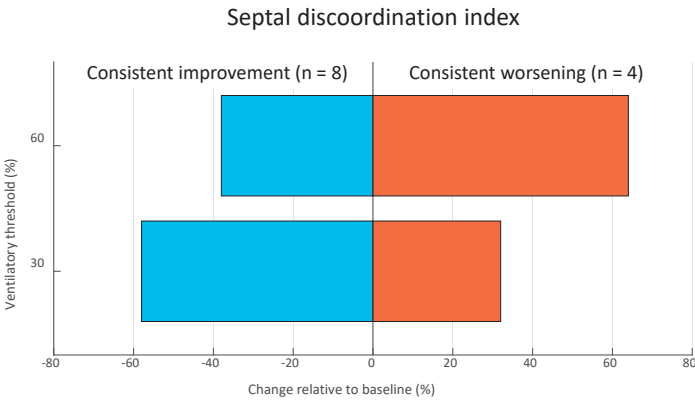
Fig. 5 Heterogeneous effect of exercise on septal discoordination index. Relative to rest, exercise at 30% and 60% of the ventilatory threshold elicits either a consistent improvement (blue) or consistent further deterioration of septal coordination (orange).

DISCUSSION

Our findings show that measurement of longitudinal strain of the septum (i.e. systolic rebound stretch and systolic shortening) during exercise stress tests is challenging but feasible (84% feasibility in obtained image sequences). In addition, SRSsept during exercise has a reproducibility comparable to that of measurements performed at rest, up to a moderate (60% of ventilatory threshold) level of exercise, using the present protocol. We were able to identify heterogeneous exercise-induced alterations in SDI relative to rest, which were in moderate to good agreement at both intensity levels.

Feasibility

We report a feasibility of 84% for measuring strain during exercise when cine-loops could be acquired successfully. Where cine-loops could not be acquired, reasons for this were likely inherent to the complexity and demandingness of performing echocardiography at multiple exercise intensity levels and/or patients prematurely ceasing the exercise protocol. Exercise stress-tests introduce several confounding elements (e.g. greater body motion and increased respiration) into otherwise routine echocardiographic measurements, thereby significantly affecting image quality.

Temporal consistency of the image plane is vital in speckle tracking analysis, since strain is calculated based on the inter-frame displacement of pixels. Complete or partial occlusion, or out-of-plane motion of the region-of-interest during tracking causes decorrelation during displacement estimation. This in turn has a significant negative effect on the accuracy of strain estimation. The image quality criteria we deemed necessary for accurate displacement tracking were therefore stricter than those that were sufficient for measurement of end-systolic and diastolic volumes.

Test-retest reproducibility and reliability

Resting test-retest septal strain curve correlation was excellent and comparable to previous studies concerning SRSsept measured at rest [27]. During exercise at 30% and 60% of the VT and during post-exercise recovery, test-retest variability of SRSsept was comparable to baseline. Our results therefore suggest adequate agreement of SRSsept between two separate visits.

These findings are in line with previous research that measured segmental longitudinal strain of the LV [28]. Here, depending on the commercial vendor, an absolute difference of up to 5% between first and second image acquisition was demonstrated. Some variability is always expected due to measurement variability, differences in the acquired acoustic window, and physiological fluctuations that occur over time. Because the present study performed echocardiographic examinations on two separate days, more pronounced physiological variation is to be expected (and therefore a lower mea-

8

surement repeatability) when compared to research that performed both examinations at most two hours apart, thereby increasing our test-retest variability [28,29]. Similarly, poor test-retest reliability is shown in the SRSsept ICCs, which was in contrast to the relatively good ICC for intra-observer and inter-observer.

Intra- and interobserver reproducibility

As expected, intra- and inter-observer reproducibility was better than test-retest agreement, owed primarily to the lack of physiological variation in these measurements. We acknowledge that variability of 2.8% for SRSsept between different observers is likely to be clinically relevant in regard to predicting response to CRT. Importantly however, because repeated analyses of identical image datasets were performed using the same software, inter-observer variability can solely be attributed to differences in either cycle-selection or segmentation. Variability may therefore be inherent to regional STE-based strain-analysis.

In line with these findings, similar variability (i.e. $1.0 \pm 2.0\%$) of SRSsept between different vendors is found by Van Everdingen et al., resulting in varying C-statistic values and different cut-off values [27]. Since a variability of up to 5% can be expected when measuring segmental strain [28], it is reasonable to suspect that, perhaps, similar amounts of variability were present in studies that investigated SRSsept (at rest) in a clinical setting [17,18]. Importantly, these studies have already proven the importance of SRSsept in the selection of patients with HF eligible for CRT, regardless of the underlying variability there. Future studies, with larger sample sizes, are warranted to establish more accurate estimates of variability for SRSsept during exercise, and directly compare these values to SRSsept at rest.

Exercise-dependent mechanical (dis)coordination in heart failure

In almost all patients, pronounced but variable exercise-induced changes in SDI were observed. These findings agree with previous research [12,15] that investigated timing-based parameters of dyssynchrony. Although exercise-induced response was heterogeneous (i.e. either improved or worsening of septal coordination), the interpretation at either exercise intensity level (i.e. 30% and 60% of VT) was consistent with moderate to good agreement.

Importantly, SDI reflects the *ratio* between wasted and constructive systolic strain of the septum during systole. SDI therefore allows for better inter- and intra-individual comparison at various exercise intensity levels than SRSsept alone, which is more sensitive to changes in blood pressure [30]. Changes in SDI during exertion may therefore indicate (lack of) cardiac compensation mechanisms during mild to moderate exertion. The heterogeneity of exercise-induced changes in SDI may therefore in part explain the

vast range of symptom-severity many patients with HF experience during daily activities, despite having similar echocardiographic function at rest.

In line with this hypothesis, previous research demonstrated the association between (the degree of) exercise-induced improvement of mechanical dyssynchrony and non-response to CRT [14,15]. Whether this also holds true for strain-based indices of discoordination is unknown. Therefore, further investigation is required in a larger cohort to ascertain the clinical utility of these measurements.

Limitations and future work

Since the goal of the present study is hypothesis-generating, the preliminary nature of our findings must be acknowledged, and our results should be interpreted accordingly. First, cycle ergometry measurements were performed several days apart because of the exertion patients had to undergo, increasing physiological variation and thereby reducing test-retest reliability compared to other studies. Although 'zoomed' high frame-rate ultrasound allowed for high quality imaging of the septum, the narrow aperture prevented capture of the whole septum in some cases. Whilst the practical benefits of SRSsept as a deformation parameter during exercise are clear, it is limited by its high variability, which are largely inherent to regional strain indices. Sample size in this explorative study was too low in order to produce a meaningful coefficient of variation (i.e. accurately reflecting the corresponding population with a sufficiently narrow confidence interval) and were therefore not calculated.

The poor image quality caused by breathing and body movement during exercise meant that measurement of consecutive cardiac cycles was not possible. Often only a single cycle was of a sufficient quality for strain analysis at a given measurement point. Because of the difficulty of acquiring pulsed-wave Doppler of the aortic valve during exercise, AVC had to be scaled based on estimated systolic and diastolic times for a given heart rate during exercise. This reduced the accuracy of SRSsept measurements and lead to an error of unknown magnitude for both systolic shortening and SRSsept. This is a significant limitation of the present study. The lack of simultaneous blood pressure measurements throughout the exercise protocol may hamper clinical understanding of our results. Finally, the strain analysis software used in this study was not standard commercially available software, however it has previously been compared to such software on clinical data where it was found to produce similar results [31].

Future studies should ensure that the exact timing of aortic valve closure is known, either assessed visually or with Doppler flow measurements. Improvements could be made to the protocol and quality of data by: use of full field-of-view imaging at a high (> 90Hz) frame rate to allow measurement of strain over the complete septal region; inclusion of simultaneous blood pressure measurement throughout the exercise protocol; minimizing time between measurement days to reduce physiological variation; and

8

minimizing the effects of exercise on image quality, for instance by use of an ultrasound probe fixation device.

CONCLUSION

Measuring mechanical discoordination using STE during exercise is feasible when high frame-rate image acquisition with semi-automated and vendor-independent analysis is ensured, but various challenges remain. During exercise up to 60% of the ventilator threshold, both test-retest agreement and inter-operator variability remained comparable to measurements performed at rest, with moderate baseline SRSsept variability prior to exercise. Moreover, exercise may elicit either a consistent improvement or deterioration of septal coordination in patients with dyssynchronous heart failure. Although interesting, its potential clinical utility remains to be further explored in larger trials with CRT recipients.

REFERENCES

1.	P. Ponikowski, A. A. Voors, S. D. Anker, *et al.* 2016 ESC Guidelines for the diagnosis and treatment of acute and chronic heart failure: The Task Force for the diagnosis and treatment of acute and chronic heart failure of the European Society of Cardiology (ESC)Developed with the special contribution of. *Eur. Heart J.* **37**, 2129–2200 (2016).

2.	J. 3rd Gorcsan, O. Oyenuga, P. J. Habib, *et al.* Relationship of echocardiographic dyssynchrony to long-term survival after cardiac resynchronization therapy. *Circulation*. **122**, 1910–1918 (2010).

3.	B. W. L. De Boeck, A. J. Teske, M. Meine, *et al.* Septal rebound stretch reflects the functional substrate to cardiac resynchronization therapy and predicts volumetric and neurohormonal response. *Eur. J. Heart Fail.* **11**, 863–871 (2009).

4.	A. Ghani, P. P. H. M. Delnoy, A. Adiyaman, *et al.* Septal rebound stretch as predictor of echocardiographic response to cardiac resynchronization therapy. *Int. J. Cardiol. Hear. Vasc.* **7**, 22–27 (2015).

5.	J. Lumens, B. Tayal, J. Walmsley, *et al.* Differentiating Electromechanical from Non-Electrical Substrates of Mechanical Discoordination to Identify Responders to Cardiac Resynchronization Therapy. *Circ. Cardiovasc. Imaging*. **8**, e003744 (2015).

6.	E. S. Chung, A. R. Leon, L. Tavazzi, *et al.* Results of the Predictors of Response to CRT (PROSPECT) trial. *Circulation*. **117**, 2608–2616 (2008).

7.	J. Holzmeister, C. Leclercq. Implantable cardioverter defibrillators and cardiac resynchronisation therapy. *Lancet (London, England)*. **378**, 722–730 (2011).

8.	A. Auricchio, F. W. Prinzen. Non-responders to cardiac resynchronization therapy: The magnitude of the problem and the issues. *Circ. J.* **75**, 521–527 (2011).

9.	A. Ghani, P. P. H. M. Delnoy, A. Adiyaman, *et al.* Response to cardiac resynchronization therapy as assessed by time-based speckle tracking imaging. *Pacing Clin. Electrophysiol.* **38**, 455–464 (2015).

10.	A. Zweerink, G. J. de Roest, L. Wu, *et al.* Prediction of Acute Response to Cardiac Resynchronization Therapy by Means of the Misbalance in Regional Left Ventricular Myocardial Work. *J. Card. Fail.* **22**, 133–142 (2016).

11.	J. Duchenne, J. M. Aalen, M. Cvijic, *et al.* Acute redistribution of regional left ventricular work by cardiac resynchronization therapy determines long-term remodelling. *Eur. Heart J. Cardiovasc. Imaging* (2020), doi:10.1093/ehjci/jeaa003.

12.	S. Lafitte, P. Bordachar, M. Lafitte, *et al.* Dynamic Ventricular Dyssynchrony. An Exercise-Echocardiography Study. *J. Am. Coll. Cardiol.* **47**, 2253–2259 (2006).

13.	A. M. Bernheim, Y. Nakajima, P. A. Pellikka. Left Ventricular Dyssynchrony in Patients with Normal Ventricular Systolic Function Referred for Exercise Echocardiography. *J. Am. Soc. Echocardiogr.* **21**, 1145–1149 (2008).

14.	M. Kuhne, R. Blank, B. Schaer, *et al.* Effects of physical exercise on cardiac dyssynchrony in patients with impaired left ventricular function. *Eur. Eur. pacing, arrhythmias, Card. Electrophysiol. J. Work. groups Card. pacing, arrhythmias, Card. Cell. Electrophysiol. Eur. Soc. Cardiol.* **13**, 839–844 (2011).

15.	G. Rocchi, M. Bertini, M. Biffi, *et al.* Exercise stress echocardiography is superior to rest echocardiography in predicting left ventricular reverse remodelling and functional improvement after cardiac resynchronization therapy. *Eur. Heart J.* **30**, 89–97 (2009).

16.	Y.-C. Wang, J.-J. Hwang, C.-C. Yu, *et al.* Provocation of masked left ventricular mechanical dyssynchrony by treadmill exercise in patients with systolic heart failure and narrow QRS complex. *Am. J. Cardiol.* **101**, 658–661 (2008).

8

17. O. A. E. Salden, A. Zweerink, P. Wouters, *et al*. The value of septal rebound stretch analysis for the prediction of volumetric response to cardiac resynchronization therapy. *Eur. Heart J. Cardiovasc. Imaging*. **22**, 37–45 (2021).

18. P. C. Wouters, G. E. Leenders, M. J. Cramer, *et al*. Acute recoordination rather than functional hemodynamic improvement determines reverse remodelling by cardiac resynchronisation therapy. *Int. J. Cardiovasc. Imaging*. **37**, 1903–1911 (2021).

19. J. Vecera, M. Penicka, M. Eriksen, *et al*. Wasted septal work in left ventricular dyssynchrony: a novel principle to predict response to cardiac resynchronization therapy. *Eur. Heart J. Cardiovasc. Imaging*. **17**, 624–632 (2016).

20. G. E. Leenders, B. W. L. De Boeck, A. J. Teske, *et al*. Septal rebound stretch is a strong predictor of outcome after cardiac resynchronization therapy. *J. Card. Fail*. **18**, 404–412 (2012).

21. K. V Bunting, R. P. Steeds, L. T. Slater, *et al*. A Practical Guide to Assess the Reproducibility of Echocardiographic Measurements. *J. Am. Soc. Echocardiogr. Off. Publ. Am. Soc. Echocardiogr*. **32**, 1505–1515 (2019).

22. W. L. Beaver, K. Wasserman, B. J. Whipp. A new method for detecting anaerobic threshold by gas exchange. *J. Appl. Physiol*. **60**, 2020–2027 (1986).

23. T. Bombardini, V. Gemignani, E. Bianchini, *et al*. Post-exercise contractility, diastolic function, and pressure: operator-independent sensor-based intelligent monitoring for heart failure telemedicine. *Cardiovasc. Ultrasound*. **7**, 21 (2009).

24. R. G. P. Lopata, M. M. Nillesen, H. H. G. Hansen, *et al*. Performance evaluation of methods for two-dimensional displacement and strain estimation using ultrasound radio frequency data. *Ultrasound Med. Biol*. **35**, 796–812 (2009).

25. C.-L. Wang, B. D. Powell, M. M. Redfield, *et al*. Left ventricular discoordination index measured by speckle tracking strain rate imaging predicts reverse remodelling and survival after cardiac resynchronization therapy. *Eur. J. Heart Fail*. **14**, 517–525 (2012).

26. E. Galli, C. Leclercq, A. Hubert, *et al*. Role ofmyocardial constructive work in the identification of responders to CRT. *Eur. Heart J. Cardiovasc. Imaging*. **19**, 1010–1018 (2018).

27. W. M. Van Everdingen, A. H. Maass, K. Vernooy, *et al*. Comparison of strain parameters in dyssynchronous heart failure between speckle tracking echocardiography vendor systems. *Cardiovasc. Ultrasound*. **15**, 25 (2017).

28. O. Mirea, E. D. Pagourelias, J. Duchenne, *et al*. Variability and Reproducibility of Segmental Longitudinal Strain Measurement: A Report From the EACVI-ASE Strain Standardization Task Force. *JACC. Cardiovasc. Imaging*. **11**, 15–24 (2018).

29. P. Barbier, O. Mirea, C. Cefalù, *et al*. Reliability and feasibility of longitudinal AFI global and segmental strain compared with 2D left ventricular volumes and ejection fraction: intra- and inter-operator, test-retest, and inter-cycle reproducibility. *Eur. Hear. journal. Cardiovasc. Imaging*. **16**, 642–652 (2015).

30. E. Donal, C. Bergerot, H. Thibault, *et al*. Influence of afterload on left ventricular radial and longitudinal systolic functions: a two-dimensional strain imaging study. *Eur. J. Echocardiogr. J. Work. Gr. Echocardiogr. Eur. Soc. Cardiol*. **10**, 914–921 (2009).

31. L. S. Fixsen, A. G. W. de Lepper, M. Strik, *et al*. Echocardiographic Assessment of Left Bundle Branch-Related Strain Dyssynchrony: A Comparison With Tagged MRI. *Ultrasound Med. Biol*. **45**, 2063–2074 (2019).

9

Does Recovery from Submaximal Exercise Predict Response to Cardiac Resynchronization Therapy?

Open Heart

Philippe C. Wouters*, Thijs Schoots*, Victor Niemeijer, Ruud F. Spee, Hareld M.C. Kemps

Contributed equally to the manuscript

ABSTRACT

Background: Exercise parameters are not routinely incorporated in decision making for cardiac resynchronization therapy (CRT). Submaximal exercise parameters better reflect daily functional capacity of heart failure patients than parameters measured at maximal exertion, and may therefore better predict response to CRT. We compared various exercise parameters, and sought to establish which best predict CRT response.

Methods: In 31 patients with chronic heart failure (61% male; age 68±7 years), submaximal and maximal cycling testing was performed before and 3 months after CRT. Submaximal oxygen onset (τVO_2 onset) and recovery kinetics (τVO_2 recovery), peak oxygen uptake (VO_2 peak), and oxygen uptake efficiency slope (OUES) where measured. Response was defined as ≥ 15% relative reduction in end-systolic volume.

Results: After controlling for age, NYHA, and VO_2 peak, fast submaximal VO_2 kinetics were significantly associated with response to CRT, measured either during onset or recovery of submaximal exercise (AUC = 0.719 for both; p < 0.05). By contrast, VO_2 peak (AUC = 0.632; p = 0.199) and OUES (AUC = 0.577; p = 0.469) were not associated with response. Among patients with fast onset and recovery kinetics, below 60 seconds, a significantly higher percentage of responders was observed (91% and 92% vs 43% and 40%, respectively).

Conclusions: Impaired VO_2 kinetics may serve as an objective marker of submaximal exercise capacity that is age-independently associated with non-response following CRT, whereas maximal exercise parameters are not. Assessment of VO_2 kinetics is feasible and easy to perform, but larger studies should confirm their clinical utility.

INTRODUCTION

Cardiac resynchronisation therapy (CRT) is an effective treatment for patients with chronic heart failure (HF) and a reduced left ventricular (LV) ejection fraction (EF). Although patient eligibility is currently primarily based on the presence of left bundle branch block (LBBB) on the ECG, approximately 30-40% of patients are non-responders [1,2]. Research has focussed on deriving new and more advanced markers from the ECG or echocardiogram to better predict response after CRT [3,4]. However, sensitivity and specificity should be further improved in order to truly affect clinical decision making [5].

Incorporation of exercise parameters may further improve patient selection, but these are not yet part of routine clinical decision making for CRT. However, several studies showed a positive relationship between pre-implantation maximal exercise capacity (peak oxygen uptake; VO_2 peak) and CRT response [6,7], suggesting that more severely impaired HF patients are less likely to achieve an echocardiographic response. This may be because their exercise capacity is more severely limited by peripheral derangements. Yet, studies investigating the influence of baseline *'exercise'* characteristics on echocardiographic response are relatively scarce, as opposed to trials investigating electrical and mechanical substrates [4].

A barrier for the widespread implementation of assessment of maximal exercise capacity is that symptom limiting exercise testing is burdensome, and often not truly achievable for patients with severe HF. Therefore, '*submaximal*' exercise testing could be a valuable alternative. One of the submaximal exercise parameters that reflect exercise capacity are oxygen kinetics [8–11]. Oxygen kinetics describe the rate of increase of oxygen uptake during a short constant-load submaximal exercise bout (VO_2 onset kinetics), and the rate of decline during recovery (VO_2 recovery kinetics). Assessment of VO_2 kinetics is safe, feasible and not physically burdensome for severely impaired patients, as it only requires an exercise effort of several minutes below the anaerobic threshold. In HF patients, oxygen kinetics were shown to be reproducible and well correlated with exercise capacity and prognosis [11–13]. In addition, VO_2 recovery kinetics were shown to be useful as a predictor of the effect of an exercise training program [14].

The main goal of the present study was to investigate whether submaximal exercise testing, and in particular oxygen uptake kinetics, can be used to predict the response to CRT. In addition, use of submaximal exercise parameters was compared to conventional parameters that require maximal exertion

9

METHODS

Patient population and study protocol

We performed a prospective multicentre trial in an open cohort of patients. A total of 34 patients with HF eligible for CRT were enrolled. Inclusion criteria were based on ESC guidelines implemented at the time of inclusion: 1) New York Heart Association (NYHA) II or III HF despite optimal medical treatment; 2) EF ≤ 35% and 3) QRS-duration ≥ 120ms. Participation in an exercise training program in the last year and during the study were excluded.

Resting echocardiography and two cardiopulmonary exercise tests (CPET) were performed at baseline and three months after CRT implantation. After echocardiography, patients performed a submaximal constant load CPET followed by a symptom limited maximal CPET, both with respiratory gas analysis. In order to familiarize the patient with the test procedure, and to determine the workload for the constant load CPET, an additional symptom limited CPET was performed at baseline. Implantation of CRT devices was performed according to standard techniques and local protocols in the Catharina Hospital, Eindhoven and University Medical Center, Utrecht, the Netherlands. Algorithms based on the intracardiac electrogram were used for device optimization.

Echocardiographic response was used as a well-accepted surrogate marker of long-term prognosis after CRT, and was defined as a decline in end-systolic volume (ESV) ≥ 15%, three months after implantation [15]. A clinical response was defined as an increase in VO_2 peak ≥ 1 ml·kg^{-1}·min^{-1} [16,17]. The study complied with the Declaration of Helsinki, and study got approved by the local Medical Ethics Committee of Máxima MC. All participants gave written informed consent.

Echocardiography

Standard two-dimensional, colour and spectral Doppler measurements were performed using a Phillips Epic 7C echo machine and a X5-1 transducer. LV dimensions were measured in the parasternal long axis view. EF was determined using the Simpson's rule algorithm by tracing the LV 2D-area in both standard apical two- and four-chamber view at end-systole and end-diastole. Images were analysed independently by two physicians.

Exercise testing

All exercise tests were performed in an upright seated position on an electromagnetically braked cycle ergometer (Lode Corrival; Lode BV, Groningen, The Netherlands). A 12-lead electrocardiogram was registered continuously. During the test, ventilatory parameters were measured breath-by-breath (ZAN 680 USB; ZAN Messgeräte, Oberthulba, Germany) and were averaged over 10–second intervals after the removal of outliers

(values > 3 standard deviations from the local mean). Volume and gas analysers were calibrated before each test.

Maximal CPET consisted of a symptom-limited test using an individualised ramp protocol for a total test duration of 8–12 minutes. The test was preceded by 4 minutes of unloaded pedalling and ended when the patient was unable to maintain the required pedalling frequency. The results of this baseline test were used in order to determine the workload for the submaximal CPET. Exercise performance was determined as the maximally achieved resistance at the end of the exercise. VO_2 peak was defined as the final 20-second averaged value of the maximal CPET. Ventilatory aerobic threshold (VAT) was assessed by the V-slope method, using the mean of the value calculated by two blinded physicians. The efficiency of CO_2 exchange was measured by assessing the required minute ventilation for CO_2 elimination. Finally, the oxygen uptake efficiency slope (OUES) was measured as it is a reliable and reproducible measure of effort-independent cardiopulmonary reserve. The OUES was derived from the logarithmic relation between VO_2 and VE during incremental exercise [18].

Submaximal constant load exercise testing commenced with a 2–minute resting period, followed by a 6–minute bout at 80% of the workload corresponding to the VAT achieved during the preceding maximal exercise test. Patients were instructed to maintain a pedalling frequency of 70 rotations per minute. After the load phase, there was a 5-minute recovery phase with no movement of the leg in order to assess VO_2 kinetics.

Analysis of oxygen uptake kinetics

Analysis of VO_2 kinetics during onset and recovery of the constant load tests was reported previously[10]. All data were resampled into 10-second intervals and the first 20 seconds of the VO_2 data (e.g., exercise onset) were omitted. This was done because during this period (cardiodynamic phase), increases in VO_2 merely reflect an increase in pulmonary blood flow, rather than actual changes in tissue gas exchange. A non-linear least squares regression procedure (Matlab 8.6 R2015b, MathWorks, US) was applied to the onset phase in order to calculate the time constant of VO_2 onset (formula 1).

Formula 1. *VO_2 kinetics for onset phase.*

$$VO_{2\ onset}\ (t) = Y_{baseline} + A \cdot \left(1 - e^{-(t - Td)/\tau}\right)$$

where A = amplitude during exercise onset; Td = time delay (seconds); and τ = time constant (seconds). Recovery kinetics of VO_2 were calculated as well (formula 2); Y= VO_2.

Formula 2. *VO_2 kinetics for recovery phase.*

$$VO_{2\ recovery}\ (t) = Y_{steady\ state} - A \cdot \left(1 - e^{-(t - Td)/\tau}\right)$$

where A = amplitude during recovery from steady state; Td = time delay (seconds); and τ = time constant (seconds); Y= VO_2

Statistical analysis

Data were analysed using SPSS statistics (version 25.0, SPSS Inc, Chicago, IL, USA). Continuous variables were tested for normality using a Shapiro-Wilk test and were expressed as the mean ± standard deviation. Data with a normal distribution were evaluated using the paired samples t-test for within group differences and by independent samples t-test concerning between-group differences. Categorical data were presented as absolute count and were compared with a Fisher exact test.

Receiver-operator characteristic curves were created for exercise-related predictors of CRT outcome. Optimal cut-off values were based on the level that resulted in the highest (sensitivity – [1 – specificity]), and subsequently an integer within this numeric range was selected in order to prevent unjustified overfitting of data. The relationship between these predictors and echocardiographic response was established using analysis of covariance (ANCOVA) with age, NYHA class and peak VO_2 as covariates. Agreement between exercise kinetics and NYHA class was assessed using Cohen's kappa coefficient. All statistical tests performed were two-tailed and a p-value < 0.05 was considered statistically significant.

RESULTS

A total of 34 patients were included. One patient did not complete the CPET on the visit after CRT implantation due to dizziness when sitting on the bike, two other patients did not show up for the examinations post-CRT without giving reason. A total of 31 patients completed all tests; all patients underwent CRT implantation, without complications. Paired respiratory gas analysis data during (sub)maximal exercise testing could be successfully retrieved. The majority of the population were male (61%) with non-ischemic cardiomyopathy (58%) and a mean age of 68±7 years **(Table 1)**. An overview of changes in echocardiographic- and exercise parameters before and after CRT of the total study population is presented in **Online Supplemental Table 1.**

Echocardiographic responders versus non-responders

Relative changes in exercise-related variables between the group of echocardiographic non-responders versus responders are presented in **Table 2**. In contrast with non-responders, only responders showed a significant increase in peak power output (P peak), VO_2 peak, OUES and VE/VCO_2 slope. Yet, no significant between-group differences were observed. Although τVO_2 recovery was significantly reduced after CRT on group level (77±39 versus 61±18; p = 0.030), no significant changes were seen when stratified according to response groups. In both responders and non-responders, the extent of LVESV-reduction and clinical improvement (ΔVO_2 peak) after CRT were not correlated significantly (R = 0.284; p = 0.135).

Table 1. Characteristics at baseline of study population.

Characteristic	Total (n = 31)	Non-responder (n = 11)	Responder (n = 20)	P-value
Age (years)	68.4 ± 7.1	72.2 ± 4.0	66.3 ± 7.6	0.026
Male (%)	19 (61)	10 (91)	9 (45)	0.020
Ischemic aetiology – n (%)	13 (42)	7 (64)	6 (30)	0.128
NYHA III – n (%)	21 (69)	10 (91)	11 (55)	0.055
HF duration (months)	42.4 ± 48.3	49.4±47.7	38.6 ± 49.4	0.562
Sinus rhythm – n (%)	23 (82)	8 (73)	18 (90)	0.224
LBBB – n (%)	26 (84)	8 (80)	18 (95)	0.267
QRS width (ms)	154 ± 17	157±21	153±15	0.556
LVEF (%)	26.6 ± 8.1	24.5 ± 8.6	27.7±7.7	0.298
ACE/ARB – n (%)	31 (100)	11 (100)	20 (100)	1.000
Beta Blocker – n (%)	28 (90)	10 (91)	18 (90)	1.000
VO_2 peak (ml/kg/min)	16.4 ± 5.4	14.8 ± 3.9	17.3 ± 6.1	0.215

Values are presented as mean ± standard deviation (SD), number or percentage. LBBB: left bundle branch block, NYHA: New York Heart Association, LVEF: left ventricular ejection fraction, SR: sinus rhythm, AF: atrial fibrillation, ACE: angiotensin-converting enzyme inhibitor, ARB: angiotensin II receptor blocker, VO_2 peak: peak oxygen uptake capacity.

Exercise-related predictors for echocardiographic response

The optimal cut-off values of various exercise parameters to predict echocardiographic response are shown in **Table 3**. For τVO_2 onset and τVO_2 recovery the highest AUC was found at a cut-off of 60 seconds (AUC 0.719; p < 0.05 for both). τVO_2 onset ≤ 60 seconds predicted echocardiographic response with a specificity of 90% and a sensitivity of 61%, whereas τVO_2 recovery predicted echocardiographic response with a specificity of 90% and a sensitivity of 67%. Maximal exercise parameters (VO_2 peak, VE/VCO_2 slope, OUES) showed lower AUC's (0.632, 0.600, 0.577 respectively), which were all not significant (**Online Supplemental Table 2**).

Only among patients with fast onset and recovery kinetics (τVO_2 onset and τVO_2 recovery ≤ 60 seconds), a significantly higher percentage of responders were observed (92% and 92% versus 44% and 40%, respectively). By contrast, maximal parameters (VO_2 peak, OUES, VE/VCO_2 slope) could not differentiate response after CRT. Controlling for age, NYHA class and VO_2 peak as covariates did not significantly influence these results **(Figure 1)**. Patients with fast τVO_2 recovery demonstrated significantly more ESV-reduction than patients with delayed τVO_2 recovery (32±14 versus 17±21; p = 0.033), and also had significantly better increase in LVEF (**Online Supplemental Table 3**). A scatterplot with individual values of submaximal VO_2 kinetics and their association with reverse remodelling is shown in **Figure 2**. Onset and recovery VO_2 kinetics were not correlated to each other (R = 0.092; P = 0.640), which suggests their interaction with echocardiographic response is due to independent mechanisms.

9

Table 2. Relative changes in echocardiographic and exercise-related variables in patients with or without echocardiographic response, before and three months after CRT implantation.

Variable	Non-responder (n=11)		Responder (n=20)	
	Baseline	3 months	Baseline	3 months
Rest				
EF (%)	24.5±8.6	24.7±8.0	27.7±7.7	40.5±8.8*
EDV (ml)	289±105	287±101	221±72	171±52*
ESV (ml)	223±102	218±92	161±59	106±45*
Maximal				
P peak (W)	97±35	102±39	107±47	118±47*
VO$_2$ peak (ml/kg/min)	14.8±3.9	16.0±3.2	17.3±6.1	19.7±6.6*
OUES	1445±479	1610±520	1610±521	1943±586*
VE/VCO$_2$ slope	38.9±9.9	37±6.1	34.9±8.4	31.7±7.0*
Submaximal				
τVO$_2$ on (s)	87.2±39.1	90.1±48.8	58.6±34.2	55.4±32.2
τVO$_2$ rec (s)	79.5±21.4	67.0±19.4	75.0±47.3	57.6±17.3

*Values presented as mean ± stand deviation. CRT: Cardiac Resynchronization Therapy; EF: ejection fraction; ESV: end-systolic volume; EDV: end-diastolic volume; τVO2: time constant of oxygen uptake; P: performance; OUES: oxygen uptake efficiency slope; VE/VCO$_2$ slope: minute ventilation for CO$_2$ elimination. * P<0.05 within-group difference.*

Table 3. Baseline test characteristics of exercise-related predictors for echocardiographic response three months after CRT implantation.

| Predictor	AUC	p-value	Cut-off value	Met?	Total	Sens (%)	Spec (%)
τVO$_2$ onset	0.719	0.029	≤ 60s	Yes	11	61	90
				No	16		
τVO$_2$ recovery	0.719	0.025	≤ 60s	Yes	12	67	90
				No	15		
VO$_2$ peak	0.632	0.199	≥ 18 ml·kg^{-1}·min^{-1}	Yes	12	50	82
				No	18		
VE/VCO$_2$ slope	0.600	0.371	≤ 40	Yes	22	80	45
				No	8		
OUES	0.577	0.469	≥ 1500	Yes	14	55	73
				No	16		

Total = number of patients in cohort that met cut-off value; sens = sensitivity spec = specificity; AUC = area under the curve; other abbreviations as in Table 2.

Comparison with NYHA functional class

NYHA functional class was not significantly associated with response (AUC = 0.680; p = 0.103). When comparing NYHA II and NYHA III, similar reductions in ESV were observed (28±15 versus 20±21; p = 0.289). In patients classified as NYHA III functional impairment, fast τVO$_2$ onset and recovery kinetics < 60 seconds were seen in 35% of patients regardless. There was no agreement between NYHA class and VO$_2$ kinetics dichotomised at 60 seconds (Cohen's Kappa = 0.000), or NYHA class and VO$_2$ peak (Cohen's Kappa = 0.000).
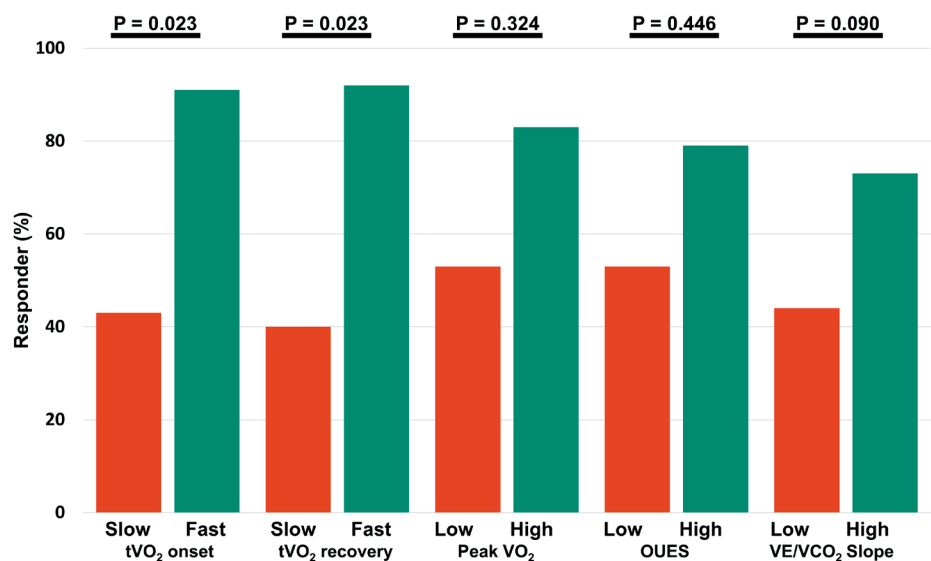
Figure 1. *Difference in echocardiographic response based on various exercise-related parameters at baseline, with significance corrected for age, NYHA and VO₂ peak. Patients with poor (red) and good (green) testing results during (sub)maximal exercise. Abbreviations as in Table 2.*

9
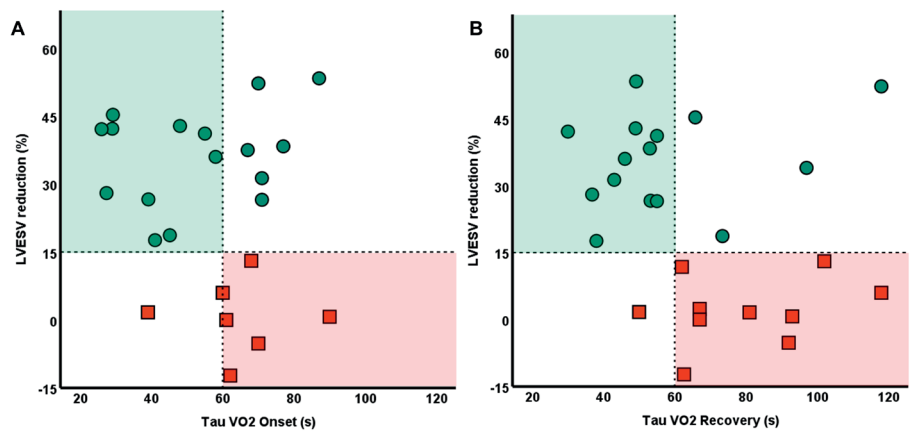
Figure 2. *Distribution of patients with (green squares) and without (red dots) echocardiographic response relative to their submaximal exercise performance at baseline. Responders, defined as at least 15% decrease in left ventricular end-systolic-volume (LVESV), are characterized by faster baseline oxygen uptake kinetics (VO₂) during onset (left graph) and recovery (right graph) of exercise.*

Factors associated with oxygen kinetics

Patients were stratified according to fast and slow τVO$_2$ recovery, i.e. below or above 60 seconds, respectively. Age was significantly higher in patients with prolonged VO$_2$ recovery, as compared to fast recovery time (72±4 versus 64±8; p = 0.001). Importantly,
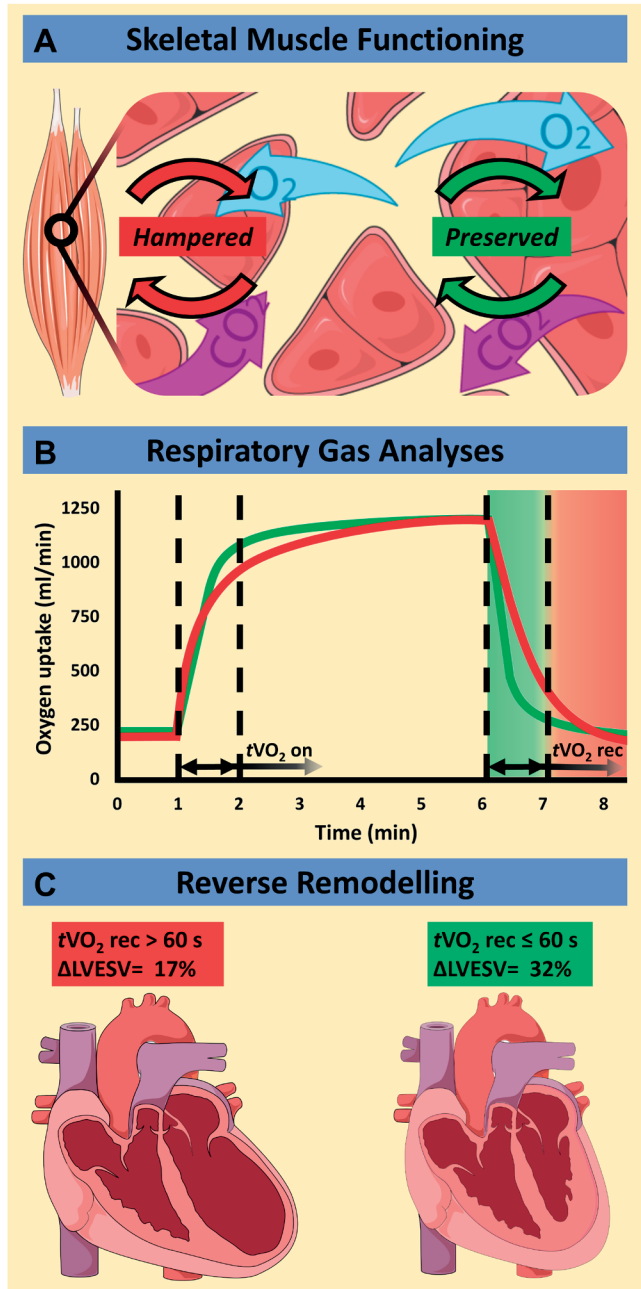
Graphical Abstract. *Derangements in tissue oxygenation (O_2 delivery) and local metabolic capacity (O_2 utilization) limit the rate change of oxygen uptake (VO_2) during onset and recovery from submaximal exercise **(red arrows, panel A)**. Respiratory gas analysis can objectively reveal patients with prolonged VO_2 kinetics **(red line, panel B)**, adapted from Kemps et al [10]. Before CRT, a prolonged duration to increase VO_2 to peak levels and normalize to baseline levels (τVO_2 onset and recovery respectively) is associated with non-response to CRT **(panel C)**. Legend: CRT, cardiac resynchronization therapy; LVESV, left ventricular end-systolic volume.*

besides peak VO_2, no other associations were found with other well-known patient char-acterises associated with response, including sex, aetiology, NYHA, LBBB morphology or QRS duration (**Online Supplemental Table 4**). Age correlated with τVO_2 recovery (R = 0.453; p = 0.016), but not with τVO_2 onset (R = 0.164; p = 0.403). Lastly, no significant differences were found when comparing patients with fast and slow oxygen kinetics during *onset* of submaximal exercise.

DISCUSSION

The present study suggests that oxygen uptake kinetics during onset and recovery from submaximal exercise may add to the prediction of the effect of CRT. An association with volumetric response was seen independently of age, VO_2 peak, and NYHA class. Conversely, more conventional exercise parameters such as VO_2 peak, OUES, and VE/VCO_2 slope, measured during peak exercise intensity, were not significantly associated with CRT response. Moreover, both submaximal VO_2 kinetics and VO_2 peak were not signifi-cantly associated with NYHA functional class, suggesting limited clinical representability of this assessment.

Exercise-related predictors of response to CRT

To our knowledge this is one of the first studies that show that submaximal exercise parameters can help in predicting outcome of CRT. Previously Berger et al. showed that the OUES at baseline was related to the CRT response [19]. However, we were unable to reproduce the high sensitivity and specificity of OUES that was reported. Rather, our results point towards a superior predictive value of VO_2 kinetics, also when directly compared to maximal exercise parameters that were previously shown to be related to the CRT response, such as VO_2 peak and VE/VCO_2 slope [6,7]. Moreover, determining a valid OUES in patients with severe HF requires exercise testing above anaerobic threshold [20], whereas this is not required for determining VO_2 kinetics.

Lastly, although very easy to use and therefore widely adopted into clinical practice, assessment of NYHA functional class is subjective and non-specific. Indeed, inter-ob-server agreement for NYHA is only 54% [21], and NYHA poorly reflects exercise capacity [22]. This in line with our results, which showed no agreement with objective assessments of (sub)maximal exercise capacity, and no significant association with response to CRT.

Pathophysiology of impaired submaximal exercise performance

The association between *low* VO_2 peak at baseline and better CRT-induced improve-ments in VO_2 peak has been established previously [23]. It should however be noted that increasingly worse VO_2 peak may be associated with improved clinical response of the

same parameter. As such, and in line with our findings, actual *prognostic* benefit from CRT has been linked to higher levels of VO_2 peak at baseline in 181 CRT-recipients before [24]. Conversely, τVO_2 recovery kinetics can be used to objectively quantify one's (in) ability to physiologically recover from submaximal exercise. Hence, opposed to VO_2 peak and NYHA, submaximal testing may be more representative of the *functional* capacity of patients with HF during ordinary daily activity.

A possible explanation for the finding that patients with slow VO_2 kinetics are less likely to respond to CRT lies in the pathophysiological background of delayed VO_2 kinetics in HF. In fact, submaximal VO_2 kinetics not only reflect the ability of the heart to increase cardiac output, but in particular also the capacity of skeletal muscles to increase oxygen utilization **(Graphical Abstract)**. This, in turn, is determined by peripheral vascular function and the metabolic capacity of skeletal muscles [25]. In fact, previous studies showed that peripheral vascular function is impaired [26,27] and related to prolonged recovery after submaximal exercise in HF patients [28]. Peripheral vascular function is, among others, influenced by neuro-humoral and systemic inflammatory processes. Impaired peripheral hemodynamics, reflected in impaired VO_2 kinetics, could therefore point towards a pro-inflammatory state and an unbalanced neuro-humoral system, which also impairs myocardial adaptation to CRT.

Submaximal exercise-capacity and age

Age is a well-documented independent cause of CRT non-response, but the actual reason for this has remained largely unexplained [3,4]. In our study, older age was associated with both echocardiographic non-response and prolonged peripheral oxygen uptake recovery kinetics, irrespective of sex or HF aetiology. This link is not surprising, since decreased skeletal muscle performance has been shown to be age-dependent before [29,30]. However, VO_2 recovery kinetics were more strongly associated with non-response, also when corrected for differences in age, NYHA class, and peak exercise capacity. Submaximal exercise capacity may therefore be a more specific marker of response to CRT than age, whilst also being more objective than assessment of NYHA functional class. Moreover, submaximal VO_2 recovery kinetics can be assessed as a continuum, as opposed to NYHA functional class.

Although current prediction models of CRT-response incorporate age and indices of electrical and mechanical dyssynchrony [3], clinical information of exercise capacity is currently lacking and perhaps insufficiently explored in this context. To date, no literature has related VO_2 kinetics to CRT response. Our results therefore point for the first time towards the potential role of impaired oxygen uptake kinetics as a mechanism of non-response. Clearly, future studies are warranted to investigate whether performing submaximal exercise tests in patients with dyssynchronous heart failure can be of added value in the refinement of patient selection criteria.

Clinical implications

To our knowledge this is the first study that shows that submaximal exercise parameters can be used to predict CRT-response. Although we acknowledge that larger prospective studies are warranted to establish definite cut-off values, the utility of submaximal VO_2 kinetics for predicting echocardiographic response after CRT was superior to VO_2 peak. Previous research [31] has suggested VO_2 peak to be more predictive than submaximal prognostic markers such as the 6-min walking test [32,33]. However, submaximal VO_2 kinetics provides physicians with reliable prognostic and objective information on the functional status of the individual patient, i.e. the ability to adapt to and recover from daily activities. Assessment of VO_2 kinetics may therefore be a more accurate and potentially better reproducible method to determine one's submaximal exercise capacity as opposed to better known and more widely implemented indices such as the six-minute walking test [34]. In addition, assessment of VO_2 kinetics is non-invasive, objective, affordable and can easily be performed repetitively over time as an indicator of clinical status.

Limitations

First, as a relatively small number of patients were included, statistical power was limited and no adequate subgroup analyses could be performed. Therefore, especially results concerning exercise-related predictors should be interpreted with caution, and larger prospective trials are warranted before finite conclusions can be drawn as to whether potential predictors should be applied in clinical practice. Nonetheless, to our best knowledge, incorporation of submaximal exercise-related predictors has not been performed previously, and therefore extends our current knowledge of eligible CRT patients. Secondly a relatively short follow-up duration was carried out, possibly resulting in overestimation of the percentage of non-responders as a consequence of a potential delayed effect. Alternatively, some patients illustrate temporary effects after CRT that diminish over time, and our response percentages were similar to those observed in larger trials (8,9).

Conclusion

The present study showed that delayed onset and recovery of peripheral oxygen uptake kinetics at baseline are associated with non-response in CRT, whereas parameters measured during maximal exertion were not. Although this association was independent from age, prolonged recovery from submaximal exercise may also – in part – explain the relative lack of reverse remodelling as more frequently seen in older individuals. Since assessment of VO_2 kinetics is feasible, objective and easy to perform, requiring only a short bout of submaximal exercise, this method is promising for use in clinical practice. However, additional research in larger populations, allowing for multivariate analysis, is needed to establish definite cut-off values, and show whether submaximal exercise testing can be of added value in the clinical decision process of CRT as a whole.

9

REFERENCES

1. C.-M. Yu, W. T. Abraham, J. Bax, *et al.* Predictors of response to cardiac resynchronization therapy (PROSPECT)--study design. *Am. Heart J.* **149**, 600–605 (2005).

2. A. Auricchio, F. W. Prinzen. Non-responders to cardiac resynchronization therapy: The magnitude of the problem and the issues. *Circ. J.* **75**, 521–527 (2011).

3. A. H. Maass, K. Vernooy, S. C. Wijers, *et al.* Refining success of cardiac resynchronization therapy using a simple score predicting the amount of reverse ventricular remodelling: results from the Markers and Response to CRT (MARC) study. *Europace.* **20** (2018). pp. e1–e10.

4. P. C. Wouters, W. M. van Everdingen, K. Vernooy, *et al.* Does mechanical dyssynchrony in addition to QRS area ensure sustained response to cardiac resynchronization therapy? *Eur. Hear. journal. Cardiovasc. Imaging* (2021), doi:10.1093/ehjci/jeab264.

5. E. S. Chung, A. R. Leon, L. Tavazzi, *et al.* Results of the Predictors of Response to CRT (PROSPECT) trial. *Circulation.* **117**, 2608–2616 (2008).

6. M. H. Mastenbroek, J. Van't Sant, H. Versteeg, *et al.* Relationship between Reverse Remodeling and Cardiopulmonary Exercise Capacity in Heart Failure Patients Undergoing Cardiac Resynchronization Therapy. *J. Card. Fail.* **22**, 385–394 (2016).

7. M. F. Piepoli, G. Q. Villani, U. Corrà, D. Aschieri, G. Rusticali. Time course of effects of cardiac resynchronization therapy in chronic heart failure: Benefits in patients with preserved exercise capacity. *PACE - Pacing Clin. Electrophysiol.* **31**, 701–708 (2008).

8. V. M. Niemeijer, T. Snijders, L. B. Verdijk, *et al.* Skeletal muscle fiber characteristics in patients with chronic heart failure: Impact of disease severity and relation with muscle oxygenation during exercise. *J. Appl. Physiol.* **125**, 1266–1276 (2018).

9. K. E. Sietsema, I. Ben-Dov, Yong Yu Zhang, C. Sullivan, K. Wasserman. Dynamics of oxygen uptake for submaximal exercise and recovery in patients with chronic heart failure. *Chest.* **105**, 1693–1700 (1994).

10. H. M. Kemps, G. Schep, M. L. Zonderland, *et al.* Are oxygen uptake kinetics in chronic heart failure limited by oxygen delivery or oxygen utilization? *Int. J. Cardiol.* **142**, 138–144 (2010).

11. R. Belardinelli, T. J. Barstow, P. Nguyen, K. Wasserman. Skeletal muscle oxygenation and oxygen uptake kinetics following constant work rate exercise in chronic congestive heart failure. *Am. J. Cardiol.* **80**, 1319–1324 (1997).

12. C. S. Bailey, L. T. Wooster, M. Buswell, *et al.* Post-Exercise Oxygen Uptake Recovery Delay: A Novel Index of Impaired Cardiac Reserve Capacity in Heart Failure. *JACC Hear. Fail.* **6**, 329–339 (2018).

13. M. Fortin, P. Y. Turgeon, É. Nadreau, *et al.* Prognostic Value of Oxygen Kinetics During Recovery From Cardiopulmonary Exercise Testing in Patients With Chronic Heart Failure. *Can. J. Cardiol.* **31**, 1259–1265 (2015).

14. H. M. Kemps, G. Schep, W. R. de Vries, *et al.* Predicting effects of exercise training in patients with heart failure secondary to ischemic or idiopathic dilated cardiomyopathy. *Am. J. Cardiol.* **102**, 1073–8 (2008).

15. C.-M. Yu, G. B. Bleeker, J. W.-H. Fung, *et al.* Left Ventricular Reverse Remodeling but Not Clinical Improvement Predicts Long-Term Survival After Cardiac Resynchronization Therapy. *Circulation.* **112**, 1580–1586 (2005).

16. A. M. Swank, J. Horton, J. L. Fleg, *et al.* Modest increase in peak VO2 is related to better clinical outcomes in chronic heart failure patients: results from heart failure and a controlled trial to investigate outcomes of exercise training. *Circ. Heart Fail.* **5**, 579–585 (2012).

17. J. O. O'Neill, J. B. Young, C. E. Pothier, M. S. Lauer. Peak oxygen consumption as a predictor of death in patients with heart failure receiving β-blockers. *Circulation*. **111**, 2313–2318 (2005).

18. R. Baba, M. Nagashima, M. Goto, *et al.* Oxygen uptake efficiency slope: A new index of cardiorespiratory functional reserve derived from the relation between oxygen uptake and minute ventilation during incremental exercise. *J. Am. Coll. Cardiol.* **28**, 1567–1572 (1996).

19. T. Berger, R. H. Zwick, M. Stuehlinger, *et al.* Impact of oxygen uptake efficiency slope as a marker of cardiorespiratory reserve on response to cardiac resynchronization therapy. *Clin. Res. Cardiol.* **100**, 159–66 (2011).

20. V. M. Niemeijer, M. Van 'T Veer, G. Schep, *et al.* Causes of nonlinearity of the oxygen uptake efficiency slope: A prospective study in patients with chronic heart failure. *Eur. J. Prev. Cardiol.* **21**, 347–353 (2014).

21. C. Raphael, C. Briscoe, J. Davies, *et al.* Limitations of the New York Heart Association functional classification system and self-reported walking distances in chronic heart failure. *Heart*. **93**, 476–482 (2007).

22. F. Y. Lim, J. Yap, F. Gao, *et al.* Correlation of the New York Heart Association classification and the cardiopulmonary exercise test: A systematic review. *Int. J. Cardiol.* **263**, 88–93 (2018).

23. S. Arora, M. Aarones, S. Aakhus, *et al.* Peak oxygen uptake during cardiopulmonary exercise testing determines response to cardiac resynchronization therapy. *J. Cardiol.* **60**, 228–235 (2012).

24. A. M. Stelken, L. T. Younis, S. H. Jennison, *et al.* Prognostic value of cardiopulmonary exercise testing using percent achieved of predicted peak oxygen uptake for patients with ischemic and dilated cardiomyopathy. *J. Am. Coll. Cardiol.* **27**, 345–352 (1996).

25. D. C. Poole, A. M. Jones. Oxygen uptake kinetics. *Compr. Physiol.* **2**, 933–996 (2012).

26. E. M. Van Craenenbroeck, V. M. Conraads. Mending injured endothelium in chronic heart failure: a new target for exercise training. *Int. J. Cardiol.* **166**, 310–4 (2013).

27. V. M. Conraads, E. M. Van Craenenbroeck, C. De Maeyer, *et al.* Unraveling new mechanisms of exercise intolerance in chronic heart failure: role of exercise training. *Heart Fail. Rev.* **18**, 65–77 (2013).

28. H. M. C. Kemps, J. J. Prompers, B. Wessels, *et al.* Skeletal muscle metabolic recovery following submaximal exercise in chronic heart failure is limited more by O 2 delivery than O 2 utilization. *Clin. Sci.* **118**, 203–210 (2010).

29. M. Tieland, I. Trouwborst, B. C. Clark. Skeletal muscle performance and ageing. *J. Cachexia. Sarcopenia Muscle*. **9**, 3–19 (2018).

30. D. S. Delorey, D. H. Paterson, J. M. Kowalchuk. Effects of ageing on muscle O2 utilization and muscle oxygenation during the transition to moderate-intensity exercise. *Appl. Physiol. Nutr. Metab.* **32**, 1251–1262 (2007).

31. B. Lamp, J. Vogt, H. Schmidt, D. Horstkotte. Impact of cardiopulmonary exercise testing on patient selection for cardiac resynchronisation therapy. *Eur. Hear. Journal, Suppl.* **6**, 5–9 (2004).

32. G. H. Guyatt, M. J. Sullivan, P. J. Thompson, *et al.* The 6-minute walk: a new measure of exercise capacity in patients with chronic heart failure sur sa capacite dans les activites de la vie quotidienne. colleagues'0 introduced the 12-minute walking test, in. *Can Med Assoc J.* **132**, 919–923 (1985).

33. C. Lucas, L. W. Stevenson, W. Johnson, *et al.* The 6-min walk and peak oxygen consumption in advanced heart failure: Aerobic capacity and survival. *Am. Heart J.* **138**, 618–624 (1999).

34. G. V. Guimarães, V. O. Carvalho, E. A. Bocchi. Reproducibility of the self-controlled six-minute walking test in heart failure patients. *Clinics*. **63**, 201–206 (2008).

9

SUPPLEMENTARY MATERIAL

Online Supplemental Table 1. Changes in cardiac function and exercise parameters.

Parameter	n	Before CRT	After 3 months	Δ (%)	P-value
EF (%)	31	26.6±8.1	34.9±11.4	7±7 [a]	<0.001
ESV (ml)	30	183.8±81.7	146.8±85.3	-22±19	<0.001
EDV (ml)	29	244.7±89.5	209.5±90.9	-15±14	<0.001
P peak (W)	30	103.4±41.9	112.1±44.5	10±18	<0.001
VO_2 peak (ml/kg/min)	30	16.2±5.3	18.4±5.8	15±23	<0.001
OUES	30	1528±496	1821±577)	22±26	<0.001
VE/VCO_2 slope	30	36.6±9.1	33.7±7.1	-7±10	<0.010
τVO_2 onset (s)	26	70.2±38.4	70.9±40.4	15±65	0.930
τVO_2 recovery (s)	26	76.7±38.9	61.3±18.3	-11±27	0.030

Cardiac resynchronization therapy (CRT) induces significant improvement in cardiac function, peak performance, peak oxygen uptake (VO_2) and VO_2 recovery kinetics in the total study population. a = absolute change.

Online Supplemental Table 2. Receiver operator curves for exercise-dependent variables for prediction of an echocardiographic response.

Parameter	Minimum	Maximum	Chosen value	P-value AUC
τVO_2 onset	> 59.0000	≤ 60.5000	60	**0.029**
τVO_2 recovery	> 59.0000	≤ 62.3023	60	**0.025**
VO_2 peak	≥ 17.7106	< 18.0863	18	0.199
OUES	≥ 1491.7186	< 1500.1439	1500	0.371
VE/VCO_2 slope	> 39.8589	≤ 41.5227	40	0.371

Legend: time constant of oxygen uptake ($\tau VO2$); oxygen uptake (VO_2); oxygen uptake efficiency slope (OUES); minute ventilation for CO2 elimination (VE/VCO_2 slope).

Online Supplemental Table 3. Differences in cardiac function based on exercise capacity.

Parameter	ΔLVESV (%)		ΔLVEF (%-point)		Echo responder (%)	
Cut-Off value met?	No	Yes	No	Yes	No	Yes
Exercise characteristics						
τVO_2 onset ≤ 60 s	18±21	31±14	6±8	10±6	**44**	**92***
τVO_2 recovery ≤ 60 s [a]	**17±21**	**32±14***	**4±8**	**10±5***	**40**	**92***
VO_2 peak ≥ 18 ml/kg/min [a]	**17±20**	**31±16***	6±7	9±7	53	83
OUES > 1500 [a]	18±19	27±19	6±7	8±7	53	79
VE/VCO_2 < 40	13±10	26±21	2±4	9±7	44	73

*[a] age significantly different between groups; * = statistically significant (p < 0.05).*

Online Supplemental Table 4. Characteristics associated with oxygen uptake recovery.

Characteristic	Slow VO$_2$ recovery (> 60 seconds)	Fast VO$_2$ recovery (≤ 60 seconds)	P-value
Age (years)	72±4	64±8	**0.001**
VO$_2$ Peak (ml/kg/min)	14±3	20±6	**0.002**
Male – n (%)	8 (54)	9 (69)	0.460
HF-duration (months)	43±49	49±52	0.759
NYHA III – n (%)	13 (87)	7 (54)	0.096
ICM – n (%)	7 (47)	5 (39)	0.718
LBBB – n (%)	12 (86)	11 (92)	1.000
QRS-duration (ms)	151±18	154±14	0.656
EDV (ml)	249±113	234±60	0.683
ESV (ml)	188±104	173±49	0.644
EF (%)	26±9	29±5	0.292

Values presented as mean ± stand deviation. Abbreviations as in Table 1.

9

10

Exercise Physiology in Heart Failure: Symptom Aetiology and Comparing Exercise Training with Cardiac Resynchronization Therapy

Philippe C. Wouters, Ruud F. Spee, Thijs Schoots, Pieter A. Doevendans, Victor M. Niemeijer, Hareld M. Kemps.

ABSTRACT

Background: Central and peripheral derangements often co-exist in chronic heart failure (CHF). In contrast to cardiac resynchronisation therapy (CRT), exercise training is infrequently considered in these patients, which leaves peripheral skeletal muscles derangements unaddressed. We sought to differentiate the effects of CRT and high-intensity interval training (HIT) on central and peripheral exercise physiology in functionally impaired CHF patients.

Methods: In 66 patients (77% male, age 66±8 years, 56% NYHA III), baseline maximal and submaximal cardiopulmonary exercise testing was performed with simultaneous assessment of central haemodynamics using a radial artery pulse contour analysis method, and skeletal muscle deoxygenation using near infrared spectroscopy. Differences in resting cardiac function, cardiac output (CO), and oxygen uptake (VO_2) kinetics during (sub)maximal exercise were compared after three months of usual care, HIT, or CRT.

Results: When comparing NYHA functional class II and III, no differences in adverse remodelling and resting ejection fraction were seen. However, NYHA III was characterised by slower cardiac CO and VO_2 kinetics during onset and recovery of submaximal exercise. After CRT, cardiac reserve remained unaltered, but improved significantly by 39% following HIT (ΔCR 2.5±3.2 L/min; p = 0.034). After both, CRT and HIT, maximal workload capacity increased by about 10%, and submaximal VO_2 recovery time decreased.

Conclusions: Differences in CO and VO_2 kinetics during submaximal exercise distinguish the severity of NYHA functional impairment in CHF. HIT and CRT have differential effects on central haemodynamics, but either improve submaximal exercise recovery. Combining both interventions may therefore optimise functional recovery.

INTRODUCTION

In patients with chronic heart failure (CHF), besides 'central' cardiac pathology, so called 'peripheral' derangements of skeletal muscle function occur as well [1]. Importantly, both mechanisms may limit oxygen uptake (VO_2) in CHF. Peripheral alterations can be characterized by limited oxygen '*delivery*' to exercising muscles (i.e., compromised macro- and microvascular blood flow), and by limited local tissue oxygen '*extraction*' through impaired skeletal muscle metabolism.

To this end, various strategies can be implemented into heart failure care-pathways, each serving their own purpose. Cardiac resynchronisation therapy (CRT) aims to restore cardiac efficiency, whereas exercise-training generally provokes a wider variety of systemic and local effects [1]. Although CRT is well-implemented and thoroughly investigated, it is only indicated in a selected few CHF patients [2]. By contrast, exercise-training has a class I recommendation and can be implemented in most patients [2]. Unfortunately, uptake for exercise-training in CHF is strikingly low, with 80% of European countries considering cardiac rehabilitation seldomly, or never at all [3]. Moreover, '*combined*' effects of CRT and exercise-training may improve outcome, but outcomes vary [4–6]. At present, further research is warranted to elucidate the cause of these variable results.

Better insights in the physiological causes of functional impairment in CHF, and improved understanding of the effects of HIT and CRT, especially during exertion, is therefore warranted. These insights may potentially guide clinical decision-making, and promote uptake of exercise training in CHF. To this end, VO_2 kinetics can be assessed, which describe the *rate change* of VO_2 during onset or recovery of submaximal exercise. VO_2 kinetics thereby reflect the ability to adapt to and recover from exertion, respectively. Additional insights can be gained by simultaneously investigating central haemodynamics (i.e., cardiac output [CO]) and peripheral skeletal muscle oxygenation (i.e., tissue saturation index [TSI]). This allows us to distinguish between central and peripheral dysfunction, and reversal thereof. Importantly, assessment of CO kinetics, VO_2 kinetics, and TSI to evaluate symptom severity, or compare the effects of HIT and CRT, has not been previously conducted.

The present study aims to further improve our understanding of mechanisms contributing to CHF symptoms, and to differentiate between the effects of cardiac resynchronization therapy (CRT) and high-intensity interval training (HIT) on central and peripheral exercise physiology. To this end, various traits that may be associated with symptomatic severity in CHF were evaluated during (sub)maximal exercise. In addition, the effects of either high-intensity interval training (HIT) and CRT on central haemodynamics, VO_2 kinetics, and skeletal muscle tissue desaturation were evaluated and compared.

10

METHODS

Study design

To allow for comparison of the effects of HIT and CRT, datasets were derived from two studies with a similar study protocol. The first was designed as an explorative randomised controlled trial, allocating patients to either usual care (control group) or HIT in a 1:1 fashion (Netherlands Trial Register: Trial NL2895) [7]. At the same time, a cohort of prospectively enrolled patients, eligible to CRT, was included separately (Netherlands Trial Register: Trial NL2419) **(Figure 1A)** [4].

Participants of both studies underwent the same measurements, whilst adhering to the same follow-up duration of three months. Baseline assessment consisted of resting echocardiography and (sub)maximal exercise testing with respiratory gas analysis **(Figure 1B)**. During exercise testing, simultaneous measurements of cardiac output using a pulse wave contour analysis method were performed **(Figure 1C)**. In addition, changes in skeletal muscle tissue oxygenation during and after (sub)maximal exercise were assessed by near infrared spectroscopy (NIRS) **(Figure 1D)**.

Implantation of the CRT devices was performed, according to standard techniques and local protocols, in the Catharina Hospital, Eindhoven and University Medical Center, Utrecht (UMCU), the Netherlands. Cardiopulmonary and hemodynamic exercise testing was performed in UMCU and Máxima MC. The research protocol was approved by the medical ethics committee of the Máxima MC, Veldhoven, The Netherlands. The study complies with the Declaration of Helsinki. All patients provided written and signed informed consent.

Population and treatment allocation

All patients had stable CHF for at least three months prior to inclusion, and were consecutively enrolled between February 2011 and June 2018. Inclusion criteria were: 1) New York Heart Association (NYHA) class II or III CHF, secondary to ischaemic or dilated cardiomyopathy; 2) left ventricular ejection fraction (LVEF) ≤ 40%; and 3) optimal medical treatment. Exclusion criteria were: 1) recent myocardial infarction; 2) unstable angina within 3 months prior to inclusion; 3) haemodynamically significant valve disease; 4) participation in a training programme (≥2/week) in the last year; 5) significant chronic obstructive pulmonary disease; and 6) orthopaedic or neuromuscular conditions limiting the ability to perform exercise. In addition, CRT patients also had to comply with ESC guideline criteria for CRT implantation [2]. Study physician and technicians were blinded to treatment allocation during the duration of the study, including during the analysis of exercise testing results.
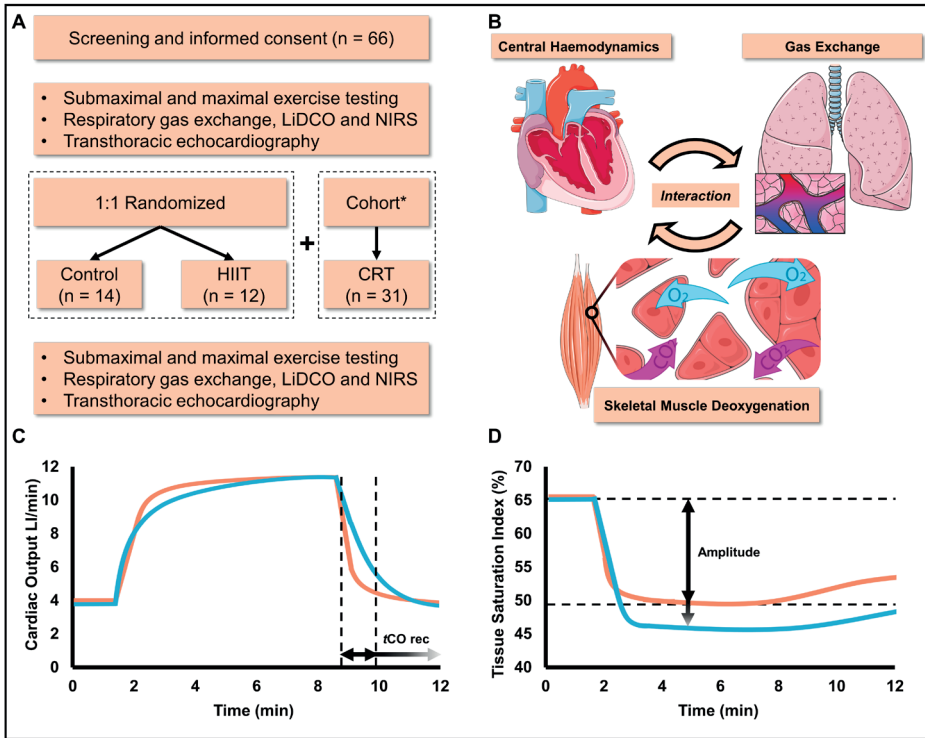
Figure 1. *Flowchart of study design and key assessments (A). The interaction between central cardiac haemodynamics, pulmonary gas exchange, and skeletal muscle function, which underlie the theoretical framework of exercise physiology in heart failure, is schematically displayed (B). Differences in physiological profiles are schematically displayed for two patients (orange and blue). Changes in cardiac output kinetics (tCO) reflect central haemodynamic performance (C), whereas skeletal muscle deoxygenation reflects the ratio between delivery and utilisation at the peripheral level (D). Legend: CRT, cardiac resynchronisation therapy; HIT, high-intensity interval training; LiDCO, lithium dilution based continuous cardiac output monitoring; NIRS, near infrared spectroscopy.*

High-intensity interval training

HIT, rather than aerobic endurance training, was chosen because of its potential effects on reversing cardiac remodelling in CHF [8]. The HIT protocol was adapted from Wisløff et al., and consisted of three sessions per week, over a 12-week period [9]. In contrast to the original treadmill-based exercise prescription, a bicycle ergometer was used. Training commenced with a five-minute warm-up period, followed by four intervals of four minutes, each separated by three-minute active pauses. A five-minute cooling down completed the protocol. High-intensity intervals were performed at a workload corresponding to 85-95% of peak VO_2 achieved at the maximal exercise test. All subjects were trained in the hospital under the direct supervision of trained physiotherapists. The control group was advised to remain physically active, in keeping with recommendations for physical activity.

Cardiopulmonary exercise testing

Exercise testing was performed on a cycle ergometer (Lode Corrival; Lode BV, Groningen, The Netherlands) in an upright seated position. During exercise testing, continuous 12-lead electrocardiogram was registered, and ventilatory parameters were measured breath-by-breath (ZAN 680 USB; ZAN Messgeräte, Oberthulba, Germany). Ventilatory parameters were averaged over 10-second intervals after removal of outliers (values > 3 SD from the local mean) [10].

First, *maximal* exercise testing was performed, which consisted of a four-minute phase of unloaded cycling, followed by a symptom limited test using an individualized ramp protocol (target duration 8–12 minutes). Tests were ended when the patient was unable to maintain the required pedaling frequency. Exercise performance was determined as the maximally achieved power (P peak) at the end of the exercise. VO2 peak was defined as the final 20-second averaged value of the maximal exercise test. Ventilatory aerobic threshold (VAT) was assessed by two blinded physicians using the V-slope method [11]. The results of this baseline test were used in order to determine the workload for the submaximal test.

Afterwards, submaximal constant load exercise testing was performed to assess submaximal VO_2 kinetics. This test commenced with a two–minute resting period, followed by a six–minute bout at 80% of the workload corresponding to the VAT achieved during the preceding maximal exercise test to ensure aerobic oxidation. Patients were instructed to maintain a pedaling frequency of 70 rotations per minute. After the loaded phase, a final 5-minute recovery phase followed, with a fixed leg position.

Assessment of exercise haemodynamics

Assessment of exercise haemodynamics was performed by a radial artery pulse contour analysis method (LiDCO; LiDCO Ltd, London, UK). This technique provides beat-to-beat changes in central haemodynamics by calculating nominal stroke volume (SV) from a pressure–volume transform of the radial artery pressure waveform [12]. In a study using the Fick method as a reference, we showed that this technique is highly accurate for the continuous assessment of CO during incremental symptom-limited exercise testing in CHF patients [13]. Shortly before the exercise protocol was started, a 20-gauge arterial catheter was inserted into the radial artery. The system was calibrated using echocardiographic assessment of stroke volume at rest [14]. Resting CO was defined as the 60-second average during the resting phase, whereas peak CO was defined as the 20-second average at the end of maximal exercise. Cardiac reserve (CR) was defined as peak minus baseline CO.

Skeletal muscle deoxygenation

A portable continuous wave near-infrared spectrophotometer (Portamon; Artinis, Elst, The Netherlands) was used to perform NIRS measurements. The NIRS probe was

connected to the right thigh with an elastic strap, located over the centre of the m. vastus lateralis. In this study, NIRS is based on the modified Lambert–Beer law and the principles of spatially resolved spectroscopy, and its clinical utility is described in detail elsewhere [15]. In brief, oxygenated (O_2Hb) and deoxygenated haemoglobin (HHb) is distinguished by detecting device-emitted light at two different wavelengths, 841 nm and 760 nm respectively. We used the tissue saturation index (TSI) during submaximal exercise as an absolute measure of skeletal muscle tissue oxygen saturation. The TSI is the ratio of O_2Hb, divided by total Hb, expressed as a percentage. We calculated TSI amplitude (TSI_{AMP}), as a measure of skeletal muscle deoxygenation, defined as baseline TSI, minus the lowest 5–second averaged value during the first three minutes of submaximal exercise. We previously demonstrated good reliability for absolute TSI amplitudes, with an intraclass correlation coefficient of 0.74-0.90 [16].

Kinetic analysis

Analysis of VO_2 and Q during onset and recovery of the constant load tests was reported previously [17]. All data were resampled into 10-second intervals and the first 20 seconds of the VO_2 data (e.g. exercise onset) were omitted. This was done because during this period (cardiodynamic phase), increases in VO_2 merely reflect an increase in pulmonary blood flow, rather than actual changes in tissue gas exchange. A non-linear least squares regression procedure (Python 2.7; Python Software Foundation, Beaverton, USA) was applied to the onset phase in order to calculate the time constant of VO_2 onset (formula 1).

10

Formula 1. *CO or VO_2 kinetics for onset phase.*

$$Y(t) = Y_{baseline} + A \cdot \left(1 - e^{-(t-Td)/\tau}\right)$$

where Y = VO_2 or CO; A = amplitude during exercise onset; Td = time delay (seconds); and τ = time constant (seconds). Recovery kinetics were calculated as well (formula 2).

Formula 2. *CO or VO_2 kinetics for recovery phase.*

$$Y(t) = Y_{steady\ state} - A \cdot \left(1 - e^{-(t-Td)/\tau}\right)$$

where Y = VO_2 or CO; A = amplitude during recovery from steady state; Td = time delay (seconds); and τ = time constant (seconds).

Statistical analysis

Data were analysed using SPSS statistics (version 26.0, SPSS Inc, Chicago, IL, USA). Continuous variables were tested for normality using visual assessment the Shapiro-Wilk test, and were expressed as the mean ± standard deviation (SD). Non-normal data was expressed as median with interquartile range (IQR). Data with a normal distribution were evaluated using the t-test. Differences in baseline characteristics of the three groups were calculated with one-way analysis of variance (ANOVA) or Kruskal-Wallis test,

where appropriate. The influence of potential confounders, owed to between-group differences (e.g. age), was evaluated using analysis of covariance (ANCOVA). Categorical data were presented as absolute count and were compared with a Chi-squared or Fisher exact test. All statistical tests performed were two-tailed and a p-value < 0.05 was considered statistically significant.

Table 1. Baseline characteristics.

Variable	Control (n = 14)	HIT (n = 12)	CRT (n = 31)	P-value
Age (years)	67±9	58±8	68±7	0.001[†]
Male – n (%)	13 (93)	10 (83)	19 (61)	0.058
ICM – n (%)	6 (43)	8 (67)	13 (42)	0.321
HF duration (months)	11 [5-37]	33 [10-81]	16 [6-72]	0.448
NYHA class III – n (%)	7 (50)	3 (25)	21 (68)	0.038
Sinus rhythm – n (%)	9 (64)	11 (92)	26 (84)	0.170
LVEDV (ml)	239 [191-333]	214 [178-260]	239 [170-299]	0.677
LVESV (ml)	175 [98-216]	144 [110-186]	171 [116-217]	0.441
LVEF (%)	32±12	33±9	27±8	0.074
Beta-blocker – n (%)	14 (100)	11 (92)	28 (90)	0.491
ACEi/ARB – n (%)	13 (93)	12 (100)	31 (100)	0.209

Results are presented as mean ± SD, median with IQR, numbers or percentages. Legend: ACEi, angiotensin-converting enzyme inhibitor; ARB, angiotensin II receptor blockers; HF, heart failure; ICM, ischemic cardiomyopathy; LVEDV, left ventricular end diastolic volume; LVEF, left ventricular ejection fraction; LVESV, left ventricular end systolic volume; NYHA, New York Heart Association. P-value for between group-difference. [†] significant between HIT and both other groups.

RESULTS

Of the 35 eligible patients who gave informed consent for the randomized part of the study, nine were excluded *before* randomization due to severe anxiety, withdrawn consent, improved LVEF > 35%, and death following CHF progression. Two patients, randomized to the training group, could not complete the protocol due to orthopaedic complaints. In the CRT cohort, 31 patients were included. At baseline, age and NYHA distribution were significantly different among the three groups **(Table 1)**.

Determinants of baseline functional impairment in CHF
Patients with NYHA II (n = 29), compared with NYHA III (n = 37), were significantly younger (age 61±7 versus 69±8; p <0.001), but there was no significant difference in duration of CHF (19 versus 24 months; p = 0.453). No significant differences were found in terms of adverse remodelling or LVEF at rest **(Supplemental Table 1; Figure 2A)**. Resting haemodynamics and oxygen uptake, i.e. baseline levels of CO and VO_2 respectively, were also similar in both groups (P > 0.05).

Without correction, CO kinetics and CR were more severely hampered in NYHA III patients (all $p \leq 0.001$), with similar results for VO_2 kinetics and VO_2 peak (all $p \leq 0.05$). Conversely, when corrected for age, NYHA III demonstrated significantly slower CO kinetics and VO_2 kinetics, during both onset and recovery of submaximal exercise **(Figure 2B)**. Patients in NYHA III also had significantly lower CR (4.8 ± 2.9 versus 7.1 ± 3.1 L/min; $p = 0.022$) when compared to NYHA II, but when corrected for age this difference was not significant ($p = 0.262$). There were no significant differences between NYHA II and NYHA III patients with respect to the amount of skeletal muscle deoxygenation during submaximal exercise (TSI_{AMP}: 8.2% versus 7.4%; $p = 0.618$; $n = 44$). Moreover, baseline LVEF was poorly related to peak performance ($R = 0.326$; $p = 0.10$) and peak VO_2 ($R = 0.339$; $p = 007$). By contrast, the association of baseline CR with peak performance ($R = 0.703$; $p < 0.001$) and peak VO_2 was strong ($R = 0.708$; $p < 0.001$).
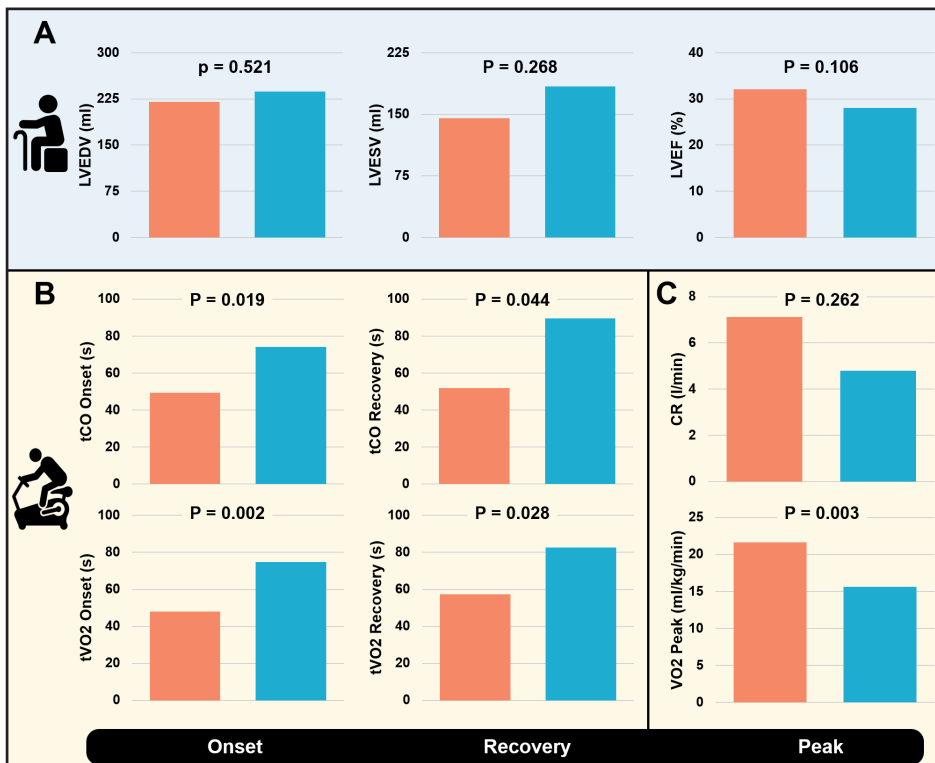
Figure 2. *NYHA III (blue) heart failure symptoms were unrelated to resting cardiac function (A). However, when corrected for age, NYHA III was associated with worse central haemodynamics and peripheral oxygen uptake during submaximal (B) and maximal (C) exercise, relative to NYHA II (orange). Legend: CO, cardiac output; CR, cardiac reserve; EDV, end-diastolic volume; EF, ejection fraction; ESV, end-systolic volume; LV, left ventricular; NYHA, New York Heart Association; tVO_2, time constant of oxygen uptake.*

Changes in resting versus exercising haemodynamics

Reverse remodelling (ΔLVESV -22$\pm$19%; p < 0.001) and subsequent improvements in *resting* haemodynamics (ΔLVEF 8$\pm$7%; p < 0.001) occurred exclusively following CRT **(Figure 3A; Supplemental Table 1)**. Conversely, *exercising* haemodynamics remained unaltered in CRT patients (ΔCR 0.1$\pm$2.5 L/min; p = 0.890), but improved significantly by 39% following HIT (ΔCR 2.5$\pm$3.2 L/min; p = 0.034) **(Figure 3B)**. HIT-induced changes in CR were largely owed to increased CO peak (12.5$\pm$3.8 versus 15.0$\pm$4.4 L/min; p = 0.073), since CO baseline remained unaltered (5.3$\pm$2.2 versus 5.7$\pm$1.5; p = 0.389). No significant changes were found in CO kinetics. Age, NYHA and LVEF were no significant confounders when comparing differences in haemodynamic changes following either HIT or CRT.

Peak exercise capacity and workload

After 3 months, CRT significantly increased VO_2 Peak by 2.2$\pm$2.7 ml/kg/min (p < 0.001) **(Figure 3C; Supplemental Table 2)**. VO_2 Peak increased non-significantly following HIT (ΔVO_2 Peak 1.3$\pm$3.1 ml/kg/min; p = 0.169). In both CRT and HIT patients, maximal workload capacity increased on average by 10%, but remained unaltered in control patients **(Figure 3D; Supplemental Table 2)**. Baseline LVEF partially accounted for between-group differences in altered peak workload capacity (p = 0.027).

Submaximal exercise kinetics

Significant reductions in submaximal exercise recovery times of 11% and 16% were seen following CRT (tVO_2 recovery 77$\pm$39 versus 61$\pm$18 seconds; P = 0.03) and HIT (tVO_2 recovery 71$\pm$19 versus 59$\pm$14 seconds; P = 0.005), respectively **(Figure 3E; Supplemental Table 3)**. In control patients, no significant changes were observed (tVO_2 recovery 69$\pm$24 versus 68$\pm$23 seconds; p = 0.722). No significant reduction in skeletal muscle deoxygenation was observed during the symptom-limited exercise test following either HIT or CRT **(Figure 3F; Supplemental Table 3)**. No significant interactions were found for age, NYHA, or LVEF.
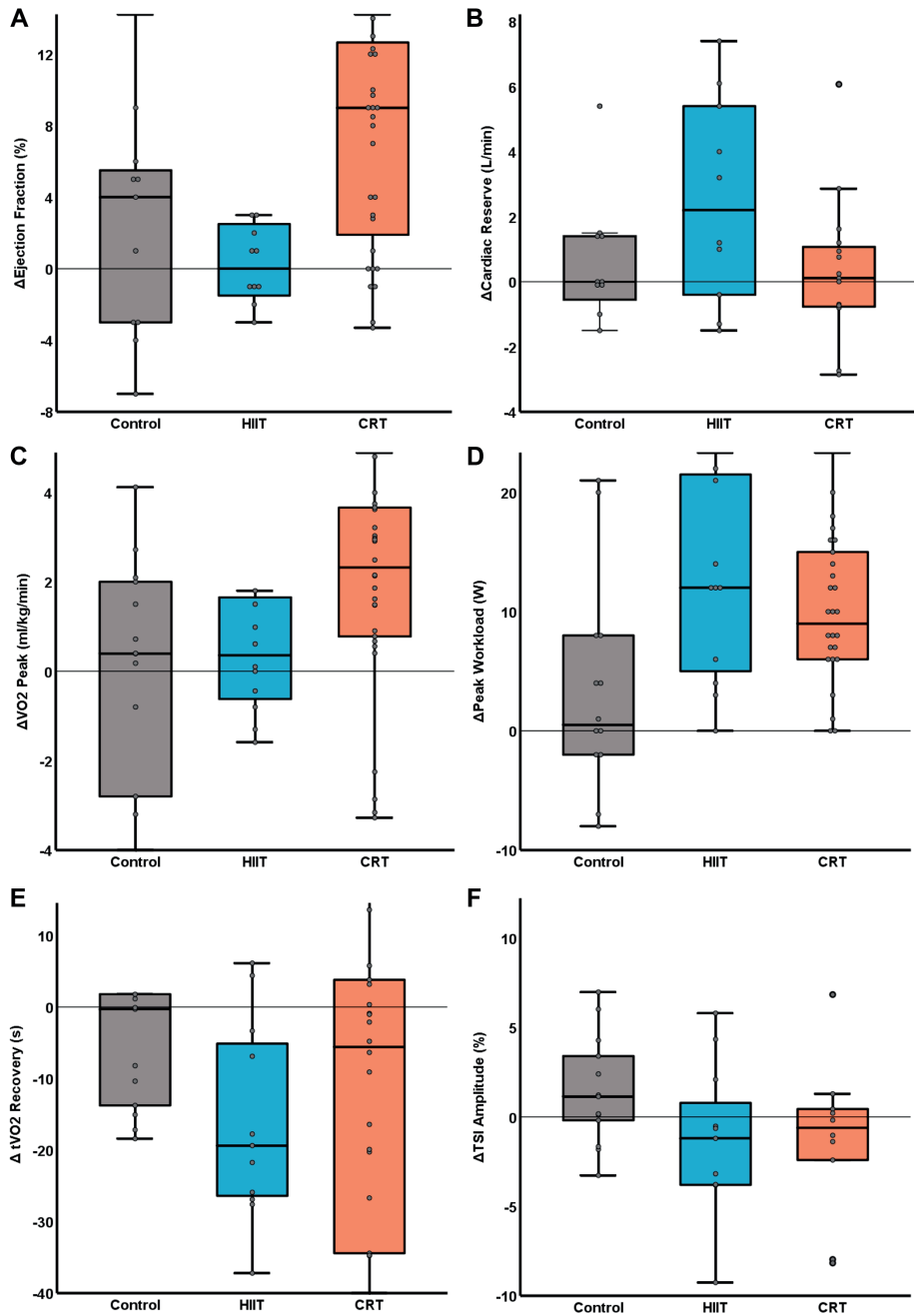
Figure 3. *Discrepancy between changes in haemodynamics at rest (A) or during exercise (B), and changes and within-group variability in exercise physiology and capacity following HIT and CRT (C-F). Abbreviations as in Figure 1.*

10

DISCUSSION

This study showed that, irrespective of resting cardiac function, a more severely reduced functional capacity in CHF patients is not only associated with worse central hemodynamic performance during exercise, but also with slower recovery from submaximal exercise. Hence, peripheral oxygen delivery and oxygen utilization are impaired in CHF patients, and these traits distinguish NYHA class II from III patients. In addition, HIT and CRT were shown to have differential effects on central haemodynamics, during exercise and at rest, respectively. However, either approach improved recovery from submaximal exercise, indicating improved efficiency of peripheral skeletal muscle [18]. Both interventions may therefore be combined to achieve an optimal and synergistic effect, particularly in CHF patients where functional capacity is markedly reduced.

Symptom aetiology in chronic heart failure

As evidenced before, cardiac function *at rest* does not explain the cause and extent of symptoms of fatigue in CHF patients, and better understanding of physiological processes that determine exercise tolerance may guide treatment selection [19]. In line with this, we found that symptomatic burden of CHF was related to impaired central haemodynamics (tCO) and skeletal muscle dysfunction (tVO$_2$) during dynamic exercise-transitions, rather than decreased resting cardiac function. Since exercise training improves VO$_2$ kinetics and exercise haemodynamics, NYHA III patients may benefit the most from (additional) exercise training, according to our results. Importantly, worse functional class and exercise capacity decreases patient motivation and adherence to exercise-training, prohibiting treatment effect [20]. It therefore stands to reason that timely intervention, thereby *'preventing'* further deconditioning due to HF-progression, is preferred.

Resting and exercising haemodynamics

In the present study, only HIT induced substantial improvements in CR (on average 37%), illustrating better cardiac performance during exercise, possibly through improved LV contractility or decreasing peripheral resistance [21]. Because CR is a marker of haemodynamic performance, it is also an important determinant of exercise capacity [22,23]. Moreover, CR has shown to be independently associated with all-cause mortality in 219 CHF patients (hazard ratio 0.682 per L/min increase in CR) [24]. Therefore, increase in CR is clinically meaningful, regardless of LVEF.

Conversely, only CRT was able to induce significant reverse remodelling and subsequent improvement in LVEF, but CR remained unaltered. This suggests exercise training may be a requirement for cardiac function to adapt at dynamic haemodynamic conditions. Although reverse remodelling does not occur in all CRT recipients (typically

60-70%), reverse remodelling is associated with a clear reduction in mortality [25]. Hence, in responding individuals, both interventions are capable of significantly improving survival [20].

Peripheral improvements in skeletal muscle

Three months of either HIT or CRT both significantly accelerated VO_2 recovery kinetics during submaximal exercise, although response was heterogeneous. In principle, acceleration of VO_2 recovery kinetics can be explained by a smaller O_2 debt, either due to improved O_2 delivery and/or faster O_2 utilisation at the level of skeletal tissue [17]. However, since no concomitant changes in CO kinetics were seen, centrally-mediated *'bulk'* O_2-delivery is unlikely to be a key mechanism for improving VO_2 recovery kinetics during submaximal exercise. Rather, *'locally'* improved matching of microvascular O_2-delivery to O_2-utilization, in the skeletal muscle, plays a more important role [26]. In line with these findings, faster VO_2 recovery in HIT patients has been associated with less severe skeletal muscle deoxygenation following submaximal exercise (i.e., TSI_{AMP}) [7].

Because accelerated VO_2 recovery essentially reflects faster recovery from submaximal exercise, improvements in VO_2 kinetics are clinically relevant. VO_2 kinetics may even be superior to VO_2 peak in predicting CHF prognosis [27]. It remains to be investigated whether peripheral derangements, as frequently encountered in HF patients, are also associated with achieving functional or echocardiographic response after CRT.

Prognostic implications

10

Adverse cardiac remodelling is typically associated with poor outcome in CHF, whereas its reversal is a hallmark of response in recipients of CRT [28]. CRT is therefore highly effective in improving survival, and may even increase exercise haemodynamics in CHF patients [23]. However, as indicated by our results, although CRT may improve exercise performance, it does not *'necessarily'* improve CR and skeletal muscle oxygenation. The discrepancy between echocardiographic response and functional outcome following CRT, in part, underscores this phenomenon [29]. By contrast, exercise training is capable of improving multiple aspects of CHF, including improving skeletal muscle functioning and (sub)maximal exercise capacity [1,4,9]. Importantly, NYHA functional class and exercise capacity are important factors associated with prognosis [30], and even a modest increase in VO_2 peak of just 1 ml/kg/min is associated with reduced mortality [31]. Hence, exercise-training is likely to improve prognosis as well, especially in those willing and motivated [20]. Unfortunately, despite these important contributions, exercise training remains frequently overlooked, and is therefore scarcely prescribed [32,33].

Combining CRT and exercise training: the best of both worlds?

The importance of combined interventions is underscored by the fact that the nature of exercise limitations in CHF patients is heterogeneous [34,35]. A combined approach, as also reported by our group, should therefore be considered feasible [4]. Even in addition to CRT, HIT further improves exercise capacity and VO_2 peak in CHF patients [4–6]. Moreover, exercise training after CRT may also further improve exercise haemodynamics, thereby further increasing CRT-induced benefits [5]. Lastly, we should acknowledge the systemic effects of exercise-training, including its ability to reduce peripheral resistance, induce skeletal muscle hypertrophy, and improve oxidative capacity [1]. In the end, heart failure is a debilitating and systemic disease [1], and effective treatment plans should actively target *both,* the alleviation of symptoms and improvement of quality and duration of life.

Limitations

The present explorative study is primarily limited by its sample size, and is therefore potentially underpowered. As a result, the relation between symptom aetiology and treatment effect could not be investigated. Second, the use of a non-randomized CRT cohort resulted in potential confounding, owed to differences in patient characteristics. Although we evaluated the influence of age, NYHA and LVEF when comparing effects of HIT with CRT, their effect cannot be reliably excluded. Third, since CRT *'acutely'* induces acute improvement in mechanical and haemodynamic function, the relatively short 3-month follow-up may have disproportionally under-estimated training-induced changes [36]. Fourth, because long-term serial assessment of exercise parameters is missing, no causal relationship with NYHA class can be established. Lastly, although NIRS amplitudes can reliably discriminate between individuals, they are less suitable to detect treatment effects over time, and should be interpreted with caution [16].

Conclusions

Rather than echocardiographic function at rest, delayed submaximal exercise VO_2 and CO kinetics characterise symptomatic burden in CHF. These results indicate that both central and peripheral derangements contribute to functional impairments in CHF patients. HIT and CRT were shown to have differential effects on central haemodynamics, namely predominantly during exercise or at rest, respectively. However, either approach improved recovery from submaximal exercise, indicating improved efficiency of peripheral skeletal muscle. Here, different but synergistic mechanisms are likely involved, since CRT focusses on cardiac function, but HIT provokes a more systemic and local effect. Hence, clinicians should be prompted to more actively pursue adequate exercise training or cardiac rehabilitation in patients undergoing interventions aimed primarily at improving cardiac function, such as CRT.

REFERENCES

1. T. A. Rehn, M. Munkvik, P. K. Lunde, I. Sjaastad, O. M. Sejersted. Intrinsic skeletal muscle alterations in chronic heart failure patients: a disease-specific myopathy or a result of deconditioning? *Heart Fail. Rev.* **17**, 421–436 (2012).

2. T. A. McDonagh, M. Metra, M. Adamo, *et al.* 2021 ESC Guidelines for the diagnosis and treatment of acute and chronic heart failure: Developed by the Task Force for the diagnosis and treatment of acute and chronic heart failure of the European Society of Cardiology (ESC) With the special contributio. *Eur. Heart J.* **42**, 3599–3726 (2021).

3. B. Bjarnason-Wehrens, H. McGee, A.-D. Zwisler, *et al.* Cardiac rehabilitation in Europe: results from the European Cardiac Rehabilitation Inventory Survey. *Eur. J. Cardiovasc. Prev. Rehabil.* **17**, 410–418 (2010).

4. R. F. Spee, V. M. Niemeijer, T. Schoots, *et al.* High intensity interval training after cardiac resynchronization therapy: An explorative randomized controlled trial. *Int. J. Cardiol.* **299**, 169–174 (2020).

5. A. Y. Patwala, P. R. Woods, L. Sharp, *et al.* Maximizing patient benefit from cardiac resynchronization therapy with the addition of structured exercise training: a randomized controlled study. *J. Am. Coll. Cardiol.* **53**, 2332–2339 (2009).

6. V. M. A. Conraads, M. Vanderheyden, B. Paelinck, *et al.* The effect of endurance training on exercise capacity following cardiac resynchronization therapy in chronic heart failure patients: a pilot trial. *Eur. J. Cardiovasc. Prev. Rehabil.* **14**, 99–106 (2007).

7. R. F. Spee, V. M. Niemeijer, P. F. Wijn, P. A. Doevendans, H. M. Kemps. Effects of high-intensity interval training on central haemodynamics and skeletal muscle oxygenation during exercise in patients with chronic heart failure. *Eur. J. Prev. Cardiol.* **23**, 1943–1952 (2016).

8. Ø. Ellingsen, M. Halle, V. Conraads, *et al.* High-Intensity Interval Training in Patients With Heart Failure With Reduced Ejection Fraction. *Circulation*. **135**, 839–849 (2017).

9. U. Wisløff, A. Støylen, J. P. Loennechen, *et al.* Superior cardiovascular effect of aerobic interval training versus moderate continuous training in heart failure patients: a randomized study. *Circulation*. **115**, 3086–3094 (2007).

10. N. Lamarra, B. J. Whipp, S. A. Ward, K. Wasserman. Effect of interbreath fluctuations on characterizing exercise gas exchange kinetics. *J. Appl. Physiol.* **62**, 2003–2012 (1987).

11. W. L. Beaver, K. Wasserman, B. J. Whipp. A new method for detecting anaerobic threshold by gas exchange. *J. Appl. Physiol.* **60**, 2020–2027 (1986).

12. M. M. Jonas, S. J. Tanser. Lithium dilution measurement of cardiac output and arterial pulse waveform analysis: an indicator dilution calibrated beat-by-beat system for continuous estimation of cardiac output. *Curr. Opin. Crit. Care*. **8**, 257–261 (2002).

13. H. M. C. Kemps, E. J. M. Thijssen, G. Schep, *et al.* Evaluation of two methods for continuous cardiac output assessment during exercise in chronic heart failure patients. *J. Appl. Physiol.* **105**, 1822–1829 (2008).

14. R. M. Lang, L. P. Badano, V. Mor-Avi, *et al.* Recommendations for cardiac chamber quantification by echocardiography in adults: an update from the American Society of Echocardiography and the European Association of Cardiovascular Imaging. *Eur Hear. J Cardiovasc Imaging*. **28**, 1-39.e14 (2015).

15. M. Ferrari, M. Muthalib, V. Quaresima. The use of near-infrared spectroscopy in understanding skeletal muscle physiology: recent developments. *Philos. Trans. Ser. A, Math. Phys. Eng. Sci.* **369**, 4577–4590 (2011).

10

16. V. M. Niemeijer, R. F. Spee, J. P. Jansen, *et al.* Test-retest reliability of skeletal muscle oxygenation measurements during submaximal cycling exercise in patients with chronic heart failure. *Clin. Physiol. Funct. Imaging*. **37**, 68–78 (2017).

17. H. M. Kemps, G. Schep, M. L. Zonderland, *et al.* Are oxygen uptake kinetics in chronic heart failure limited by oxygen delivery or oxygen utilization? *Int. J. Cardiol.* **142**, 138–144 (2010).

18. H. M. C. Kemps, J. J. Prompers, B. Wessels, *et al.* Skeletal muscle metabolic recovery following submaximal exercise in chronic heart failure is limited more by O 2 delivery than O 2 utilization. *Clin. Sci.* **118**, 203–210 (2010).

19. A. J. Coats. Heart failure: What causes the symptoms of heart failure? *Heart*. **86**, 574–578 (2001).

20. L. B. Cooper, R. J. Mentz, J.-L. Sun, *et al.* Psychosocial Factors, Exercise Adherence, and Outcomes in Heart Failure Patients: Insights From Heart Failure: A Controlled Trial Investigating Outcomes of Exercise Training (HF-ACTION). *Circ. Heart Fail.* **8**, 1044–1051 (2015).

21. R. Hambrecht, S. Gielen, A. Linke, *et al.* Effects of exercise training on left ventricular function and peripheral resistance in patients with chronic heart failure: A randomized trial. *JAMA*. **283**, 3095–3101 (2000).

22. L. B. Tan. Evaluation of cardiac dysfunction, cardiac reserve and inotropic response. *Postgrad. Med. J.* **67 Suppl 1**, S10-20 (1991).

23. D. Schlosshan, D. Barker, C. Pepper, *et al.* CRT improves the exercise capacity and functional reserve of the failing heart through enhancing the cardiac flow- and pressure-generating capacity. *Eur. J. Heart Fail.* **8**, 515–521 (2006).

24. S. G. Williams, M. Jackson, G. A. Cooke, *et al.* How do different indicators of cardiac pump function impact upon the long-term prognosis of patients with chronic heart failure? *Am. Heart J.* **150**, 983 (2005).

25. P. W. X. Foley, S. Chalil, K. Khadjooi, *et al.* Left ventricular reverse remodelling, long-term clinical outcome, and mode of death after cardiac resynchronization therapy. *Eur. J. Heart Fail.* **13**, 43–51 (2011).

26. B. R. McKay, D. H. Paterson, J. M. Kowalchuk. Effect of short-term high-intensity interval training vs. continuous training on O2 uptake kinetics, muscle deoxygenation, and exercise performance. *J. Appl. Physiol.* **107**, 128–138 (2009).

27. C. Schalcher, H. Rickli, M. Brehm, *et al.* Prolonged Oxygen Uptake Kinetics During Low-Intensity Exercise Are Related to Poor Prognosis in Patients With Mild-to-Moderate Congestive Heart Failure[*]. *Chest*. **124**, 580–586 (2003).

28. A. Alberto, G. H. K., B. Andrea, E. Michele, J. J. L. Imaging, Biomarker, and Clinical Predictors of Cardiac Remodeling in Heart Failure With Reduced Ejection Fraction. *JACC Hear. Fail.* **7**, 782–794 (2019).

29. B. K. Fornwalt, W. W. Sprague, P. BeDell, *et al.* Agreement is poor among current criteria used to define response to cardiac resynchronization therapy. *Circulation*. **121**, 1985–1991 (2010).

30. R. Kazem, B. Derrick, C. Nathalie, *et al.* Risk Prediction in Patients With Heart Failure. *JACC Hear. Fail.* **2**, 440–446 (2014).

31. A. M. Swank, J. Horton, J. L. Fleg, *et al.* Modest increase in peak VO2 is related to better clinical outcomes in chronic heart failure patients: results from heart failure and a controlled trial to investigate outcomes of exercise training. *Circ. Heart Fail.* **5**, 579–585 (2012).

32. H. Golwala, A. Pandey, C. Ju, *et al.* Temporal Trends and Factors Associated With Cardiac Rehabilitation Referral Among Patients Hospitalized With Heart Failure: Findings From Get With The Guidelines-Heart Failure Registry. *J. Am. Coll. Cardiol.* **66**, 917–926 (2015).

33. T. M. H. Eijsvogels, M. F. H. Maessen, E. A. Bakker, *et al.* Association of Cardiac Rehabilitation With All-Cause Mortality Among Patients With Cardiovascular Disease in the Netherlands. *JAMA Netw. Open*. **3**, e2011686–e2011686 (2020).

34. R. F. Spee, V. M. Niemeijer, T. Schoots, *et al.* The relation between cardiac output kinetics and skeletal muscle oxygenation during moderate exercise in moderately impaired patients with chronic heart failure. *J. Appl. Physiol.* **121**, 198–204 (2016).

35. R. F. Spee, V. M. Niemeijer, B. Wessels, *et al.* Characterization of exercise limitations by evaluating individual cardiac output patterns: a prospective cohort study in patients with chronic heart failure. *BMC Cardiovasc. Disord.* **15**, 57 (2015).

36. P. C. Wouters, G. E. Leenders, M. J. Cramer, *et al.* Acute recoordination rather than functional hemodynamic improvement determines reverse remodelling by cardiac resynchronisation therapy. *Int. J. Cardiovasc. Imaging*. **37**, 1903–1911 (2021).

10

SUPPLEMENTARY MATERIAL

Supplemental Table 1. Baseline differences stratified to NYHA classification.

Variable	NYHA 2 (n = 29)	NYHA 3 (n = 37)	P-value
Age (years)	61±7	69±8	<0.001
Male – n (%)	24 (83)	27 (73)	0.391
ICM – n (%)	12 (41)	20 (54)	0.332
HF duration (months)	19 [6-61]	24 [7-98]	0.453
Sinus rhythm – n (%)	26 (90)	28 (76)	0.203
LVEDV (ml)	220 [178-282]	237 [185-293]	0.521
LVESV (ml)	145 [99-211]	184 [135-216]	0.278
LVEF (%)	32±11	28±8	0.106
Beta-blocker – n (%)	26 (90)	35 (95)	0.647
ACEi/ARB – n (%)	28 (97)	37 (100)	0.439

Results are presented as mean ± SD, median with IQR, numbers or percentages. Legend: ACEi, angiotensin-converting enzyme inhibitor; ARB, angiotensin II receptor blockers; HF, heart failure; ICM, ischemic cardiomyopathy; LVEDV, left ventricular end diastolic volume; LVEF, left ventricular ejection fraction; LVESV, left ventricular end systolic volume; NYHA, New York Heart Association

Supplemental Table 2. Changes in resting haemodynamics and peak exercise capacity.

	Control (n=14)		HIT (n=12)		CRT (n= 31)	
	Before	After	Before	After	Before	After
Resting haemodynamics						
EDV (mL)	239 [191-333]	236 [147-300]	214 [178-260]	207 [179-263]	**239 [170-299]**	**195 [148-253] †**
ESV (mL)	175 [98-216]	259 [86-218]	144 [110-186]	136 [105-206]	**171 [116-217]**	**115 [84-183] †**
EF (%)	32.9±11.7	35.5±12.4	32.8±8.6	33.5±10.4	26.6±8.1	34.9±11.4*
Peak exercise capacity						
VO$_2$ peak (ml/min/kg)	20.2±6.0	19.9±6.7	20.8±5.4	22.2±5.3	**16.2±5.4**	**18.4±5.8***
P peak (W)	130±57	132±64	**135±47**	**150±51***	103±42	112±44*

*Results are presented as mean ± SD or median with IQR. Legend: HIT, high-intensity interval training; CRT, cardiac resynchronisation therapy; * p < 0.05 relative to baseline of same group. † p < 0.001*

Supplemental Table 3. Changes in central haemodynamics and peripheral oxygen utilisation during (sub)maximal exercise testing.

	Control (n=14)		HIT (n=12)		CRT (n= 31)	
	Before	**After**	**Before**	**After**	**Before**	**After**
Exercising haemodynamics						
tCO onset (s)	52±39	48±31	62±27	49±17	64±33	72±37
tCO recovery (s)	66±49	60±25	52±23	55±23	77±64	59±26
CO peak (L/min)	17.5±25.0	17.6±25.4	12.5±3.8	15.0±4.4	11.1±4.0	10.8±5.0
CR (L/min)	5.8±4.3	5.8±5.7	**7.2±2.6**	**9.7±4.1***	5.9±2.9	5.9±3.8
Peripheral oxygen utilisation						
tVO_2 onset (s)	60±28	56±23	57±22	49±17	70±38	71±40
tVO_2 recovery (s)	68±23	69±24	**71±19**	**59±14***	**77±39**	**61±18***
TSI_{AMP} (%)	7.4±5.2	8.9±5.7	10.1±7.2	7.9±4.9	6.2±2.6	4.9±4.5

*Legend: CO, cardiac output; CR, cardiac reserve; CRT, cardiac resynchronisation therapy; HIT, high-intensity interval training; TSI, tissue saturation index; tVO2, time constant of oxygen uptake. * $p < 0.05$ relative to baseline of same group.*

10

11

General Discussion

BACKGROUND

The main goals of clinical research on cardiac resynchronization therapy (CRT) are preventing unwarranted procedures and further improving outcome after CRT implantation. In patients with dyssynchronous heart failure, a crucial but complex interplay between electrical dyssynchrony and subsequent left ventricular (LV) mechanical dyscoordination (LVMD) exists. Such electrical and mechanical markers, often derived from the ECG and cardiac imaging modalities, have been linked to outcomes after CRT [1–4]. However, the clinical value of electrical markers is limited [5, 6], and routine evaluation of imaging markers of LVMD is still lacking in everyday clinical practice [1, 7]. In the first part of this thesis, novel approaches to better use electrical and mechanical markers are investigated to improve patient selection criteria for CRT **(Figure 1 – Part I)**. We found that combining deep-learning or QRS$_{AREA}$ with strain-based discoordination likely allows for optimal and objective assessment of the electromechanical substrate. Electrical and mechanical parameters are also used to help navigate the LV lead towards sites of late electrical [8, 9] or mechanical activation [10, 11], and away from scar [12]. Although LV-leads placed in these positions may result in more favourable outcomes, results have shown to vary. Hence, in the second part, current challenges and opportunities for optimising LV-lead placement were identified, and the feasibility of a patient-specific targeting approach using real-time image-guidance was evaluated **(Figure 1 – Part II)**. Lastly, because heart failure is a systemic disease that induces symptoms during exertion and limits exercise tolerance [13], the role of exercise testing before and exercise training after CRT was explored as well **(Figure 1 – Part III)**. We found that exercise-testing may provide diagnostic and prognostic information in CRT patients, whereas exercise may also provide additional therapeutic benefits in these patients .

11
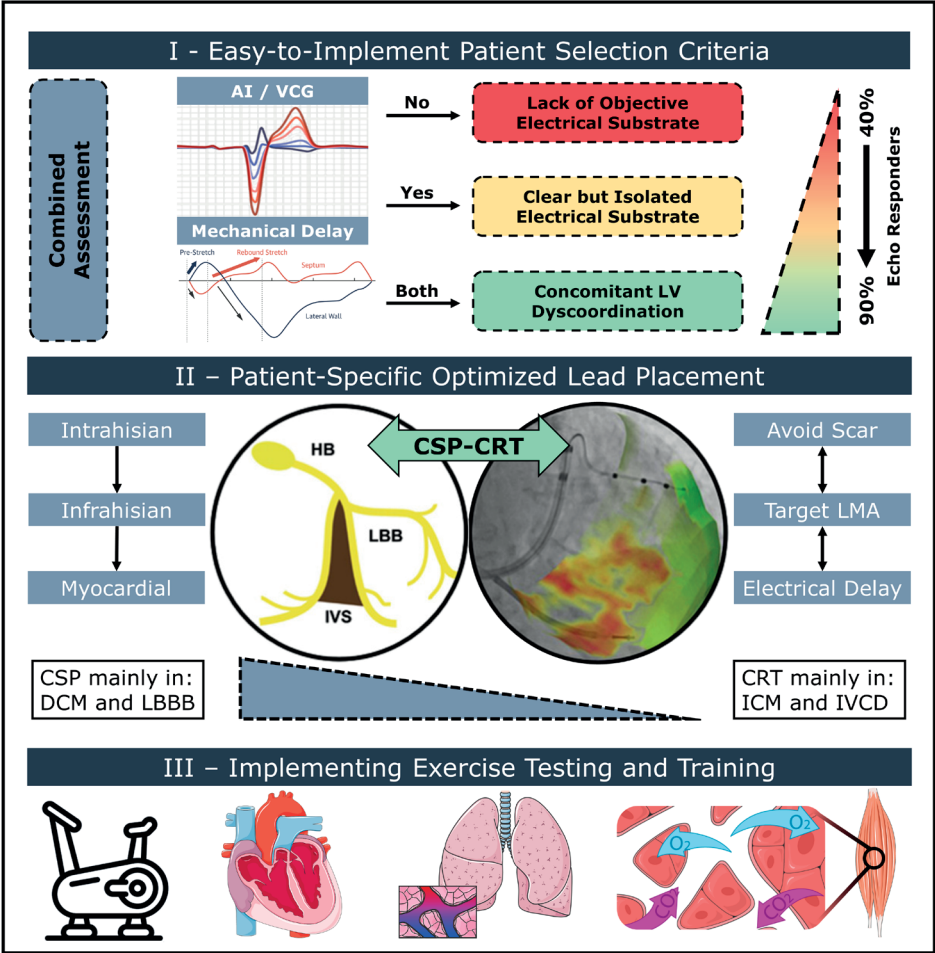
Figure 1. *Summary of the concepts elucidated in the present thesis. In part I, the importance of simultaneous assessment of electrical and mechanical markers of dyssynchrony is demonstrated. In part II, we discuss the role of image-guided left ventricular lead placement, which is likely most important in patients with scar and/or without left bundle branch block. Lastly, part III explores the diagnostic, prognostic and therapeutic implications of exercise in patients with dyssynchronous heart failure. Legend: AI, artificial intelligence; CRT, cardiac resynchronization therapy; CSP, conduction system pacing; DCM, dilating cardiomyopathy; ICM, ischemic cardiomyopathy; IVCD; intraventricular conduction delay; LBBB, left bundle branch block; VCG, vectorcardiography.*

PART I – OPTIMZING PATIENT SELECTION

The importance of predicting response

A recent position paper has criticised the usefulness of prediction models, as they argue that they cannot justify withholding patients from CRT with sufficient certainty, and patients with a guideline indication may derive some benefit, even when they show no clear signs of reverse remodelling [7]. Indeed, because heart failure is a progressive

disease, preventing further decline in cardiac function may be considered an improvement as well. By itself, an echocardiographic response may therefore be a suboptimal surrogate predictor of clinical outcome after CRT, with a specificity of 62-70% and sensitivity of 61-70% [14–17]. Still, because the patient serves as their own control, assessment of reverse remodelling remains a valuable tool to determine the intra-patient effect of CRT. Regardless, large meta-analyses indicate that *'on group level'* CRT is unlikely to improve clinical outcome in patients with non-LBBB or QRS <150 ms [18–20]. Because a considerable portion of patients with non-LBBB and/or QRS < 150 ms (i.e. non-class I indication) do benefit, the search for selecting patients that derive significant benefit from CRT is still ongoing. The uncertainty of implanting CRT in these patients is further evidenced by the ongoing NICD-CRT study (NCT02454439). This is the first trial to prospectively investigate CRT in patients with QRS ≥ 130 ms and non-LBBB. Clearly, refining patient selection criteria should not be discarded as unimportant.

Baseline electrical substrate

In **chapter 2**, vectorcardiographic QRS_{AREA} and a deep learning-based approach on the whole ECG were both shown to provide more accurate and objective approaches to identify the LV baseline electrical substrate than contemporarily used guideline criteria. Importantly, because FactorECG evaluated ECG factors beyond the QRS-complex, it also significantly outperformed QRS_{AREA} for prediction of outcome. Because we identified clusters of predicted echocardiographic non-response *'and'* poor clinical outcome, the FactorECG approach may exclude potential treatment effect in CRT with sufficient reliability. Of course, randomized studies with a control group (i.e. CRT-OFF) are still warranted to provide more definitive evidence. Moreover, both methods have the advantage that they omit the need for human interpretation of the QRS-complex, namely its width and morphology. Indeed, the subjectivity and large inter-observer disagreement following human interpretation of the QRS-complex is a major pitfall of ECG interpretation [6, 21, 22], and thereby also an inherent limitation of the NICD-CRT study. It would, however, be interesting to evaluate the role of the objective FactorECG or QRS_{AREA} approach in the NICD-CRT study population.

Mechanical dyscoordination

Clear advancements have been made to further improve and objectify the identification of the baseline electrical substrate preceding implantation with CRT. However, using the ECG alone, no information regarding LV mechanical discoordination (LVMD) is provided. After all, it is likely that pump function relates most to 'mechanical' rather than electrical dyssynchrony. In **Chapter 3**, we demonstrated that strain-based systolic rebound stretch (SRS) '*acutely*' decreases after CRT. Moreover, acute *'intra-ventricular recoordination'*, as reflected by reduction of SRS, was more strongly associated with echocardiographic

11

response than acute '*inter-ventricular resynchronisation*'. Hence, although both param-eters likely reflect different aspects of mechanical dysfunction in the dyssynchronous heart, SRS is the better index of a functional mechanical substrate, amenable to CRT and reflecting subsequent LV reverse remodelling. However, important limitations still need to be addressed before mechanical dyssynchrony can be incorporated into the guideline criteria for CRT.

Indeed, ever since the disappointing results of the often-cited PROSPECT study, the added value of mechanical dyssynchrony to refine patient selection criteria for CRT has been under constant debate [23]. Critics typically focus on the lack of sufficient sensitivity, and rightfully claim that, despite continuous efforts, the absence of LV mechanical dys-synchrony cannot reliably justify withholding patients of CRT [7]. However, PROSPECT was a non-randomised study, published well over a decade ago, that primarily investigated markers of dyssynchrony that are now considered obsolete [23]. Indeed, for a marker of mechanical dyssynchrony to be of added value in everyday clinical practice, its simplic-ity, high inter-observer agreement, and low test-retest variability should be demon-strated in a clinical setting. Moreover, as evidenced by the PROSPECT study, markers of dyssynchrony should not be based on the 'time-to-peak mechanical activation' concept. Rather, strain-based measurements are likely more promising. To this extent, our group has previously made many efforts to further improve the clinical utility of SRSsept [24–26]. However, to date, SRSsept has not yet been investigated in the context of optimally as-sessed electrical substrate. Combined assessment may further increase sensitivity and specificity of SRSsept.

A combined approach in clinical setting

In **Chapter 4**, simultaneous assessment of QRS_{AREA} and various markers of mechanical dyssynchrony was performed in a real-world database of CRT recipients (Markers and Predictors of Response [MARC]) [4]. Here, a simple 4-variable logistic regression model (Age, QRS_{AREA}, SRSsept, ApRock) resulted in an AUC of 0.77 for '*sustained*' volumetric response at both 6 and 12-month follow-up **(Figure 1 – Part I)**. These patients thereby demonstrate stable disease remission, and likely benefit from continued prognostic benefits[14–17]. Moreover, it was shown that measuring SRSsept is only of additional benefit for the prediction of response to CRT in the presence of a clear and objective electrical substrate at baseline, i.e. when QRS_{AREA} is high. We also demonstrate how combined evaluation of electromechanics allows for '*reliably inclusion*' of patients that derive a sustained echocardiographic response. This may be particularly beneficial to patients in countries that maintain lower cost-effectiveness thresholds, or where CRT is espe-cially under-utilised [7, 27]. Indeed, previous work already suggested that lack of sufficient electrical dyssynchrony (i.e. QRS-duration < 130 ms) generally precludes benefit from CRT, regardless of the presence of mechanical dyssynchrony [28, 29]. Conversely, computer

modelling studies demonstrated that non-electrical substrates such as (septal) scarring and myocardial stiffness may affect mechanical dysynchrony, but these cannot be corrected by CRT [30, 31]. The implications of this work are important, because now the practical (i.e. "clinical work-up") and clinical implications (i.e. "what does it mean") of electromechanical concordance are demonstrated in a real-world clinical setting. In our study, SRSsept was assessed using vendor-independent software, with focussed septal views in 61% of patients.

Future Studies

In the meantime, efforts should therefore be made to integrate these aspects into a single and easy-to-use metric that can rapidly be investigated in a prospective, randomised, controlled trial. The AMEND-CRT trial (NCT04225520) set out to investigate this by using the simple Apical Rocking index. This study will randomize patients either to guideline-recommended CRT implantation, versus treatment recommendation based on presence (CRT-ON) or absence (CRT-OFF) of mechanical dyssynchrony. Although the arrival of the first prospective randomised trial that addresses the role of imaging in CRT in patients with a guideline CRT indication is applauded, two major limitations should be addressed. First, in AMEND-CRT, apical rocking is investigated without critical evaluation of the baseline electrical substrate. As shown by our study, sensitivity and specificity of apical rocking in patients with low QRS_{AREA} is of no value (<50% for both; AUC = 0.471). It should be emphasized that a relative lack of QRS_{AREA} (i.e., < 120 µVs) is common. This is evidenced by a prevalence of ~40% in our study, despite all patients complying with guideline criteria for CRT. Secondly, although Apical Rocking is easy to assess and can reliably rule out CRT-response due to its high sensitivity (84%; when QRS_{AREA} is high), its specificity is low when compared to SRSsept (61% versus 79%; when QRS_{AREA} is high). Perhaps for this reason, SRSsept and Apical Rocking have shown to be able to complement each other when combined into a single model [32]. As a result, further studies may be warranted before mechanical dyssynchrony can be used as a selection criterium. Currently, clinical outcome data is being collected as part of the MARC Long-Term Outcome (MARC: LTO) registry, which will address whether combined electrical and mechanical assessment also affect prognosis. At the same time, the MARC2 trial is being undertaken in a large number of international centres, which will validate the role of QRS_{AREA} in improving patient selection in individuals who are deemed to have non-LBBB [33].

11

PART II – TAILORING LEAD PLACEMENT

The fallacy of empirical lead placement

In part I, the importance of judicious patient selection was discussed, since the absence of sufficient electrical substrate prohibits effective resynchronisation altogether [28, 29]. However, a poor LV-lead position may preclude CRT response as well, regardless of favourable characterises. This is, in part, also reflected in **Chapter 2** by the large differences in the FactorECG performance when comparing non-ICM and ICM patients (AUC = 0.77 versus AUC = 0.63). This is because in ICM, optimizing LV-lead position is especially critical. Regardless, there is an ongoing debate concerning the 'who' and 'how' of optimizing LV-pacing site, with many implanting physicians disagreeing on the optimal strategy. **Chapter 5** therefore thoroughly discusses the many challenges of determining the optimal pacing site, and how these can be overcome in everyday clinical practice. Accumulated evidence in over 4200 patients showed that, on group level, no pacing site is consistently superior [34–36]. However, there is considerable intra-patient variability in acute haemodynamic response following comparison of different pacing sites [37–43]. As a result, *'individual'* optimization of LV-lead placement may improve response and long-term outcome after CRT. Because optimization of lead position further promotes reduction in total LV activation time [11], it may even increase the total '*proportion*' of patients eligible for CRT **(Figure 2)**. We therefore argue that we should abandon the guideline-directed dogma of empirically targeting the mid-posterolateral wall [1], and should determine the optimal site using patient-specific characteristics. Although reaching individualised targets may prove challenging when encountering restricted venous anatomy, new ultrathin quadripolar micro-leads are being developed (ASTRAL-4LV; NCT04463641). These leads are only 0.4m m in diameter, which may help to better navigate narrow and tortuous veins.

Determining the optimal pacing site

From a physiological point of view, conduction system pacing (CSP) provides an exciting and promising alternative to resynchronizing the heart. Because of its potential use in CRT patients in the future, the differences between CSP and transvenous LV-lead placement were also discussed in **chapter 5**. CSP has shown to provide better electrical resynchronization and similar acute haemodynamic benefits when compared to biventricular pacing [44]. However, a large LBBAP registry demonstrated failure of the implantation procedure in 15% of 325 heart failure patients, and demonstrated echocardiographic response in 72% [45]. In non-LBBB, implantation was unsuccessful in 35%, and response was lower at 67%. Hence, in total, only 44% of non-LBBB patients benefited directly from LBBAP, despite possible selection bias following non-consecutive patient recruitment. The first trial that actually randomised to either BVP or CSP (all LBBB patients, 78%
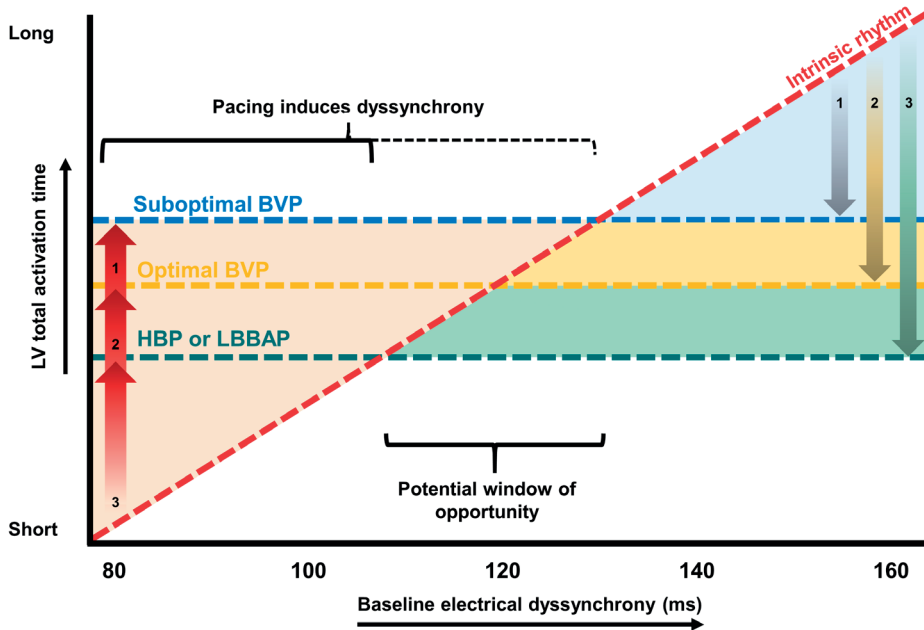
Figure 2. *Effect of various pacing modalities on left ventricular (LV) activation time. The effect of biventricular pacing (BVP) and conduction system pacing (CSP) on LV total activation time are illustrated. Depending on the amount of baseline electrical dyssynchrony without pacing (dotted red line), pacing can be beneficial (downward arrows) or potentially detrimental (upward arrows).*

non-ICM) demonstrate that His-bundle pacing provided near-similar echocardiographic and clinical improvement compared with biventricular CRT, at the expense of higher pacing thresholds [46]. In the meantime, we should not forget that contemporary CRT is an extremely well-investigated and safe device therapy, which has proven its worth in drastically improving outcome in heart failure patients with a class I indication [18, 19]. Until randomized trials that directly compare CSP and CRT have long-term data that demonstrates superiority of CSP with a similar safety profile as CRT, there is no reason to divert from the current 2021 pacing guidelines [1].

Image-guided approach: the 'who' and the 'how'

By comparison, our real-time image-guided approach (69% LBBB, 62% non-ICM) resulted in 86% responders, or 67% in non-LBBB **(chapter 6)**. This indirect comparison is admittingly crude, as our study was a prospective non-randomised study with only 30 patients, albeit from three centres. However, it does underscore the important notion that the potential of targeted transvenous lead placement should not yet be discarded. Targeted approaches are likely most useful in patients with ICM [47] and in patients with non-LBBB or a QRS-duration below 150 ms **(Figure 1 – Part II)** [11]. This is important, because these patients tend to demonstrate poor response after CRT [33]. Indeed, in LBBB

patients without any LV lateral wall scar, any targeted approach is likely of minimal added value, and electrical or mechanical guidance are non-inferior to each other [8]. This is likely because these patients have a clear electrical substrate [48], and thereby have a large region that suffers significant late electromechanical activation, perhaps as large as 40% of the LV free wall [49]. In non-LBBB, image-guided LVLP resulted in superior outcome compared to contemporary placement, whereas a QLV-guided approach failed to do so [11, 50]. However, our study was the first to demonstrate the feasibility of real-time image-fusion in a multicentre setting, with in 76% procent a near-optimal lead location **(chapter 6)**. This study thereby confirms the importance of real-time guidance discussed in **chapter 7**, which highlights the large difference in the percentage of 'in-target' pacing, achieved [...] in studies with (71-83%) and without (30-63%) real-time image-fusion. Of course, firm conclusions concerning the clinical efficacy of our approach can only be drawn after results from the multicentre randomised-controlled double-blinded ADVISE trial. The protocol of this trial, which is currently enrolling patients in six Dutch hospitals, is carefully discussed in **chapter 7**, and at the same time describes the potential economic implications. Although one other randomised trial also investigates the use of real-time MRI guided implantation (TACTIC CRT; NCT03992560), this study is limited to patients with ICM, limiting generalizability of the results.

PART III − EXPLORING EXERCISE PHYSIOLOGY

Diagnostic and prognostic importance of exercise testing

Exercise testing has an established role with proven diagnostic and prognostic utility, and its use extends to all segments of the heart failure population [51]. By contrast, exercise physiological aspects in patients with '*dyssynchronous'* heart failure are rarely investigated, and its implications are therefore not fully understood. This is in part due to the complexity involved when dealing with stress echocardiography **(chapter 8)**, submaximal exercise testing **(chapter 9)**, or haemodynamics and skeletal muscle function during dynamic transitions **(chapter 10)**. Hence, in **part III**, we sought to explore the exercise physiology of patients with dyssynchronous heart failure.

In **chapter 8,** we illustrate that strain-measurements during exercise, although challenging, is feasible up to 60% of the ventilatory threshold. Improved high frame-rate image acquisition may increase its feasibility [52]. In addition, it was shown that the extent of wasted mechanical work can be influenced by exercise, and is therefore dynamic. As a proof-of-concept, this study partly provides an explanation for the heterogeneity and variability in exercise-induced symptom-severity encountered across patients with LBBB, despite having similar cardiac function at rest. **Chapter 9** compares predictors exercise-related predictors of CRT response, as measured [...] during either submaximal

exercise or peak exertion. It was demonstrated how oxygen uptake (VO_2) kinetics during submaximal effort are significantly associated with response to CRT. This is of relevance, because many CRT patients are not accustomed to peak exertion during daily life, and, consequently, are frequently afraid or incapable of performing symptom-limited exercise testing [51]. Moreover, as also evidenced in **chapter 10**, symptomatic severity in heart failure is also characterised by peripheral derangements in skeletal muscle function, which are frequently overlooked [13, 53, 54]. As a result, true VO_2 Peak derived from cardiopulmonary exercise tests is often not truly achieved, thereby reducing the validity of these tests. By contrast, VO_2 recovery kinetics reflects one's capacity to recover from ordinary daily activities and thereby objectively quantify one's submaximal exercise capacity, while reflecting skeletal muscle functioning [53, 55] . This may also explain why, in our study, submaximal VO_2 kinetics were more strongly associated with volumetric response after CRT than VO_2 Peak. Of course, larger studies are required before firm conclusions can be drawn regarding non-inferiority submaximal exercise testing with regard to its prognostic and diagnostic value, preferably in conjunction with electrical and mechanical parameters. Moreover, these studies need to validate the proposed cut-off values of 60 seconds. Ultimately, because HF symptoms are typically experienced during submaximal exertion, both stress echocardiography **(chapter 8)** and submaximal exercise testing **(chapter 9)** may provide diagnostic and prognostic information in patients with heart failure, but further research is warranted.

Therapeutic effects of exercise in heart failure

Because heart failure is a debilitating and systemic disease, an integrated approach that also treats 'peripheral' derangements of skeletal muscle function may be beneficial **(Figure 1 – Part III)**. In **chapter 10**, high-intensity interval training (HIT) and CRT were shown to have differential effects on cardiac function, and similar effects on (sub)maximal exercise capacity. For instance, both interventions improved submaximal exercise capacity, but only CRT improved resting cardiac function. By contrast, only three months of HIT improved exercise haemodynamics, which has been shown to be independently associated with all-cause mortality in over 200 heart failure patients [56]. This may be one of multiple reasons why exercise training in heart failure is proven clinically and prognostically important [57–59]. It is therefore all the more striking that uptake of exercise training or cardiac rehabilitation is so poor. Although exercise training has a class I indication in patients with heart failure [60], a mere 5% of Dutch patients with chronic HF are estimated to participate in a cardiac rehabilitation program [58]. Furthermore, in 80% of European countries, cardiac rehabilitation is considered seldomly or never at all [61]. This may also explain the clear discrepancy between clinical, echocardiographic and functional outcome encountered across heart failure patients after CRT [62]. This is not necessarily surprising, considering CRT can only improve cardiac function and subsequent organ perfusion,

11

but by itself does not promote exercise tolerance or train the peripheral skeletal muscles. Hence, efforts should be directed towards promoting the uptake of exercise training in heart failure. Although **chapter 10** illustrates that symptomatic severity is related to reduced exercise haemodynamics and skeletal muscle function, earlier consideration is likely of higher importance. Not only does timely intervention increase the likeliness to adhere to training programs [57], it may also limit further deterioration of skeletal muscle function and exercise capacity [13]. Although various questions remain to be answered before exercise physiology in dyssynchronous heart failure is fully understood, promoting uptake of exercise should be considered a priority.

REFERENCES

1. M. Glikson, J. C. Nielsen, M. B. Kronborg, *et al.* 2021 ESC Guidelines on cardiac pacing and cardiac resynchronization therapy: Developed by the Task Force on cardiac pacing and cardiac resynchronization therapy of the European Society of Cardiology (ESC) With the special contribution of the European Hear. *Eur. Heart J.* (2021), doi:10.1093/eurheartj/ehab364.

2. B. W. L. De Boeck, A. J. Teske, M. Meine, *et al.* Septal rebound stretch reflects the functional substrate to cardiac resynchronization therapy and predicts volumetric and neurohormonal response. *Eur. J. Heart Fail.* **11**, 863–871 (2009).

3. G. E. Leenders, B. W. L. De Boeck, A. J. Teske, *et al.* Septal rebound stretch is a strong predictor of outcome after cardiac resynchronization therapy. *J. Card. Fail.* **18**, 404–412 (2012).

4. A. H. Maass, K. Vernooy, S. C. Wijers, *et al.* Refining success of cardiac resynchronization therapy using a simple score predicting the amount of reverse ventricular remodelling: results from the Markers and Response to CRT (MARC) study. *Europace.* **20** (2018). pp. e1–e10.

5. A. M. W. van Stipdonk, R. Hoogland, I. ter Horst, *et al.* Evaluating Electrocardiography-Based Identification of Cardiac Resynchronization Therapy Responders Beyond Current Left Bundle Branch Block Definitions. *JACC Clin. Electrophysiol.* **6**, 193–203 (2020).

6. A. M. W. van Stipdonk, S. Vanbelle, I. A. H. Ter Horst, *et al.* Large variability in clinical judgement and definitions of left bundle branch block to identify candidates for cardiac resynchronisation therapy. *Int. J. Cardiol.* **286**, 61–65 (2019).

7. W. Mullens, A. Auricchio, P. Martens, *et al.* Optimized implementation of cardiac resynchronization therapy: a call for action for referral and optimization of care. *Eur. J. Heart Fail.* **22**, 2349–2369 (2020).

8. C. Stephansen, A. Sommer, M. B. Kronborg, *et al.* Electrically vs. imaging-guided left ventricular lead placement in cardiac resynchronization therapy: a randomized controlled trial. *EP Eur.* (2019), doi:10.1093/europace/euz184.

9. M. R. Gold, U. Birgersdotter-Green, J. P. Singh, *et al.* The relationship between ventricular electrical delay and left ventricular remodelling with cardiac resynchronization therapy. *Eur. Heart J.* **32**, 2516–2524 (2011).

10. S. Saba, J. Marek, D. Schwartzman, *et al.* Echocardiography-Guided Left Ventricular Lead Placement for Cardiac Resynchronization Therapy. *Circ. Hear. Fail.* **6**, 427–434 (2013).

11. J. J. Marek, S. Saba, T. Onishi, *et al.* Usefulness of echocardiographically guided left ventricular lead placement for cardiac resynchronization therapy in patients with intermediate QRS width and non-left bundle branch block morphology. *Am. J. Cardiol.* **113**, 107–116 (2014).

12. F. Leyva, P. W. Foley, S. Chalil, *et al.* Cardiac resynchronization therapy guided by late gadolinium-enhancement cardiovascular magnetic resonance. *J. Cardiovasc. Magn. Reson.* **13**, 29 (2011).

13. T. A. Rehn, M. Munkvik, P. K. Lunde, I. Sjaastad, O. M. Sejersted. Intrinsic skeletal muscle alterations in chronic heart failure patients: a disease-specific myopathy or a result of deconditioning? *Heart Fail. Rev.* **17**, 421–436 (2012).

14. C.-M. Yu, G. B. Bleeker, J. W.-H. Fung, *et al.* Left Ventricular Reverse Remodeling but Not Clinical Improvement Predicts Long-Term Survival After Cardiac Resynchronization Therapy. *Circulation.* **112**, 1580–1586 (2005).

15. C. Ypenburg, R. J. van Bommel, C. J. W. Borleffs, *et al.* Long-term prognosis after cardiac resynchronization therapy is related to the extent of left ventricular reverse remodeling at midterm follow-up. *J. Am. Coll. Cardiol.* **53**, 483–490 (2009).

11

16.   P. W. X. Foley, S. Chalil, K. Khadjooi, *et al.* Left ventricular reverse remodelling, long-term clinical outcome, and mode of death after cardiac resynchronization therapy. *Eur. J. Heart Fail.* **13**, 43–51 (2011).

17.   M. Kloosterman, A. M. W. van Stipdonk, I. ter Horst, *et al.* Association between heart failure aetiology and magnitude of echocardiographic remodelling and outcome of cardiac resynchronization therapy. *ESC Hear. Fail.* **7**, 645–653 (2020).

18.   I. Sipahi, J. C. Chou, M. Hyden, *et al.* Effect of QRS morphology on clinical event reduction with cardiac resynchronization therapy: meta-analysis of randomized controlled trials. *Am. Heart J.* **163**, 260–7.e3 (2012).

19.   I. Sipahi, T. P. Carrigan, D. Y. Rowland, B. S. Stambler, J. C. Fang. Impact of QRS Duration on Clinical Event Reduction With Cardiac Resynchronization Therapy: Meta-analysis of Randomized Controlled Trials. *Arch. Intern. Med.* **171**, 1454–1462 (2011).

20.   J. G. Cleland, W. T. Abraham, C. Linde, *et al.* An individual patient meta-analysis of five randomized trials assessing the effects of cardiac resynchronization therapy on morbidity and mortality in patients with symptomatic heart failure. *Eur. Heart J.* **34**, 3547–3556 (2013).

21.   M. L. Caputo, A. van Stipdonk, A. Illner, *et al.* The definition of left bundle branch block influences the response to cardiac resynchronization therapy. *Int. J. Cardiol.* **269**, 165–169 (2018).

22.   E. B. Engels, M. Mafi-Rad, A. M. W. van Stipdonk, K. Vernooy, F. W. Prinzen. Why QRS Duration Should Be Replaced by Better Measures of Electrical Activation to Improve Patient Selection for Cardiac Resynchronization Therapy. *J. Cardiovasc. Transl. Res.* **9**, 257–265 (2016).

23.   E. S. Chung, A. R. Leon, L. Tavazzi, *et al.* Results of the Predictors of Response to CRT (PROSPECT) trial. *Circulation.* **117**, 2608–2616 (2008).

24.   W. M. Van Everdingen, A. H. Maass, K. Vernooy, *et al.* Comparison of strain parameters in dyssynchronous heart failure between speckle tracking echocardiography vendor systems. *Cardiovasc. Ultrasound.* **15**, 25 (2017).

25.   W. M. van Everdingen, A. Zweerink, R. Nijveldt, *et al.* Comparison of strain imaging techniques in CRT candidates: CMR tagging, CMR feature tracking and speckle tracking echocardiography. *Int. J. Cardiovasc. Imaging.* **34**, 443–456 (2018).

26.   W. M. van Everdingen, J. Walmsley, M. J. Cramer, *et al.* Echocardiographic Prediction of Cardiac Resynchronization Therapy Response Requires Analysis of Both Mechanical Dyssynchrony and Right Ventricular Function: A Combined Analysis of Patient Data and Computer Simulations. *J. Am. Soc. Echocardiogr.* **30**, 1012-1020.e2 (2017).

27.   M. J. P. Raatikainen, D. O. Arnar, K. Zeppenfeld, *et al.* Statistics on the use of cardiac electronic devices and electrophysiological procedures in the European Society of Cardiology countries: 2014 report from the European Heart Rhythm Association. *Eur. Eur. pacing, arrhythmias, Card. Electrophysiol. J. Work. groups Card. pacing, arrhythmias, Card. Cell. Electrophysiol. Eur. Soc. Cardiol.* **17 Suppl 1**, i1-75 (2015).

28.   J. Beshai, R. Grimm, S. Nagueh, *et al.* Cardiac-resynchronization therapy in heart failure with narrow QRS complexes. *Hear. Metab.* **369**, 38 (2008).

29.   F. Ruschitzka, W. T. Abraham, J. P. Singh, *et al.* Cardiac-Resynchronization Therapy in Heart Failure with a Narrow QRS Complex. *N. Engl. J. Med.* **369**, 1395–1405 (2013).

30.   J. Lumens, B. Tayal, J. Walmsley, *et al.* Differentiating Electromechanical from Non-Electrical Substrates of Mechanical Discoordination to Identify Responders to Cardiac Resynchronization Therapy. *Circ. Cardiovasc. Imaging.* **8**, e003744 (2015).

31. J. M. Aalen, E. Donal, C. K. Larsen, *et al*. Imaging predictors of response to cardiac resynchronization therapy: left ventricular work asymmetry by echocardiography and septal viability by cardiac magnetic resonance. *Eur. Heart J.* **41**, 3813–3823 (2020).

32. O. A. E. Salden, A. Zweerink, P. Wouters, *et al*. The value of septal rebound stretch analysis for the prediction of volumetric response to cardiac resynchronization therapy. *Eur. Heart J. Cardiovasc. Imaging*. **22**, 37–45 (2021).

33. O. A. E. Salden, K. Vernooy, A. M. W. van Stipdonk, *et al*. Strategies to improve selection of patients without typical left bundle branch block for cardiac resynchronization therapy. *JACC Clin. Electrophysiol*., in press, doi:10.1016/j.jacep.2019.11.018.

34. F. Leyva, A. Zegard, R. J. Taylor, *et al*. Long-term outcomes of cardiac resynchronization therapy using apical versus nonapical left ventricular pacing. *J. Am. Heart Assoc.* **7**, e008508 (2018).

35. L. A. Saxon, B. Olshansky, K. Volosin, *et al*. Influence of left ventricular lead location on outcomes in the COMPANION study. *J. Cardiovasc. Electrophysiol.* **20**, 764–768 (2009).

36. J. P. Singh, H. U. Klein, D. T. Huang, *et al*. Left ventricular lead position and clinical outcome in the multicenter automatic defibrillator implantation trial-cardiac resynchronization therapy (MADIT-CRT) trial. *Circulation*. **123**, 1159–1166 (2011).

37. C. Butter, A. Auricchio, C. Stellbrink, *et al*. Effect of resynchronization therapy stimulation site on the systolic function of heart failure patients. *Circulation*. **104**, 3026–3029 (2001).

38. A. L. A. J. Dekker, B. Phelps, B. Dijkman, *et al*. Epicardial left ventricular lead placement for cardiac resynchronization therapy: Optimal pace site selection with pressure-volume loops. *J. Thorac. Cardiovasc. Surg.* **127**, 1641–1647 (2004).

39. M. R. Gold, A. Auricchio, J. D. Hummel, *et al*. Comparison of stimulation sites within left ventricular veins on the acute hemodynamic effects of cardiac resynchronization therapy. *Hear. Rhythm*. **2**, 376–381 (2005).

40. M. D. Bogaard, P. A. Doevendans, G. E. Leenders, *et al*. Can optimization of pacing settings compensate for a non-optimal left ventricular pacing site? *EP Eur.* **12**, 1262–1269 (2010).

41. N. Derval, P. Steendijk, L. J. Gula, *et al*. Optimizing hemodynamics in heart failure patients by systematic screening of left ventricular pacing sites: the lateral left ventricular wall and the coronary sinus are rarely the best sites. *J. Am. Coll. Cardiol.* **55**, 566–575 (2010).

42. M. Strik, S. Ploux, P. R. Huntjens, *et al*. Response to cardiac resynchronization therapy is determined by intrinsic electrical substrate rather than by its modification. *Int. J. Cardiol.* **270**, 143–148 (2018).

43. A. Zweerink, O. A. E. Salden, W. M. van Everdingen, *et al*. Hemodynamic Optimization in Cardiac Resynchronization Therapy: Should We Aim for dP/dtmax or Stroke Work? *JACC Clin. Electrophysiol.* **5**, 1013–1025 (2019).

44. F. C. W. M. Salden, J. G. L. M. Luermans, S. W. Westra, *et al*. Short-Term Hemodynamic and Electrophysiological Effects of Cardiac Resynchronization by Left Ventricular Septal Pacing. *J. Am. Coll. Cardiol.* **75**, 347–359 (2020).

45. P. Vijayaraman, S. Ponnusamy, Ó. Cano, *et al*. Left Bundle Branch Area Pacing for Cardiac Resynchronization Therapy: Results From the International LBBAP Collaborative Study Group. *JACC Clin. Electrophysiol.* **7**, 135–147 (2021).

46. M. Vinther, N. Risum, J. H. Svendsen, R. Møgelvang, B. T. Philbert. A Randomized Trial of His Pacing Versus Biventricular Pacing in Symptomatic HF Patients With Left Bundle Branch Block (His-Alternative). *JACC. Clin. Electrophysiol.* **7**, 1422–1432 (2021).

47. F. Leyva. Cardiac resynchronization therapy guided by cardiovascular magnetic resonance. *J. Cardiovasc. Magn. Reson.* **12**, 64 (2010).

11

48.   S. Ploux, R. Eschalier, Z. I. Whinnett, *et al.* Electrical dyssynchrony induced by biventricular pacing: Implications for patient selection and therapy improvement. *Hear. Rhythm*. **12**, 782–791 (2015).

49.   R. H. Helm, M. Byrne, P. A. Helm, *et al.* Three-dimensional mapping of optimal left ventricular pacing site for cardiac resynchronization. *Circulation*. **115**, 953–961 (2007).

50.   J. P. Singh, R. D. Berger, R. N. Doshi, *et al.* Targeted Left Ventricular Lead Implantation Strategy for Non-Left Bundle Branch Block Patients: The ENHANCE CRT Study. *JACC. Clin. Electrophysiol.* **6**, 1171–1181 (2020).

51.   U. Corrà, P. G. Agostoni, S. D. Anker, *et al.* Role of cardiopulmonary exercise testing in clinical stratification in heart failure. A position paper from the Committee on Exercise Physiology and Training of the Heart Failure Association of the European Society of Cardiology. *Eur. J. Heart Fail.* **20**, 3–15 (2018).

52.   P. Joos, J. Porée, H. Liebgott, *et al.* High-Frame-Rate Speckle-Tracking Echocardiography. *IEEE Trans. Ultrason. Ferroelectr. Freq. Control*. **65**, 720–728 (2018).

53.   R. F. Spee, V. M. Niemeijer, T. Schoots, *et al.* The relation between cardiac output kinetics and skeletal muscle oxygenation during moderate exercise in moderately impaired patients with chronic heart failure. *J. Appl. Physiol.* **121**, 198–204 (2016).

54.   V. M. Niemeijer, T. Snijders, L. B. Verdijk, *et al.* Skeletal muscle fiber characteristics in patients with chronic heart failure: Impact of disease severity and relation with muscle oxygenation during exercise. *J. Appl. Physiol.* **125**, 1266–1276 (2018).

55.   H. M. C. Kemps, J. J. Prompers, B. Wessels, *et al.* Skeletal muscle metabolic recovery following submaximal exercise in chronic heart failure is limited more by O 2 delivery than O 2 utilization. *Clin. Sci.* **118**, 203–210 (2010).

56.   S. G. Williams, M. Jackson, G. A. Cooke, *et al.* How do different indicators of cardiac pump function impact upon the long-term prognosis of patients with chronic heart failure? *Am. Heart J.* **150**, 983 (2005).

57.   L. B. Cooper, R. J. Mentz, J.-L. Sun, *et al.* Psychosocial Factors, Exercise Adherence, and Outcomes in Heart Failure Patients: Insights From Heart Failure: A Controlled Trial Investigating Outcomes of Exercise Training (HF-ACTION). *Circ. Heart Fail.* **8**, 1044–1051 (2015).

58.   T. M. H. Eijsvogels, M. F. H. Maessen, E. A. Bakker, *et al.* Association of Cardiac Rehabilitation With All-Cause Mortality Among Patients With Cardiovascular Disease in the Netherlands. *JAMA Netw. Open.* **3**, e2011686–e2011686 (2020).

59.   R. Hambrecht, S. Gielen, A. Linke, *et al.* Effects of exercise training on left ventricular function and peripheral resistance in patients with chronic heart failure: A randomized trial. *JAMA*. **283**, 3095–3101 (2000).

60.   T. A. McDonagh, M. Metra, M. Adamo, *et al.* 2021 ESC Guidelines for the diagnosis and treatment of acute and chronic heart failure: Developed by the Task Force for the diagnosis and treatment of acute and chronic heart failure of the European Society of Cardiology (ESC) With the special contributio. *Eur. Heart J.* **42**, 3599–3726 (2021).

61.   B. Bjarnason-Wehrens, H. McGee, A.-D. Zwisler, *et al.* Cardiac rehabilitation in Europe: results from the European Cardiac Rehabilitation Inventory Survey. *Eur. J. Cardiovasc. Prev. Rehabil.* **17**, 410–418 (2010).

62.   B. K. Fornwalt, W. W. Sprague, P. BeDell, *et al.* Agreement is poor among current criteria used to define response to cardiac resynchronization therapy. *Circulation*. **121**, 1985–1991 (2010).

FUTURE PERSPECTIVES

Better application of prediction models

Objective identification of an absent electrical substrate may reliably exclude a meaningful treatment effect after CRT **(chapter 2),** whereas the presence of electrical substrate with concomitant mechanical dysfunction **(chapter 4)**, instigating acute recoordination **(chapter 3)** reliably ensures sustained response. However, a study where FactorECG and mechanical dyssynchrony are combined is still lacking, and studies with a control group (CRT-OFF) are still warranted before definite conclusions can be drawn. Moreover, official thresholds that result in acceptable predicted probabilities of poor response/outcome that justify denial of CRT in patients that are currently deemed eligible should still be established. Besides improving risk stratification of CRT outcome, deep-learning on the ECG can also be used to promote early detection of patients with asymptomatic LV dysfunction with LVEF ≤ 35% with an AUC of 0.90-0.93 [1,2]. Applying these algorithms on smartwatch ECGs may further accelerate early and easy detection. When also combined with the FactorECG approach to detect a CRT-eligible electrical substrate, the possibility arises to allow for early intervention with CRT. Although evidence of CRT in patients with NYHA I is relatively scarce, these patients are likely to derive significant clinical benefit [3,4]. Considering the ineffectiveness of pharmacological therapy in patients with LBBB, early intervention with CRT may drastically impact patients, even when they are asymptomatic. Indeed, despite guideline-directed medical therapy in patients with LVEF ≤35%, improvement in LVEF in LBBB is marginal with an absolute improvement of 2%, which is nearly 4-fold lower as compared to patients with a narrow QRS duration [5]. Improvement in LVEF above the guideline-indicated threshold of 35% for CRT implantation should therefore be considered unlikely after medical treatment, and direct referral to CRT in LBBB may be more beneficial.

11

Implications of novel resynchronization approaches

We should consider that CSP and (targeted) biventricular pacing are not necessarily at odds with each other **(chapter 5)**. In case of mixed conduction disease (i.e., LBBB + nonspecific intraventricular conduction delay), CSP can be used to resynchronize the septum, whereas the additional transvenous LV lead may further reduce LV total activation time through ventricular fusion pacing [6-9]. This may be because most non-LBBB patients have intact His-Purkinje activation and exhibit LV activation onset within the septum comparable to that of patients with narrow QRS [10,11]. As a result, benefits of left bundle branch area pacing by activating fast conducting superficial subendocardial fibres may be relatively limited [12], and optimally targeted **(part II)** leads at the lateral wall are still warranted to overcome nonspecific myocardial conduction delay in this important patient subgroup [13]. Although these combinations (HOT-CRT or LOT-CRT)

have shown to provide better resynchronization through a further reduction in LV total activation time when compared to CSP alone, future studies should evaluate potential benefits concerning acute haemodynamic response, reverse remodelling, and clinical outcome. Importantly, should CSP prove its worth when compared to BVP, generalisability of prediction models **(part I)** cannot be assumed. Hence, these models will also need to be evaluated in patient cohorts that receive CSP. This is important, because CSP may be used to treat a broad range of heart failure patients, including HFmrEF [14], QRS < 130 ms [15], and RBBB [16].

Establish the role of exercise in workup of CRT patients

A major cause of the low participation rates of cardiac rehabilitation and prescribed exercise training in HF is likely related to patient frailty, lack of physician referral, or more practical barriers such as lack of transportation. Fortunately, many alternatives exist, including forms of home-based or telerehabilitation [17]. Importantly, these alternatives seem to be similarly effective in improving clinical and health-related quality of life outcomes in patients with heart failure [18], and are likely to be cost-effective [19,20]. We should focus on more widespread adoption of the aforementioned alternatives to centre-based rehabilitation in a cost-effective way.

REFERENCES

1. R. R. van de Leur, M. N. Bos, K. Taha, *et al.* Inherently explainable deep neural network-based interpretation of electrocardiograms using variational auto-encoders. *medRxiv*, in press, doi:10.1101/2022.01.04.22268759.

2. Z. I. Attia, S. Kapa, F. Lopez-Jimenez, *et al.* Screening for cardiac contractile dysfunction using an artificial intelligence-enabled electrocardiogram. *Nat. Med.* **25**, 70–74 (2019).

3. C. Linde, W. T. Abraham, M. R. Gold, C. Daubert. Cardiac Resynchronization Therapy in Asymptomatic or Mildly Symptomatic Heart Failure Patients in Relation to Etiology: Results From the REVERSE (REsynchronization reVErses Remodeling in Systolic Left vEntricular Dysfunction) Study. *J. Am. Coll. Cardiol.* **56**, 1826–1831 (2010).

4. I. Goldenberg, V. Kutyifa, H. U. Klein, *et al.* Survival with Cardiac-Resynchronization Therapy in Mild Heart Failure. *N. Engl. J. Med.* **370**, 1694–1701 (2014).

5. E. Sze, Z. Samad, A. Dunning, *et al.* Impaired Recovery of Left Ventricular Function in Patients With Cardiomyopathy and Left Bundle Branch Block. *J. Am. Coll. Cardiol.* **71**, 306–317 (2018).

6. L. Padeletti, P. Pieragnoli, G. Ricciardi, *et al.* Simultaneous His Bundle and Left Ventricular Pacing for Optimal Cardiac Resynchronization Therapy Delivery. *Circ. Arrhythmia Electrophysiol.* **9**, e003793 (2016).

7. V. Pugazhendhi, H. Bengt, E. K. A., G. Jacek. His-Optimized Cardiac Resynchronization Therapy to Maximize Electrical Resynchronization. *Circ. Arrhythmia Electrophysiol.* **12**, e006934 (2019).

8. A. Zweerink, S. Zubarev, E. Bakelants, *et al.* His-Optimized Cardiac Resynchronization Therapy With Ventricular Fusion Pacing for Electrical Resynchronization in Heart Failure. *JACC Clin. Electrophysiol.* **7**, 881–892 (2021).

9. M. Jastrzębski, P. Moskal, W. Huybrechts, *et al.* Left bundle branch-optimized cardiac resynchronization therapy (LOT-CRT): Results from an international LBBAP collaborative study group. *Hear. Rhythm*. **19**, 13–21 (2022).

10. N. Derval, J. Duchateau, S. Mahida, *et al.* Distinctive Left Ventricular Activations Associated with ECG Pattern in Heart Failure Patients. *Circ. Arrhythmia Electrophysiol.* **10**, e005073 (2017).

11. M. Potse, D. Krause, L. Bacharova, *et al.* Similarities and differences between electrocardiogram signs of left bundle-branch block and left-ventricular uncoupling. *EP Eur.* **14**, v33–v39 (2012).

12. F. C. W. M. Salden, J. G. L. M. Luermans, S. W. Westra, *et al.* Short-Term Hemodynamic and Electrophysiological Effects of Cardiac Resynchronization by Left Ventricular Septal Pacing. *J. Am. Coll. Cardiol.* **75**, 347–359 (2020).

13. O. A. E. Salden, K. Vernooy, A. M. W. van Stipdonk, *et al. JACC Clin. Electrophysiol.*, in press, doi:10.1016/j.jacep.2019.11.018.

14. E. S. Chung, R. P. Katra, S. Ghio, *et al.* Cardiac resynchronization therapy may benefit patients with left ventricular ejection fraction >35%: a PROSPECT trial substudy. *Eur. J. Heart Fail.* **12**, 581–587 (2010).

15. P. S. Sharma, N. R. Patel, V. Ravi, *et al.* Clinical outcomes of left bundle branch area pacing compared to right ventricular pacing: Results from the Geisinger-Rush Conduction System Pacing Registry. *Hear. Rhythm*. **19**, 3–11 (2022).

16. P. S. Sharma, A. Naperkowski, T. D. Bauch, *et al.* Permanent His Bundle Pacing for Cardiac Resynchronization Therapy in Patients With Heart Failure and Right Bundle Branch Block. *Circ. Arrhythmia Electrophysiol.* **11**, e006613 (2018).

17. R. J. Thomas, A. L. Beatty, T. M. Beckie, *et al.* Home-Based Cardiac Rehabilitation: A Scientific Statement From the American Association of Cardiovascular and Pulmonary Rehabilitation, the

11

American Heart Association, and the American College of Cardiology. *J. Am. Coll. Cardiol.* **74**, 133–153 (2019).

18. L. Anderson, G. A. Sharp, R. J. Norton, *et al.* Home-based versus centre-based cardiac rehabilitation. *Cochrane database Syst. Rev.* **6**, CD007130 (2017).

19. R. W. M. Brouwers, E. K. J. van der Poort, H. M. C. Kemps, M. E. van den Akker-van Marle, J. J. Kraal. Cost-effectiveness of Cardiac Telerehabilitation With Relapse Prevention for the Treatment of Patients With Coronary Artery Disease in the Netherlands. *JAMA Netw. Open.* **4**, e2136652–e2136652 (2021).

20. M. Scherrenberg, M. Falter, P. Dendale. Cost-effectiveness of cardiac telerehabilitation in coronary artery disease and heart failure patients: systematic review of randomized controlled trials. *Eur. Hear. J. - Digit. Heal.* **1**, 20–29 (2020).

A

ENGLISH SUMMARY

Better characterisation of the electromechanical substrate **(part I)** may promote more appropriate patient selection for cardiac resynchronization therapy (CRT) implantation. By developing an and-to-end automated and explainable deep learning-based approach, we were able to identify a patient cluster with the predicted combination of non-response and poor outcome after CRT **(chapter 2)**. This approach allows for objective risk-stratification that outperforms contemporary electrocardiogram characteristics and QRS_{AREA}, and thereby reliable excludes the presence of a CRT-amendable substrate. **Chapter 3** illustrates how incorporating the mechanical substrate may extend the accuracy of such prediction models, which in turn is illustrated in the form of a combined assessment of the electrical substrate and mechanical dysfunction in **chapter 4**. Here, a simple four-variable model was shown to be associated with a sustained volumetric response, which indicates stable disease remission.

Optimizing left ventricular (LV) lead position **(part II)** may improve outcome after CRT, whereas poor placement may preclude response despite an underlying amendable substrate or favourable patient characteristics. Hence, **chapter 5** discusses the importance of optimizing LV-lead placement. It is shown how the optimal pacing site is highly variable, patient-specific, difficult to predict *during* implantation, and especially critical in the presence of atypical LV activation or myocardial scar. In these patients, image-guidance, rather than electrical-guidance, is likely the most important approach for achieving the optimal transvenous lead position. Hence, **chapter 6** demonstrates that real-time navigation of the LV-lead is feasible in a multicentre setting. Not only were leads adequately positioned in 76% of patients, echocardiographic response was achieved in 86% of patients. **Chapter 7** then discusses the protocol of the multicentre randomised controlled 'Advanced Image Supported Lead Placement in Cardiac Resynchronization Therapy' (ADVISE) trial, which will further investigate the clinical efficacy of this approach.

Lastly, **part III** explores the potential diagnostic **(chapter 8)**, prognostic **(chapter 9)**, and therapeutic **(chapter 10)** implications of exercise in heart failure. In **chapter 8**, the feasibility of strain-based discoordination-imaging during stress echocardiography was demonstrated. Stress echocardiography could unmask dynamic changes in mechanical dyscoordination. Although feasible, many challenges remain to overcome. **Chapter 9** demonstrates that submaximal oxygen uptake (VO_2) kinetics are associated with volumetric response to CRT. While at least equally effective as measuring VO_2 Peak, submaximal VO_2 kinetics may provide a more relevant characterisation of exercise tolerance, which is also more reliable and patient-friendly. Finally, in **chapter 10**, we illustrate how differences in cardiac output and VO_2 kinetics during submaximal exercise distinguish the severity of functional impairment in chronic heart failure, rather than differences in

resting echocardiography. Moreover, we demonstrate that both high-intensity interval training and CRT improve submaximal exercise tolerance. By contrast, only CRT induces cardiac reverse remodelling, whereas only an exercise training program improved exercising haemodynamics. Hence, combining both therapies may further improve functional recovery through differential effects.

NEDERLANDSE SAMENVATTING

Indicatiestelling voor cardiale resynchronisation therapie (CRT) kan worden verbeterd door de mate van elektromechanische dysfunctie te bepalen bij patiënten met dyssynchroon hartfalen **(deel I)**. In **hoofdstuk 2** werd een inherent uitlegbare *deep learning* methode op het standaard pre-implantatie elektrocardiogram toegepast. Hierdoor konden patiëntclusters worden geïdentificeerd waar non-respons in combinatie met een slechte klinische uitkomst na CRT werden voorspeld. Deze aanpak staat daarmee volledig geautomatiseerde en objectieve risico-stratificatie toe. Daarnaast is deze aanpak nauwkeuriger dan QRS_{AREA} en hedendaagse criteria die uit het elektrocardiogram worden geïnterpreteerd. **Hoofdstuk 3** toont dat het bepalen van het mechanische substraat dergelijke voorspelmodellen verder kan verbeteren. De gecombineerde aanpak van het gelijktijdig bepalen van het elektrische substraat én mechanische linkerkamer dysfunctie werd daartoe in **hoofdstuk 4** onderzocht. Een simpel voorspelmodel met slechts vier variabelen bleek sterk voorspellend voor aanhoudende echorespons, wat stabiele ziekteremissie aangeeft.

Een optimaal geplaatste linkerkamerdraad **(deel II)** kan de uitkomsten na CRT verbeteren, terwijl een slechte plaatsing respons kan belemmeren ongeacht gunstige patienteigenschappen. In **hoofdstuk 5** werd het belang van de optimale linkerkamerdraad positie bediscussieerd. Deze is zeer variabel, patiënt-specifiek, moeilijk te voorspellen *tijdens* de procedure, en met name cruciaal in de aanwezigheid van atypische linkerkamer activatie of littekenweefsel. Met name in deze patiënten kan beeld-gestuurde draadplaatsing een belangrijke rol spelen, hetgeen in **hoofdstuk 6** werd onderzocht. Middels *live* beeld-sturing werd de linkerkamerdraad goed gepositioneerd in 76% van de patiënten, met een echorespons in 86% van de patiënten. De 'Advanced Image Supported Lead Placement in Cardiac Resynchronization' (ADVISE) studie zal de klinische effectiviteit van deze methode verder onderzoeken. Het protocol van deze vervolgstudie met gerandomiseerde controlegroep werd in **hoofdstuk 7** toegelicht.

In **deel III** werden de diagnostische **(hoofdstuk 8)**, prognostische **(hoofdstuk 9)**, en therapeutische **(hoofdstuk 10)** implicaties van inspanning bij hartfalen verkend. **Hoofdstuk 8** toont de toepasbaarheid van op *strain* gebaseerde maten van discoördinatie tijdens inspanning aan. Inspanningsechocardiografie bracht dynamische veranderingen in mechanische discoördinatie aan het licht, maar verdere ontwikkelingen zijn nodig om de reproduceerbaarheid van deze techniek te verbeteren. De associatie van zuurstofopname (VO_2) kinetiek, zoals verkregen tijdens submaximale inspanning, en echorespons na CRT werd aangetoond in **hoofdstuk 9**. Submaximale VO_2 kinetiek is minstens zo effectief als piek VO_2 capaciteit tijdens maximale inspanning, maar is waarschijnlijk betrouwbaarder en patiëntvriendelijker. Tot slot toont **hoofdstuk 10** aan dat de ernst van symptomatische beperking bij chronisch hartfalen wordt gekarakteriseerd

door verschillen in cardiale outputkinetiek en VO_2 kinetiek tijdens submaximale inspanning, maar niet door cardiale functie zoals gemeten in rust. Daarnaast werd duidelijk dat zowel CRT als een trainingsprogramma de submaximale inspanningscapaciteit verbeteren. Echter, waar CRT zorgt voor remodellering van het hart, kan enkel een inspanningsprogramma de haemodynamiek tijdens inspanning verbeteren. Beide therapieën spelen daardoor een rol in het functionele herstel van patiënten met hartfalen.

LIST OF PUBLICATIONS

PUBLISHED

Wouters PC, van de Leur RR, Vessies MB, van Stipdonk AMW, Ghossein MA, Hassink RJ, Doevendans PA, van der Harst P, Maass AH, Prinzen FW, Vernooy K, Meine M, van Es R. Explainable electrocardiogram-based deep learning outperforms guideline criteria and QRS_{AREA} for prediction of cardiac resynchronization therapy outcome. *European Heart Journal*

Wouters PC, Schoots T, Niemeijer V, Spee RF, Kemps HMC. Does recovery from submaximal exercise predict response to cardiac resynchronisation therapy? *Open Heart*

Wouters PC, van Slochteren FJ, Tuinenburg AE, Doevendans PA, Cramer MJ, Delnoy, PPHM, van Dijk VF, Meine M. Real-time image-guided lead placement in cardiac resynchronisation therapy: feasibility and outcome in a multicentre setting. *Heart Rhythm O2*

Fixsen LS, **Wouters PC**, Lopata RGP, Kemps HMC. Strain-based discoordination imaging during exercise in heart failure with reduced ejection fraction: Feasibility and reproducibility. *BMC Cardiovasc Disorders*. **25**; 22(1):127 (2022).

Salden FCWM, Huntjens PR, Schreurs R, Willemen E, Kuiper M, **Wouters PC**, Maessen JG, Bordachar P, Delhaas T, Luermans J, Meine M, Allaart CP, van Stipdonk AMW, Prinzen FW, Lumens J, Vernooy K. Pacing therapy for atrioventricular dromotropathy: a combined computational-experimental-clinical study. *Europace*. **24**, 784-795 (2022).

Wouters PC, van Everdingen WM, Vernooy K, Geelhoed B, Allaart CP, Rienstra M, Maass AH, Vos MA, Prinzen FW, Meine M, Cramer MJ. Does mechanical dyssynchrony in addition to QRS area ensure sustained response to cardiac resynchronization therapy? *Eur. Heart J. Cardiovasc. Imaging*. (2021). Online ahead of print.

Wouters PC, van Lieshout C, van Dijk VF, Delnoy PPHM, Doevendans PAFM, Cramer MJ, Frederix, GWJ, van Slochteren FJ, Meine M. Advanced image-supported lead placement in cardiac resynchronisation therapy: protocol for the multicentre, randomised controlled ADVISE trial and early economic evaluation. *BMJ Open*. **11** (2021).

Wouters PC, Vernooy K, Cramer MJ, Prinzen FW, Meine M. Optimizing lead placement for pacing in dyssynchronous heart failure: The patient in the lead. *Heart Rhythm*. **18**, 1024-1032 (2021).

Wouters PC, Leenders GE, Cramer MJ, Meine M, Prinzen FW, Doevendans PAFM, de Boeck BWL. Acute recoordination rather than functional hemodynamic improvement determines reverse remodelling by cardiac resynchronisation therapy. *Int J Cardiovasc Imaging*. **37**, 1903-1911 (2021).

Ghossein MA, van Stipdonk AMW, Plesinger F, Kloosterman M, **Wouters PC**, Salden OAE, Meine M, Maass AH, Prinzen FW, Vernooy K. Reduction in the QRS area after cardiac resynchronization therapy is associated with survival and echocardiographic response. *J Cardiovasc Electrophysiol*. **3**, 813-822 (2021).

Salden OAE, Zweerink A, **Wouters PC**, Allaart CP, Geelhoed B, de Lange FJ, Maass AH, Rienstra M, Vernooy K, Vos MA, Meine M, Prinzen FW, Cramer MJ. The value of septal rebound stretch analysis for the prediction of volumetric response to cardiac resynchronization therapy. *Eur Heart J. Cardiovasc Imaging*. **22**, 37-45 (2021).

van Middendorp LB, Kuiper M, Munts C, **Wouters PC**, Maessen JG, van Nieuwenhoven FA, Prinzen FW. Local microRNA-133a downregulation is associated with hypertrophy in the dyssynchronous heart. *ESC Heart Failure*. **4**, 241–251 (2017).

SUBMITTED/UNDER REVIEW

van Bavel JJA, Beekman HDM, Schot A, **Wouters PC**, van Emst MG, Takken T, van der Heyden MAG, Vos MA. The exercising AV block dog model: remodeling is essential in tolerating moderate treadmill activity. *Submitted*

Wouters PC, Spee RF, Schoots T, Doevendans PA, Niemeijer V, Kemps HMC. Exercise physiology in heart failure: symptom aetiology and comparing exercise training with cardiac resynchronisation therapy. *Under review*

Rijks J, Ghossein MA, **Wouters PC**, Dural M, Maass AH, Meine M, Kloosterman M, Luermans J, Prinzen FW, Vernooy K, van Stipdonk AMW. Comparison of the relation of the ESC 2021 and ESC 2013 definitions of Left Bundle Branch Block with clinical and echocardiographic outcome in cardiac resynchronization therapy. *Under review*

IN PREPERATION

Wouters PC, Zweerink A, van Everdingen WM, Ghossein MA, Cramer MJ, Doevendans PA, Vernooy K, Prinzen FW, Allaart CP, Meine M. Clinical outcome after different strategies of hemodynamic optimization in cardiac resynchronization therapy: Stroke Work increases pressure on dP/dtmax. *In preparation*

REVIEW COMMITTEE

Prof. dr. P. van der Harst
Prof. dr. B.K. Velthuis (chair)
Prof. dr. ir. H.M. den Ruijter
Prof. dr. L.M.G. Hartgens
Prof. dr. C.P. Allaart

IV

DANKWOORD

En dan resteert enkel nog het dankwoord. Hét onderdeel dat door menig lezer als eerste, en soms als enige, zal worden gelezen. Zonder de hulp van zo veel mensen was dit boekje nooit tot stand gekomen. In de eerste plaats wil ik **alle patiënten** die hebben bijgedragen aan de onderzoeken uit dit proefschrift bedanken. Ik heb grote bewondering voor de bereidheid om, juist op zo'n kwetsbaar en onzeker moment in het leven, bij te dragen aan de medische kennis. Zonder iemand te willen overslaan wil ik de volgende mensen bij naam noemen:

Mijn promotoren, **prof. dr. Doevendans** en **prof. dr. Prinzen**:
Prof. dr. Doevendans, beste Pieter, ik wil je bedanken voor de mogelijkheid te promoveren bij de cardiologie in het UMCU. Ik vind het knap hoe jij leiding weet te geven aan zo'n groot aantal promovendi, hetgeen wordt weerspiegeld door de enorme waslijst aan publicaties die op jouw naam staan. Onze contactmomenten waren misschien schaars, ze waren altijd concreet en nuttig. Ook kan ik je voorkeur om pragmatisch te werk te gaan erg waarderen, al moet ik bekennen dat de e-mails van mijn kant wel vaak iets uitgebreider waren. Bij revisies kreeg ik vaak dezelfde dag nog te horen of een stuk verduidelijking behoefte, of juist jouw 'seal of approval' ontving. Bedankt voor alle mogelijkheden en de begeleiding deze jaren.

Prof. dr. Prinzen, beste Frits. Vanuit historisch perspectief had ik je ook als eerste kunnen noemen. Je stond namelijk al sinds mijn bachelor aan de wieg van mijn prille wetenschappelijke carrière. Ik ken niemand die het linker bundel tak blok zo beheerst als jij. Een typerende uiting daarvan is dat je alle literatuur die ooit hierover is geschreven paraat hebt (ik denk onder andere aan "Narula, 1977"). Je bent pijlsnel, benaderbaar, en discussies leverden steevast inzichten die een extra dimensie gaven aan onze stukken. Echter, nog belangrijker voor mij is de manier waarop jij jonge onderzoekers weet te begeleiden en inspireren. Dat heeft indruk gemaakt op mij, en zal altijd als een voorbeeld blijven dienen. Ik ben enorm dankbaar dat je mijn promotie wilde begeleiden, ondanks dat ik de stap van het mooie Maastricht naar Utrecht heb gezet.

Mijn co-promotoren, **dr. M. Meine** en **dr. M.J. Cramer**:
Beste **Mathias**, ik bof maar met jou als co-promotor. Jij was altijd beschikbaar voor overleg en advies. Tegelijkertijd gaf jij mij vanaf het begin af aan het vertrouwen en de mogelijkheden om zelfstandig te werk te gaan. Hierdoor was er altijd ruimte voor eigen ideeën… of om soms "stiekem" te sporten. Nog steeds leer ik iedere implantatie wat bij over de oneindige mogelijkheid aan pacing configuraties. Of ik net als jij het merk en type lead uit een X-thorax ga kunnen herkennen betwijfel ik, maar jouw advies voor de

V

kliniek zal ik zeker opvolgen: "wees vooral jezelf als dokter". Mathias, ik hoop dat ik nog lang mag genieten van je politiek (in)correcte humor, en vooral, dat we nog lang samen mogen werken.

Beste **Maarten-Jan**, mijn tweede co-promotor. Jij hebt mij weten te overtuigen om te komen promoveren in het UMCU. Ik heb je leren kennen als een onuitputbare bron van energie, enthousiasme, ideeën, en creatieve slogans. Ieder jaar wordt de rol van beeldvorming bij CRT weer een stukje duidelijker. Jouw rol binnen die onderzoekslijn, ook als netwerker, is onmiskenbaar daarin. Jouw energie is ook de reden dat het analyseren van de vrachtlading MARC-2 echo's op de maandagmiddag een stuk dragelijker werd. Jouw grote voorliefde voor 'central illustrations' is al snel overgewaaid naar mij. Die hebben zonder twijfel vaak net dat extra zetje richting publicatie gegeven.

Ik wil de leden van de leescommissie, **prof. dr. B.K. Velthuis, prof. dr. P. van der Harst, prof. dr. ir. H.M. den Ruijter, prof. dr. L.M.G. Hartgens** en **prof. dr. C.P. Allaart** graag bedanken. Dank voor de tijd en het kritisch beoordelen van mijn proefschrift.

Stafleden van het UMC, dank voor de samenwerking, de onderwijsmomenten, en de interesse tijdens de onderzoeksbesprekingen. In het bijzonder dank aan de EFO-dokters, **Anton Tuinenburg, Nick Clappers, Rutger Hassink, Peter Loh en Astrid Hendriks.** Jullie ECG kennis is intimiderend, daar kan voorlopig geen AI-algoritme tegenop. Beste Anton, jou wil ik afzonderlijk bedanken. Niet alleen hield jij mij steevast op de hoogte van geschikte patiënten, je was ook altijd bereid voor een praatje over van alles en nog wat. Ook dank voor je geduld bij de implantaties, en de moeite die je deed om zo vaak mogelijk onze ambitieuze targets te bereiken.

Heren van **CART-Tech,** de toekomst van jullie bedrijf is ongetwijfeld in goede handen. **Frebus**, mijn soms kritische houding kon nooit tippen aan jouw eeuwig enthousiasme. Onze samenwerken was daarom altijd relaxed. Al werd soms de toon al gezet wanneer onze afspraken 30 minuten later dan gepland van start gingen. Ik wens je veel succes met het combineren van ondernemen, research, en de belangrijkere nieuwe rol die je inmiddels hebt toebedeeld gekregen. **Paul**, onder het mom van "trust, but verify" hou jij je als geen ander bezig met de studievoortgang en de inclusies. Dank voor jouw betrokkenheid, en natuurlijk de leuke borrels en diners. **Emanuele**, thank you for your flexibility and assistance at the cath lab. Without your help, the addition of three centers would not be possible.

Beste **Geert Leenders** en **Bart de Boeck**, ik heb met name aan het begin van mijn promotie met jullie mogen samenwerken. Dank voor jullie inspanningen om mij het

concept van SRS machtig te maken. Ik ben vereerd dat ik jullie persoonlijke inspanningen als grondleggers daarin heb mogen oppakken en kunnen voortzetten. **Odette Salden**, als jouw opvolger wil ik je bedanken voor jouw bereidheid mij te introduceren aan het onderzoeksleven in het UMCU. Desondanks ben ik bang dat ik je verstrooidheid wat betreft dossier huishouding heb overgenomen.

Dan de vele collega's buiten Utrecht, te beginnen bij het Máxima MC. Beste **Hareld Kemps**, tijdens mijn semi-arts stage in het Máxima MC leerde jij mij al dat in de onderzoekswereld alles vanzelf wel goed komt. En inderdaad, toen de initiële plannen door trage patiënten-inclusie niet liepen zoals gepland, maakte jij het mogelijk om de inspanningsfysiologie bij CRT patiënten te onderzoeken. Jouw nuchtere houding en soms tikkeltje donkere humor helpt om het hoofd koel te houden. Veel dank ook aan **Ruud Spee, Victor Niemeijer** en **Thijs Schoots,** zonder de door jullie vergaarde data en de hulp bij het interpreteren hiervan waren onze stukken er nooit gekomen!

De onderzoekers van de **ADVISE-2** studies, **Vincent van Dijk** en **Peter-Paul Delnoy**. Mede dankzij jullie input, betrokkenheid en vertrouwen in deze studie hebben we de haalbaarheid van een image-guided aanpak kunnen aantonen in Nederland. Op naar de resultaten van de **ADVISE-3!** Inmiddels is inclusie gestart in zes centra, mede dankzij de inzet van **Alexander Maass, Vokko van Halm**, en **Kevin Vernooy**. Beste Kevin, jou wil ik extra bedanken voor je betrokkenheid bij onze review. Zonder jouw inzichten over conductie systeem pacing was dit overzicht over optimale draadplaatsing in CRT niet zo compleet geweest als nu. Dank voor je scherpe feedback en bereidbaarheid tot meedenken over steeds weer nieuwe projecten.

De onderzoekers van de **MARC** studie wil ik bedanken voor de mogelijkheid om een sub-analyse te mogen verrichten in deze prachtig uitgebreide database. **Cor Allaart, Marc Vos, Bastiaan Geelhoed, Michiel Rienstra**, allen veel dank voor de hulp bij data-analyse en de feedback die heeft bijgedragen aan dit mooie stuk. Jullie enthousiasme en vertrouwen hebben bijgedragen aan het initiatief om eindelijk die langverwachte lange termijn uitkomsten te verzamelen. Alexander Maass en Kevin Vernooy, jullie zijn naast ADVISE-3 en MARC óók al betrokken bij de **MUG** database. Geweldig dat we de mogelijkheid kregen om hier ons deep learning project in uit te voeren. Zonder de inspanningen van **Twan van Stipdonk** en **Moedi Ghossein** was dit nooit gelukt, jullie hebben enorm veel werk verzet in deze database. Dank voor jullie bereidbaarheid en betrokkenheid bij deze projecten.

En dan volgt, niet te vergeten, het wetenschappelijk hoofdkantoor van het UMCU; **de Villa**. Een plek waar golven, darten, en forten bouwen van katheterdozen de normaalste

V

zaak van de wereld is. Ook papers schijnen hier geschreven te worden, al zijn CD's hier nog nooit succesvol gebrand. Met jullie valt altijd wat te beleven in de villa: **René van Es** (als nestor duidelijk niet op je mondje gevallen: mooi dat je altijd in bent voor een discussie), **Sanne** en **Marijn** (hét duo achter bijna iedere borrel en het onvergetelijke PhD-weekend), **Feddo** (met je escalatiemix en traditioneel ontknoopte hemd op alle borrels, dank dat je mij op sleeptouw nam om echo's te maken), **Karim** (strain-expert, eeuwig vraagbaken, en mede fitness fanaat) en **Melle** (het nieuwe AI wonderkind van de Villa). **Rutger**, samen hebben we San Francisco in stijl uitgespeeld door een onuitputbare bron aan Hazy IPA's, dreigend tekort aan Tesla superchargers, overstekende hertjes, en veel te brakke hoogtemeters in Yosemite. Als kers op de taart delen we ook de 1^e auteursplek op ons mooie FactorECG-paper. Zeven reviewers verder, maar dan heb je ook wat! Ik ben blij dat je als paranimf aan mijn zijde staat tijdens mijn verdediging!

Ook dank aan alle (ex-)collega-onderzoekers, binnen en buiten de Villa: **Agnieszka, Anne-Mar, Arjan, Bas, Diantha, Evangeline, Fahima, Hugo, Joanne, Lieke, Lisa, Machteld, Mark, Markella, Max, Mimount, Nicole, Rob, Rosanne, Steven, Thomas, Timion** en **Vera**. Met name veel dank voor alles wat niét met onderzoek te maken had, ik kijk uit naar het volgende PhD-weekend.

Studenten **Cheyenne** en **Rens**, jullie zijn een enorme hulp geweest bij het verzamelen en analyseren van data. Ik wil jullie bedanken voor jullie inzet en leergierigheid. Ik weet zeker dat de opbrengst van jullie werk nog zal worden vervolgd!

De **echocardiografisten** van het UMCU, in het bijzonder **Jeanette, Elly, Ineke, Grianne** en **Roshni**. Dank voor jullie hulp bij het leren maken van echo's, en voor jullie geduld wanneer ik weer niet wist hoe een bepaalde meting moest worden verricht in IntelliSpace. Alle **medewerkers op de HCK**, dank voor jullie geduld en ondersteuning bij de pressure-volume loop metingen, of wanneer we weer een lastig target op het beeldscherm toverden. De **device technici, Jeroen, Hiske, Rolf, Maaike** en **Lars** dank voor de ondersteuning tijdens de implantaties (is het nu Q-LV of Q-RV?), en de follow-up van studiepatiënten. Dank aan **Jos** van Abbott, voor zijn ondersteuning en flexibiliteit bij de ADVISE-patiënten. **Ronald Groenemeijer**, dank voor jouw technische ondersteuning en de hulp met VDICOM. Zonder jouw hulp bevonden we ons nog in de steentijd. **Manon**, samen hebben wij zowel de **MARC-2** als de **ADVISE-3** studies op orde gehouden. Dank voor de samenwerking en het uit de brand helpen bij de monitorvisites.

Vrienden van **de Oude Garde**, ondanks al die jaren blijft het een feest om elkaar weer te zien. Ons halve leven hebben wij met elkaar gedeeld, en we kennen elkaar daardoor beter dan eigenlijk goed voor ons is. Geen grap, vaak onder de gordel, gaat ons te ver.

Laten we echter ook vooral het beste in elkaar naar boven blijven halen. Dank voor de vele borrels, gezamenlijk vakanties, festivals, sloopweekenden, filosofische discussies, eigenaardige tradities en onzinnige gesprekken.

Bonobo's, jullie zijn een bijzonder en gevarieerd stelletje ongeremde apen. In Maastricht hebben we teveel meegemaakt om op te noemen. Een 'gezelligere' studententijd zonder jullie kan ik mij dan ook niet voorstellen. Ik hoop dat er ruimte blijft voor het herleven van zulke momenten, ondanks de gestage verburgerlijking waar we aan toe moeten geven. **Wouter**, in het bijzonder dank aan jou als netwerker en vraagbaken. Mooi dat wij nog samen een paper gepubliceerd hebben. Overigens zijn je schoenen inmiddels wat uitgelopen.

Mijn paranimf, **Aise**, en huisgenoot van het eerste uur. Al sinds mijn bachelor weet jij, zonder enige achtergrond in de geneeskunde, prikkelende vragen te stellen over mijn werk. Onze discussies hebben meer dan eens geholpen om overzicht te krijgen over mijn eigen gedachtes. Waren je opruimvaardigheden maar net zo sterk aanwezig als je eeuwige nieuwsgierigheid. **Sammy**, je bent een aanwinst geweest voor de TP-crew, op meer vlakken dan als (opruim)partner van Aise.

Ook mijn familie wil ik bedanken. Lieve **pa en ma**, ik ben opgegroeid in een klein maar gezegend nest met jullie als ouders. Dat is iets dat ik altijd zal waarderen, en nooit zal vergeten. Vanaf dag 1 hebben jullie mij gesteund met jullie onvoorwaardelijke liefde. Zonder jullie was ik nooit gekomen waar ik nu ben. Ook **de Koentjes** zijn een enorme steun geweest tijdens dit avontuur. Dank dat jullie mij altijd zó thuis hebben laten voelen en al mijn flauwe grappen en geplaag zijn blijven tolereren. Ik kan niet wachten tot de volgende verhitte discussies over alle problemen in de zorg, bij voorkeur tijdens het keten in een Grieks restaurant.

En tot slot, mijn lieve **Carolien**. Niemand heeft de ups-and-downs van mijn promotie van zo dichtbij gemaakt als jij. Jij doorstond de vele avonden wanneer ik als nachtuil weer mijn ideeën moest wegschrijven, en tolereerde hoe de eetkamertafel progressief een weerspiegeling van mijn verstrooide gedachtes werd. De term "linker bundel tak blok" spreek je inmiddels vloeiend uit, maar of je écht begrijpt wat ik precies heb gedaan weet ik niet. Veel belangrijker is dat ik me geen betere 'partner in crime' kan wensen dan jij. Geef alsjeblieft nooit op om de balans tussen werk en privé te blijven bewaken met mij. Ik hou van je.

V

CURRICULUM VITAE

Philippe Constant Wouters was born April 15th 1994, and raised by his parents, Theo and Myriam, in Terheijden. After graduating high school, he moved to Limburg in 2012 to study Biomedical Sciences at the University of Maastricht. Here he gained his first experience with research under supervision of prof. dr. Prinzen, who instantly sparked his ambition in the field of cardiovascular research. With his bachelor's degree completed in 2015, he seized the opportunity to combine his interests in research and medicine by enrolling in the 4-year 'AKO-master'. He concluded his master with an internship at the department of cardiology at Máxima MC under supervision of dr. Kemps. In 2019 he officially became a physician and clinical investigator. Upon completion of his medical training, he continued his path to start a PhD program under supervision of prof. dr. Doevendans, prof. dr. Prinzen and co-promotors dr. Meine and dr. Cramer. At the department of cardiology at the UMC Utrecht, Philippe studied various strategies to advance the role of imaging and exercise in patients with heart failure that are to be treated with cardiac resynchronization therapy. During this period, he had the opportunity to collaborate with many cardiologist and researchers, including colleagues he was grateful to have met during his past education. These joint efforts have led to the scientific work provided in this thesis. Philippe will continue his career in academia and medicine. In august 2022, he started a residency at the department of cardiology in the Diakonessenhuis in Utrecht.

VI